National Library of Canada
Acquisitions and Bibliographic Services Branch
395 Wellington Street
Ottawa, Ontario
K1A 0N4

Bibliothèque nationale du Canada
Direction des acquisitions et des services bibliographiques
395, rue Wellington
Ottawa (Ontario)
K1A 0N4

Your file Votre référence

Our file Notre référence

NOTICE

The quality of this microform is heavily dependent upon the quality of the original thesis submitted for microfilming. Every effort has been made to ensure the highest quality of reproduction possible.

If pages are missing, contact the university which granted the degree.

Some pages may have indistinct print especially if the original pages were typed with a poor typewriter ribbon or if the university sent us an inferior photocopy.

Reproduction in full or in part of this microform is governed by the Canadian Copyright Act, R.S.C. 1970, c. C-30, and subsequent amendments.

AVIS

La qualité de cette microforme dépend grandement de la qualité de la thèse soumise au microfilmage. Nous avons tout fait pour assurer une qualité supérieure de reproduction.

S'il manque des pages, veuillez communiquer avec l'université qui a conféré le grade.

La qualité d'impression de certaines pages peut laisser à désirer, surtout si les pages originales ont été dactylographiées à l'aide d'un ruban usé ou si l'université nous a fait parvenir une photocopie de qualité inférieure.

La reproduction, même partielle, de cette microforme est soumise à la Loi canadienne sur le droit d'auteur, SRC 1970, c. C-30, et ses amendements subséquents.

Canada

UNIVERSITY OF ALBERTA

CHARACTERIZATION OF ANAEROBIC *sn*-GLYCEROL-3-PHOSPHATE DEHYDROGENASE IN *ESCHERICHIA COLI* : AN INVESTIGATION INTO THE MEMBRANE-BOUND SUBUNIT GLPB

BY

© MONICA ELIZABETH ROSE VARGA

A THESIS

SUBMITTED TO THE FACULTY OF GRADUATE STUDIES AND RESEARCH IN PARTIAL FULFILLMENT OF THE REQUIREMENTS FOR THE DEGREE OF DOCTOR OF PHILOSOPHY

DEPARTMENT OF BIOCHEMISTRY

EDMONTON, ALBERTA

FALL, 1994

National Library
of Canada

Acquisitions and
Bibliographic Services Branch

395 Wellington Street
Ottawa, Ontario
K1A 0N4

Bibliothèque nationale
du Canada

Direction des acquisitions et
des services bibliographiques

395, rue Wellington
Ottawa (Ontario)
K1A 0N4

Your file Votre référence

Our file Notre référence

The author has granted an irrevocable non-exclusive licence allowing the National Library of Canada to reproduce, loan, distribute or sell copies of his/her thesis by any means and in any form or format, making this thesis available to interested persons.

L'auteur a accordé une licence irrévocable et non exclusive permettant à la Bibliothèque nationale du Canada de reproduire, prêter, distribuer ou vendre des copies de sa thèse de quelque manière et sous quelque forme que ce soit pour mettre des exemplaires de cette thèse à la disposition des personnes intéressées.

The author retains ownership of the copyright in his/her thesis. Neither the thesis nor substantial extracts from it may be printed or otherwise reproduced without his/her permission.

L'auteur conserve la propriété du droit d'auteur qui protège sa thèse. Ni la thèse ni des extraits substantiels de celle-ci ne doivent être imprimés ou autrement reproduits sans son autorisation.

ISBN 0-315-95275-X

Canada

UNIVERSITY OF ALBERTA

RELEASE FORM

NAME OF AUTHOR:	Monica Elizabeth Rose Varga
TITLE OF THESIS:	Characterization of Anaerobic *sn*-Glycerol-3-phosphate Dehydrogenase in *Escherichia coli* : An Investigation into the Membrane-bound Subunit GlpB
DEGREE:	Doctor of Philosophy
YEAR THIS DEGREE GRANTED:	Fall 1994

Permission is hereby granted to the University of Alberta Library to reproduce single copies of this thesis and to lend or sell such copies for private, scholarly or scientific research purposes only.

The author reserves all other publication and other rights in association with the copyright in the thesis, and except as hereinbefore provided neither the thesis nor any substantial portion thereof may be printed or otherwise reproduced in any material form whatever without the author's prior written permission.

Monica E. R. Varga

PERMANENT ADDRESS:

2904 Park Lane S. W.
Calgary, Alberta
CANADA
T2S 2L7

Date: July 20, 1994

"Once in a lifetime..."

David Byrne, Talking Heads

UNIVERSITY OF ALBERTA

FACULTY OF GRADUATE STUDIES AND RESEARCH

The undersigned certify that they have read, and recommend to the Faculty of Graduate Studies and Research for acceptance, a thesis entitled CHARACTERIZATION OF ANAEROBIC *sn*-GLYCEROL-3-PHOSPHATE DEHYDROGENASE IN *ESCHERICHIA COLI*: AN INVESTIGATION INTO THE MEMBRANE-BOUND SUBUNIT GLPB submitted by MONICA ELIZABETH ROSE VARGA in partial fulfillment of the requirement for the degree of DOCTOR OF PHILOSOPHY.

Dr. Joel H. Weiner [Supervisor]

Dr. William A. Bridger

Dr. Carol E. Cass

Dr. Mark S. Peppler

Dr. Janet M. Wood

Date: July 20, 1994

To my parents

ABSTRACT

Anaerobic *sn*-Glycerol-3-phosphate dehydrogenase (G3PDH) of the bacterium *Escherichia coli* catalyzes the oxidation of glycerol-3-phosphate to dihydroxyacetone phosphate and passes the electrons, via the membrane bound menaquinone pool, to the terminal acceptor. G3PDH is specified by the *glpACB* operon which encodes three polypeptide chains. GlpA and GlpC comprise a soluble catalytic dimer (which has been previously purified and characterized). The third subunit, GlpB, is essential for anaerobic growth, as shown in complementation studies with a mutant strain deleted for the *glpACB* operon. GlpB appears to be associated with the cytoplasmic membrane as indicated by expression studies and sucrose gradient sedimentation, although it exhibits unusual membrane protein behavior as it is resistant to detergent solubilization except with denaturing detergents like sarkosyl or SDS and this has hampered the investigation of GlpB structure and function. Crucial to a proposed electron transfer role of GlpB, I have demonstrated the existence of a redox center within the protein using electron paramagnetic resonance (EPR) spectroscopy. EPR studies were conducted on a preparation of GlpB as a fusion with the *Schistosoma japonicum* glutathione S-transferase (GST). Although evidence for a paramagnetic center was obtained with the GSTGlpB fusion, anomalous results suggested that the center was not present in the fusion protein representative of the physiological state. EPR analysis of cells anaerobically overexpressing the *glpACB* operon showed that the reduction of the center was possible not only by artificial reductants but with the physiological substrate, glycerol-3-phosphate. This result confirmed the functional association of GlpB with the catalytic dimer, and that electron transfer occurred through GlpB into the respiratory chain. The redox center has been tentatively assigned as a [2Fe-2S] center with an E_m of - 320 mV ± 30 mV at pH 7.0. The cluster was very labile, susceptible to over reduction with dithionite, oxidative damage and changes in pH as well as the iron-chelator, o-phenanthroline. Mutagenesis of cysteine residues (C12S, C59S) for coordinating the proposed cluster showed that C59S appeared to act as a ligand whereas C12S did not, but C12S it destabilized the local environment. The atypical behavior of the center as determined from EPR studies may be an indication that the paramagnetic center in GlpB is not a [2Fe-2S] center but a novel type of cluster.

ACKNOWLEDGMENTS

I would like to thank my supervisor, Joel Weiner for the opportunity to work in his laboratory, for his patience, enthusiasm and guidance during my years of study. I would also like to thank the members of my committee; Carol Cass, Mark Peppler and Bill Bridger for their interest in my progress and giving freely of their time and knowledge. I must also thank Bill for keeping his office door wide open - our scientific and personal discussions were always truly enlightening and he always managed to be give that little ounce of encouragement when it was needed the most. I will always remember Billy Bob in the fondest ways, even though I never did get to work in his lab.

Many past and current members of the department have lent advice, support, and encouragement to me in my years as a graduate student. I would especially like to thank Gillian Shaw, who helped me tremendously in my early years in the lab, while I was a 'green' scientist and for her continued support and friendship during my stay in the lab. To Brittan Pasloske, for his active interest in my research throughout the years and for his generous hospitality whenever I have visited him in Palo Alto. To Dave Stuart, who was instrumental in my decision to complete a Ph. D. in this department - thanks for the confidence in my abilities. To Douglas Hogue, for his helpful suggestions in the world of membrane proteins and along with Calla Shank-Hogue, their wonderful conversation and company at all our delectable dinner parties. To Cheryl Helgason, for her weekly reminder that time must be spent outside the lab. I would also like to thank Darrin Bailey, for his thoughtfulness and consideration during the 'rough' times. To Mae Wylie, for her expert editorial assistance and also for lending an ear and some cheer. I wish them continued success in all of their lives.

I would like to thank Richard Cammack for introducing me to the artistry of EPR, and for his hospitality while visiting King's College in London in April 1992. His comments and suggestions were always appreciated. To Richard Rothery for his assistance with my EPR studies here in the department. To Russell Bishop, for showing me that within science there is not just a great deal of frustration but also a great degree of luck. I would also like to thank the many and varied people who were members of the lab, for the scientific discussions at our weekly group meetings and for their contribution to the way I perceive science and the scientific community.

I am grateful to the Alberta Heritage Foundation for Medical Research, the Medical Research Council of Canada, the Province of Alberta and the Department of

Biochemistry for financial support.

I would like to offer a special thank you to Andrea Opgenorth who understands me better than I understand myself at times and for her calming influence she has had on me in times of stress. Thanks so much for knowing when a celebration was in order.

Finally, and most of all, I would like to thank the members of my family, especially my parents, for their moral and financial support over the years . My career change may have not been totally understood, but their never ending love and support has always been the cornerstone of my life. I am sincerely grateful to them for allowing me to develop and grow as I have.

TABLE OF CONTENTS

	Page
CHAPTER 1: INTRODUCTION	1
A. Energy Coupling / Chemiosmotic Theory	1
B. F_0-F_1 ATPase	3
C. Components and Pathways for Electron Transport in *E. coli*	5
1. Aerobic Growth	6
a) Components	6
b) Coupling Sites of the Aerobic Chain	7
2. Anaerobic Growth	8
a) Regulation	9
1. FNR Regulation	10
2. The ArcAB System	11
3. Nitrate Regulation	12
b) Components of the Anaerobic Chain	12
1. Primary Dehydrogenases	12
a. Formate Hydrogenlyase System	12
b. D-lactate Dehydrogenase	13
c. NADH Dehydrogenase	14
d. Other Dehydrogenases	15
2. Terminal Reductases of the Anaerobic Pathway	15
a. Nitrate Reductase [*narGHJI*]	15
b. Trimethylamine N-oxide Reductase [*torA*]	15
c. Dimethyl Sulfoxide Reductase [*dmsABC*]	16
d. Fumarate Reductase [*frdABCD*]	16
D. Glycerol Metabolism	18
1. Regulation of the *glp* genes	19
2. The Proteins	21
a) The Repressor, GlpR	21
b) The Glycerol Facilitator, GlpF	21
c) The G3P Transporter, GlpT	22
d) Aerobic Glycerol-3-phosphate Dehydrogenase [*glpD*]	22
e) Anaerobic Glycerol-3-phosphate Dehydrogenase [*glpACB*]	24

E. Iron-Sulfur Proteins 26
1. General Types of Iron Sulfur Clusters 26
a) [4Fe-4S] Clusters 27
b) [3Fe-4S] Clusters 28
c) [2Fe-2S] Clusters 28
2. Electron Paramagnetic Resonance (EPR) Spectroscopy 29
3. Oxidation - Reduction Potentiometry 32
F. Membrane Proteins 33
G. Thesis Objective 35

CHAPTER II. MATERIALS AND METHODS 46

A. Materials 46
1. Chemicals 46
2. Molecular Biology Products 46
3. Bacterial Strains 47
4. Growth Media 47
B. Methods 48
1. Molecular Genetic Procedures 48
2. Plasmid Constructions 50
a) Bacteriophage T7 Promoter Plasmids [pGLP90 Series] 50
b) Glutathione S-transferases (GST) Fusions with pGEX-3X Vector [pGLP100 Series] 51
3. Construction of Mutant Strain, MERV84 52
4. Site Directed Mutagenesis 52
5. DNA Sequence Analysis 53
6. T7 Expression Studies 53
a) Radiolabelling of Plasmid Encoded Polypeptides Using Plasmid Encoded T7 RNA Polymerase 53
b) Expression of Plasmid Encoded Polypeptides Using Chromosomally Encoded T7 RNA Polymerase 54
7. GSTGlpB Fusion Studies 55
a) Growth and Induction 55
b) Affinity Purification of the GSTGlpB Fusion Protein 55
c) Site Specific Factor X_a Proteolysis 55
8. Preparation of Purified GlpAC Dimer 56

9. General Preparation of Cellular Fractions 56
10. Subcellular Localization of GlpB 57
11. Solubilization Attempts 57
a) Membrane bound GlpB 57
b) Insoluble Aggregates or Inclusion Bodies 58
12. Chymotrypsin Digestion of GlpA 58
13. SDS-Polyacrylamide Gel Electrophoresis 59
14. Determination of Protein Concentration 59
15. Enzymatic Activity 59
a) G3P Dehydrogenase Activity 59
b) Glycerol Dehydrogenase Assay 60
16. Iron-Sulfur Protein Analysis 60
a) Non-heme Iron Determination 60
b) Non-heme Iron Stain 60
c) Acid Labile Sulfide Analysis 60
17. EPR Spectroscopy 60
a) Preparation of Samples 61
b) Preparation of Well Maintained Anaerobic Samples 61
c) Preparation of EPR Samples Poised at Defined Redox Potentials 62
d) Preparation of EPR Samples at Various pH 63
18. Electron Microscopy 63
19. Fluorescence 63

CHAPTER III. AMPLIFICATION OF THE *GLPACB* OPERON 70

A. Overexpression of *glp* Genes Using the T7 RNA Polymerase/Promoter Expression System 71
1. Identification of the *glp* gene Products 71
a) Expression of the Genes 71
b) Subcellular Localization of the Glp Polypeptides 72
c) Expression of *glpB* 73
d) Expression Using BL21(DE3) 73
2 GlpA Forms an Insoluble Aggregate 74
a) Expression of GlpA 74
b) Properties of Enriched GlpA 74

c) Solubilization of GlpA 75
3. Enzymatic Activity of Aerobically Expressed *glpACB* 76
B. Overexpression of *glp* Genes Using Anaerobic Growth Conditions 77
1. Localization of GlpB 77
2. Enzymatic Activity by Anaerobic Expression of *glpACB* 78
C. Discussion 79

CHAPTER IV. PHYSIOLOGICAL ROLE OF GLPB 98

A. Complementation Studies with MERV84 99
1. GlpB is Required for Growth 100
2. *glpX* Does Not Complement MERV84 101
B. GlpB Exhibits a Paramagnetic Center 101
1. EPR Visible Center Exhibited in the Reduced State of Whole Cells 101
2. Analysis of Membrane Fraction 103
C. G3P Reduction of GlpB 103
D. Discussion 104

CHAPTER V. ANALYSIS OF GLPB REGIONS BY GST FUSIONS 115

A. Full Length GSTGlpB [Expression of pGLP100] 116
1. Expression of GSTGlpB 116
2. Localization of GSTGlpB 116
3. Affinity Enrichment 117
4. Site-Specific Cleavage with Factor X_a 117
5. Visible Spectroscopy 118
6. EPR Spectral Analysis of GSTGlpB 118
a) EPR Signals of Whole Cells, Soluble and Particulate Fractions 119
b) Time Course of Reduction 120
c) Temperature and Microwave Power Dependence of the GSTGlpB EPR Siganl 120
d) Redox Potentiometry of the GSTGlpB 120

7. Other Studies 121
a) Activity Measurements 121
b) Nonheme Iron and Acid Labile Sulfide Determinations 122
B. The Amino Terminal GSTGlpB Truncate [Expression of pGLP101] 122
1. Characteristics of GSTGlpB' 122
2. EPR Spectral Analysis 123
3. Nonheme Iron Stain 123
C. Discussion 124
1. Characterization of Paramagnetic Center 125
2. Determination of Cluster - Analytical Quantitation 128
3. Structural Considerations of the GSTGlpB Fusion Protein 129
4. The N terminal Region Appears to Hold the Paramagnetic Center of GlpB 130

CHAPTER VI. CHARACTERIZATION OF THE GLPB PARAMAGNETIC CENTER 152

A. Visible Spectroscopy 153
B. EPR Spectra of Anaerobically Maintained JM83/pGLP1 154
C. Temperature Dependence of Reduced Spectra 156
D. Power Saturation Behavior of JM83/pGLP1 Reduced Signal 157
E. Redox Potentiometry of the GlpB Cluster 158
1. Aerobically Prepared Cell Suspensions 158
2. Anaerobically Prepared Cell Suspension at pH 7.0 158
3. Anaerobically Prepared Cell Suspension at pH 9.0 159
F. Effects of Other Variables on the Signal 160
1. pH 160
2. Treatment with Denaturants 160
3. Treatment with O-Phenanthroline 161
4. Treatment with 80 % DMSO 161
G. Effect of Oligonucleotide Site-Directed Mutagenesis on the GlpB Signal 162
1. Expression of the Mutant GlpB Polypeptides 162
2. Visible Absorption Spectroscopy 163

3. EPR Spectroscopy 163
H. Spin Quantitation 164
I. Discussion 165
1. Presence of an Iron-Sulfur Center 166
2. Oxidation - Reduction Potentiometry 170
3. Temperature Dependence and Power Saturation Behavior 172
4. Environmental Effects on the GlpB [2Fe-2S] Cluster 173

CHAPTER VII. CONCLUDING REMARKS 214

A. Summary 214
B. Future Directions 217
1. Mode of Membrane Binding of GlpB 218
2. Interaction of GlpAC with GlpB 219
3. Electron Transfer Porperties of GlpB 220
a) [Fe-S] Cluster Coordination 220
b) Quinone Binding to GlpB 221
c) Role of Histidines 222
d) Role of the Carboxy Terminal Cys Motif 222
4. Studies with GlpAC 223

BIBLIOGRAPHY 225

LIST OF TABLES

		Page
Table 1	*Escherichia coli* Strains Utilized	63
Table 2	Plasmids and Phage Utilized	64
Table 3	List of Oligonucleotide Primers	68
Table 4	G3P Dehydrogenase Activity from T7 Promoter During Aerobic Expression	92
Table 5	G3P Dehydrogenase Activity from *glp* Promoter During Anaerobic Expression	97

LIST OF FIGURES

		Page
Figure 1	A Schematic of the Chemiosmotic Systems in *E. coli*	38
Figure 2	Regulatory Scheme for Control of the Aerobic and Anaerobic Pathway Operons in *E. coli*	39
Figure 3	A Schematic of Metabolism of Glycerol in *E. coli*	40
Figure 4	The Amino Acid Sequence of GlpB	41
Figure 5	Schematic of the Folding Pattern of Iron-Sulfur Centers	42
Figure 6	A Schematic of EPR Spectra of a Paramagnet with Anisotropic g	43
Figure 7	A Schematic Representation of the Construction of the T7 Expression Plasmids [pGLP90 Series]	65
Figure 8	Construction of GST Fusion Plasmids [pGLP100 Series]	69
Figure 9	Autoradiogram of [^{35}S]-Methionine Labelling of *glpACB* Genes in *E. coli* Strains K38 and JM83	84
Figure 10	Autoradiogram of the Cytoplasmic and Particulate Fractions of [^{35}S]-Methionine Labelled Cells	86
Figure 11	Electron Micrographs of JM83 Cells Overexpressing GlpA	88
Figure 12	Analysis of GlpA Inclusion Body Preparation	90
Figure 13	Membrane Association of GlpB	93
Figure 14	Solubilization of GlpB from the Cytoplasmic Membrane by Detergents	95
Figure 15	Complementation of MERV84 with *glp* Genes	108
Figure 16	*glpX* Does Not Complement MERV84	109
Figure 17	EPR Spectra of the Paramagnetic Center of JM83/pGLP1 at 20 K	110
Figure 18	EPR Spectra of Whole Cells at 20 K of GlpACB in MI1443 [*frdABCD*-]	112
Figure 19	EPR Spectra at 20 K of Yamato Inner Membranes of JM83/pGLP1	113
Figure 20	EPR Spectra at 20 K of Whole Cells Incubated with Physiological Substrates	114

Figure 21	A Schematic Highlighting Interesting Residues or Regions of GlpB	133
Figure 22	Electrophoretic Gels of Expression, Localization and Affinity Enrichment of GSTGlpB from BNN103	134
Figure 23	The Visible Absorption Spectra of GSTGlpB and GSTGlpB'	137
Figure 24	EPR Spectra of Enriched GSTGlpB Fusion Protein.	139
Figure 25	Effect of pH and Methyl Viologen on the Reduced EPR Spectra of GSTGlpB	142
Figure 26	EPR Signals of the Various Cellular Fractions of BNN103/pGLP100	143
Figure 27	Time Course Study of Reduction with Purified GSTGlpB	144
Figure 28	Temperature Dependence of GSTGlpB Purified Fusion Protein	145
Figure 29	Microwave Power Saturation Behaviour of Purified GSTGlpB	146
Figure 30	Estimation of Midpoint Potential of GSTGlpB Redox Species	148
Figure 31	Representative Spectra of GSTGlpB During Redox Titration at pH 9.0	149
Figure 32	EPR Spectra of Purified Truncated GSTGlpB'	151
Figure 33	Visible Absorption Spectra of JM83/pGLP1 Whole Cells	178
Figure 34	Wide Band EPR Spectra at 5 K of Anaerobically Handled JM83/pGLP1 Whole Cells	181
Figure 35	A Narrow Band EPR Spectrum at 20 K of Anaerobically Handled JM83/pGLP1 Whole Cells	183
Figure 36	EPR Spectra at 20 K of Intact and Anaerobically Lysed Cells	184
Figure 37	EPR Spectra at 20 K of Anaerobically Handled Intact Cells Reduced with G3P	185
Figure 38	EPR Spectra of Anaerobically Prepared JM83/pGLP1 Whole Cells at 20 dB	186
Figure 39	Temperature Dependence of the Signal Amplitude in JM83/pGLP1 Intact Cells	187

Figure 40	Representative EPR Spectra of Anaerobically Prepared JM83/pGLP1 Whole Cells at 20 K With Varying Power Levels	189
Figure 41	Microwave Power Saturation Behaviour of JM83/pGLP1 Intact Cells	191
Figure 42	Temperature Dependence of Power Saturation at Half Saturation	193
Figure 43	Representative Spectra of JM83/pGLP1 Anaerobically Lysed Cell Suspension During Redox Titration at pH 7.0	194
Figure 44	Estimation of Midpoint Potential of JM83/pGLP1 Signal	196
Figure 45	A Wide Band EPR Spectrum at 5K of a JM83/pGLP1 Lysed Cell Suspension Sample Poised at - 425 mV	197
Figure 46	Representative EPR SPectra of JM83/pGLP1 Anaerobically Lysed Cell Suspension During Redox Titration at pH 9.0	199
Figure 47	Estimation of Midpoint Potential of JM83/pGLP1 Signal at pH 9.0	201
Figure 48	pH Effects on EPR Spectra of JM83/pGLP1 Whole Cells	203
Figure 49	Effect of Denaturants on JM83/pGLP1 Lysed Cells	205
Figure 50	Effect of the Iron Chelator o-Phenanthroline on JM83/pGLP1 Lysed Cells	206
Figure 51	EPR Spectrum of JM83/pGLP1 Whole Cells Resuspended in 80 % DMSO	207
Figure 52	Yamato Inner Membanes of JM83/pGLP90C12S and JM83/pGLP90C59S	208
Figure 53	The Visible Absorption Spectrum of JM83/C12S and JM83/C59S Mutants	210
Figure 54	EPR Spectra at 20 K of C12S and C59S Mutants	211
Figure 55	Representative EPR Spectra of a Redox Titration of JM83/pGLP90C12S Anaerobically Lysed Cell Suspension at pH 7.0	212

LIST OF SYMBOLS AND ABBREVIATIONS

ADP	adenosine-5'-diphosphate
Ap	ampicillin
ATP	adenosine-5'-triphosphate
CHAPS	3-[(3-Cholamidopropyl)-dimethylammonio]-1-propane-sulfonate
CHES	2,[N-cyclohexylamino]ethane sulfonic acid
Cm	chloramphenicol
CO	carbon monoxide
CO_2	carbon dioxide
COL	cholate
CTAB	cetyl-trimethyl ammonium bromide
Cys, cys	cysteine
C12S	cysteine to serine substitution at residue 12
C59S	cysteine to serine substitution at residue 59
cyt	cytochrome
DDAPS	N-dodecyl-N,N-dimethyl-3-ammonio-1-propane-sulfonate
DH	dehydrogenase
DHA	dihydroxyacetone
DHAP	dihydroxyacetone phosphate
DMN	2,3-dimethyl-1,4-naphthoquinone
DMSO	dimethyl sulfoxide
DNAse	deoxyribonuclease
DOC	deoxycholate
DTT	dithithreitol
EDTA	Ethylene diamine tetraacetate
EPPS	N-[2-Hydroxyethyl]piperazine-N'-[3-propanesulfonic acid
EPR	electron paramagnetic resonance
ETC	electron transport chain
F_0	membrane domain of the ATP synthase

F_1	catalytic domain of the ATP synthase
FAD	Flavin adenine dinucleotide
Fd	ferredoxin
Fe-S	non-heme iron and acid labile sulfur
FMN	flavin mononucleotide
FNR	Fumarate nitrate regulator
FRD	fumarate reductase
G/F	glycerol/fumarate
G3P	glycerol-3-phosphate
G3PDH	Glycerol-3-phosphate dehydrogenase
GLP	G3P dehydrogenase
Gly	glycine
GST	glutathione S-transferase
GSTGlpB	glutathione S-transferase;GlpB protein fusion
GTP	guanosine-5'-triphosphate
$HCOO^-$	formate
HCO_3^-	bicarbonate
HOQNO	2-n-heptyl-4-hydroxyquinoline N-oxide
IHF	intergration host factor
IPTG	isopropyl β-D-thiogalactopyranoside
kbp	kilo-basepair
kDa	kilo-Dalton
K_m	Michaelis constant
Kn	kanamycin
LB	Luria broth
LDH	lactate dehydrogenase
LSB	Laemmli solubilization buffer
MK	menaquinone
MOPS	3-[N-Morpholino]propanesulfonic acid
MTT	3(4,5-dimethylthiazolyl-2)-2,5-diphenyl tetrazolium bromide
mV	millivolt

NaPi	sodium phosphate
NADH/NAD^+	nicotinamide adenine dinucleotide
ND	Not detectable
NDH	NADH dehydrogenase
NH_4OH	ammonium hydroxide
NMR	nuclear magnetic resonance
NO_2^-	nitrite
NO_3^-	nitrate
ORF	open reading frame
P_i	inorganic phosphate
PAGE	polyacrylamide gel electrophoresis
PBS	phosphate buffered saline
PCMPS	p-chloromercuriphenylsulphonate
PCR	polymerase chain reaction
P/F	peptone/fumarate
pmf	proton motive force
PMS	phenazine merthosulphate
PMSF	phenylmethylsulfonyl flouride
Pro	proline
RNAse	ribonuclease
SDS	sodium dodecyl dulfate
Ser	serine
TAE	Tris-acetate-EDTA
TBE	Tris-borate-EDTA
TCA	trichloroacetic acid
TEMED	tetramethylethlylenediamine
Tet	tetracycline
TMAO	trimethylamine N-oxide
UHNQ	3-undecyl-2-hydroxy-1,4-napthoquinone
UQ	ubiquinone

$A_{ox,\ red}$	redox species oxidized, reduced
b	inhomogeneity parameter
B_o	appplied static magnetic field, guass or mT
E	energy state
E_m	redox midpoint potential, mV
e^-	electron
F	Faraday's constant
g	EPR variable to designate features of spectra
h	Plank's constant
H^+	proton
n	number of electrons transferred [Nernst equation]
P	microwave power, mW
$P_{1/2}$	power at half saturation, mW
Δp	proton motive force
ΔpH	transmembrane pH difference
R	Universal gas constant
S	signal height or amplitude [EPR spectrum]
T	temperature, K
T_1	spin-lattice relaxation time
T_2	spin-spin relaxation time
ϕ	bacteriophage ϕ
λ	bacteriophage λ
ν	microwave frequency, Ghz
μ_B	Bohr magnetron constant
$\Delta\psi$	membrane potential
Z	conversion factor [Equation 2]

CHAPTER I. INTRODUCTION

The facultative anaerobic bacterium, *Escherichia coli*, is capable of growing by aerobic or anaerobic electron transfer [respiration] as well as fermentation. This bacterium has long been considered to be a dominant organism of the human large intestine - populations establishing themselves shortly after birth and persisting to death. Although *E. coli* has the ability to utilize oxygen as a terminal electron acceptor, which may give it an ecological advantage over strict anaerobes within the gut (Savage *et al.*, 1977), its persistence in the gut reflects its efficiency in growth during anaerobic conditions. Bacterial anaerobic electron transport is considered one of the simplest bioenergetic processes and thus has been extensively studied by microbiological, biochemical and biophysical means.

This introduction highlights the various concepts which underlie the experimental work presented in this thesis. Although most areas will be briefly touched upon, it is by no means an exhaustive review of the literature nor of the theories and the experimental evidence to date. However, whenever possible, comprehensive reviews in each of the subject areas will be referenced. I have organized the introduction with general principles discussed first, narrowing to the specific system on which I have concentrated my efforts in the last years of study, namely the inducible anaerobic Glycerol-3-phosphate dehydrogenase [*glpACB*] in *E. coli*.

A. Energy Coupling / Chemiosmotic Theory

Living cells require energy to drive the diverse functions within the cell and for building of its structural components. Whether the energy comes from light [photosynthesis] or from the oxidation of organic compounds [respiration], most of the energy is used in the manufacture of adenosine triphosphate (ATP), which is considered the cell's currency. The conversion of electron flow to biological work requires molecular transducers. Bacteria, as well as mitochondria and chloroplasts, possess specialized membranes which house the components of the energy-transducing machinery. Energy transduction in bacteria is associated with the cytoplasmic membrane and the machinery couples the electron flow from the oxidation of substrates to the production of a transmembrane pH difference accomplishing osmotic and electrical work. Potential energy is stored within the proton gradient thus formed.

The electron transport chain catalyzes the 'downhill' transfer of electrons from

substrates to final acceptors such as oxygen and results in the reoxidation of reduced coenzymes [schematically shown in Figure 1]. This transfer of electrons involves a series of oxidation - reduction reactions of membrane carrier molecules with the eventual reduction of a terminal electron acceptor. The transfer of electrons from the reduced coenzymes to the terminal electron acceptor establishes a hydrogen ion gradient across the membrane. The intermediate electron carriers of the electron transfer chain are asymmetrically distributed across the cytoplasmic membrane, and are arranged in decreasing order of their reduction potential [redox potential] which is a measure of their reductive power relative to a standard [hydrogen] electrode. The movement of hydrogen ions across the membrane as a result of electron transport establishes an electrochemical gradient. This oxidation-reduction energy of electron transfer through the respiratory chain, coupled to the outward translocation of protons across the membrane was proposed by Mitchell in 1961 (Mitchell, 1961). The diffusive counterflow of hydrogen ions back across the membranes though a proton channel established by the membrane bound ATP synthase, or ATPase, which catalyzes the synthesis of ATP from ADP + P_i, drives the synthesis of ATP. Hence the electrochemical proton gradient or protonmotive force (Δp) created by the extrusion of hydrogen ions across the membrane establishes the chemiosmotic mechanism for generating ATP. It is a means of coupling electron transport with phosphorylation, thus generating the universal energy currency of biochemical reactions.

It can be mathematically described as:

$$\Delta p = \Delta \Psi - Z \Delta \text{ pH} \qquad (1)$$

where: Δp protonmotive force or force that is generated by physically creating a proton gradient across the membrane, mVolts

$\Delta \Psi$ electrochemical component [membrane potential]

ΔpH transmembrane pH difference, due to the higher concentration of protons outside the membrane sac, and

Z factor to convert pH to electrical units and is defined by:

$$Z = 2.303\ RT/nF \qquad (2)$$

where: R Universal gas constant [1.987 cal $K^{-1}mol^{-1}$]

T temperature, K

n number of electrons transferred

F Faraday's constant [23062 cal $mol^{-1}Volt^{-1}$]

Crucial to the chemiosmotic theory as proposed by Mitchell are a number of basic requirements. First, the membrane is considered impermeable to both protons and hydroxyl ions. The maintenance of the integrity of the membrane as an intact, closed sac is essential if the proton gradient is to be maintained. Secondly, the respiratory chains are organized in 'redox loops' to allow for vectorial translocation of protons across the membrane. Thirdly, the existence of a reversible membrane spanning ATPase capable of reversibly interconverting the energy stored in the proton gradient, Δp, with the chemical energy stored in ATP, must also be present. A fourth requirement is that the other energy dependent processes such as metabolite transport and bacterial mobility should be capable of using the proton gradient directly. Other hypotheses have been proposed for the mechanism of energy transduction, namely a) chemical coupling (Slater, 1953); b) conformational coupling (Boyer, 1972); and c) localized proton pumping hypothesis (Williams, 1978). However, Mitchell's chemiosmotic hypothesis is now generally accepted (reviewed in Cramer & Knaff, 1991). Very little information is available on the biochemical mechanism of proton translocation. The efficiency of anaerobic electron transport has relied on the determination of the protons translocated per pair of electrons.

B. F_0-F_1 ATPase

In accordance with the chemiosmotic hypothesis, the membrane-bound ATPases couple the energy stored in the electrochemical gradient of protons to the chemical energy of ATP. In *E. coli*, as in other species, it is the class of F_0-F_1 ATPase which fulfills this function. The *E. coli* F_0-F_1 ATPase accounts for about 15 % of total membrane protein (Datta, 1987). This multi-subunit complex has a molecular weight of about 450 kDa and is composed of two major domains. The F_0 membrane bound domain forms a proton channel across the membrane (Fillingame *et al.*, 1983), and the F_1 extrinsic domain contains the catalytic sites for synthesis and hydrolysis of ATP (Downie *et al.*, 1979). Binding of the F_1 'head or knob' on the F_0 'stalk' blocks the proton pore of the latter domain (Futai & Kanazawa, 1983).

The assembly of the *E. coli* multimeric enzyme is reviewed in Brusilow (1993). The F_0 complex consists of three subunits [a, b, c] with the F_1 complex having five subunits [α, β, γ, δ, ε]. The stoichiometry of the complex is $ab_2c_{10}\alpha_3\beta_3\gamma\delta\varepsilon$. The

subunits are encoded by a series of nine genes in the *unc* operon. Although the assembled ATPase complex contains different numbers of each subunit, the operon contains only a single copy of each gene arranged as:

unc operon	I	B	E	F	H	A	G	D	C
Subunits	i	a_1	c_{10}	b_2	δ_1	α_3	γ_1	β_3	ε_1

The arrangement of the genes in the operon and the corresponding stoichiometry of the subunits implies the expression of the individual genes must rise and fall three times from one end of the operon to the other. The function of UncI is as yet unknown as it is not part of the final complex, but it may be involved in activation of the complex. It has been demonstrated that the F_1 subunits are not required for the functional integration of the F_0 subunits into the membrane (Aris *et al.*, 1985; Fillingame *et al.*, 1986). It is believed that the F_0 complex is synthesized in the membrane as an 'immature closed' form [proton impermeable] and then converted to its 'mature, proton-conducting' form by interaction with the F_1 subunits (Brusilow, 1993). All three of the F_0 subunits are required to create a proton channel in the phospholipid bilayer. Recent work has demonstrated a direct effect of the δ subunit on the F_0 complex which produces increased proton permeability but a direct association between δ and any of the F_0 subunits has not been demonstrated (Monticello & Brusilow, 1994).

The F_0-F_1 ATPase from bovine heart mitochondria has been purified as a 16 subunit complex (Lutter *et al.*, 1993). The mitochondrial ATPase is more complex than the bacterial enzyme with additional subunits present in the complex, namely the subunits A6L, oligomycin sensitivity conferral protein (OSCP), F_6, d and an inhibitor protein. The purification protocol utilized solubilization of the proteins from the mitochondrial membrane by the detergent dodecyl-β-D-maltoside, with a combination of ion-exchange and gel filtration chromatography and ammonium sulphate precipitation yielding a highly pure enzyme suitable for crystallization trials. Purification of the intact complex required detergents to maintain the solubility of the highly hydrophobic F_0 domain. The purified preparation retained the ATP hydrolase activity, which can be inhibited by oligomycin, and after reconstitution into phospholipid vesicles, was able to pump protons. The inhibition of hydrolytic activity by oligomycin was an indication of an intact proton channel. The F_1 domain was functionally associated with the membrane domain as the preparation retained its ATPase hydrolysis activity.

The structure of the F_1 complex from mitochondria has been determined by x-ray

crystallographic studies at 6.5 Å resolution (Abrahams *et al.*, 1993)) and by electron microscopy and image processing (Boekema *et al.*, 1986). The F_1 ATPase is approximately a spherical globule 110 Å in diameter, on a 40 Å stem which contains two α-helices in a coiled-coil. One of the α-helices extends through the entire particle from the base of the stem to the top of the roughly spherical domain. The roughly spherical particle is composed of three α and three β subunits alternating in a hexagonal arrangement around the central stem. The 'coiled-coil' stem, consisiting of the γ, δ and ε subunits, is believed to interact with the F_0 domain in the intact F_0-F_1 ATPase complex. A pit or depression next to the stem penetrates ~ 35 Å into the F_1 'αβ' domain, which may be occupied by a F_0 subunit in the intact complex (Abrahams *et al.*, 1993). The central helix provides a possible mechanism for transmission of conformational changes induced by the proton gradient from the stalk to the catalytic sites of the enzyme.

Probable functions of the various subunits in the *E. coli* F_0-F_1 ATPase have been deduced from genetic and molecular biological studies. The F_1 complex, by sequence comparison, is thought to have a total of six adenine nucleotide binding sites. Only three of these sites, corresponding to the three β subunits, show any evidence for catalyic function using ATP-γ^{32}P. The role of the other three adenine nucleotide binding sites, which may be on the α-chains or the αβ interfaces, continues to be uncertain. δ is considered as the 'interface between proton flow and ATP synthesis' (Engelbrecht & Junge, 1990) as it is necessary for binding of F_1 to F_0, whereas γ, by mutational analysis also appears to be involved in proton permeability, as it can plug the proton channel of F_0 (Brusilow, 1993).

The ATPase is responsible for coupling the proton gradient to the formation of the γ-phosphate bond of ATP, and it is capable of using either the $\Delta\Psi$ or the ΔpH component of Δp for this purpose. Either component can drive ATP synthesis only if the total driving force is about 150 mV [or ΔpH > 2.5 pH units] (Jones, 1982). During fermentation, hydrolysis of ATP, derived from substrate level phosphorylation, occurs to produce a Δp, while during oxidative growth the energy of the electrochemical potential is used to make ATP.

C. Components and Pathways for Electron Transport in *E. coli*

E. coli, like other respiratory bacteria, is able to grow aerobically and anaerobically. This is due to the presence of a variety of electron transfer chains, which are all organized in roughly the same manner, with primary dehydrogenases passing on

the reducing equivalents via the membrane bound quinone pool to the terminal electron acceptors. The electron transfer chains are composed of dehydrogenases, oxidases, flavins, quinones, iron-sulfur proteins and cytochromes, similar to those of eukaryotic mitochondria, but more diverse. Specifically, bacterial electron transport chains are usually branched or have alternative routes for electron transfer in a single cell, which allow the bacteria to respond more efficiently to their environment of changing substrates. Major changes in cellular protein composition accompany the transition from aerobiosis to anaerobiosis in *E. coli* (Smith & Neidhart, 1983a,b). The most readily observed changes are those resulting from the variance in the cytochrome content and visible absorption spectroscopy patterns prepared from cells grown in the presence of oxygen or alternative respiratory chain oxidants such as fumarate, nitrate or dimethylsulfoxide (Ingledew & Poole, 1984). The cytochromes are identified due to their distinctive visible spectra and are most readily resolved on the basis of their α-absorption bands in the 550 - 610 nm region.

1. Aerobic Growth

a) Components

A comprehensive review of aerobically induced electron transport chains in *E. coli* is given by Poole & Ingledew (1987) and Anraku & Gennis (1987) and can be summarized below:

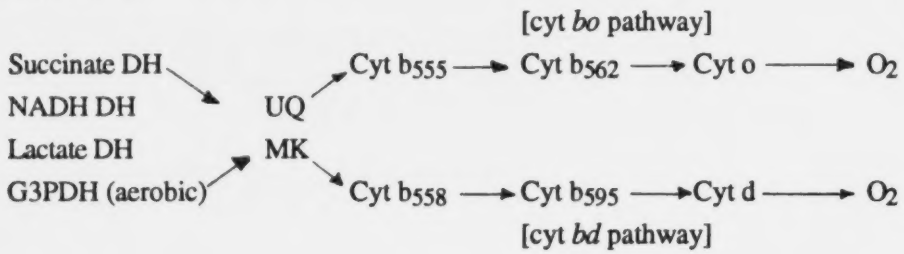

It is interesting to note the following points regarding the aerobic chains:

1) Several dehydrogenases feed into the chain. Among these are formate dehydrogenase, nicotinamide adenine dinucleotide (NADH) dehydrogenase, D [constitutive] or L [induced]-lactate dehydrogenase, glycerol-3-phosphate (G3P) dehydrogenase [aerobic], and succinate dehydrogenase. All of the dehydrogenases have

flavin adenine dinucleotide (FAD) or flavin mononucleotide (FMN) prosthetic groups (summarized in Poole & Ingledew, 1987). The presence and concentrations of the different respiratory complexes are regulated by the growth conditions and the media supplements. The series of flavoprotein dehydrogenases thus result in the oxidation of a number of substrates, namely, NADH, succinate, malate, D- and L- lactate, α-hydroxybutyrate, L-glycerol-3-phosphate, formate, dihydroorotate and pyruvate (Bragg, 1979).

2) The reducing equivalents from the dehydrogenases are passed to the membrane bound quinone pool. *E. coli* can synthesize two quinones, ubiquinone-8 (UQ) and menaquinone-8 (MK) (Polglase *et al.*, 1965) which act to carry the hydrogen atoms between the primary dehydrogenases and the terminal oxidases or reductases. Au *et al.* (1984) suggest that the location of the quinone can only be placed on the dehydrogenase side of all the cytochromes [in cytochrome *bo* or cyt *bo* pathway] as they could find no evidence for a role of the quinones elsewhere in the respiratory chain. UQ is the primary hydrogen carrier in high oxygen aeration and nitrate respiration, with a switch to MK at low O_2 tension or fumarate respiration (Poole & Ingledew, 1987).

3) There is no cytochrome c dependent branch in *E. coli* [as seen in mitochondria or *Paracoccus*].

4) *E. coli* has two terminal oxidase enzymes, known as cyt *bo* and cyt *bd*, both of which can directly oxidize the quinol. Cyt *bo* is the primary system in high aeration to early log phase growth of cells. Visible absorption spectral analysis of cytoplasmic membranes indicates the presence of cyt b_{555} and cyt b_{562}, with cyt o detected by the Soret band [410 - 420 nm] absorbance of its reduced form with bound CO relative to its reduced form in the absence of CO (Ingledew & Poole, 1984). Cyt *bo* comprises four polypeptides and contains a copper. As availability of oxygen decreases, cyt *bd* is expressed [low oxygen tension or stationary phase (Au *et al.*, 1985)]. The presence of the cyt *bd* complex can be spectrally followed by the presence of cyt b_{558} and b_{595} and two cyt d [628 nm]. The presence of the second terminal oxidase allows the Gram negative bacteria to adapt to environments where the surrounding O_2 content can vary appreciably. Neither complex is used when the bacteria are grown fermentatively.

Many of the recent studies have focused on the properties of the two aerobic terminal oxidases of *E. coli* (Puustinen *et al.*, 1991). Both oxidases, which are located in the plasma membrane, have been isolated, purified and characterized. Gennis and coworkers (Calhoun *et al.*, 1993; Thomas *et al.*, 1993) have concentrated their efforts on site-directed mutagenesis of various conserved residues in the cyt *bo* complex, in an

attempt to understand ligand binding and residues essential for conveying protons to the binuclear center. Also, they have contributed, along with other investigators, in the study of the mechanism of synthesis and assembly of the heme d component in the cyt *bd* complex (Georgiou *et al.*, 1988). In addition to the two genes *cydA* and *cydB* which encode the constituent subunits of the cyt *bd* complex, *cydC* and *cydD*, encode proteins which show homology to the ABC membrane transporters (Higgins, 1992) and are essential for the formation of the cyt *bd* ubiquinol complex (Poole *et al.*, 1993).

5) *E. coli*, when reduced, also exhibits a visible absorption spectral band lying between 585 and 596 nm, which is similar to a *Acetobacter* sp. cyt a_1 band (Poole & Ingledew, 1987). No clear function for the a_1-like pigment has as yet been determined, but speculation exists that it may be able to interact with cyt *bd* to form a terminal oxidase. It is proposed to aid in the removal of peroxide that may be generated by the primary reaction of cyt *bd* with O_2 (Ingledew & Saraste, 1979)].

b) Coupling Sites of the Aerobic Chain

The aerobic electron transport chain appears to consist of two energy conserving sites, a low potential site associated with the NADH dehydrogenase and a high potential site associated with each of the terminal oxidase complexes. Studies have indicated that the NADH dehydrogenase region of the aerobic respiratory chain contains a coupling site [site 1] (Poole & Ingledew, 1987). In aerobically grown cells, an H^+/O ratio of 4 for respiration-driven proton translocation for malate oxidation has been reported, in contrast with a value of 2 for each of succinate, D-lactate, and DL-glycerol-3-phosphate oxidation. These results strongly suggest a proton-translocating site associated with NADH dehydrogenase (Lawford & Haddock, 1973). In some cases, the ratio drops to two for NADH dehydrogenase, as reported in the case of sulfate limitation (Poole & Haddock, 1975), indicative of the loss of the coupling site.

For the latter portion of the chain, the presence of a coupling site is considered to pertain to each of the cyt *bd* and cyt *bo* pathways. The H^+/O ratio for the terminal segment of the electron transport chain has been reported to be an integer of two. Brice *et al.* (1974) examined the stoichiometries at various growth conditions, namely early-logarithmic [cyt *bo* predominant] phase and O_2 limited [cyt *bd* predominant] cells and found that the ratios were almost the same. The H^+/O ratio indicates that the oxidases function as a conventional proton translocation loop with the quinone as the H^+ carrier, being reduced on the cytoplasmic side of the membrane, with reoxidation of the quinol

on the periplasmic side of the membrane by an electron carrier with 2 H^+ being released. The electrons are then transferred to oxygen and the scalar oxidase protons are consumed on the cytoplasmic side of the membrane (Anraku & Gennis, 1987). Purification of complexes containing either cyt *bo* or cyt *bd* (Kita *et al.*, 1984a,b) have supported the assignment of an energy coupling site in each of the cyt *bd* and cyt *bo* pathways of the chain. Although the 'scalar' mechanism of proton translocation is sufficient to account for the ratio of one H^+/e^-, studies of the cyt *bo* oxidase in spheroplasts yielded a ratio of $2H^+/e^-$ (Puustinen *et al.*, 1991). This indicated that cyt *bo* functions as a proton pump in addition to separating charges of quinol oxidation [$2H^+/e^-$], whereas cyt *bd* only catalyzes the separation of the protons and electrons of ubiquinol oxidation [$1H^+/e^-$]. To date though, proton pumping has not been demonstrated in reconstituted proteoliposomes with the cyt *bo* complex. The failure of the reconstituted system to act as a vectorial pump has been suggested to be due to the loss of the subunit E which although is not essential for oxidase turnover, is essential for the assembly of the functional oxidase (Hosler *et al.*, 1993).

2. Anaerobic Growth

E. coli is able to grow on a number of substrates during anaerobic growth. Just as various routes are available during aerobic growth, there is a diverse series of electron transport chains which are induced during anaerobic growth. Lin & Kuritzkes (1987) provide a detailed summary of the various components of the anaerobic electron transport chains. For each of the substrates [i.e. H_2, formate, NAD, glycerol-3-phosphate and lactate] a primary dehydrogenase exists, and upon oxidation of the substrate, passes on the reducing equivalents to the terminal electron acceptor via the quinone pool. Instead of oxygen as the terminal electron acceptor, *E. coli* can use nitrate [+ 420 mV], fumarate [+ 30 mV], trimethylamine N-oxide (TMAO) [+ 130 mV], dimethyl sulfoxide (DMSO) [+ 160 mV] (Cole *et al.*, 1985) and other poorly characterized acceptors. The potential free energy available from the reduction of the alternative respiratory substrate can be correlated with the synthesis of the alternative respiratory enzymes, with a hierarchy for substrate use as follows: oxygen > nitrate > DMSO > TMAO > fumarate. When several electron acceptors are present, the choice of terminal oxidant is the one for which the most energetically favorable acceptor is present (Lin & Kuritzkes, 1987; Gunsalus, 1992).

a) Regulation

E. coli employs the electron donor-acceptor couple which yields the most energy and there is a tight regulation and coordination of the expression of the respiratory pathway genes. The primary level of regulation is in response to anaerobiosis with further regulation in response to nitrate availability. The regulatory control scheme of the aerobic and anaerobic respiratory operons in *E. coli* is shown in Figure 2, adapted from reviews by Gunsalus (1992) and Iuchi & Lin (1991). There are three global regulators which provide the indicated negative and positive transcriptional control to coordinate enzyme synthesis:

1. The anaerobic switch mechanism [FNR regulation]
2. The second level of aerobic-anaerobic control [ArcAB system]
3. The availability of nitrate [NarX, NarL, and NarQ regulatory system]

During aerobic growth, the predominant pathway expressed [during high aeration] is the cyt *bo* oxidase complex or *cyoABCDE* operon. With decreasing oxygen availability, the cyt *bd* oxidase complex or *cydAB* operon is expressed. The affinity for oxygen of cyt *bo* oxidase is lower than that of cyt *bd* oxidase [K_m = 1.4 to 2.9 μM versus K_m = 0.23 to 0.38 μM, respectively] (Poole & Ingledew, 1987). A threefold elevation in the level of the *cydAB* expression is observed when oxygen is absent suggestive that the cell remains poised and ready to scavenge oxygen as it may be encountered in the environment (Gunsalus, 1992). Furthermore, the levels of expression of the anaerobic terminal electron acceptors are elevated upon a shift to oxygen-free conditions [nitrate reductase, *narGHJI*, 25-fold; dimethyl sulfoxide reductase, *dmsABC*, 65-fold; fumarate reductase, *frdABCD*, 10 fold] (Stewart, 1982; Spiro & Guest, 1990; Cotter & Gunsalus, 1989; Jones & Gunsalus, 1987).

1. FNR Regulation

The primary level of regulation is the anaerobic switch mechanism, regulated by the FNR [fumarate-nitrate-regulator] protein. In the absence of oxygen, FNR not only activates synthesis of anaerobic respiratory enzymes [i.e. glycerol-3-phosphate dehydrogenase, *glpACB*; *frdABCD*; *dmsABC*; and *narGHJI*], but also represses synthesis of some of the aerobic respiratory enzymes like the cyt *bo* and cyt *bd* terminal oxidase complexes (Spiro & Guest, 1990). FNR is structurally related in its proposed DNA binding region to a number of transcription factors, including the cyclic-AMP

receptor protein, CRP, which controls catabolite repression in *E. coli* (Shaw *et al.*, 1983). It stimulates transcription at target promoters by binding to a 22-base pair (bp) repeat sequence, which has been identified by comparison of a number of FNR regulated genes: 5'-aaatTTGATatatAATCAAattt-3' (Eiglmeier *et al.*, 1989). *In vitro* DNA-footprinting experiments have shown that purified FNR (Trageser *et al.*, 1990; Green *et al.*, 1991)] binds specifically to the consensus target site and spans a region of DNA requiring a FNR dimer (Green *et al.*, 1991). As *fnr* is constitutively expressed, and neither DNA-binding nor transcriptional activation by purified FNR is dependent on oxygen deprivation *in vitro* (Sharrocks *et al.*, 1991) it is uncertain how it senses the oxygen level and binds to the promoter region to initiate RNA polymerase transcription. Lazazzera *et al.* (1993) using studies with constitutively active FNR* mutants and dominant negative mutants, which inhibit the activity of wild type FNR, have suggested that under anaerobic conditions FNR is a dimer that is active for binding, and under aerobic conditions, it is inactivated by conversion to a monomer. Bell & Busby (1994) recently identified a location of an activating region in FNR, by describing a number of mutations that cause defects in transcriptional activation without preventing DNA binding. As none of the substitutions totally abolished FNR-dependent transcription, they proposed there may be more than one activating region. The physiological factor that regulates FNR in response to oxygen deprivation is unclear, although it has been suggested that Fe^{2+} is required for FNR activity *in vivo* (Spiro *et al.*, 1989) and has also been shown to bind to FNR (Green *et al.*, 1991). The mechanism remains to be resolved.

2. The ArcAB System

A second level of regulation in response to anaerobiosis is the ArcAB system, which, during oxygen deprivation, mediates expression of aerobically induced electron transfer proteins (Iuchi & Lin, 1988; Iuchi *et al.*, 1989). The ArcAB proteins make up another two component regulatory system with ArcB functioning as the "sensor-transmitter" (Iuchi *et al.*, 1990a) and ArcA as the "receiver-regulator" to mediate transcriptional control of the *cyoABCDE, cydAB* operons and other operons encoding enzymes involved in aerobic respiratory pathways. Two component systems generally allow rapid adaptation to environmental change and so ArcA activation may prepare the cell for new conditions in response to the change in the cellular redox state. ArcA represses *cyoABCDE* expression by 1/70 (Cotter & Gunsalus, 1992). Interestingly, ArcA activates *cyd* expression by 3-fold aerobically and 12-fold anaerobically (Cotter &

Gunsalus, 1992; Iuchi *et al.*, 1990b). As well, FNR and ArcA appear to mediate control of the *cyoABCDE* genes independent of one another, but FNR control of *cydAB* expression is dependent on active ArcA protein (Cotter & Gunsalus, 1992). These results were recently confirmed by Compan & Touati (1994) who demonstrated that FNR exerts no control in a Δ*arcA* background. Using *arcA-lac* transcriptional and translational fusions, they showed that *arcA* expression increases about fourfold in anaerobiosis and that both FNR and ArcA are required for full expression. These investigators also identified the upstream regulatory region of *arcA* which revealed that transcription occurs in aerobiosis from three constitutive upstream promoters, and during anaerobiosis, an FNR-dependent transcript is present.

The block in the expression of genes involved in aerobic metabolism [i.e. aerobic glycerol-3-phosphate dehydrogenase (*glpD*)] by ArcA repression, may become complete only with FNR-dependent induction of anaerobic functions [i.e. *glpACB*]. It thus appears that FNR activation of *arcA* transcription may play an important role in the coordination of expression of genes associated with aerobic and anaerobic metabolism during environmental changes (Compan & Touati, 1994).

3. Nitrate Regulation

The energetically most favorable anaerobic respiratory pathway utilizes formate (HCO_2^-) as an electron donor for nitrate (NO_3^-) reduction (Stewart, 1993). It has been found that better electron acceptors repress the expression of enzymes for less favorable substrates. From the hierarchy, nitrate is better than fumarate and hence blocks the expression of fumarate reductase but not TMAO reductase (Pascal *et al.*, 1984). As well, the expression of the *narGHJI* operon is elevated ten-fold in response to nitrate availability. This process involves a two component regulatory system [NarLX] which is part of a family of response regulators to environmental conditions (Stock *et al.*, 1990). NarL (Gunsalus *et al.*, 1989) functions as a response regulator that binds DNA, while NarX is a membrane bound sensor-transmitter for detecting nitrate availability (Nohno *et al.*, 1989; Stewart *et al.*, 1989). The integration host factor (IHF) greatly stimulates nitrate induction of the target operons, by bringing the NarL protein into the proximity of the promoter for transcriptional activation (Rabin *et al.*, 1992; Schroder *et al.*, 1993). An additional gene, *narQ*, has been identified and analysis of mutants reveals that NarQ can sense and respond to nitrate availability, and requires NarL to effect nitrate-dependent transcription (Chiang *et al.*, 1992). Rabin & Stewart (1993) recently identified a second response regulator, *narP*, encoding a 22 kDa protein that is highly

similar in both sequence and organization to the NarL protein. It is interesting to note that the regulation by the NarX, NarQ and NarL system has no direct effect on the expression of the aerobic *cyoABCDE* and *cydAB* operons (Cotter & Gunsalus, 1992). A review of nitrate regulation of anaerobic respiratory gene expression in *E. coli* is given by Stewart (1993).

b) Components of the Anaerobic Chain

1. Primary Dehydrogenases

a. Formate Hydrogenlyase System

The formate hydrogenlyase system is induced by formate and repressed by anaerobic growth with nitrate or during aerobic growth (Lin & Kuritzkes, 1987). When no endogenous substrate is present, the induction of the system is dependent upon the presence of pyruvate formate lyase [which is dependent upon positive induction by FNR]. The complex is composed of a formate dehydrogenase [FDH_H] and a hydrogenase, catalyzing the following reaction:

$$HCOO^- + H^+ \xrightarrow[FDH_H + \text{hydrogenase}]{} CO_2 + H_2 \qquad (3)$$

The formate induced enzyme does not couple to the electron transport chain, but does remove one proton from the cytoplasm in the scalar reaction defined above.

The dehydrogenase, encoded by *fdhF* is an 80 kDa protein and requires selenium and molybdate for activity. As with most enzymes requiring molybdate, chlorate resistance mutations affect the synthesis, assembly or attachment of the Mo cofactor, thus abolishing FDH_H activity. A high concentration of formate reverses the repression of nitrate but not repression due to aerobic growth.

The hydrogenase is specifically induced by formate and does not show a strong dependence for activation by FNR. It is, however, like the dehydrogenase, repressed by aerobic growth, as well as nitrate or some other high redox potential environment. The hydrogenase component of the formate hydrogenlyase complex accounts for > 90 % of the hydrogenase activity in *E. coli* grown anaerobically. The enzyme appears to require both Ni and Fe for activity (Lin & Kuritzkes, 1987). A number of other isozymes have been identified by their requirement during various other growth conditions i.e. isoenzyme 2 for enhanced growth on H_2 and fumarate.

Another formate dehydrogenase, FDH_N, is associated with nitrate reduction and is distinct from FDH_H. The *fdnGHI* operon is induced by nitrate and repressed by aerobic conditions. The FDH_N complex is purified as a three protein unit containing Se, Mo cofactor, heme and a non-heme iron-sulfur subunit. Subunit A [110 kDa], a selenopolypeptide, and Subunit B [32 kDa] span the cytoplasmic membrane. Subunit C [20 kDa] is generally considered to be a *b*-type cytochrome. The synthesis or the stability of the enzyme is impaired in the absence of Mo. Contrary to the formate induced enzyme, the nitrate induced enzyme donates the hydrogen extracted from formate to the quinone pool, resulting in the extrusion of two protons per formate oxidized (Lin & Kuritzkes, 1987).

b. D-Lactate Dehydrogenase

D-Lactate dehydrogenase [D-LDH] is a flavoenzyme found on the inner surface of the cytoplasmic membrane (Futai & Tanaka, 1975). The protein is composed of 571 amino acid residues with a molecular weight of ~ 65 kDa and contains an FAD cofactor (Rule *et al.*, 1985; Futai, 1973; Kohn & Kaback, 1973). Detergent is required for isolation and purification of the enzyme, and the enzyme requires lipids or detergent for functional activity (Fung *et al.*, 1979; Kovatchev *et al.*, 1981). Despite its localization to the inner membrane, D-LDH does not appear to be an integral membrane protein as it can be eluted from membranes by washing with 0.6 M guanidine hydrochloride (Reeves *et al.*, 1973). This observation supports the analysis of the amino acid sequence, as the composition is not particularly hydrophobic and it does not appear to contain any hydrophobic structures for transmembranal association (Rule *et al.*, 1985). However, the requirement for a lipid environment suggests that the enzyme is not a peripheral membrane protein bound by electrostatic interactions. Peerson *et al.* (1990) using site-directed incorporation of 5-fluorotryptophan, probed the structure and function of the enzyme. Their results suggested that the enzyme may have a two domain structure of many cytoplasmic dehydrogenases but with the addition of a membrane-binding domain between the catalytic and cofactor domains. Recently, Sun *et al.* (1993) proposed a model for membrane association based on ^{19}F-NMR studies to investigate the structure of D-LDH and its association with the phospholipids. They were able to establish the membrane binding area of the protein to include the region between Tyr_{228} and Phe_{369}, but binding was not continuous in the region.

c. NADH Dehydrogenase

E. coli membranes contain two biochemically distinct NADH dehydrogenase activities which are also encoded by two distinct genes. The enzyme, NDH-1, encoded by the structural genes *nuoF* and *nuoM* (Calhoun & Gennis, 1993; Zambrano & Kolter, 1993) is a proton-pumping NADH:ubiquinone oxidoreductase, which contains FMN and nonheme iron. It is believed to be related to the mitochondrial complex I (Matsushita *et al.*, 1987). The second enzyme, NDH-II, encoded by *ndh* (Young *et al.*, 1981), is a single, FAD-containing polypeptide which does not participate in proton-pumping (Matsushita *et al.*, 1987). The two dehydrogenases can be further differentiated on the basis of their substrate specificity and sensitivity to inhibitors. NDH-I is able to oxidize NADH as well as reduced nicotinamide hypoxanthine dinucleotide [deamino-NADH], and is more sensitive to inhibition by myxothiazol, piericidin A and 3-undecyl-2-hydroxy-1,4-naphthoquinone (UHNQ) (Matsushita *et al.*, 1987). NDH-II utilizes only NADH and its oxidation is not coupled to the generation of an electrochemical gradient. The absence of either enzyme produces no obvious growth defect, but simultaneous mutations in both enzymes are deleterious to cell growth (Calhoun & Gennis, 1993).

d. Other Dehydrogenases

L-Lactate flavodehydrogenase also serves as an electron donor to most of the anaerobic transport chains. Its induction is dependent on the appropriate substrate and is also expressed during aerobic growth. The characteristics of this dehydrogenase are listed in Poole & Ingledew (1987).

The anaerobically induced sn-Glycerol-3-phosphate Dehydrogenase, encoded by the *glpA* locus, is the subject of this thesis and will be introduced in the upcoming section on glycerol metabolism.

2. Terminal Reductases of the Anaerobic Pathway

a. Nitrate Reductase [*narGHJI*]

Nitrate reductase is a membrane-bound complex of three subunits [2:2:4 ratio]: NarG [150 kDa], NarH [60 kDa] and NarI [20 kDa]. NarI is a hydrophobic subunit containing a b_{556}-type cytochrome which receives electrons from the quinone pool and transfers them to the iron-sulfur subunit, NarH. Nar I is also considered to act as the membrane attachment subunit(s) for the soluble NarG and NarH subunits (Blasco *et al.*, 1992). The electrons complete their path to reduction of nitrate by being delivered from

NarH to the molybdenum cofactor within NarG, where the actual reduction of nitrate [NO_3^-] to nitrite [NO_2^-] occurs. The NarJ polypeptide is not part of the final enzyme but is implicated in the activation of the NarGH complex, as it is involved in the insertion of the molybdenum cofactor (Blasco *et al.*, 1992). Much of the current research involves mutational analysis of the iron-sulfur centers within NarH, in an attempt to understand the electron pathway through the enzyme (Augier *et al.*, 1993).

b. Trimethylamine N-oxide Reductase [*torA*]

Trimethylamine N-oxide (TMAO) serves as an anaerobic electron acceptor with molecular hydrogen, NADH, formate, or lactate as donor (Lin & Kuritzkes, 1987). Proton extrusion and the generation of a membrane potential coupled to TMAO reduction has been observed in anaerobically grown *E. coli* (Takagi *et al.*, 1981). Pascal *et al.* (1984) showed that the major inducible enzyme accounts for 93 % of the total TMAO reductase activity and is coded for by the *torA* gene. TMAO is also a substrate for DMSO reductase described below. Sambasivarao & Weiner (1991) using a double mutant in *torA* and *dmsABC* showed that TorA, encoded by *torA* gene of the *torCAD* operon (Mejean *et al.*, 1994), is the only inducible TMAO reductase under physiological conditions. Mutations in *fnr* result in a dramatic loss of TMAO activity, but the synthesis of TorA is not regulated by *fnr* nor nitrate, but by induction by TMAO [with the two-component regulatory system TorST] and TorR, an anaerobic switch regulator specific for the system (Pascal *et al.*, 1991). TMAO reductase is a molybdenum cofactor containing periplasmic enzyme composed of a single subunit of 110 kDa which can exist in crude extracts as a monomer or a dimer (Yamamoto *et al.*, 1986; Silvestro *et al.*, 1988; Silvestro *et al.*, 1989). The *torB* gene product is proposed to be involved in the insertion of the molybdenum cofactor in the enzyme, while TorC and TorD encode a c-type cytochrome and a protein of unknown function, respectively (Mejean *et al.*, 1994). TorC is proposed to act as an intermediary electron carrier providing the electrons to TorA.

c. Dimethyl Sulfoxide Reductase [*dmsABC*]

E. coli is capable of growing anaerobically on DMSO as the terminal electron acceptor, with glycerol, H_2, formate and substrates which generate NADH, but apparently not by D- or L- lactate (Bilous & Weiner, 1985a,b). DMSO reductase is encoded by the *dmsABC* operon which has been cloned (Bilous & Weiner, 1988) and sequenced (Bilous *et al.*, 1988). *dmsABC* is under control of *fnr* regulation, and is

repressed by nitrate or aerobic conditions. The purified enzyme (Weiner *et al.*, 1988) consists of three polypeptides: DmsA [82 kDa], DmsB [23 kDa] and DmsC [31 kDa]. The enzyme has very broad substrate specificity and is able to reduce many S- or N-oxide compounds as well as chlorate (Weiner *et al.*, 1992). DmsA is a molybdopterin-containing enzyme, and is most likely the catalytic subunit (Weiner *et al.*, 1992). DmsB is an iron-sulfur protein, containing four [4Fe-4S] clusters. Initial characterization of the clusters was reported by Cammack & Weiner (1990), with titration of four midpoint potentials of -50, -120, -240 and -370 mV. DmsC, is a membrane bound subunit, with eight transmembranal segments (Weiner *et al.*, 1993) required for quinol oxidation and as an anchor for DmsAB. Ongoing current studies are focusing on the assignment of the iron-sulfur clusters, the molybdopterin cofactor - type and binding characteristics, as well as investigations of interaction of DmsC with the DmsA and DmsB (Weiner-personal communication).

d. Fumarate Reductase [*frdABCD*]

When *E. coli* is grown anaerobically in the presence of fumarate and the absence of nitrate, a membrane-bound fumarate reductase is induced. Under aerobic growth conditions, the *frd* operon is repressed and succinate dehydrogenase is induced (Poole & Ingledew, 1987). Although fumarate is not a strong oxidant in comparison to the other terminal electron acceptors discussed so far, it can serve as the electron sink allowing the reoxidation of NADH (Poole & Ingledew, 1987). Glycerol-3-phosphate, formate, NADH, lactate, hydrogen and dihydroorortate have been shown to act as donors in the electron transport chain coupled to fumarate (Poole & Ingledew, 1987). The use of mutants has demonstrated that menaquinone is essential for fumarate reduction (Newton *et al.*, 1971). Respiration driven proton translocation has been demonstrated in anaerobic cell suspensions and when glycerol-3-phosphate is used as substrate, a ratio of $2H^+$/dihydroxyacetone is obtained (Miki & Lin, 1975). The standard redox potentials of the glycerol-3-phosphate/dihydroxyacetone phosphate and of the fumarate/succinate couples are - 190 mV and + 30 mV respectively (Cole *et al.*, 1985).

Fumarate reductase is encoded by the *frdABCD* operon, which is under *fnr* control. *frdABCD* expression is also dependent on the level of alanine in the cell via an attenuation mechanism (Latour & Weiner, 1988). The reductase is composed of two membrane extrinsic, catalytic subunits [FrdA and FrdB] bound to the membrane by two hydrophobic anchors [FrdC and FrdD] in equimolar ratio (Cole *et al.*, 1985). The enzyme catalyzes the interconversion of fumarate and succinate, with a $K_{mFumarate}$ of

420 μM and a $K_{mSuccinate}$ of 2 mM (Dickie & Weiner, 1979; Robinson & Weiner, 1982). The enzyme activity has been purified as the tetrameric holoenzyme [FrdABCD] and as a dimer catalytic unit [FrdAB], but only the tetramer is capable of oxidizing the quinone analog 2,3-dimethylnaphthoquinone [DMN] and this activity is inhibited by another quinone analog, HOQNO (Cole *et al.*, 1985). The FrdA polypeptide, 69 kDa, contains the covalently bound flavin prosthetic group and the active site (Weiner & Dickie, 1979). The FrdA polypeptide, however, in the absence of FrdB, is soluble and nonfunctional, but still contains the flavin cofactor (Latour & Weiner, 1989). FrdB [27 kDa] is an iron-sulfur containing subunit, and the centers have been identified and characterized to be one of each of a [2Fe-2S] (center 1, - 20 mV), an [3Fe-4S] (center 3, - 70 mV) and an [4Fe-4S] (center 2, - 330 mV) clusters by electron spin resonance and magnetic circular dichroism spectroscopy (Morningstar *et al.*, 1985; Johnson *et al.*, 1985; Cammack *et al.*, 1985b). The FrdC and FrdD subunits have extremely hydrophobic amino acid compositions and are known to reside within the inner membrane (Cole *et al.*, 1985; Latour & Weiner, 1989). Both FrdC and FrdD are required for membrane association and for the oxidation of reduced quinone analogues (Condon & Weiner, 1988; Latour & Weiner, 1989). Furthermore, the separation of the DNA coding for the FrdC and FrdD polypeptides affects the ability of the fumarate reductase to assemble into a functional complex (Condon & Weiner, 1988). Recent work has focused on determination of the quinone binding domains within the membrane subunits. Westenberg *et al.* (1993) have shown that the positive charge at $FrdC_{H82}$ is required for stabilization of the quinone radical intermediate and the negative charge at $FrdC_{E239}$ for deprotonation of menaquinol.

D. Glycerol Metabolism

An overview of glycerol metabolism within *E. coli* (Lin, 1987) is shown in Figure 3. Glycerol enters the cell by facilitated transport mediated by the *glpF* gene product. Once inside the cell, glycerol is phosphorylated by an ATP-dependent kinase (*glpK*) to glycerol-3-phosphate (G3P). As the membrane is permeable to glycerol, after being actively accumulated in the cytoplasm, glycerol would be free to move down its concentration gradient out of the cell. However, by being phosphorylated, glycerol is trapped immediately within the cell. The GlpK kinase is subject to noncompetitive allosteric inhibition by fructose 1,6-biphosphate and the nonphosphorylated form of enzyme III^{Glc}, thus preventing glycerol consumption during glucose utilization (Lin,

1987). G3P can also be actively accumulated in the cell via several transport systems: 1) The *glpT* transport system (Hayashi *et al.*, 1964), is highly specific for the utilization of G3P; 2) highly specific *ugp* transport system which is part of the *pho* regulon, and hence functional in a *pho*$^-$ constitutive strain or when phosphate is limiting (Argast & Boos, 1980); 3) non specific hexose phosphate transport system (*uhp*). G3P is then oxidized to dihydroxyacetone phosphate (DHAP) by one of two dehydrogenases, *glpD* or *glpA*. *glpD*, encodes the aerobic G3P dehydrogenase and its activity is maximal under well oxygenated growth conditions. *glpA*, encodes the anaerobic G3P dehydrogenase which exhibits maximal activity during anaerobic growth with fumarate present as the electron acceptor. Anaerobiosis results in the repression of the *glpD* operon by the *arcAB* regulatory system and the FNR dependent activation of the *glpACB* operon (Iuchi *et al.*, 1990c). Under anaerobic conditions, nitrate respiration is observed to lower the expression of *glpA* by two (Iuchi *et al.*, 1990c).

In the absence of oxygen, *E. coli*, can be induced to express a simple respiratory electron transfer chain, when the growth medium is supplemented with glycerol and a terminal electron acceptor such as fumarate (Lin & Kuritzkes, 1987). Glycerol, after phosphorylation to G3P, is oxidized by the anaerobic G3P dehydrogenase to DHAP. The electrons then pass via menaquinone to a terminal electron transfer enzyme such as fumarate reductase or DMSO reductase (Cole *et al.*, 1985; Bilous & Weiner 1985a,b). DHAP is then available for further metabolism. During growth on carbon sources other than glycerol, G3P is made by direct reduction of DHAP with NADH by the G3P synthase (*gpsA*). GpsA is very sensitive to inhibition by its product, G3P, and hence acts to regulate the intracellular level of G3P (Cronan & Rock, 1987). Anaerobically, with fumarate as the exogenous hydrogen acceptor, glycerol and G3P support a doubling time of 245 and 190 min, respectively (Lin, 1976). Aerobically, glycerol is utilized faster than G3P, with the reverse true for anaerobic growth, but the growth rates reported depend upon the particular strain and the composition of the medium.

A minor secondary pathway has also been reported which bypasses the phosphorylation of glycerol to G3P. An NAD^+ linked glycerol dehydrogenase was first reported by Asnis & Brodie (1953), which oxidized glycerol to dihydroxyacetone (DHA). A multistep mutant strain 424 (*glpK*$^-$, *glpD*$^-$) was isolated in which the innate glycerol pathway described previously is replaced by a new pathway with an NAD^+ linked dehydrogenase as the first step (St. Martin *et al.*, 1977). The DHA can then be phosphorylated by the glycerol kinase, for which DHA is also a substrate (Hayashi & Lin, 1967), however with strain 424, DHA was observed to be released into the culture

medium. The synthesis of the enzyme first appeared to be constitutive, but the level of the enzyme appears to be highly dependent on the physiological state of the cell (Tang *et al.*, 1982) and is weakly expressed in the wild type strain. Recently, Truniger *et al.* (1992) identified and reported the sequence of the *glpX* gene [*glpFKX* operon], of whose function is as yet unknown. It was speculated however that *glpX* may encode for glycerol dehydrogenase (*gld*), based on its similar apparent molecular weight [40 kDa] with that previously reported [39 kDa] (Tang *et al.*, 1979). This speculation was short lived though as Truniger & Boos (1994) subsequently reported the identification and sequence of the glycerol dehydrogenase gene [*gldA*], located at 89.2 minutes [rather than 88 minutes for the *glpFKX* operon].

1. Regulation of the *glp* Genes

The genes involved in glycerol metabolism in *E. coli* are part of the *glp* regulon. These genes are arranged in five different operons positioned at three different locations on the chromosome. The *glpTQ* operon is located at the 49-minute position and is transcribed in the counterclockwise direction. The operon encodes for the glycerol-P permease, GlpT, (Eiglmeier *et al.*, 1987) and the periplasmic glycerophosphodiesterase, GlpQ (Tommassen *et al.*, 1991). The *glpACB* operon, encoding the anaerobic G3P dehydrogenase (Cole *et al.*, 1988), is directly adjacent to and transcribed divergently from the *glpTQ* operon (Ehrmann *et al.*, 1987). The first two open reading frames (ORF) of the *glpACB* operon downstream of the promoter, which were originally termed *glpA* and *glpB*, have been renamed to conform with genetic observations and are now referred to as *glpA* and *glpC*. The distal ORF, now called *glpB*, is the third open reading frame (Cole *et al.*, 1988). The *glpFKX* operon is located near 88 minutes and is transcribed counterclockwise. It encodes for the cytoplasmic membrane-associated glycerol diffusion facilitator, GlpF, (Sweet *et al.*, 1990) and the cytoplasmic kinase, GlpK (Pettigrew *et al.*, 1988). As mentioned, the function of GlpX is unknown (Truniger *et al.*, 1992). The *glpD* gene for the aerobic G3P dehydrogenase (Austin & Larson, 1991) is located near 75 minutes and is transcribed clockwise from the *glpEGR* operon. *glpE* and *glpG* encode proteins whose functions are as yet unknown (Schweizer *et al.*, 1986), but *glpR* encodes the repressor protein, which regulates the *glp* regulon.

The *glp* genes comprise a regulon because they are all negatively regulated by the specific *glpR* repressor (Freedberg & Lin, 1973; Larson *et al.*, 1987). Repression can

be relieved to differing extents, depending on the operon in the presence of G3P the inducer for the system (Lin, 1987). There are three kinds of control affecting the expression of the *glp* regulon, namely: 1) specific repression by *glpR*; 2) catabolite repression during growth in the presence of glucose; and 3) respiratory repression, with each operon showing a different pattern of response to each control (Freedberg & Lin, 1973). The order of sensitivity of the operons to control by the *glp* repressor during aerobic growth is *glpFKX* > *glpD* > *glpTQ* > *glpACB*, while during anaerobic growth the order of sensitivity is *glpFK* > *glpACB* = *glpD* > *glpTQ* (Weissenborn *et al.*, 1992). The order of sensitivity is reversed for catabolite repression (Lin, 1987). As previously mentioned, anaerobiosis causes a decreased expression of *glpD* due to its repression by the *arcAB* regulatory system and increased expression of *glpACB* due to activation by the FNR dependent mechanism (Iuchi *et al.*, 1990c). The repressor binding sites in the control region for the *glpD* operon have been identified (Ye & Larson, 1988) and as well the various operator control regions for the divergently transcribed *glpTQ-glpACB* operons (Larson *et al.*, 1992). Comparison of the sequences of the repressor-binding sites between the operons showed that the repressor binding sites are tandem repetition of the operator, suggesting cooperative binding at adjacent sites. The formulated consensus operator sequence is: 5'-(A/T)ATGTTCG(A/T)TA(A/T)CGAACAT(A/T)-3'. A region was also identified for the binding of the cAMP-CRP complex in the *glpTQ* operator region and as well two regions for *glpACB*, which coincided with the FNR binding site. This is not surprising considering that the FNR and CRP proteins recognize very similar DNA sequences (Bell & Busby, 1994). It was also suggested that *glpACB* operator(s) are involved in control of *glpTQ* expression perhaps via a formation of a repression loop. Insertion mutagenesis has shown that the distance between the operator sites is important for complete repression of the *glpTQ* and *glpACB* operons (Larson *et al.*, 1992). Recent studies (Zhao *et al.*, 1994) have investigated altered consensus operator regions *in vivo*, which showed that all base substitutions at positions 3, 4, 5, and 8 from the center of the palindromic operator caused a decrease in repressor binding. Strong cooperative binding of the repressor to tandem operators was also demonstrated, with maximal cooperativity observed when two 20 bp operators were directly repeated or when 2 bp separated the two operators. Cooperative binding to multiple operator sites may greatly increase the responsiveness to control by the repressor, as well as allowing for a flexibility from absolute sequence specificity for repressor binding.

2. The Glp Proteins

a) The Repressor, GlpR

The repressor protein, GlpR, has been purified and characterized (Larson *et al.*, 1987). The protein migrated with an apparent molecular weight of 30 kDa, as assessed by sodium dodecyl sulfate (SDS)-polyacrylamide gel electrophoresis (PAGE). The apparent size of the repressor by gel filtration under nondenaturing conditions was 130 kDa, suggesting a tetramer. Interaction of the repressor with DNA fragments confirmed its specific binding to the control regions of *glpD*, *glpK* and *glpT-A* genes, with diminished binding in the presence of the inducer G3P.

b) The Glycerol Facilitator, GlpF

The glycerol facilitator, GlpF, is the only known example in *E. coli* of a plasma membrane transporter believed to catalyze facilitated diffusion (Nikaido & Saier, Jr, 1992). A variety of small straight-chain molecules are admitted by GlpF, including compounds such as polyhydric alcohols, as well as glyceraldehyde, glycine and urea. On the other hand, 4-, 5-, and 6- carbon sugars and G3P do not have ready access through GlpF, most likely being impeded by size and charge (Heller *et al.*, 1980). The protein has an apparent molecular weight of 25 kDa as analyzed by SDS-PAGE (Sweet *et al.*, 1990). This is in relative agreement with the predicted molecular weight for the derived amino acid sequence of 29.8 kDa (Weissenborn *et al.*, 1992) and its localization within the inner membrane was confirmed by active protein fusions to periplasmic alkaline phosphatase and cytoplasmic β-galactosidase (Sweet *et al.*, 1990). From hydropathy analysis, the 281-residue GlpF is predicted to contain six transmembranal spanning regions, with homology with several eukaryotic proteins involved in solute transport (Pao *et al.*, 1991). The characterization of GlpF has been hampered by the lack of a test system in which its activity can be examined in the absence of other bacterial proteins, particularly glycerol kinase. Maurel *et al.* (1994) studied the transport of glycerol mediated by GlpF following injection of *glpF* mRNA into *Xenopus laevis* oocytes. GlpF selectively transported glycerol but not water or ions. Glycerol transport via GlpF proved to be nonsaturable up to 200 mM and exhibited a low activation energy, confirming earlier reports (Heller *et al.*, 1980) that GlpF mediates glycerol diffusion via a pore type mechanism.

c) The G3P Transporter, GlpT

GlpT is located within the inner membrane, and shows an apparent molecular weight of 44 kDa as analyzed by SDS-PAGE (Larson *et al.*, 1982). This permease is a member of a class of bacterial organophosphate permeases which transport substrates by antiport with inorganic phosphate (Ambudkar *et al.*, 1986). The transport protein has a predicted molecular weight of 50.3 kDa, but its very hydrophobic nature, with 12 predicted membrane-spanning α-helical segments, may account for its aberrant mobility in SDS-PAGE (Eiglmeier *et al.*, 1987). GlpT showed extensive homology to other transport proteins, i.e. UHPT, lactose, melibiose, citrate, arabinose, xylose and glucose transporters (Gott & Boos, 1988; Eiglmeier *et al.*, 1987). Analysis of the topology of the protein by *phoA* and *lacZ* fusions suggested a transmembrane organization consistent with the predicted model (Gott & Boos, 1988).

d) Aerobic Glycerol-3-phosphate Dehydrogenase [*glpD*]

The aerobic G3P dehydrogenase is encoded by the *glpD* gene (Austin & Larson, 1991). GlpD is maximally expressed during aerobic growth, but anaerobic repression of the *glpD* operon can be relieved by mutations either in *arcA* or *arcB* (Iuchi *et al.*, 1990c). A mutant possessing only aerobic G3PDH can grow on glycerol or G3P with nitrate or oxygen, but not fumarate. Analysis of the amino acid sequence revealed a possible transmembrane helix, from residues 6 to 32, but this region was also indicated to contain a flavin binding domain and hence considered unlikely to be involved in localization of the protein (Austin & Larson, 1991). Aerobic G3P dehydrogenase showed no apparent homology to the anaerobic enzyme [*glpACB*], except in the FAD-binding region and another region which may be the G3P binding site (Austin & Larson, 1991). The enzyme has 51 % apolar residues with few cysteines or histidines [0.8 and 2.8 %, respectively] (Schryvers, 1981). The cysteines are not clustered in any pattern typical of iron-sulfur centers [refer to Chapter I, section E]. It is believed that GlpD is similar to D-lactate dehydrogenase of *E. coli* which is overall hydrophilic but is tightly membrane associated (Poole & Ingledew, 1987).

The GlpD protein is a membrane-bound dehydrogenase localized on the internal surface of the inner membrane (Weiner, 1974). The enzyme comprises about 1% of the membrane proteins in a mutant constitutive for the enzyme. It was originally purified

after presolubilization from the membrane with 0.1 % sodium deoxycholate in 0.25 M NaCl and shown to be a dimer [~ 80 kDa] containing an FAD cofactor (Weiner & Heppel, 1972). Recent studies have suggested that the extreme amino-terminal region of GlpD is sufficient for membrane localization (Austin & Larson, 1991).

Aerobic G3PDH has been well characterized within the laboratory (Schryvers, 1981; Robinson, 1982). Modification of the original purification protocol with the addition of a hydroxylapatite chromatography step resulted in identification of the polypeptide of 58 kDa, contrary to the originally reported 35 kDa (Schryvers *et al.*, 1978). The purified protein exists as a dimer [chemical cross linking studies; (Robinson, 1982)] and was confirmed to contain a noncovalently bound flavin [FAD] which is reduced by substrate. It has an apparent K_{mG3P} of 1.1 mM and 10 mM in the purified and crude membrane preparations respectively, with maximal activity between pH 7 and 9.5 and at a temperature of 44°C. The difference in K_m is believed to be a reflection of the relative accessibility of the active site to substrate in the preparations rather than an alteration in binding properties of the enzyme (Schryvers, 1981). Removal of detergent resulted in a dramatic reduction in activity, but activity could be restored with the addition of phospholipid. This was suggestive of GlpD's proper conformation and interaction within the membrane. Despite the dependence of detergent or phospholipid for full electron transfer activity, the purified GlpD showed a temperature and pH profile similar to the membrane-bound form, indicative that the enzyme had not undergone any drastic alterations during purification. Circular dichroism studies also indicated that the detergent caused minor conformational change of the enzyme (Robinson, 1982). The purified, detergent-depleted enzyme can be reconstituted with *E. coli* membrane vesicles to support G3P-dependent active transport of L-proline. Further studies on the purified enzyme have shown that it is competitively inhibited by a number of structural analogs [i.e. $K_{I\text{-}DHAP}$ ~ 0.5 mM] and is also regulated in a complex manner by ATP or GTP. Enzyme activity is also inhibited by the addition of sulfhydryl reagents or the iron chelator, o-phenanthroline (Schryvers, 1981; Robinson, 1982).

e) Anaerobic Glycerol-3-phosphate Dehydrogenase [*glpACB*]

Anaerobic G3P dehydrogenase [*glpACB*] has been isolated and characterized as a soluble dimeric enzyme (Schryvers & Weiner, 1981). The purified enzyme is composed of subunits of 62 kDa [GlpA] and 43 kDa [GlpC] in a 1:1 ratio. The enzyme contains 1 mol of noncovalently bound FAD and 2 mol of non-heme iron per dimer. The presence

of 20 % ethylene glycol stabilized the enzyme by preventing disassociation of the subunits. Addition of exogenous flavins, both FAD and FMN, are required for maximal activity *in vitro*. The stimulation of the two flavins are independent, and hence it was suggested that the FMN is acting at an "allosteric" site distinct from the active site. The K_{mG3P} in the presence and absence of exogenous FMN was 0.339 ± 0.011 mM and 0.100 ± 0.004 mM, respectively. The purified enzyme was sensitive to sulfhydryl reagents but was not inhibited by the iron chelator 1,10-phenanthroline.

Although the purified enzyme [GlpAC] is now considered the soluble catalytic dimer, DNA sequence analysis of the operon encoding the dehydrogenase led to the finding that three open reading frames were transcribed (Cole *et al.*, 1988). It has been suggested that the third ORF or GlpB is a membrane receptor for the catalytic dimer and while some interaction of GlpAC with the membrane can be observed in GlpB containing membranes, the interaction *in vitro* is not quantitative (Kuritzkes *et al.*, 1984; Cole *et al.*, 1988). The role of this subunit in G3P dehydrogenase activity and anaerobic electron transport is the subject of this thesis. In earlier studies, GlpB was assigned to a Coomassie blue stained 44 kDa polypeptide which sedimented with the membrane fraction in broken cell preparations but there was no direct evidence to support this assignment (Cole *et al.*, 1988). The inferred amino acid sequence of GlpB [Figure 4] does not resemble a transmembranal polypeptide, as it lacks stretches of hydrophobic amino acids typical of membrane spanning regions (Cole *et al.*, 1988). It does however have a segment, amino acid residues 261-279, with a large hydrophobic moment (Eisenberg, 1984) which may form an amphipathic helix in the membrane. Calculation of the potential β-strand amphiphilicity did not reveal any regions that could be interpreted as candidates for the strands of a transmembrane β-barrel (Cole *et al.*, 1988) which are often present in porins and specific channels (Nikaido, 1992).

The amino acid sequence of GlpB encodes many interesting features which are highlighted in Figure 4. One of the key features in the sequence is the presence of two cysteine motifs which resemble the ligands of typical [4Fe-4S] clusters [described in the upcoming section on iron-sulfur proteins]. The conserved sequence Cys-X-X-Cys-X-X-Cys-X-X-X-Cys-Pro is found in the GlpB sequence at residues 9 to 20 and 56 to 67, displaying marked sequence homology to *Clostridium* type ferredoxins and other iron-sulfur proteins such as fumarate reductase and DMSO reductase of *E. coli* (Bruschi & Guerlesquin, 1988; Cammack, 1991). Secondly, two Cys-Cys-Gly motifs [C_{201}-G_{203}; C_{329}-G_{331}] are present, which have been shown to act as membrane attachment sites in rhodopsin by addition of palmitic acid (Khorana, 1992). These motifs are considered

very rare within bacteria, and as yet it is not known whether these Cys motifs play any role in the interaction of GlpB with the inner membrane. Another salient feature of the GlpB sequence is that there are a number of histidine residues in the central portion of the sequence. Histidines are of interest as they are found to interact with heme groups for binding (Degli-Esposti, 1989; Fu *et al.*, 1994) and zinc-containing metalloproteases (Hase & Finkelstein, 1993), as well as for interaction with the quionol pool within the membrane [i.e. H_{82} in FrdC] (Weiner *et al.*, 1986). The fourth interesting feature in the GlpB amino acid sequence is the presence of a motif in the C-terminal end of the polypeptide which shows some homology to a [2Fe-2S] cluster (Cammack, 1991) or a metal binding domain, again due to the presence of a number of Cys residues. Except for the highlighted motifs, GlpB does not show any sequence homology to any reported protein.

Based on these interesting features within the GlpB sequence, a number of questions arise, namely:

1. Although *glpB* is identified as a gene in the *glpACB* operon, is the gene expressed and is it required for structural and/or functional association with the GlpAC dimer in physiologic conditions?
2. If GlpB is expressed, where is it localized within the cell?
3. If it is within the membrane, how is it associated and does GlpB act as a membrane anchor for the soluble dimer?
4. Is GlpB involved in an electron transfer role?
5. Do the cysteine motifs coordinate the proposed [Fe-S] centers and what role do the many histidines play in the function of the polypeptide?

E. Iron-Sulfur Proteins

Iron-sulfur proteins are found throughout nature. There are an increasing number of proteins containing these iron-sulfur clusters which participate in a more recently defined role such as catalysis, i.e. aconitase (Kent *et al.*, 1985; Klausner *et al.*, 1993). In *E. coli* endonuclease III the [Fe-S] cluster appears to act in a strictly structural role (Kuo *et al.*, 1992). Recently, bacterial L-serine dehydratases have been shown to be a new family of enzymes containing Fe-S clusters (Grabowski *et al.*, 1993), but as these enzymes have counterpart enzymes which do not contain the prosthetic group, the function of the Fe-S center is as yet unknown. Human ferrochelatase, which catalyzes the insertion of iron into the porphyrin molecule as the terminal step in the heme

biosynthetic pathway, has also recently been shown to be an iron-sulfur protein (Dailey *et al.*, 1994). The most recent novel function of an iron-sulfur center has been reported to be essential for transcriptional activation by the redox-sensing SoxR protein in *E. coli* (Hildago & Demple, 1994). The majority of iron-sulfur proteins characterized to date (Cammack, 1991), however, are particularly found in the membrane-bound electron transfer chains of bioenergetic systems, namely the mitochondria, chloroplasts and bacteria. These clusters are known to act as secondary electron carriers, within or between redox enzyme systems. Various redox partners (Cammack, 1991) include heme, flavin, chlorophyll [plant ferredoxin], molybdenum [DMSO reductase], ubiquinone, iron, nickel, copper and an other iron-sulfur cluster [fumarate reductase]. The clusters undergo one-electron redox reactions at characteristic midpoint potentials (Cammack, 1986).

1. General Types of Iron Sulfur Clusters

The iron-sulfur proteins are distinguished from other non-heme iron proteins by the special coordination of the iron to cysteine residues of the protein and generally the presence of acid labile sulfur. Figure 5 is a schematic showing the general coordination of the clusters. High resolution X-ray crystallography of simple iron-sulfur proteins have confirmed the existence of [2Fe-2S], [3Fe-4S], and [4Fe-4S] clusters (listed in Cammack, 1991). Moura *et al.* (1992) recently reported the presence of a [6Fe-6S] cluster in *Desulfovibrio desulfuricans* but no crystal structure is available as yet. Bacterial ferredoxins (Fds) have been studied extensively and are classified according to the type of [Fe-S] cluster they bind i.e. [4Fe-4S]. They are distinguished from other non-heme iron proteins by a number of key features (Bruschi & Guerlesquin, 1988): a) their ability to transfer electrons; b) their 1:1 ratio of non-heme iron:labile sulfur; c) molecular weight around 6000 - 13000; d) general acidic amino acid composition of the polypeptide over basic residues; e) a low reduction potential [< 350 mV]; f) visible adsorption spectrum which decreases reversibly on reduction; and g) an electron paramagnetic resonance (EPR) signal in the oxidized or reduced states at low temperature characteristic of the cluster type.

a) [4Fe-4S] Clusters

The majority of the Fds share a common ancestor and evolved after gene

duplication (George *et al.*, 1985; Bruschi & Guerlesquin, 1988; Fukuyama *et al.*, 1988). The *Clostridium*-type Fds are considered the classic bacterial Fd, each consisting of two 28-residue domains. Each domain contains the conserved Cys motif: Cys-XX-Cys-XX-Cys-XXX-Cys-Pro, which again is characteristic of the *Clostridial*-type Fds. These Fds contain 2[4Fe-4S] clusters, with the cysteines acting as the ligands for the nonheme iron. The two clusters often display weak dipolar and exchange coupling between the spins, as observed with EPR spectroscopy (Mathews *et al.*, 1974). Each cluster appears to act as a single electron transfer site and has an oxidation-reduction potential of about - 400 mV (Buchanan & Arnon, 1970).

Monocluster [4Fe-4S] centers are also common, with cluster coordination as defined by the Cys motif described above. Generally, not all eight cysteines are present, with one of the clusters being replaced by an α-helix in the protein (Fukuyama *et al.*, 1988). These monoclusters have been isolated and characterized from *Bacillus polymyxa*, *Desulfovibrio gigas*, *D. desulfuricans* Norway and *D. africanus* (Bruschi & Guerlesquin, 1988). The [4Fe-4S] clusters are generally similar in reduction potential to those in the 2[4Fe-4S] Fds, but the observed EPR spectra are more simplified by the absence of magnetic interaction associated with the loss of one cluster.

b) [3Fe-4S] Clusters

The formation of a [3Fe-4S] center usually involves cluster coordination with omission of one of the cysteines. The second cysteine in the 28-residue domain of a [4Fe-4S] cluster is usually the residue which has been altered to another residue, such as in nitrate reductase, NarH, with a tryptophan residue replacing the cysteine (Blasco *et al.*, 1989). The different ligand binding in [3Fe-4S] clusters has recently been used to investigate predictions about iron-sulfur cluster composition, utilizing site-specific mutagenesis, where cysteine residues or other putative ligands to the cluster are substituted by other amino acids. In some cases, this caused the loss of the cluster, or failure of the protein to assemble, and in other cases, the protein retained its structure and function (Cammack, 1991). Rothery & Weiner (1991), reported successful conversion of a [4Fe-4S] center to a [3Fe-4S] center in DmsB of DMSO reductase from *E. coli* [Cys_{102}], with the loss of the g = 1.99 peak in the EPR spectrum in the reduced state with formation of features in the oxidized spectrum. The oxidized spectrum was qualitatively similar to that reported for other [3Fe-4S] centers. Mutagenesis experiments with ferredoxin I from *Azotobacter vinelandii*, where Cys_{20} was replaced by an alanine,

showed that the mutant protein retained both of its [4Fe-4S][3Fe-4S] clusters (Martin *et al.*, 1990). X-ray crystallographic studies demonstrated that Cys_{20} was indeed a ligand in the native protein, but a structural rearrangement took place in the mutant, in which the missing cysteine was replaced by the free Cys_{24}. Although one would generally conclude that if the cluster is not altered, the cysteine is not a ligand, the results of mutagenesis experiment may be unpredictable.

c) [2Fe-2S] Clusters

The [2Fe-2S] Fds do not exhibit as defined a cysteine motif as the [4Fe-4S] clusters. Although 4 cysteine residues are also required to act as ligands for the nonheme iron, the spacing between the cysteines is variable. In fumarate reductase, the [2Fe-2S] center is coordinated by the motif, starting at residue 57, $CX_4CX_2CX_{11}C$, while the [2Fe-2S] Fd from *Spirulina platensis* is coordinated within the region, starting at residue 40, $CX_4CX_2CX_{29}C$ (Beinert, 1990). A comparison of the sequence of the [2Fe-2S] Fd isolated from *C. pasteurianum* failed to detect any homology with the other ferredoxin sequences containing 2Fe, 3Fe and 4Fe active sites. In particular, the cysteine spacing is different in the *C. pasteurianum* [2Fe-2S] Fd and in [2Fe-2S] Fds of the chloroplast type. (Bruschi & Guerlesquin, 1988). Furthermore, additional cysteine residues may be present within the ligand spanning region, but are not utilized as such [*C. pasteurianum*]. Hence, it appears that the stabilization of [2Fe-2S] clusters in Fds is not achieved in a unique and characteristic pattern of cysteine ligands.

2. Electron Paramagnetic Resonance (EPR) Spectroscopy

Electron paramagnetic resonance spectroscopy is a technique that probes the environment of a paramagnetic center [unpaired electron] within a molecule. It is rather a selective technique as most materials have paired electrons (Cammack, 1991). The major use of EPR of transition ions in biological systems is to identify metal centers and to determine their redox state and the state of coordination. Although EPR spectra of iron sulfur proteins are indicative of the type of centers present, use of this method to identify and quantitate the centers can be difficult since the EPR of all iron-sulfur proteins of even a single type are not all the same and other paramagnetic centers interfere (Mortenson & Gillum, 1980). Furthermore, even under the best experimental conditions, not all the protein is in the state that has the known EPR signal and hence quantitation of the signal

may not give an accurate value for the number and kind. An undesired change in the folding arrangement of the polypeptide holding the iron sulfur clusters may occur during preparative handling of the samples [i.e. denatured] which can further complicate the analysis. In the Fds, it is found that minor perturbations, such as changes in salt concentration, can change the lineshape of the observed spectrum (Cammack & Watts, 1994). Despite the drawbacks to EPR, low-temperature EPR spectroscopy, introduced by Beinert & Sands (1960) for the study of the mitochondrial respiratory chain remains the most versatile method for characterizing iron sulfur clusters in complex systems (Cammack, 1991).

For a complete description of the technique, the reader is referred to the following reviews: Orme-Johnson & Sands (1973) and Cammack & Watts (1994). EPR detects changes in the energy state of an excitable species [unpaired electron] upon absorption of incident electromagnetic radiation. In a typical biological sample, the unpaired electrons [magnetic moment s = 1/2] will be separated from each other in the sample and their spins randomly oriented. Once a magnetic field is applied, it gives direction to which the magnetic moments of the electrons are aligned. By applying radiation, such as microwave frequency in EPR, the electron can take up only one of two possible energy states, alignment with [parallel] or against [anti-parallel] the field. The two energy states differ by an amount:

$$\Delta E = h\nu = g\,\mu_B B_o \qquad (4)$$

where: h Planck's constant
ν microwave frequency, GHz [fixed by the resonant frequency of the cavity of the instrument]
g dimensionless spectroscopic variable whose value is characteristic of the paramagnetic center
μ_B Bohr magneton constant
B_o applied static magnetic field, mT or Gauss

Generally, the aim is to solve for the g-tensor or g, which is dependent on the microwave frequency [most common experiments use 9.0 - 9.5 GHz, X band] and the magnetic field. g is treated as a dimensionless spectroscopic variable whose value is characteristic of the paramagnetic center. The g value of a free electron is g = 2.00232, and deviation from this value is a measure of the additional interactions which the

electron spin system has with its surroundings. g values are used as markers to locate maxima, crossing points, minima and other positions in the EPR spectra. In order to obtain a spectrum over a wide range of values of g, the magnetic field, B_o, is varied as the microwave frequency is fixed by the resonant frequency of the cavity of the spectrometer. The EPR spectrum usually presented is the first derivative of the microwave power absorption detected and the intensity is revealed as the double integration of the derivative signal.

As can be deduced from earlier discussion, the value of ΔE is orientation dependent; the spectrum collected is a summation of individual spectra taken as an average of all possible orientations of the molecule. Individual molecules carrying paramagnetic centers may exist in a range of conformations and are hard to distinguish, but give g values distributed about a mean value and hence contribute to the linewidth seen with most spectra. The g-value can be considered as having a set of three orthogonal principal axes, x, y and z. Three cases of symmetry arise: 1) Cubic [$g_x = g_y = g_z$]; 2) Axial [$g_x = g_y \neq g_z$]; and 3) Rhombic [$g_x \neq g_y \neq g_z$]. Figure 6 is a schematic illustrating respective spectra of the listed symmetry. A comprehensive listing of various iron-sulfur proteins is given in Cammack (1991).

In a spectroscopic experiment, the energy which is absorbed by the sample is dissipated to its surroundings [the lattice] by a spin relaxation mechanism (Gayda *et al.*, 1976). In EPR, the important ways in which the spin system loses energy to the lattice are the direct process, the Orbach process and the Raman process. These processes are characterized by the spin relaxation time, T_1, and may be identified by the variation of T_1 with temperature (T). T_1 is a measure of the lifetime of an electron in one of the energy states and is inversely proportional to the relaxation rate. The region below 4 K is dominated by a T^2 temperature dependence characteristic of the direct process. Above this temperature, a second order Raman process becomes important [T^9 dependence], which eventually gives way to the very rapid higher temperature Orbach process which has a more elaborate temperature dependence based on antiferromagnetic exchange coupling among the high-spin iron atoms (Blum *et al.*, 1983; Gayda *et al.*, 1976). T_1 has practical consequences for the detection of the EPR signal, namely it determines the power saturation characteristics of the spectrum and thus the optimum temperature for a measurement. For instance, if T_1 is too long, microwave power saturation sets in, and the signal becomes weaker and distorted. This may be alleviated by using a lower microwave power or a higher temperature. If T_1 is too short, the width of the spectrum may become too great and the absorption lines become undetectable. Most systems

studied have followed one of the three relaxation mechanisms proposed. In each case, the transverse relaxation time, T_2, [spin-spin relaxation time], is considered constant.

The microwave power saturation behaviour of a sample can reveal much about the nature of the spin system. To obtain quantitative and undistorted spectra, it is necessary to obtain spectra at microwave powers below those that cause significant saturation of the EPR spectrum. In the literature, $P_{1/2}$ is commonly used as the saturation parameter and it is the incident microwave power at which the EPR signal is half the amplitude it would have been in the absence of saturation. Under normal non-saturating conditions, the intensity of the EPR signal should be proportional to the square root of microwave power. A common presentation of the saturation behaviour is the Beinert/Orme-Johnson plot, where the normalized signal amplitude (S) is divided by the square root of the power (P) and plotted as a function of the square root of power [i.e. log ($S/\sqrt{P}$) vs log ($\sqrt{P}$)]. The result is a straight line parallel to the abscissa where no saturation occurs, and slopes downward toward the abscissa when saturation occurs. The $P_{1/2}$ value is determined as the point at which the two curves intersect (Rupp *et al.*, 1978).

Although greater sensitivity is usually obtained at higher power, this may result in saturation, especially at lower temperatures, since relaxation rates are strongly temperature dependent. The signal amplitude observed tends to be inversely proportional to the absolute temperature. With increasing temperature, relaxation is more efficient and a line broadening is generally observed. For each system, there will be usually an optimum temperature at which the linewidth is minimum. Hence, one tends to work at temperatures as low as possible [i.e. < 77 K]. Furthermore, the temperature dependence of the amplitude of the spectra can often be used to aid in the characterization of the type of [Fe-S] signal. [4Fe-4S] centers are generally visible at lower temperatures [< 30 K], with [2Fe-2S] centers being more readily observed at higher temperatures [70 K] (Gayda *et al.*, 1979). At temperatures below 20 K, the Orbach relaxation process is inefficient, so that T_1 is long and the EPR signal becomes readily saturated with microwave power. This saturation is more pronounced for the [2Fe-2S] clusters. In complex iron-sulfur proteins, the relaxation may be more rapid because of the spin-spin interactions between paramagnetic clusters (Cammack & Watts, 1994).

3. Oxidation - Reduction Potentiometry

Oxidation - reduction [redox] potentiometry is of interest for the study of

paramagnetic centers involved in biological electron transfer enzymes. Combined with EPR spectroscopy, in complex systems where several redox species are present, it can be used as an aid in identification of a particular redox species. Determination of the redox midpoint potential [E_m] of the center can also help elucidate the electron pathway within the protein. The E_m is a measure of the relative ability of the species to be an oxidizing or reducing agent, with a more positive potential indicating a better oxidizing agent. A description of the theory of the redox technique is given by Dutton (1978).

In poising the solution or membrane suspension, the entire redox chamber is kept under oxygen free argon as oxygen is a strong oxidizing agent. A number of mediator dyes which have redox potentials in the range to be studied are added together to the suspension. These mediators act as buffers for the system, and act as "go-betweens" between the measuring electrode and the biological redox couple (Dutton, 1978). However, caution must be exercised in the choice of each mediator as each may not interact efficiently with the species under investigation. In the case with some efficient mediators such as methyl and benzyl viologen, the production of free radicals in certain oxidation states may interfere with the observed EPR spectra, especially in the $g = 2$ region and thus are used sparingly (Cammack & Watts, 1994). The potential of the system is poised with the addition of chemical reductants such as dithionite, or oxidants such as potassium ferricyanide. The measuring electrode used is a platinum strip which is in direct contact with the suspension. The reference electrode is the standard saturated KCl calomel electrode, calibrated against the standard hydrogen electrode.

In order to determine the midpoint potential of the species, the signal amplitude is plotted against the recorded potential at which the sample was taken. The data are fitted to an S-shaped curve, calculated from the Nernst equation:

$$E = E_m + RT/nF \log\{ [A_{ox}]/[A_{red}]\} \qquad (5)$$

where: E_m Midpoint potential [mV at 25°C]
A_{ox} Oxidized species present
A_{red} Reduced species present, and
RT/nF as previously defined in Equation 2.

For most biological redox species, n is expected to be 1.0. Furthermore, in non pure samples, there are several redox species with different E values contributing to the EPR signal. If they are closer than 40 mV apart, these species are almost impossible to

distinguish (Cammack & Watts, 1994).

F. Membrane Proteins

The biological membrane functions as a permeability barrier that establishes the separate compartments of the bacterial cell. Many of the enzymes associated with the respiratory chains are either extrinsic proteins, which do not penetrate the lipid bilayer but are associated with the surface of the membrane, or are intrinsic [embedded within the inner membrane]. In many cases cytoplasmic subunits interact with membrane-bound subunits to form a membrane associated complex [i.e. fumarate reductase, DMSO reductase]. Most of the intrinsic proteins span the bilayer, either once or in multiple spanning regions, generally as α-helices or amphipathic [channel forming] helices (Jennings, 1989). The transmembranal segments are connected by hydrophilic loop regions.

The integral membrane proteins are difficult to purify because they are surrounded by lipid, and disruption of the interaction with the lipid may also lead to denaturation of the protein. Intrinsic membrane proteins tend not to be soluble in aqueous buffer solutions, and generally require the use of detergents, organic solvents or strong chaotropes for solubilization from the membrane (Datta, 1987). Extrinsic proteins require less treatment usually and can be extracted with changes of pH or ionic strength. Besides transmembranal segments, other means of membrane attachment occur, particularly post translational modification by fatty acid acylation (Sefton & Buss, 1987; Hartel-Schenk & Agre, 1992; Omer & Gibbs, 1994). Various reagents are sometimes necessary to aid in solubilization from the membrane [i.e. hydroxylamine for palmitic acid linkages to cysteine residues by thioester bonds, but not fatty acids linked through oxyester or amide bonds (Magee *et al.*, 1984)].

The importance of solubilization of membrane bound protein is exhibited by the need for a soluble state of the complex as the starting material for purification and crystallization. A primary goal with all membrane bound proteins is to understand the function associated with that particular membrane protein, be it in membrane transport, energy transduction, signal transduction or enzymatic, it is essential to know the structure of the protein. Despite considerable effort very few membrane proteins have yielded crystals suitable for high resolution x-ray diffraction analysis. As yet there are only a handful of crystal structures determined. In 1985, Deisenhofer *et al.* (1985) determined the three dimensional structure of the subunits from the photoreaction center

of *Rhodopseudomonas viridis* at a 3 Å resolution. Since then, the reaction center from *Rhodobacter sphaeroides* R-26, a very similar structure has been determined (Allen *et al.*, 1987), as well as the porin from the outer membrane of *E. coli* [OmpA] (Paul & Rosenbusch, 1985) which demonstrated that membrane proteins may be composed of β-sheets and not α-helices. Recently, Kuhlbrandt *et al.* (1994) reported the structure of another integral membrane protein, that of the light-harvesting chlorophyll a/b-protein complex, which has three transmembranal segments with 12 chlorophylls chelated holding two of the α-helices in place. Bacteriorhodopsin, the light-dependent proton pump, has not been amenable to X-ray structural analysis. However, the ordered arrangement of the protein in the purple membrane has allowed a number of successful electron diffraction studies of the membrane associated complex (Henderson & Unwin, 1975; Baldwin *et al.*, 1988). The protein consists of seven transmembranal α-helical rods, arranged in a crescent shape cluster with trimeric organization. Relatively few charged groups are present in the membrane bilayer, but three are suggested to be involved in the mechanism of H^+-pumping [summarized in Cramer & Knaff, 1991].

Until greater success is achieved with crystallization of membrane proteins, many algorithms exist for predicting the structure and relative orientations of transmembranal domains based on various hydropathy scales (Crimi & Degli Esposti, 1991). As well, experimental analysis by gene fusion constructs with periplasmic alkaline phosphatase (Manoil *et al.*, 1990) or β-lactamase (Broome-Smith *et al.*, 1990) also provide insight into the topology of membrane proteins. Many investigators are working on determining the orientation of the protein within the membrane and how it relates to the 'stop transfer' mechanism for proper assembly of the protein within the membrane (Yamane *et al.*, 1990; Ballesteros & Weinstein, 1992).

G. THESIS OBJECTIVE

The research within the Weiner laboratory has concentrated on attempting to understand the structure, organization and function of the components within the respiratory chains. Our attention has focused on the enzymes involved in the simple anaerobic respiratory chain induced by growth of *E. coli* cells in glycerol/fumarate media, namely the G3P/menaquinone/fumarate reductase system. The purification and partial characterization of anaerobic G3P dehydrogenase (Schryvers & Weiner, 1981) and fumarate reductase (Cole *et al.*, 1985) have previously been accomplished, yet our understanding of the way these proteins are expressed and assembled within the

membrane is still lacking. The rapid proliferation of molecular biological techniques and the availability of EPR instrumentation and technical expertise have allowed us to expand the study of the G3P dehydrogenase. The ultimate aim of the research is to be able to reconstitute an entire electron transport system comparable to that observed in the physiological state of the cell. This will aid in our understanding of other electron transport chains, such as the mitochondrial respiratory chain, and the identification of defects associated with the chain which are linked to various mitochondrial myopathies.

Specifically, I have focused on the functional analysis of the anaerobic glycerol-3-phosphate dehydrogenase or GlpACB. The *glpACB* operon has been cloned and sequenced (Cole *et al.*, 1988). With the identification of the third open reading frame, *glpB*, a number of questions were raised as previously described [Section I.D.2e]. The interaction of the soluble catalyic dimer with the membrane-bound menaquinone pool was speculated upon. It had been proposed that the dimer would transiently associate with the membrane by an interaction with a membrane anchoring subunit, but the identity of this membrane component was unknown. GlpB had been assigned as a 44 kDa polypeptide by SDS-PAGE based on comparative expression of the truncated-operon (*glpACB'*) with the full operon. The polypeptide was found in the crude membrane fraction of lysed cells. The expression of the GlpB polypeptide was questionable as clear identification on SDS- polyacrylamide gels varied from experiment to experiment. It was also uncertain whether its apparent localization was an artifact of overexpression as in the formation of insoluble aggregates or inclusion bodies (Marston, 1986), or if the polypeptide was associated with the membrane. Furthermore, the original analysis and expression of the cloned fragment containing the *glp* operon in minicell preparations (Schryvers, 1982) failed to identify the GlpB polypeptide. By analogy to other respiratory enzymes complexes [i.e. FrdABCD] it was hypothesized that GlpB, the third gene in the operon, was expressed and was part of the G3PDH enzyme complex. It was also hypothesized that GlpB acted as a membrane anchor (Kuritzkes *et al.*, 1984; Cole *et al.*, 1988) for the soluble catalytic GlpAC dimer, despite its atypical hydrophilic nature. GlpB would form a link between the catalytic dimer and the menaquinone pool, for transfer of electrons. **This led to the development of my project which was to be the investigation of the structural and functional role of GlpB as a subunit of anaerobic G3PDH; its interaction with the GlpAC dimer as well as with the membrane. A major component of the work was to identify the proposed redox centers with the aim of confirming the electron transfer function of GlpB.** I adopted a combined genetic, molecular

biological and biochemical approach to investigate these questions.

In Chapter III, I describe the results of the studies investigating the expression of the various subunits of the *glpACB* operon. I used a series of constructed recombinant clones under control of the endogenous *glp* promoter and the inducible bacteriophage T7 promoter. This approach was used to conclusively identify the gene-polypeptide relationship, as well as to overproduce the various subunits. The T7 promoter expression system was also used to investigate the aerobic expression of an anaerobically-induced enzyme. I also discuss the results of the studies investigating anaerobic expression of the entire *glp* operon using the endogenous promoter and the localization of GlpB within the cell.

In Chapter IV, the physiological role of GlpB is discussed. First, I examined the growth requirement of GlpB utilizing a multiple mutant background, which I refer to as MERV84. The construction of this strain was necessary to overcome the technical difficulties associated with the induction of glycerol dehydrogenase. I then resorted to EPR spectroscopy to investigate the presence of a paramagnetic center within GlpB.

In Chapter V, I discuss the results of studies using purified GlpB as a fusion protein with glutathione-S-transferase [GST]. I concentrated my efforts on visible absorption and EPR spectroscopy. My initial EPR experiments with the GSTGlpB protein were conducted with the help of Dr. R. Rothery who was kind enough to record and analyze various samples and redox titration attempts, until I became familiar with operation of the spectrometer. I also decribe the results of the studies done with a truncated version of the GSTGlpB fusion protein, which only encompassed the first third of the GlpB polypeptide.

In Chapter VI, I describe the further characterization the paramagnetic center in GlpB. Again, much of the work done in the characterization of the center relied on visible absorption and EPR spectroscopy. Characterization of the type of cluster was carried out in whole cell preparations overexpressing the *glpACB* operon grown in anaerobic glycerol/fumarate media. Confirmation of the cluster type and coordination of the cluster was investigated by addition of a number of reagents to the preparation and monitoring the effect on the reduced EPR signal. Site-directed mutagenesis of the conserved second cysteines in the *Clostridial*-Fd motif was performed. I examined the effect of substituting Cys_{12} and Cys_{59} to serine residues [C12S and C59S, respectively].

The final chapter summarizes the findings of this research and general ideas of the system, providing a model. In addition, questions which remain to be answered, along with possible approaches to address them, are presented.

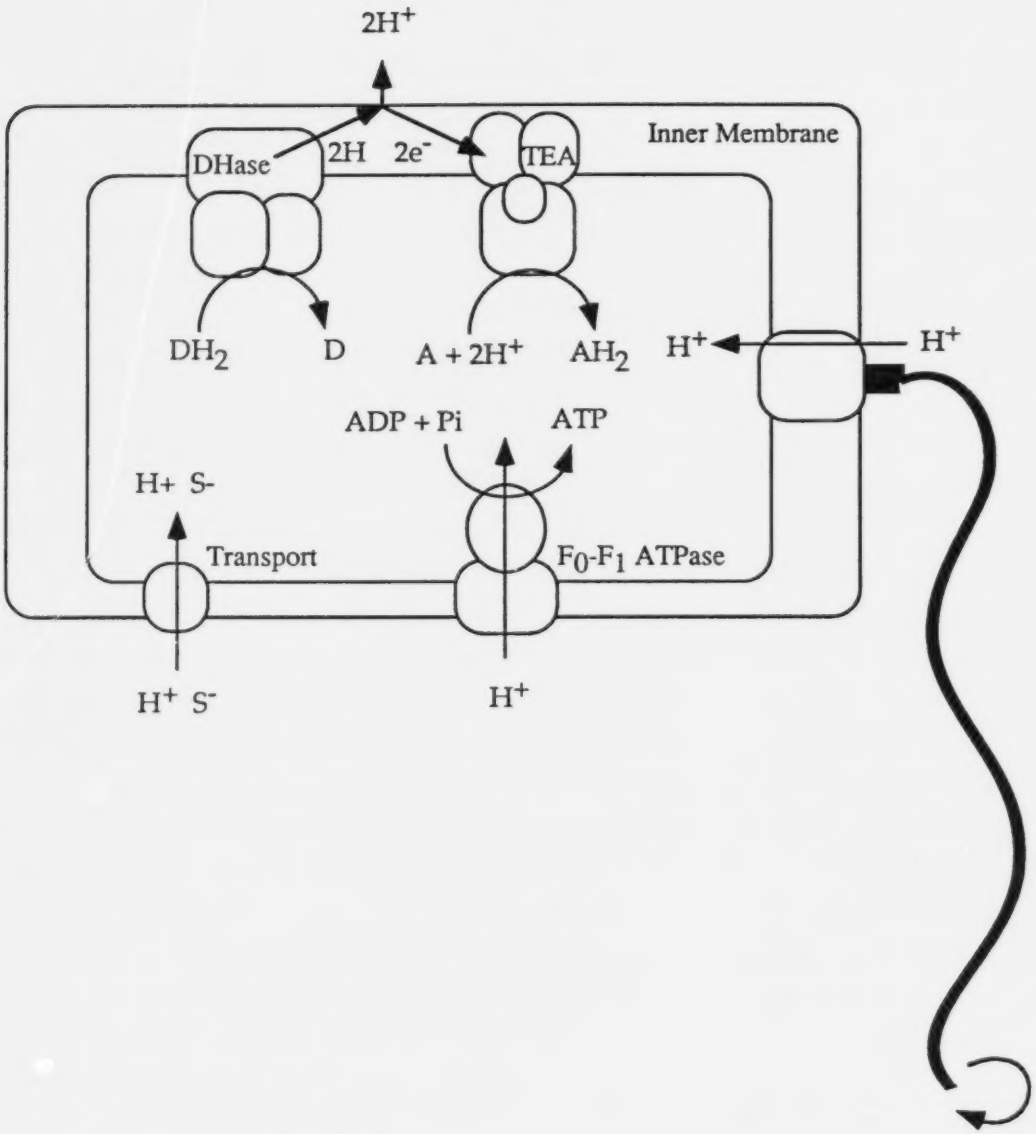

FIGURE 1. A Schematic of the Chemiosmotic Systems in *E. coli*. The electrochemical proton gradient or protonmotive force created by the extrusion of hydrogen ions (H^+) across the membrane establishes the chemiosmotic mechanism for generating ATP using the F0-F1 ATPase. The dehydrogenase (DHase) oxidizes the donor substrate (DH2) and passes on the reducing equivalents to the terminal electron acceptor enzyme (TEA) which reduces the terminal electron acceptor, A. Energy dependent processes such as metabolite transport and bacterial mobility are capable of using the proton gradient directly [adapted from Latour, 1988].

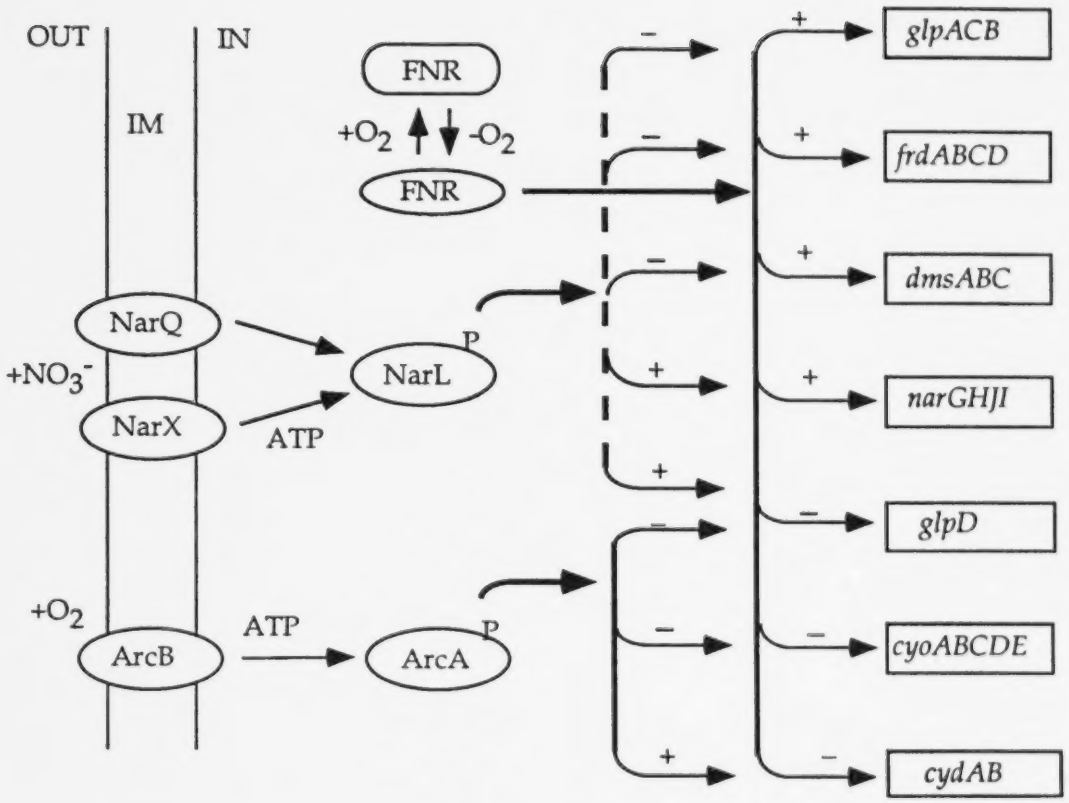

FIGURE 2. Regulatory Scheme for Control of the Aerobic and Anaerobic Pathway Operons in *E. coli*. The three global regulators provide the indicated negative (-) and positive (+) transcriptional control to coordinate enzyme synthesis. The ArcAB , NarQ, and NarXL regulatory systems are activated by the presence of oxygen and nitrate respectively, as indicated. ArcA and NarL become phosphorylated (P) upon activation. The FNR-dependent control is in response to anaerobiosis. The following genes encode the indicated enzymes: *glpACB*, anaerobic G3P dehydrogenase; *glpD*, aerobic G3P dehydrogenase; *frdABCD*, fumarate reductase; *dmsABC*, DMSO reductase; *narGHJI*, nitrate reductase; *cydAB*, cytochrome *d* oxidase; *cyoABCDE*, cytochrome *o* oxidase. Control by additional proposed regulators is not shown in this scheme [adapted from Gunsalus (1992) and Iuchi & Lin (1991)].

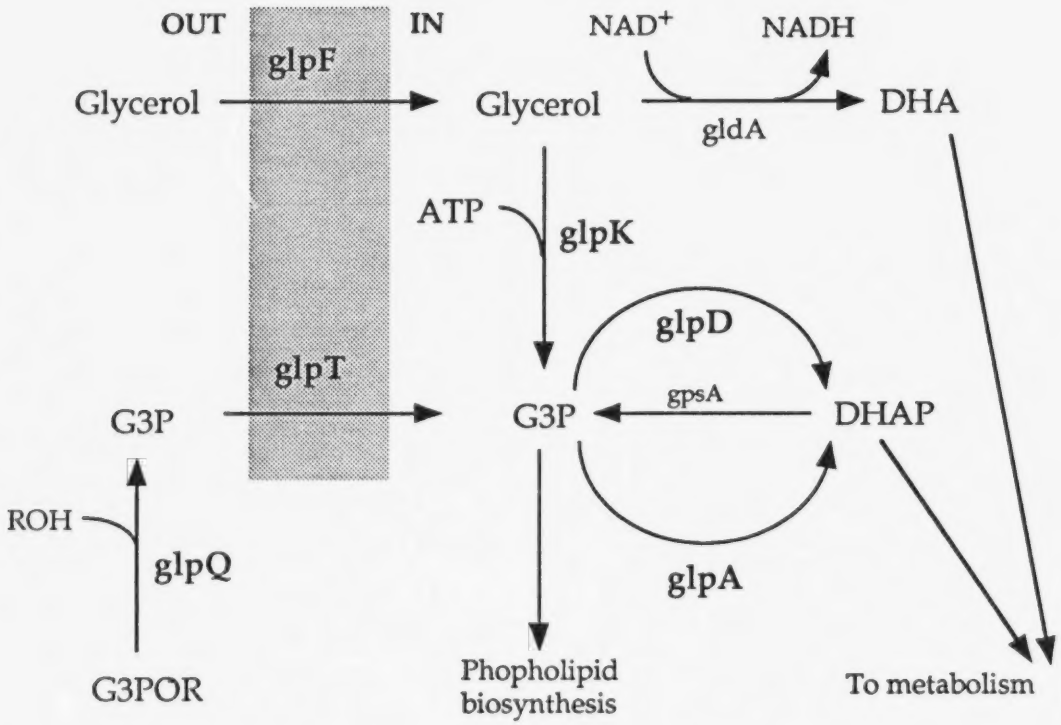

FIGURE 3. A Schematic of Metabolism of Glycerol in *E. coli*. The various components are as specified by their genetic identification: *glpA*, anaerobic G3PDH; *glpD*, aerobic G3PDH; *glpF*, glycerol facilitator; *glpK*, glycerol kinase; *glpQ*, phosphodiesterase; *glpT*, transporter; *gpsA*, G3P synthase; and *gldA*, glycerol dehydrogenase. The cytoplasmic membrane is shown as the grey region, with the periplasmic space referred to as 'OUT' and the cytosol as 'IN'.

1 MNDTSFEN**C**IK**C**TV**C**TTA**CP**VSRVNPGYPG

31 PKQAGPDGERLRLKDGALYDEALKY**C**IN**C**K

61 R**C**EVA**CP**SDVKIGDIIQRARAKYDTTRPSL

91 RNFVLS**H**TDLMGSVSTPFAPIVNTATSLKP

121 VRQLLDAALKID**H**RRTLPKYSFGTFRRWYR

151 SVAAQQAQYKDQVAFF**H**GVFVNYN**H**PQLGK

181 DLIKVLNAMGTGVQLLSKEKCCGVPVIANG

211 FTDKARKQAITNVESIREAVGVKGIPVIAT

241 SSTCTFALRDEYPEVLNVDNKGLRD**H**IELA

271 TRWLWRKLDEGKTLPLKPLPLKVVY**H**TP**CH**

301 MEKMGWTLYTLELLRNIPGLELTVLDSQCC

331 GIAGTYGFKKENYPTSQAIGAPLFRQIEES

361 GADLVVTD**C**ET**C**KWQIEMSTSLR**C**E**HP**ITL

391 LAQALA*

FIGURE 4. The Amino Acid Sequence of GlpB [Cole *et al.*, 1988]. Various regions, as described in the text [Section I.D.2e] are highlighted: 1) Ferredoxin-like motifs for [4Fe-4S] cluster coordination (solid underline); 2) histidines in bold; 3) CCG motifs (outlined letters); and 4) [2Fe-2S] cluster motif or metal binding motif (boxed).

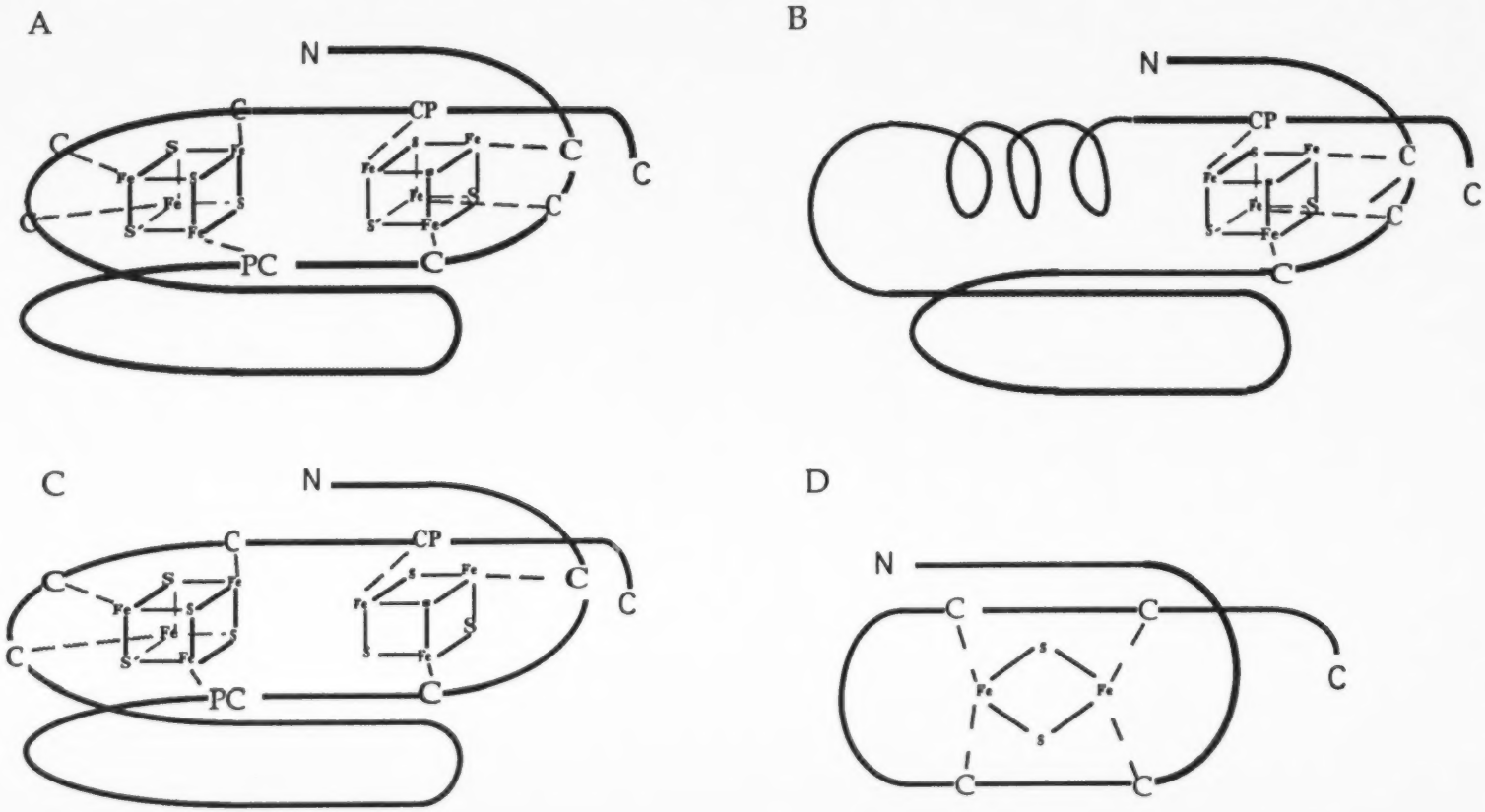

FIGURE 5. Schematic of the Folding Pattern of Iron-Sulfur Centers. The relevant cysteine and proline residues are highlighted. (A) 2[4Fe-4S] ferredoxin motif; (B) [4Fe-4S] monocluster motif; (C) Formation of a [3Fe-4S] cluster by omission of one of the cysteines; and (D) [2Fe-2S] cluster [adapted from Cammack, 1991].

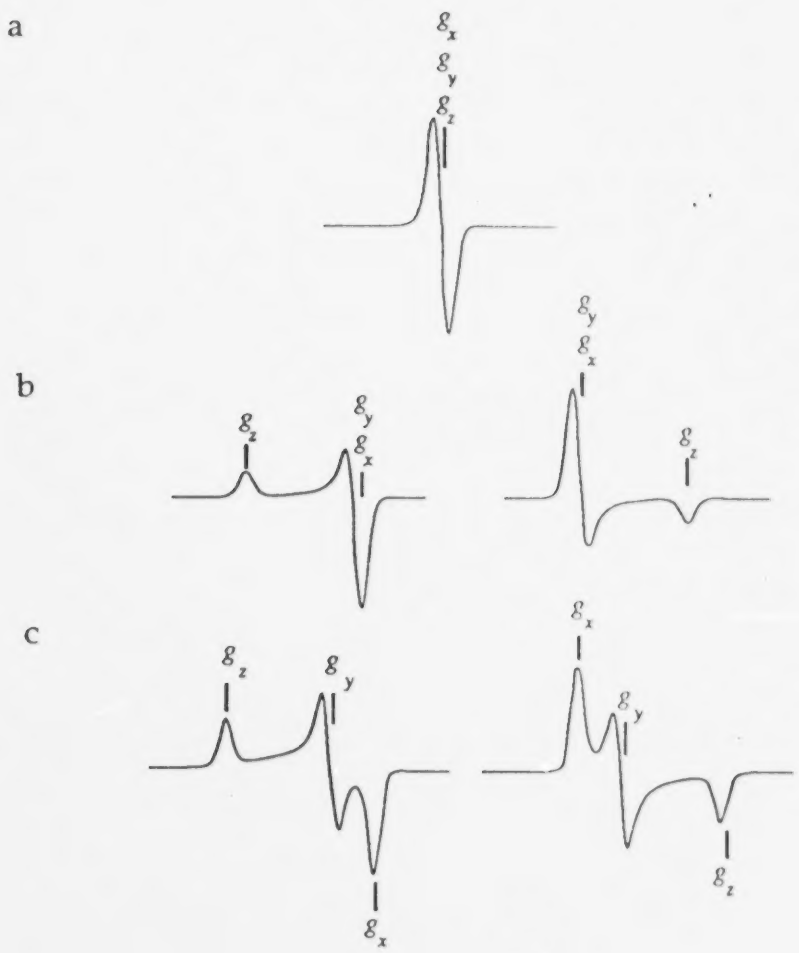

FIGURE 6. A Schematic of EPR Spectra of a Paramagnet with Anisotropic g. The g-factor is considered as having a set of three orthogonal principal axes, x, y and z. Three cases are considered; a) Cubic symmetry, $g_x = g_y = g_z$; b) Axial, $g_x = g_y \neq g_z$; and c) Rhombic, $g_x \neq g_y \neq g_z$ [adapted from (Cammack & Watts, 1994)].

CHAPTER II. MATERIALS AND METHODS

A. Materials

1. Chemicals

[^{35}S] Methionine, [^{35}S] cysteine mixture [Tran^{35}S-Label ^{TM}] [~ 10 mCi/ml] was obtained from ICN Biomedicals Canada Ltd., Mississauga, Canada. Acrylamide, bis-acrylamide, dithiothreitol (DTT), sodium dodecyl sulfate (SDS), and N,N,N',N'-tetramethylethlenediamine (TEMED) were obtained from Bio-Rad Laboratories, Richmond, U.S.A.

Rifampicin, flavin adenine dinucleotide (FAD), flavin mononucleotide (FMN), phenazine methosulfate (PMS), (3(4,5-dimethylthiazolyl-2-)2,5)diphenyl tetrazolium bromide (MTT), DL-α-glycerophosphate (G3P), adenosine triphosphate (ATP), β-nicotinamide adenine dinucleotide (NAD), sodium dithionite, potassium ferricyanide, phenylmethylsulfonyl fluoride (PMSF), 2,[N-cyclohexylamino]ethane sulfonic acid (CHES), 3-[N-Morpholino]propanesulfonic acid (MOPS), trizma, N-[2-Hydroxyethyl]piperazine-N'[3-propanesulfonic acid] (EPPS), ethylenediaminetetraacetic (EDTA), agarose, glutathione, glutathione-agarose beads [G-4510], o-phenanthroline, sodium formate, lactic acid, redox dye mediators [methylene blue, indigosulphonate, thionine, phenosafranine, anthraquinone 2-sulphonic acid, methyl viologen, benzyl viologen, duroquinone and resorufin], antibiotics [kanamycin, tetracylcine, ampicillin, chloramphenicol, and streptomycin], detergents [n-dodecyl β-D-maltoside, n-dodecyl β-d-glucopyranoside, and octyl β-d-thioglucopyranoside], proline, leucine, arginine, threonine and histidine were all from SIGMA, St. Louis, U.S.A. 2,3-dimethyl-1,4-naphthoquinone (DMN) was a gift from Prof. Dr. A. Kroger [Institut fur Mikrobiologie, Frankfurt, Germany]. Factor X_a for the cleavage of the GSTGLPB fusion protein was a gift from Dr. L. Smillie [University of Alberta]. Purified GroEL was a gift from Dr. W. A. Bridger [University of Alberta]. Isopropyl-β-D-thiogalactopyranoside (IPTG) was purchased from Jersey Glove and Lab Supply, New Jersy, U.S.A.

All other common reagents were of the highest grade required.

2. Molecular Biology Products

Restriction endonucleases *Bam*HI, *Eco*RI, *Bcl*I, *Hind*III, *Xho*I, *Sal*I, *Kpn*I,

*Sma*I, *Pst*I, *Pvu*II, bacteriophage T4 DNA ligase and polymerase, T7 DNA polymerase, and *Thermus aquaticus* (Taq) DNA polymerase were from Bethesda Research Labs (BRL). The restriction endonucleases *Sfu*I and *Bst*XI, and deoxynucleoside triphosphates were purchased from Boehringer Mannheim, Laval, Quebec. The enzymes ribonuclease (RNAse), deoxyribonuclease (DNAse), ferredoxin and lysozyme were from SIGMA, St. Louis, U.S.A.

Polymerase chain reaction (PCR) oligonucleotide primers MVA1 and MVA2 [refer to Table 3] were synthesized by Dr. K. Roy [University of Alberta]. All other DNA sequence primers and site directed mutagenesis oligonucleotides were synthesized by P. d'Obrenan or R. Whitford [University of Alberta].

Plasmid pGEX-3X was a gift from Dr. M. Michalak [University of Alberta]. Phagemids pBluescript^{TM} II KS^{-} and pBC^{TM} KS^{-} were purchased from Stratagene Cloning Systems, La Jolla, CA. pKIXX vector DNA was purchased from Pharmacia Biotech Inc, Baie d'Urfe, Quebec.

Glass milk powder, for agarose gel purification of DNA, was a gift from Dr. G. McFadden [University of Alberta].

3. Bacterial Strains

The *Escherichia coli* strains used are listed in Table 1.

4. Growth Media

All strains were subcultured aerobically in Luria Broth (LB) (Sambrook *et al.*, 1989) before inoculation into the medium of choice. Stock strains were stored frozen at -70°C in LB made with 8% [v/v] dimethyl sulfoxide (DMSO).

For anaerobic expression, cultures were routinely grown in glycerol/fumarate (G/F) medium [per litre: 5.44 g of KH_2PO_4, 10.49 g of K_2HPO_4, 2 g of $(NH_4)SO_4$, 3.75 g of NaOH, 4.64 g of fumaric acid, 0.01% metal mix [0.4 mM $MgSO_4$, 25 µM $MnSO_4 \cdot H_2O$, 10 µM $FeSO_4 \cdot 7H_2O$, 5 µM $CaCl_2$], 0.52% (v/v) glycerol, 0.05 % (w/v) casamino acids [for small scale growth i.e. < 1 l] or 0.1% peptone [for large scale growth - 20 l]. The medium was supplemented with 20 µg/ml each of thiamine, proline and leucine.

Large scale anaerobic growth occured in 4-l or 20-l carboys which were filled to the top with medium and tightly sealed with the screw-on-cap or rubber stopper

respectively. To ensure no sedimentation of the cells occurred, each carboy was gently stirred with a magnetic stir bar.

In some cases [cells unable to grow anaerobically on G/F medium], anaerobic growth was supported by a peptone/fumarate medium (P/F) [per litre: 4 g peptone, 4 g yeast extract, 6 g K_2HPO_4, 4.76 g KH_2PO_4, 4.6 g fumaric acid, 3.73 g NaOH] (Condon & Weiner, 1988). The medium was supplemented with 0.1 % glucose, 0.2 % glycerol or 40 mM G3P.

For bacteriophage T7 RNA polymerase/promoter expression studies, cells were routinely grown in Enriched medium [per litre: 20 g tryptone, 10 g yeast extract, 5 g NaCl, 0.2 % glycerol, 50 mM potassium phosphate, pH 7.2]. During labelling with [^{35}S]-methionine, [^{35}S]-cysteine Tran^{35}S-label^{TM}, M9 minimal medium (Miller, 1992) supplemented with Difco Methionine Assay Medium [0.2 %], thiamine [20 µg/ml] and glucose [1 %] was used. When using BL21(DE3), a lysogenic strain carrying the T7 RNA polymerase as a chromosomal copy [Table 1], the cells were grown in a M9 minimal medium (Miller, 1992) supplemented with 0.1 % methionine after addition of IPTG [0.1 mM].

During growth and expression of glutathione S-transferase (GST) fusion proteins, cells were routinely grown in LB supplemented with 10 µg/ml thiamine. Metal mix [as described above in the recipe for G/F medium] was routinely added [1 ml/ l]. For electron paramagnetic resonance spectroscopy studies, the $MnSO_4$ was omitted from the metal mix.

For amplification and preparation of plasmid DNA, cells were grown either in a minimal M9 medium (Sambrook *et al.*, 1989) or in Terrific broth [12 g tryptone, 24 g yeast extract, 4 ml glycerol per 900 ml containing 0.17 M KH_2PO_4/0.72 M K_2HPO_4] (Tartoff & Hobbs, 1987).

B. Methods

1. Molecular Genetic Procedures

Plasmid DNA was isolated by the cold alkaline pH method as described by Birnboim & Doly (1979). Further purification was by extraction of proteins with organic solvent [phenol/chloroform] and precipitation with polyethylene glycol, isopropanol or ethanol (Crosa *et al.*,1994). Quantitation of DNA concentration was by ultraviolet-visible (uv) absorption spectroscopy [Varian DMS100 spectrophotometer] in

1 ml quartz cuvettes using distilled water as the dilution media and blank.

Analysis of plasmid DNA was routinely carried out by restriction endonuclease digestion for 1 - 2 hour using the enzyme conditions specified by the manufacturer. When digestion was complete, the reactions were terminated by heating at 65°C for 10 minutes. For analysis on DNA agarose gels, 0.2 volumes of stop mix [0.25 % Bromophenol blue, 0.25 % xylene cyanol, 30 % glycerol in water] were added prior to heating. The size of the restriction fragments was determined relative to molecular weight standards. *Hind*III-digested bacteriophage λ DNA was routinely used as the standard for DNA [band sizes: 23.1, 9.3, 6.6, 4.4, 2.3, 2.01, 0.56 kilobase (kb)]. DNA gel electrophoresis was performed on two scales. For mini screen [small scale preparation] analysis of recombinant clones, samples were electrophoresed in 1 % agarose gels in 0.04 M Tris-acetate/0.001 M EDTA (TAE) buffer, pH 8.0 (Sambrook *et al.*, 1989) at 25 V for 12 - 15 hours. For quick analysis of double stranded DNA, 0.8 - 1.2 % agarose gels were run in 0.045 M Tris-borate/0.001 M EDTA (TBE) buffer, pH 8.0 at 160 V for 20 - 30 minutes. All gels were stained in ethidium bromide [0.5 mg/ml] for 10 minutes prior to visualization under short wave length uv light. Single-stranded DNA was electrophoresed on 1 % agarose in TAE buffer at 80 V for approximately 1 hr.

Restriction fragments recovered from 1 % agarose gels [TAE buffer] were purified by the glass milk technique (Vogelstein & Gillespie, 1979).

Transformation of *E. coli* with plasmid DNA was routinely carried out by the calcium chloride method (Mandel & Higa, 1970). For selection on kanamycin (Kn), chloramphenicol (Cm) or tetracycline (Tet), the transformation mix was grown in L-broth without antibiotics for 1 hour and then plated on selective LB agar containing Kn [40 µg/ml], Cm [42.5 µg/ml] or Tet [12.5 µg/ml] respectively. For transformation of cells with two plasmids, the bacterial strain was first transformed with the DNA encoding Km resistance and the resulting established Km^r clones were transformed with the plasmid carrying ampicillin resistance (Ap^r) or Cm^r. Isolates of transformants were stored at -70°C in L-broth containing 8% DMSO.

For triple plasmid transformation [pGP1-2, pGLP91 and pGLP97], the double transformant carrying the Km^r and Cm^r resistant plasmids was first established, as described above. Successful transformation of pGLP91 was then executed by electroporation (Hanahan *et al.*, 1991) of the competent cells [log phase cultures washed and resuspended at high cell density in 10% cold glycerol], and plating the cells onto LB agar plates containing Ap [100 µg/ml]. Electroporation was performed using the Gibco BRL Cell-Porator *E. coli* Electroporation System at 2.44 kV. Ap^r colonies were then

rechecked for the presence of all three plasmids by growth on LB plates containing all three antibiotics at the appropriate concentrations.

2. Plasmid Constructions

During construction of recombinant plasmids, transformants were screened by plasmid DNA isolation as described by Birnboim & Doly (1979). A list of plasmids and vectors used are shown in Table 2. pGLP90 is similar to pGLP1 in that both carry the intact *glpACB* operon. pGLP15, encoding *glpA*, is truncated at the *Xho*I site within *glpC* (corresponding to leucine$_{79}$) and is similar to pGLP91. pGLP20, encoding *glpAC*, is truncated at the *Sal*I site within *glpB* (corresponding to valine$_{258}$) and is similar to pGLP92. The pGLP1, pGLP15, and pGLP20 plasmids each carry an intact *glpT* gene.

a) Bacteriophage T7 Promoter Plasmids [pGLP90 Series]

A schematic outlining the construction of the bacteriophage T7 promoter plasmids is shown in Figure 7. Plasmid pGLP1 was the original recombinant plasmid carrying the *glpACB* operon as well as the *glpTQ* region [7.4 kbp *Pst*I fragment] (Cole *et al.*,1988). From pGLP1, a 0.6 kb *Sph*1 fragment was deleted in the *glpT* region [pGLP30], with the subsequent transfer of the resultant 6.8 kb *Hind*III fragment into the *Hind*III site of pACYC184 to generate plasmid pGLP22 [Figure 7, Panel A]. These plasmids had been constructed previously (J. H. Weiner, University of Alberta) and were used for subsequent constructions.

The bacteriophage T7 promoter plasmids [pGLP90 series] were constructed as follows [Figure 7, Panel B]: a 4.7 kb *Sac*II-*Hind*III fragment from pGLP22 was cloned into *Sac*II-*Hind*III cleaved pBluescript II KS$^-$ [Ap^r] to generate pGLP90 [*glpACB*]. *Xho*I digestion and religation of pGLP90 generated pGLP91 carrying only full length *glpA*. *Sal*I digestion and religation of pGLP90 generated pGLP92, encoding *glpAC* and a fragment of *glpB*. The *Kpn*I fragment which extends from within *glpA* to the site within *glpB* of pGLP90 was isolated and cloned into pBluescript II KS$^-$ to generate pGLP95 encoding *glpCB'*. The *Xho*I fragment from within *glpC* to the multicloning site of pGLP90 was isolated and cloned into pBluescript II KS$^-$ to create pGLP93 encoding only full length *glpB*. pGLP94 was generated by *Kpn*I deletion of pGLP93. It carries a truncated *glpB* gene encoding a truncated GlpB polypeptide to Gly$_{190}$.

Due to the absence of any convenient restriction endonuclease sites, construction

of pGLP97, carrying *glpCB* was carried out as follows: polymerase chain reaction [(PCR) : Saiki *et al.*, 1988] was used to replicate and amplify the *glpCB* genes from plasmid pGLP1 (Cole *et al.*,1988). The primers used for PCR as well as for oligonucleotide site-directed mutagenesis [as described in the upcoming section] are listed in Table 3. The 5' primer, MVA3, was designed to contain a *Bam*HI restriction endonuclease site prior to the amplified region of the operon [-60 nucleotides from the nucleotides encoding the initiating methionine codon, ATG, of *glpC*]. The primer was designed to anneal downstream of *glpC* to ensure inclusion of any regulatory elements which may be required for expression of *glpCB*. The 3' primer, MVA2 was designed with an added *Eco*R1 restriction endonuclease site following the termination codon of *glpB*. The PCR reaction was carried out as described (Saiki *et al.*, 1988), using *Taq* DNA polymerase. The amplification reaction was carried out for 25 cycles in the PHC-2 DNA Thermocycler [Techne Corporation]. The DNA was denatured at 94°C for 1 min, annealed at 55°C for 2 min and extended at 72°C for 3 min. The product was extracted with chloroform, to remove overlaying mineral oil, and ethanol precipitated. To further purify the product it was electrophoresed in 1.2 % agarose and the DNA band was recovered by glass powder (Vogelstein and Gillespie, 1979). The 2.6 kb amplified product was simultaneously digested with *Bam*H1 and *Eco*R1, the enzymes heat inactivated at 65°C for 15 min, and the DNA was purified once again by the glass powder technique. The fragment was cloned into pBC KS$^-$ (Cm^r) by insertion into the multicloning site [*Bam*H1/*Eco*R1].

b) Glutathione S-transferase (GST) Fusions with pGEX-3X Vector [pGLP100 Series]

The pGEX-3X vector (Smith & Johnson, 1988) is a glutathione S-tranferase (GST) gene fusion system designed for high level expression of genes or gene fragments. The protein of interest is fused to the carboxyl terminus of GST from *Schistosoma japonicum* and is easily purified from bacterial lysates by affinity chromatography (Smith & Johnson, 1988).

Recombinant plasmid pGLP100 [GSTGlpB] was constructed as follows [Figure 8]. PCR was used to replicate the *glpB* gene from plasmid pGLP1 (Cole *et al.*, 1988). The 5' primer, MVA1, was designed to contain a *Bcl*I restriction endonuclease site prior to the start of the nucleotides encoding the initiating methionine codon, ATG, of *glpB*. The 3' primer, MVA2, was that used previously for the pGLP97 construction.

The PCR reaction was carried out as previously described [Section II.B.2a]. The

amplification product was extracted with chloroform, to remove overlaying mineral oil, and ethanol precipitated. Further cleaning of the product was done by glass powder purification (Vogelstein & Gillespie, 1979) following electrophoresis in 1.2 % agarose.

The amplified product was digested with *Eco*R1, heat inactivated at 65°C for 15 min, and then digested with *Bcl*I. The 1.2 kb fragment was cleaned by glass powder purification as before, and ligated into co-digested [*Bam*HI/*Eco*RI] pGEX-3X vector. The ligation incubation was for 16 hours at 14°C. The product was transformed into *E. coli* strain TG1, and transformants screened by Ap^r and plasmid DNA characterization. The construction of the fusion point site was confirmed by DNA sequencing using oligonucleotide primer [MV1] designed to hybridize 60 nucleotides upstream from the *Bcl*I/*Bam*HI cloning site within pGEX-3X. The sequence was confirmed to about 400 nucleotides into the *glpB* gene, rather than the full gene, due to financial restrictions. The verified recombinant clone, with the in-frame fusion of *glpB* to the carboxy terminus of the GST gene, was called pGLP100.

A fusion of GST and truncated GlpB was constructed, carrying the N-terminal region of GlpB [~ 370 nucleotides or 123 amino acids]. PCR was again used to replicate and amplify the *glpB* gene [Figure 8]. The full length *glpB* 1.2 kb fragment was first isolated as described before for the full length construct, cut with *Bcl*I, phenol/$CHCl_3$ extracted, and ethanol precipitated followed by *Pvu*II digestion. The resulting ~ 370 basepair (bp) fragment was isolated by DNA gel electrophoresis, cleaned as before and ligated into codigested [*Bam*HI/*Sma*I] pGEX-3X vector. The resultant recombinant clone, after similar transformation conducted for the full length fusion, screening, and DNA sequence confirmation, was called pGLP101 [GSTGlpB'].

3. Construction of Mutant Strain, MERV84

MERV84 is a mutant strain unable to grow anaerobically on G/F medium due to its *gldA*::Tn10, *glpFKX*$^-$, and Δ*glpTACB* background. The strain was used for complementation with various recombinant plasmids carrying combinations of the *glpACB* operon as well as the *glpT* gene [i.e. pGLP1 (*glpACB*), pGLP15 (*glpA*), and pGLP20 (*glpAC*)]. The *gldA*::Tn10 marker from DLT242 was transferred to SH173 by bacteriophage P1 transduction as outlined in Miller (1992). Following transduction, bacteria were plated on M9-tetracycline agar plates supplemented with glucose/fumarate, G/F or glycerol alone. Colonies only able to grow on glucose/fumarate plates were further tested for anaerobic growth on G/F medium supplemented with tetracycline.

4. Site Directed Mutagenesis

A list of mutagenic oligonucleotide primers utilized are listed in Table 3. A brief description of location and desired mutation are also listed. Recombinant plasmid pGLP90 [*glpACB*] was used as the source for single stranded template isolation. Single stranded template was made as described (Crosa *et al.*, 1994) with helper phage M13K07 used for superinfection of strain RZ1032/pGLP90. Transformants were screened by plasmid DNA isolation as described previously.

Mutants were constructed with the Kunkel based method of site directed mutagenesis (Kunkel, 1985), which theoretically provides a strong selection against the non-mutagenized strand of double-stranded DNA. This method makes use of *dut⁻ ung⁻ E. coli* strain RZ1032 to allow incorporation of uracil in place of thymine in the single stranded template used in the mutagenesis reactions, with selection for positive clones after transformation into a restored *dut⁺ ung⁺* strain such as TG1. The specifics of single stranded template synthesis are as described in Kunkel (1985). In a *dut⁻* background, the enzyme dUTPase is inactivated resulting in higher levels of intracellular dUTP. The *ung⁻* mutation inactivates uracil N-glycosolase thus allowing for incorporated uracil to remain in the DNA. The uracil-containing single stranded DNA is then used as template for the synthesis of the complementary strand which is primed by the specific mutagenic oligonucleotide containing the desired mutation. By transformation into a nonmutant background, only the non-uracil containing strand survives. During extension of the mutagenic strand, T4 DNA polymerase was routinely used. In cases where efficiency was very low, T7 DNA polymerase was used (Tabor & Richardson, 1987). T7 DNA polymerase is highly processive, catalyzing the polymerization of thousands of nucleotides without dissociating. Mutagenic clones were confirmed by plasmid DNA isolation followed by DNA sequencing through the region of the mutagenic site [i.e 200+ nucleotides on either side of the site].

5. DNA Sequence Analysis

DNA sequence analysis based on dideoxy-DNA sequencing (Sanger *et al.*, 1977) was performed by the Department of Biochemistry DNA Synthesis and Sequencing Lab [University of Alberta] with double stranded DNA as the template in the majority of the reactions. In some cases, single stranded DNA was also sequenced. Sequencing

primers used are listed in Table 3.

6. T7 Expression Studies

a) Radiolabelling of Plasmid Encoded Polypeptides Using Plasmid Encoded T7 RNA Polymerase

E. coli K38/pGP1-2 and JM83/pGP1-2 were transformed with appropriate plasmids [pGLP90 series] and labelled with [^{35}S]-methionine as described by Tabor & Richardson (1985) with minor modifications. Transformed cells were grown overnight at 30°C with shaking in L-broth containing Ap [100 µg/ml] and/or Kn [40 µg/ml)]. The cultures were subcultured into fresh L-broth containing appropriate [Ap, Kn or both] antibiotics, and grown at 30°C to an optical density of 0.5 at 600 nm prior to use. For labelling, 900 µl samples were removed and harvested by centrifugation and washed twice with 1 ml phosphate buffered saline. The washed cells were resuspended in 1 ml of sterile M9 medium supplemented with 1% each of Difco Methionine Assay Medium, thiamine and glucose. The suspensions were incubated for 1 hr at 30°C with shaking and then transferred to 42°C for 15 minutes to induce expression of T7 RNA polymerase. Rifampicin [250 µg/ml] was added and the cells were left at 42°C for an additional 15 min. The suspension was then shifted to 30°C for 20 min at which time an aliquot of Tran^{35}S-Label [15 µCi] was added. After 30 min incubation, the cells were harvested by centrifugation.

Cytoplasmic fractions were isolated by freeze/thaw lysis after treatment with 5 mg/ml lysozyme in 0.25 M EDTA (Kaback, 1971). PMSF (2 mM) was added to the cell culture prior to the lysozyme/EDTA solution, and the suspension was incubated on ice for 60 min. Prior to freeze/thaw treatment, 10 µg of DNAse, 4 µg RNAse and 10 mM $MgCl_2$ were added to the suspension. The lysed cell suspensions were centrifuged to remove cell debris, and the supernatant fractions were centrifuged at 390,000 xg, 4°C for 25 min. The soluble proteins were concentrated by addition of one fifth volume of 50% trichloroacetic acid (TCA). After 30 min incubation on ice, the samples were washed twice with 10% TCA, and then resuspended in 25 µl Laemmli solubilization buffer (Laemmli, 1970) modified to contain 0.2 M Tris base (TCA buffer). The pellet fractions were resuspended in 40 µl TCA buffer. For analysis by SDS-PAGE [Section II.B.13], 20 µl aliquots of the various samples were loaded onto the gel.

For overproduction of plasmid encoded nonradiolabelled proteins using the T7 RNA polymerase/promoter system cultures were grown aerobically at 30°C in Enriched medium [Section II.A.4] for 3.5 hr, shifted to 42°C for 1 hr and incubated at 30°C for 2 hr prior to harvest, lysis of cells and analysis by SDS-PAGE [Section II.B.13].

b) Expression of Plasmid Encoded Polypeptides Using Chromosomally Encoded T7 RNA Polymerase

E. coli lysogen BL21(DE3) was transformed with appropriate plasmids as described previously. Cultures were grown aerobically at 30°C in M9 glucose minimal medium to an O.D.600 of ~1.0. Expression was induced with 0.4 mM IPTG. At this time methionine [3 µg/ml] was added and the cultures were allowed to grow for 2-3 hr at 30°C.

7. GSTGlpB Fusion Studies

a) Growth and Induction

Overnight cultures of *E. coli* BNN103 transformed with parental or recombinant plasmids [pGEX-3X, pGLP100 series] were diluted 1:100 in fresh Luria Broth medium (Sambrook *et al.*, 1989) and grown at 37°C to an optical density (OD_{600}) of about 0.8. In some cases, metal mix [1 ml/l], with and without manganese, was added to the growth medium. IPTG was then added to 0.1 mM. Cultures were routinely allowed to grow for an additional 3 - 5 hours at 37°C, 8 hr at 30°C or 20 hr at 20°C. The cells were pelleted and resuspended in phosphate buffered saline [PBS:4 mM NaCl, 16 mM Na_2HPO_4, 4 mM NaH_2PO_4, pH 7.3 or pH 9.0] including 1% Triton X-100 and 0.5 mM DTT. For handling of the truncated fusion protein (GSTGlpB'), Triton X-100 was omitted since it did not appear to enhance solubilization, as viewed with SDS-PAGE.

b) Affinity Purification of the GSTGlpB Fusion Protein

Cells were lysed by passage through a French press at 20,000 psi, and subjected to centrifugation at 10,000 Xg for 6 minutes at 4°C. The soluble fraction was applied to a column of pre-swollen glutathione-agarose beads (Smith & Johnson, 1988), equilibrated with PBS + 1% Triton X-100, 0.5 mM DTT. The column was washed with

PBS to remove unbound protein, and then the fusion protein was eluted with 5 mM glutathione in 50 mM Tris-HCl, pH 8.0, 0.5 mM DTT. The fractions containing GSTGlpB were pooled and concentrated by Amicon ultrafiltration. Aliquots were frozen in liquid nitrogen and stored at -70°C.

For the truncated version, GSTGlpB' [pGLP101], the detergent was omitted from the buffers.

c) Site Specific Factor X_a Proteolysis

Cleavage of purified GSTGlpB or recombinant GSTGLPB' with human Factor X_a was performed in the Tris-HCl elution buffer containing 100 mM NaCl, 1 mM $CaCl_2$, 350 µg of purified fusion protein and 0.7 µg human Factor X_a (Smith & Johnson, 1988). The reaction incubation was at 4°C or at 20°C. The reaction was stopped by addition of PMSF to a final concentration of 2.5 mM after 1 to 24 hours incubation. In some experiments the cleavage was carried out with the addition of purified GlpAC dimer [GSTGlpB:GlpAC, 1:1; (Schryvers & Weiner, 1981)] or 0.5 mM DTT.

8. Preparation of Purified GlpAC Dimer

Purifed GlpAC dimer was prepared as described by Schryvers & Weiner (1982). One hundred grams of frozen (-70°C) JM83/pGLP1 cell paste [prepared from 300 l fermentation run on G/F medium by D. MacIssac] was used. Purified GlpAC dimer was frozen in liquid nitrogen in 200 µl aliquots and thawed only as required.

9. General Preparation of Cellular Fractions

Cultures were harvested by centrifugation and the whole cells were routinely washed once and suspended in 50 mM sodium phosphate (NaPi) buffer pH 6.8 or 50 mM Tris-HCl buffer, pH 8.0 containing 50 µg/ml PMSF. Samples were kept on ice throughout the procedure. The suspension was then lysed by two passages through a French pressure cell [American Instrument Co., Silver Spring, Md.] at 16,000 psi or 20,000 psi depending upon the volume [i.e. low setting for < 3ml, high setting > 3 ml]. The crude lysates [whole cell extracts] were centrifuged at 4,000 xg for 10 min to remove cellular debris and the resulting supernatants were centrifuged at 490,000 xg for

25 min [< 3ml] or at 100,000 xg for 1 hr [> 3ml]. The crude membranes [pellet or "particulate fraction"] were resuspended in 50 mM NaPi, pH 6.8 buffer or 50 mM Tris-HCl buffer, pH 8.0 containing PMSF [50 µg/ml]. The supernatant of the high speed centrifugation is referred to as the "cytoplasmic fraction". In cases where washed membranes were used, the crude membranes, after resupension in buffer containing PMSF and homogenization, were once again subjected to ultracentrifugation at 100,000 xg for 1 hr. The washed membranes were then resuspended in the buffer containing PMSF.

10. Subcellular Localization of GlpB

JM83 and JM83/pGLP1 cells were grown anaerobically for 24 hr at 37°C in G/F medium as previously described. Cells were washed once, and resuspended in 30 mM Tris-HCl buffer, pH 8.0, containing 22 % sucrose [wt/vol]. Inner and outer membrane fractions were prepared as described by Yamato *et al.* (1975) using lysozyme/EDTA treatment and sucrose density gradient centrifugation. Final suspension was in 50 mM NaPi buffer, pH 7.5 with PMSF [0.5 mM] added. The inner [or "Yamato membrane"] and outer membrane fractions were then analyzed by gel electrophoresis to determine localization of GlpB.

11. Solubilization Attempts

a) Membrane Bound GlpB

A Yamato membrane enriched preparation of GlpB was used for detergent solubilization attempts. A typical solubilzation experiment was carried out as follows: 100 µl of Yamato membranes [50 mg/ml protein concentration] were used as starting material. A 200 µl aliquot of 50 mM NaPi buffer was added, plus 1 µl of stock [200 mM] PMSF. This diluted preparation was then divided into 25 µl aliquots in 1.5 ml microtubes. Detergent [generally 10 % (w/v) stock solution] was then added to a final concentration of 2 %. In some cases the detergent concentration was varied or multiple washings with a particular detergent were utilized. The suspension was well mixed, and then allowed to incubate at room temperature for approximately 40 minutes. The samples were then transferred to ultracentrifuge tubes and centrifuged at 450,000 xg for 25 min at 4°C. The supernatant and pellet fraction were collected and Laemmli

solubilization buffer (LSB) added. The samples were then analyzed by polyacrylamide gel electrophoresis, with approximately 1/4 the available protein loaded for the supernatant fractions [40 μg estimate] and ~ 1/2 for the membrane fractions [60 μg estimate].

The various detergents tried include: Triton X-100, Triton X-102, Triton X-45, Triton X-35, Tween 20, Brij 96, 3-[(3-Cholamidopropyl)-dimethylammonio]-1-propane-sulfonate (CHAPS), Sarkosyl, SDS, n-octyl glucoside, Thesit, N-dodecyl-N,N-dimethyl-3-ammonio-1-propane-sulfonate (DDAPS), Deoxycholate (DOC), cholate (COL), cetyl trimethyl ammonium bromide (CTAB), DOC and COL containing 0.5 - 1.5 M NaCl, n-dodecyl β-D-maltoside, n-dodecyl β-thioglucopyranoside and octyl β-D-thioglucopyranoside. Other reagents used for solubilization attempts included 0.4 or 0.8 M hydroxylamine, pH 9.0 and 0.4 M $NaHCO_3$, pH 10.

b) Insoluble Aggregates or Inclusion Bodies

During the T7 expression and GST fusion studies, the majority of the recombinant expressed proteins were found to pellet with the cellular debris [low speed pellet] which is indicative of an insoluble aggregate or inclusion body (Marston, 1986). Many of the agents used to attempt to solubilize GlpB were also tried on the inclusion body preparations as well as 1 - 3 M guanidine hydrocloride and 1 - 4 M urea.

In some cases [i.e. T7 expressed GlpA], further enrichment of the polypeptide was done by sucrose gradient sedimentation, which I refer to as a 'simplified Yamato preparation'. In this simplified preparation, cells grown in M9 minimal medium were washed once in 3 mM EDTA and lysed as described before. The crude membrane fractions were collected and resuspended by homogenization in 3 mM EDTA and the suspension was layered onto a 44 % [w/w] sucrose solution in 3 mM EDTA. The gradient was centrifuged for 18 hours at 120,000 xg. Floating banded regions were collected. The fractions were diluted with two volumes of 3 mM EDTA, pelleted at 100,000 xg for 30 minutes and suspended in 200 mM NaPi, pH 6.8 buffer.

12. Chymotrypsin Digestion of GlpA

The inclusion body preparation of GlpA [as described in the previous section] was subjected to chymotrypsin proteolysis. An aliquot of GlpA [75 μg] was resuspended in 500 μl of 50 mM Tris-HCl buffer, pH 7.5. Chymotrypsin, 0.5 μl of 1

mg/ml stock, was added and allowed to digest at room temperature for 1 hour. TCA (0.5 ml of 10 % stock) was added, incubated on ice for 30 minutes and then centrifuged. The pellet was resuspended in 40 µl TCA buffer, as described previously [Section II.B.6a]. The samples, 20 µl aliquots, were then subjected to SDS-PAGE as described below.

13. SDS-Polyacrylamide Gel Electrophoresis

Proteins were separated by electrophoresis on 7.5 - 15 % [wt/vol] acrylamide-bisacrylamide [30:0.8] SDS gels with a stacking gel of 4% acrylamide-bisacrylamide. The samples solubilized in Laemmli (1970) buffer, were heated to 95°C for 3 min and then loaded onto the gel. In cases where the proteins had been subjected to TCA precipitation, the samples were heated as described for non-TCA precipitated samples. Electrophoresis was performed on a Bio-Rad Mini Protean II electrophoresis cell following the instructions of the manufacturer except voltage applied was 160 V or 180 V. Gels were stained with 0.1 % Coomassie blue, 0.1 % cupric acetate in isopropanol [25 %]/acetic acid [10%] and destained [25 % EtOH/10% acetic acid]. Gels containing [^{35}S]-labelled proteins were dried and autoradiographed without further treatment. In some cases, gels and autoradiograms were densitometrically scanned for quantitation, using a Joyce Loebl Chromoscan 3.

A protein standard [Bio-Rad Laboratories SDS-PAGE Molecular Weight Standards - Low] was routinely loaded in an adjacent lane to the experimental samples. The molecular weight markers were: rabbit muscle phosphorylase b, 97,400; bovine serum albumin, 66,200; ovalbumin, 45,000; carbonic anhydrase, 31,000; soybean trypsin inhibitor, 21,500; and hen egg white lysozyme, 14,400.

A sample of the purified GlpAC dimer [5 - 15 µg] was also routinely loaded in an adjacent lane to the experimental samples, for ease in identification of the GlpACB polypeptides in the experimental samples.

14. Determination of Protein Concentration

Protein was determined by the modified method of Lowry using bovine serum albumin as standard (Markwell *et al.*, 1978). A Varian DMS 100 UV-Visible spectrophotometer or Gilford Instrument Spectrophotometer 250 was used for absorption measurements.

15. Enzymatic Activity

a) G3P Dehydrogenase Assay

Enzymatic assays were done as previously described by Cole *et al.* (1988). 1 unit is defined as 1 µmole of MTT reduced per minute. Specific activities are expressed as units per mg of protein. In some cases, DMN was used as an alternate for PMS.

b) Glycerol Dehydrogenase Assay

Glycerol dehydrogenase activity was assayed by following the increase in absorbance due to NADH fromation at 340 nm using a Gilford spectrophotometer (Tang *et al.*,1979). Reaction mixtures of 1 ml contained 100 mM glycerol, 0.6 mM NAD^+, 30 mM $(NH_4)_2SO_4$ and 100 mM K_2CO_3, pH 9.0. The molar extinction coefficient (ε) of NADH used was 6.22 mM. One unit of activity was taken as the amount of enzyme needed to reduce 1 µmol of NAD per minute.

16. Iron-Sulfur Protein Analysis

a) Non-heme Iron Determination

The method used for determination of nonheme iron is as previously described by Brumby & Massey [Method A: Massey (1967)]; in the presence and absence of reducing agent, the valency state of the iron in the trichloroacetic acid extract may be determined.

b) Non-heme Iron Stain

A quick method of visualizing an iron-sulfur protein is to use a specific potassium ferricyanide stain of a nondenaturing polyacrylamide gel (Leong *et al.*, 1992). The gels were prepared as described previously except that SDS was omitted from the gels and buffers. The inclusion of 0.1% Triton X-100 in the samples, gel and buffer was also tried. Samples were adjusted to 10 % [w/v] sucrose prior to loading and were not boiled. Purified ferredoxin [Sigma] was used as a control.

c) Acid Labile Sulfide Analysis

The determination of the acid-labile sulfide was done by the method described by King & Morris (1967).

17. EPR Spectroscopy

EPR spectra were recorded using a Bruker ESP300 EPR spectrometer equipped with an Oxford Instruments ESR-9 flowing helium cryostat. Instrument conditions and temperature conditions, unless otherwise indicated, were as follows: Temperature, 20 K; microwave power, 20 mW [10 dB]; frequency, 9.45 GHz; modulation frequency, 100 kHz; receiver gain, 5 X 10^4; and modulation amplitude 9.66 G. Integrations were performed by double integration with Cu(II)-EDTA as standard following base line correction of spectra prior to each integration.

a) Preparation of EPR samples

Samples of 150 µl were transferred using a microliter syringe into quartz tubes, and flushed with argon. Sodium dithionite was used as the artificial reductant [2.5 mM] and potassium ferricyanide [10 mM] as the oxidant unless otherwise specified. For physiologic substrate studies, 20 mM G3P, formate or lactate were used or 25 mM fumarate. Upon mixing, samples were allowed to equilibrate before being frozen in liquid nitrogen. In some cases, 65 µM o-phenanthroline was used as an iron chelator, and was allowed to incubate for 5 minutes - 2 hours prior to freezing. Incubation with other agents such as 1 M urea and 0.4 M guanidine hydrochloride was performed for ten minutes prior to freezing.

b) Preparation of Well Maintained Anaerobic Samples

After growth of cells [i.e. JM83 harboring the plasmids pGLP1, pGLP90C12S, and pGLP90C59S] in 4-l carboys, the cells were harvested as before, and after one washing in 50 mM Tris-HCl, pH 8.0, were placed in a sealed anaerobic 'Glove Bag' [Instruments for Research and Industry - Aldrich; USA] which was vacuum purged and filled with pure N_2 gas. The anaerobic state of the bag was confirmed by addition of

dithionite to a solution of benzyl viologen (BV). The purple color formation on the reduction of BV is maintained in the absence of oxygen. Within the bag, the cell paste [3 - 4 g] was routinely resuspended in 50 mM MOPS/ 5 mM EDTA, pH 7.0 [4 ml], and homogenized.

Whole cell samples [150 µl] were transferred to EPR quartz tubes and dithionite or physiological substrates were added. The samples were frozen in liquid nitrogen within the bag.

For analysis of lysed cells, the homogenized suspension was treated with 300 µl lysozyme/EDTA solution (10 mg/ml in 0.2 M EDTA), and incubated on ice for about 45 minutes. Prior to freeze/thaw of the suspension three times in liquid nitrogen, 200 µl of 2 mg/ml DNAse, 100 µl of 4 mg/ml RNAse, and 200 µl of 1 M $MgCl_2$ were added. Samples were transferred to EPR tubes as before.

For use in anaerobic redox chamber [Section II.B.17c], the lysed cell suspension was drawn up into a syringe, sealed on each end with parafilm, and then transferred into the anaerobic redox chamber through a needle port. The sealed redox chamber was continually being flushed with argon to maintain its anaerobic state.

c) Preparation of EPR Samples Poised at Defined Redox Potentials

Samples were placed in an anaerobic chamber similar to that described by Dutton (1978), under argon, in 100 mM MOPS/5 mM EDTA, pH 7.0 or 100 mM 2-[N-cyclohexylamino]ethane-sulfonic acid (CHES)/1 mM EDTA, pH 9.0. Mediators added together were methylene blue, indigodisulphonate, thionine, phenosafranine, anthraquinone 2-sulphonic acid, all at 50 µM, and resorufin at 40 µM. In some cases, the concentration of the mediators was increased by 50 %. The redox potential was measured with a platinum and calomel electrode, at 25°C. The redox titration was typically performed in an initial reducing direction, followed by oxidation then re-reduction. The potential was adjusted with small additions of dithionite and potassium ferricyanide solutions. After an equilibration time when the poised redox potential appeared stable, at least 5 - 10 min, samples were transferred with a microliter syringe through an anaerobic chamber into quartz tubes and frozen in liquid nitrogen. In cases where the poised potential exhibited significant drift, samples were taken after a longer stabilization time. Potentials were recorded relative to the standard hydrogen electrode.

For titrations involving the GSTGlpB full length fusion protein, the sample suspension was prepared as follows. The soluble fraction of the low speed

centrifugation step [Section II.B.7b] was centrifuged at 140 000 xg for 1 hour at 4°C. The pellet was resuspended in 100 mM CHES/1 mM EDTA, pH 9.0. As the initial steps involved detergent, this preparation is referred to as the 'cell debris and microinclusion body' preparation. In alternative preparations, the Triton X-100 was omitted from the buffer for resuspension of the cells and washed membranes were resuspended in the 100 mM CHES/ 1 mM EDTA, pH 9.0 buffer. In this case, the preparation is referred to as 'washed membranes'.

d) Preparation of EPR Samples at Various pH

JM83/pGLP1 [*glpACB*] whole cells were resuspended in 50 mM MOPS/ 5 mM EDTA, pH 7.0 [40 mg/ml] within the anaerobic bag. Aliquots of 100 µl were placed in Eppendorf tubes and 100 µl of 'buffer cocktail' mix was added and allowed to incubate for ten minutes prior to reduction with 2.5 mM dithionite and freezing as before. The 'buffer cocktail' mix was prepared as follows: a solution of 200 mM of [N-[2-Hydroxyethyl]piperazine-N'-[3-propanesulfonic acid] (EPPS), MOPS and CHES buffer was prepared. Using 5 N NaOH, the buffer mix was brought to the various pH levels [pH 5, 6, 7, 8, 9, and 10], at which time an aliquot was taken and added to the whole cell sample.

For the GSTGlp fusion studies, 10 µl of 0.45 M 'buffer cocktail' was added to 150 µl aliquots of purified GSTGlpB [3.5 mg/ml].

18. Electron Microscopy

Whole cell samples of JM83 and JM83/pGLP91 [*glpA*] were prepared for analysis of thin sections by electron microscopy. The samples were fixed by the glutaraldehyde/osmium tetraoxide method as previously described (Weiner *et al.*, 1984). The preparation of the samples and microscopy were graciously done by R. Bradley and Dr. D. Scraba [Department of Biochemistry, University of Alberta] respectively.

19. Fluorescence

Preliminary fluorescence studies were conducted with the inclusion body preparation of GlpA [refer to Section II.B.11b]. GlpA protein [75 µg] was added to 2.5 ml of 0.1 M citric acid/0.2 M Na_2HPO_4, pH 3.6 buffer in a cuvette. Excitation was at

445 nm. The Perkin Elmer Luminescence Spectrometer LS50 was used for the analysis.

TABLE 1

Escherichia coli Strains Utilized

Bacterial Strain	Relevant Genotype	Source or Reference
BL21(DE3)	F⁻ *hsdS, gal,* λcIts$_{857}$ *ind*1 Sam7 *nin5 lac* UV5-T7 gene *1*	Studier & Moffatt (1986)
BNN103	(Δ*lacIOPZYA*) U169 *proH*⁺, *lon, araD135, strA, thi, hflA150, cbr*::Tn10	J. H. Weiner, Univ. of Alberta
DLT242	F⁻, *thiA1, araD139,* Δ(*argF-lacZ*)U169, *rpsL150, relA1, flb5301, ptsF25, deoC1, rbsR,* Δ(*glpFKX*), *gldA*::Tn10	Truniger & Boos (1994)
JM83	*ara,* Δ(*lac-proAB*), *rpsL, thi,* ϕ80, *lacZ ΔM15*	Cole *et al.* (1988)
K38	HfrC *phoA4, pit-10, tonA22, ompF627, relA1*	Russel & Model (1984)
MC4100	F- *araD139,* Δ(*argF-lac*)U169 *ptsF25, deoC1, relA1 flB530, rpsL 150* λ⁻	J. H. Weiner, Univ. of Alberta
MERV84	SH173, Δ(*glpFKX*), *gldA*::Tn10	This study
MI1443	Δ*frdABCD,* Δ*ampC, recA,* Sm^r	Condon & Weiner (1988)
RZ1032	HfrKL16 *PO/45 lysA(61-62) thi-, relA1, spoT1, dut-1, ung-1, Zbd-279*::Tn10	B. Malcolm, Univ. of Alberta
SH173	F⁻ *araD139, Δ(argF-lac)U169, rpsL150, relA1, thi, gyrA, glpA593*	Ludtke *et al.* (1982)
TG1	K12, Δ(*lac-pro*), *supE, thi, hsdΔ5,* F' (*traD36, proA*⁺*B*⁺, *lacI*^{q}, *lacZ ΔM15*)	J. H. Weiner, Univ. of Alberta

TABLE 2

Plasmids and Phagemids Utilized

Plasmid/Phagemid	Relevant Characteristic	Source or Reference
pBC KS$^-$	T7 promoter, Cm^r	Stratagene
pBluescript II KS$^-$	T7 promoter, Ap^r	Stratagene
pGEX-3X	*gst* fusion, Ap^r	Pharmacia
pGP1-2	cI$_{857}$, T7 RNA polymerase under λP_2 control, Kn^r	S. Tabor
pGLP1*	pBR322, *glpACB, glpTQ*, Ap^r	Cole *et al.* (1988)
pGLP15*	pBR322, *glpA, glpTQ*, Ap^r	J. Weiner
pGLP20*	pBR322, *glpACB*# *glpTQ*, Ap^r	Cole *et al.* (1988)
pGLP22*	pACYC184, *glpACB*, Cm^r	J. Weiner
pGLP90*	pBluescript KS$^-$, *glpACB*, Ap^r	This study
pGLP91*	pBluescript KS$^-$, *glpA*, Ap^r	This study
pGLP92*	pBluescript KS$^-$, *glpACB'*, Ap^r	This study
pGLP93	pBluescript KS$^-$, *glpB*, Ap^r	This study
pGLP94	pBluescript KS$^-$, *glpB'*, Ap^r	This study
pGLP95	pBluescript KS$^-$, *glpCB'*, Ap^r	This study
pGLP97	pBC KS$^-$, *glpCB*, Cm^r	This study
pGLP100	pGEX-3X, *glpB*, Ap^r	This study
pGLP101	pGEX-3X, glpB' [1-370 nts],Ap^r	This study

\# The prime designation indicates gene truncates. pGLP90 is similar to pGLP1 in that both carry the intact *glpACB* operon. pGLP91, encoding *glpA*, is similar to pGLP15, as both are truncated at the *Xho*I site within *glpC* (corresponding to leucine$_{79}$). pGLP92, encoding *glpAC*, is similar to pGLP20, as both are truncated at the *Sal*I site within *glpB* (corresponding to valine$_{258}$). pGLP1, pGLP15 and pGLP20 also carry an intact *glpT* gene whereas the pGLP90 series plasmids do not.

* These plasmids highlighted carry the endogenous anaerobic *glp* promoter.

FIGURE 7. A Schematic Representation of the Construction of the T7 Expression Plasmids [pGLP90 Series]. The size and the *glp* genes present in the various recombinant plasmids carried in the pACYC184 and pUC vectors and the phagemids pBluescript II KS- or pBC KS- are as shown. Refer to Table 2 for a listing of the *glp* genes present in each plasmid and to text for a description of constructions [Section II.B.2a]].

Panel A: Construction of pGLP22 from pGLP1.

Panel B: Construction of the pGLP90 Series from pGLP22.

A

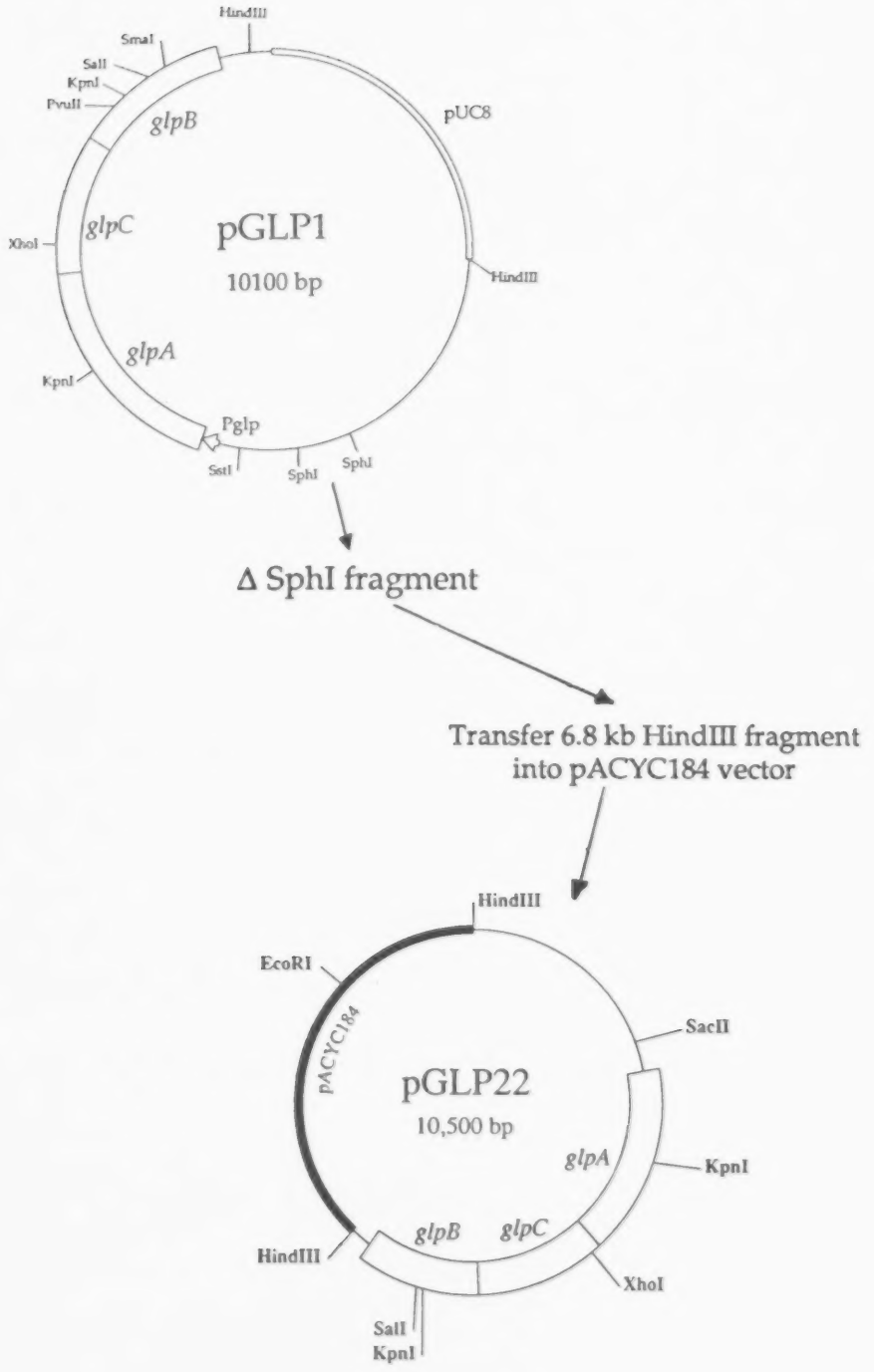
HindIII
SmaI
SalI
KpnI
PvuII
glpB
pUC8
glpC
pGLP1
10100 bp
XhoI
HindIII
glpA
KpnI
Pglp
SstI
SphI
SphI
Δ SphI fragment
Transfer 6.8 kb HindIII fragment
into pACYC184 vector
HindIII
EcoRI
pACYC184
SacII
pGLP22
10,500 bp
glpA
KpnI
glpB
glpC
HindIII
XhoI
SalI
KpnI

B

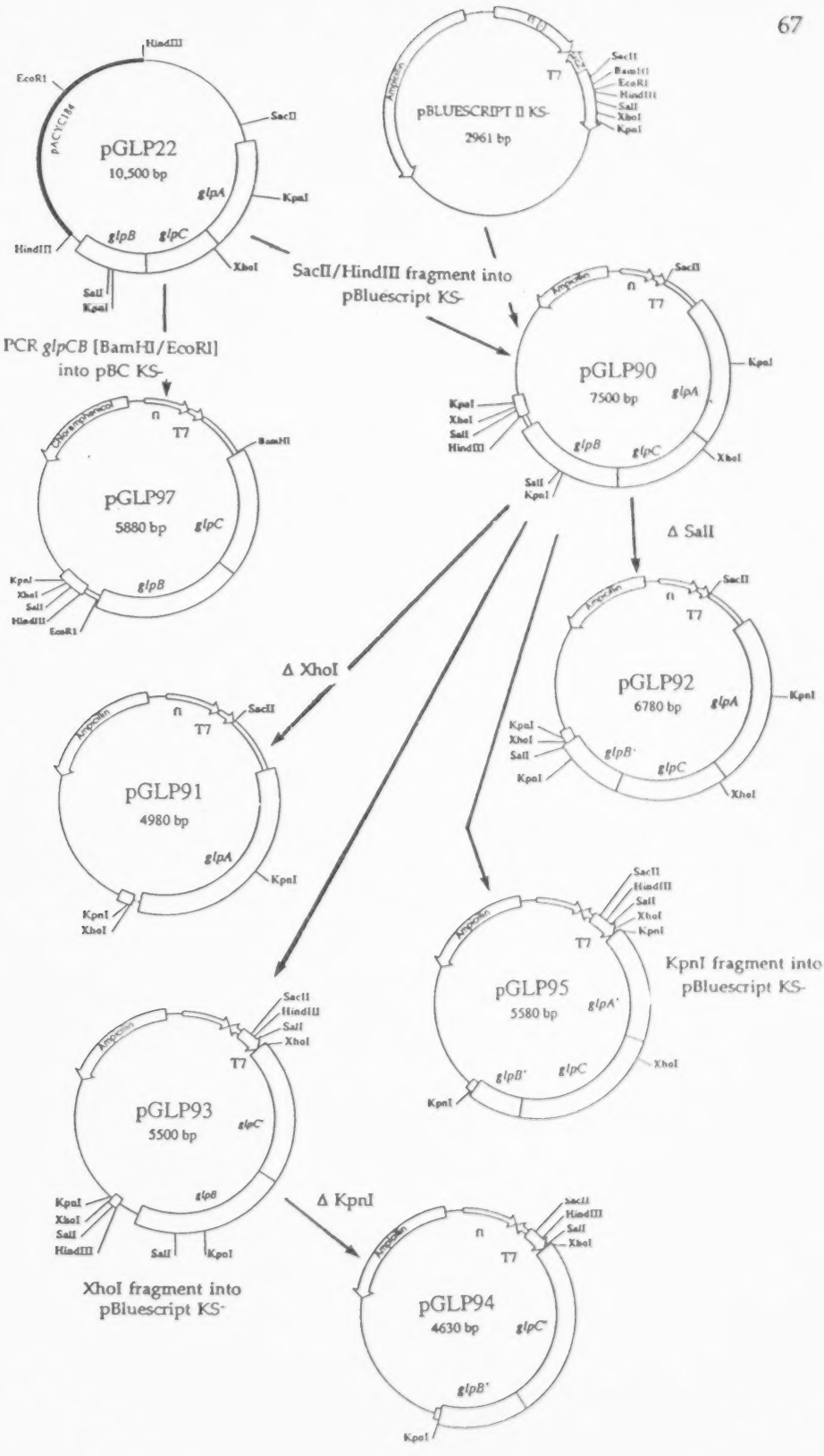
pGLP22
10,500 bp
pBLUESCRIPT II KS-
2961 bp
SacII/HindIII fragment into
pBluescript KS-
PCR glpCB [BamHI/EcoRI]
into pBC KS-
pGLP90
7500 bp
pGLP97
5880 bp
Δ SalI
Δ XhoI
pGLP92
6780 bp
pGLP91
4980 bp
pGLP95
5580 bp
KpnI fragment into
pBluescript KS-
pGLP93
5500 bp
Δ KpnI
XhoI fragment into
pBluescript KS-
pGLP94
4630 bp

TABLE 3

LIST OF OLIGONUCLEOTIDE PRIMERS

Primer Name	Sequence	Characteristic Features	Reference Within Study
MVA1	5'GGCCTATGATCATGAATGAC ACCAGCTTCCGAA	5' *glpB*, *Bcl*I restriction site	Construction of pGLP100 and pGLP101
MVA2	5'GCTAGAATTCAGGAGTTTAA GCCAGCGGCCTG	3' *glpB*, *Eco*R1 restriction site	Construction of pGLP97, pGLP100
MVA3	5'CGAAAGCGAATTTACCCGCT G	5' *glpC*, *Bam*HI restriction site	Construction of pGLP97
MV1	5'GCATGGCCTTTGCAG	pGEX-3X fusion site	Sequencing of pGLP100 and pGLP101
MV7	5'GCATCAAGCAGCTGCCGC	*Pvu*II restriction site, $glpB_{380}$*	Sequencing of GlpB C59S Mutant
MV8	5'CGCCAATCTTCACATCGG	$glpB_{180}$*	Sequencing of GlpB C12S Mutant
MV9	5'GCAGACGGTGCTCTTAATGC	$glpB_{30}$*	GlpB C12S mutagenic primer
MV10	5'CAACGTTTGCTGTTGATGC	$glpB_{230}$*	GlpB C59S mutagenic primer

* The subscript number indicates nucleotide position within the gene for which the primer is designed to anneal.

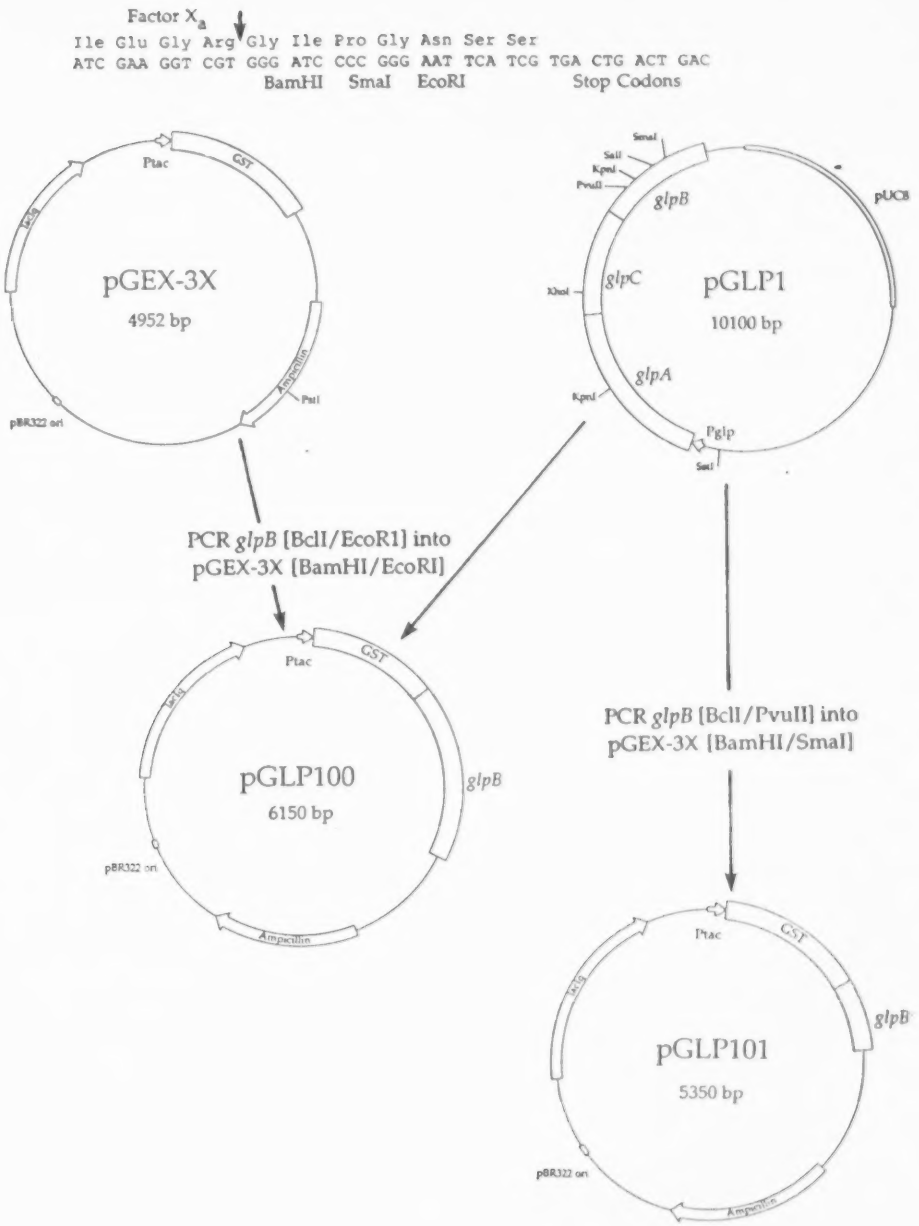

FIGURE 8. Construction of GST Fusion Plasmids [pGLP100 Series]. The fusion point sequence of the pGEX-3X vector is shown at the top of the figure, with the Factor X_a cleavage shown, as well as the restriction enzyme cloning site of the fusion point. The plasmids were constructed as described in text [Chapter II]. Refer to Table 2 for a listing of the section of *glpB* gene present in each fusion construct.

CHAPTER III. AMPLIFICATION OF THE *GLPACB* OPERON

With the identification of the third gene, *glpB* and the preliminary assignment of GlpB as a 44 kDa band, a major goal of the project was to develop a strategy for purification of the polypeptide. The aim was to be able to reconstitute a functional trimeric enzyme utilizing purified GlpB and previously purified and characterized GlpAC.

A prerequisite for purification of a particular protein is the availability of a method for identification of that protein. As GlpB has no catalytic activity associated with it, the aim was to consistently visualize a major band on SDS-polyacrylamide gels consistent with accumulation of large quantities GlpB.

The approach I adopted for the identification of GlpB and its amplification was to construct a series of recombinant plasmids of the *glpACB* operon under the control of the bacteriophage T7 promoter. The RNA polymerase of T7 is very selective for specific promoters that are rarely encountered in DNA unrelated to T7 DNA and efficient termination signals are also rare (Studier & Moffatt, 1986). The T7 RNA polymerase is thus able to make a complete transcript of almost any DNA that is placed under control of a T7 promoter. Furthermore, the T7 RNA polymerase is a very active enzyme and is able to elongate chains about five times faster than the endogenous *E. coli* RNA polymerase. Hence the system should lead to high levels of expression of the genes of interest, namely *glpA*, *glpC* and *glpB*. As developed by Tabor & Richardson (1985), the T7 RNA polymerase/promoter expression system has the RNA polymerase gene of T7 cloned into the plasmid pBR322 under the inducible control of the λ P_L promoter and the thermoinducible cI_{857} λ repressor [plasmid pGP1-2]. The gene of interest is cloned into a second plasmid or phagemid like pBluescript II^{TM}, which has a multi-cloning site with the bacteriophage T7 and T3 promoters. Induction is achieved easily by shifting the growth temperature from 30°C to 42°C, thus releasing the cI_{857} λ repressor. Selective inhibition of the *E. coli* RNA polymerase by addition of rifampicin, and radiolabelling with [^{35}S]-methionine, makes this expression system useful for identification of unknown gene products. As the RNA polymerase gene is carried on a plasmid, it can be transferred to a variety of host strains. However, if plasmids or antibiotic incompatibility exists, the strain BL21(DE3) carries the T7 RNA polymerase gene under control of the *lac*UV5 promoter as a lysogen in the *E. coli* chromosome and can be induced in this system by the addition of IPTG (Studier & Moffatt, 1986).

There was variability of expression of *glpB* as judged by the inconsistent

presence of the gene product on SDS-polyacrylamide gels. One of my first goals was to determine whether *glpB* was expressed as part of the *glpACB* operon and whether it could be expressed in the absence of GlpAC. Following conclusive identification of GlpB, the hope was to use the same expression system to produce quantities of GlpB suitable for biochemical analysis. Further, as the T7 system does not involve anaerobic regulation, I decided to examine whether or not the genes of an anaerobically expressed protein could assemble properly and function in the presence of oxygen. I also expected to obtain some preliminary information on the assembly of the subunits into a complex, as well as cofactor addition. The expression of the subunits was compared to the levels of expression of the genes under control of the endogenous promoter during anaerobic growth. The cellular localization of GlpB was investigated with the use of both the T7 RNA polymerase/promoter system and with overexpression of pGLP1 [*glpACB*] under endogenous anaerobic control.

A. Overexpression of *glp* Genes Using the T7 RNA Polymerase/Promoter Expression System

1. Identification of the *glp* Gene Products

a) Expression of the Genes

The construction of the plasmids, with various combinations of the *glp* genes behind the T7 promoter in the vector pBluescript II KS$^-$, was as described in Materials and Methods [refer to Figure 7 or Table 2].

To identify the gene products, I used [^{35}S] - methionine, [^{35}S] - cysteine mixture Tran^{35}S-Label^{TM} for radiolabelling using the T7 RNA polymerase/promoter expression system as developed by Tabor & Richardson (1985) and described in Materials and Methods [Section II.B.6a]. Due to the limitations of the experimental procedure, my use of the T7 expression system with radiolabelling was for identification of the GlpACB polypeptides in a qualitative manner. The quantitative distribution of the subunits in the various cellular fractions was not deemed appropriate. The procedure, as originally described (Tabor & Richardson, 1985), utilizes *E. coli* K38, containing plasmid pGP1-2 [Kn^r]. In initial expression and labelling experiments, I found that the *glp* polypeptides were poorly expressed in the system [Figure 9, lane 2], although the *frdABCD* operon expressed efficiently (Latour & Weiner, 1989). Furthermore, the specific activity of

anaerobic G3PDH observed in K38/pGP1-2/pGLP90 [*glpACB*] was only 0.18 U/mg. In previous studies with the cloned *glpACB* operon, *E. coli* JM83 was used as the host (Cole *et al.*, 1988). When JM83 was transformed with pGP1-2 and the *glp* recombinant plasmid, pGLP90 (*glpACB*), efficient expression of the Glp polypeptides migrating at 62 kDa and 43/44 kDa was observed [Figure 9, lane 5]. This was confirmed by the elevated levels of anaerobic G3PDH activity [Section III.A.3; 1.94 U/mg].

b) Subcellular Localization of the Glp Polypeptides

To investigate the subcellular localization of the Glp polypeptides I prepared cytoplasmic and particulate fractions using a lysozyme-osmotic shock procedure [Section II.B.6a]. Concentrated protein from T7 expression samples was examined by SDS-polyacrylamide gel electrophoresis and autoradiography [Figure 10]. No attempt was made to quantitate the distribution of each polypeptide between the cellular fractions as the amount of loading of each sample onto the SDS-polyacrylamide gel was variable. Panel A shows the soluble or cytoplasmic fractions and Panel B the particulate or membrane fractions. *E. coli* JM83/pGP1-2, without addition of rifampicin, expressed numerous proteins expected within the *E. coli* cell [lane 1]. Upon the addition of rifampicin, which inhibits *E. coli* RNA polymerase, very few proteins were detected [lane 2], although throughout the labelling experiments a band at about 44/45 kDa was among those seen in the soluble fraction. JM83/pGP1-2 with pGLP90, encoding the entire *glpACB* operon, produced three bands migrating as 62, 43 and 44 kDa [lane 3]. The 62 kDa and 43 kDa bands were observed in both fractions while the 44 kDa band was visible in the particulate fraction, migrating just above the the 43 kDa band. This upper band was faintly visible in the soluble fraction. The visualization of the third Glp polypeptide in Figure 10 [lane3], was a result of the better resolution of the 43/44 kDa band [observed in Figure 9, lane 5], due to a change in acrylamide concentration of the gel. Using pGLP92 which encodes *glpAC* and a truncated portion of *glpB*, I found the 62 and 43 kDa labelled polypeptides in the soluble fraction [Figure 10, A: lane 4]. I also observed the loss of the 44 kDa particulate band and a new 28 kDa polypeptide in the particulate fraction [B; lane 4]. From these studies I reasoned that the 44 kDa band seen in the particulate fraction of pGLP90 (*glpACB*) [B; lane 3] corresponded to the full length GlpB. To confirm that the 62 kDa polypeptide was the GlpA subunit I used pGLP91, which encodes only *glpA*. This resulted in the labelling of only the 62 kDa polypeptide [lane 5]. Surprisingly, this polypeptide was found predominantly in the

particulate fraction [Panel B]. Plasmid pGLP95 encoding *glpCB'* exhibited a 43 kDa labelled band in the soluble fraction [A: lane 6], corresponding to GlpC, and was faintly visible in the particulate fraction.

Expression of *glpCB* together on one plasmid, pGLP97 showed the localization of GlpC [43 kDa] to the soluble fraction [A; lane 8] with the 44 kDa polypeptide being localized in the particulate fraction [B; lane 8]. As well, complementation of pGLP97 (*glpCB*) with pGLP91 (*glpA*) again showed GlpC localized to the soluble fraction [A; lane 10], GlpB in the particulate fraction [B; lane 10], while GlpA was split between the two fractions. A large portion of GlpA was also seen in the crude debris or low speed pellet fraction [A, lane 11].

c) Expression of *glpB*

To test whether GlpB can be expressed independently of *glpAC*, I constructed pGLP93, carrying only *glpB*. Using JM83/pGP1-2/pGLP93 cells, I observed a band migrating at 44 kDa predominantly in the particulate fraction [Figure 9, lane 4 and Figure 10, B; lane 7]. With the recombinant plasmid, pGLP94, which does not contain the full length version of the *glpB* gene, the 44 kDa band disappeared [Figure 9, lane 3 and Figure 10, B; lane 9] and a smaller band migrating at 18 kDa was observed [Figure 9, lane 3]. The truncated polypeptide migrating at 18 kDa was not visible in Figure 10 due to the lower percentage of acrylamide gel used.

d) Expression Using BL21(DE3)

The lysogenic strain BL21(DE3) which carries an inducible chromosomal copy of T7 RNA polymerase was also used for expression of the *glpACB* operon and the various recombinant constructs. This strain was originally chosen to eliminate the need for pGP1-2 but it proved in some cases to be an efficient host for expression of the polypeptides [i.e. GlpA - next section]. I monitored the expression of the *glp* polypeptides by Coomassie blue staining of SDS-polyacrylamide gels and found that without the addition of rifampicin and [^{35}S]-radiolabelling, the identification of the two polypeptides, GlpC and GlpB, was usually inconclusive. Expression in LB or Enriched medium [Section II.A.4] enhanced the presence of other *E. coli* proteins particularly the presence of the 45 kDa background band, seen in the labelling experiments.

2. GlpA Forms an Insoluble Aggregate

a) Expression of GlpA

When GlpA was expressed in the absence of the other Glp polypeptides, it was localized to the particulate fraction under aerobic conditions [Figure 10, B; lane 5]. As well, during anaerobic growth of BL21(DE3)/pGLP91 (*glpA*) and JM83/pGP1-2/pGLP91 (*glpA*) in G/F medium, GlpA was also observed in the nonsoluble fraction. Note that only pGLP90, 91 and 92 carry the endogenous *glp* promoter as well as the T7 promoter. These observations suggested that GlpA was associating with the membrane or accumulating as an insoluble inclusion body [Williams *et al.*, 1982].

The nature of the overexpressed GlpA polypeptide as an inclusion body in nonradiolabelled cells [refer to Section II.B.6a,b] was determined by two approaches. The first strong indication that GlpA formed an insoluble aggregate was the observation that most of the GlpA collected in the particulate cell debris fraction after cell lysis and centrifugation at 9800 xg, a force too low to pellet membranes (Sprott *et al.*, 1994). The second approach to show that expression of *glpA* lead to the formation of insoluble aggregates was by electron microscopy of thin sections prepared from cells overexpressing the GlpA polypeptide. Electron micrographs of thin sections of JM83/pGP1-2/pGLP91 (*glpA*) showed the accumulation of electron dense particles, typical of inclusion bodies, in the cytoplasm which were free of the DNA/ribosome background of bacterial cytoplasm [Figure 11, Panel A]. The arrow in the diagram is showing the lighter gray region of the cell. The darker spots interspersed in the gray zone are believed to be more densely packed aggregates than the surrounding loosely packed aggregates. These gray areas or zones of clearing of the cytoplasmic material are not observed in the control strain, JM83/pGP1-2 [Panel B]. Together these results indicated that GlpA accumulated as an insoluble aggregate when expressed on its own.

b) Properties of Enriched GlpA

A lysed cell preparation of BL21(DE3)/pGLP91 (*glpA*) grown aerobically with IPTG induction [Section II.B.6b] was centrifuged at 120,000 xg. The particulate fraction was collected and layered on a 44 % sucrose solution as described - the 'simplified version' of Yamato preparation of inner membrane in Materials & Methods [Section II.B.11b]. Following centrifugation, an almost pure preparation of GlpA was

found in the pellet fraction [Figure 12, lane 3]. GlpA collected from the sucrose gradient pellet had a light brown color, and analysis of flavin fluorescence of the sample showed a very weak emission peak at 520 nm after excitation at 445 nm in citrate/phosphate buffer, pH 3.6. Although there was one major contaminating band within the brown pellet fraction [Figure 12, lane 3], these preliminary results suggested that some of the GlpA may contain FAD cofactor. However, as the FAD cofactor is noncovalently-bound (Schryvers, 1981), much of it could have been lost through the preparative handling.

Chymotrypsin digestion of purified GlpAC resulted in the cleavage of the 62 kDa GlpA band into two fragments, a 50 kDa band and a smaller band if ethylene glycol was present (Schryvers, 1981). The site for cleavage by chymotrypsin was predicted from the amino acid sequence of GlpA (Cole *et al.*, 1988). The 50 kDa band was found to contain the FAD cofactor. In the absence of ethylene glycol, there was a preferential degradation of the larger 50 kDa subunit, resulting in a preparation of intact small subunit which did not contain a flavin cofactor (Schryvers, 1981). To test whether GlpA, present as insoluble aggregates, was susceptible to chymotrypsin digestion, proteolytic digestion was conducted with the enriched fraction of GlpA [Section II.B.12]. A complete loss of the GlpA band [Figure 12, lane 4] with the subsequent formation of a smaller 28 kDa band was observed. When purified GlpAC was digested with chymotrypsin, in the absence of the stabilizer ethylene glycol, the same proteolytic fragment was seen [Figure 12, lane 2]. These results suggested that the chymotrypsin site was accessible in the inclusion body preparation of GlpA. The GlpA polypeptide was most likely in an unstable, unfolded state since degradation of the 50 kDa band occurred, similar to that seen with purified dimer in the absence of ethylene glycol.

c) Solubilization of GlpA

I attempted to solubilize the isolated GlpA inclusion bodies by a variety of methods. I used a variety of ionic and nonionic detergents, chaotropic agents and salts and found that only SDS and sarkosyl, at concentrations above 1%, were effective. I also attempted to co-express *glpA* [pGLP91] with *glpC* [pGLP97] but met with limited success. This was seen with the T7 radiolabelling expression studies where the GlpA polypeptide was still observed in the cellular debris fraction [Figure 10, Panel A, lane 11], and weakly in the soluble fraction [Figure 10, A, lane 9]. I lowered the growth temperature from 37°C to 30°C to see if a slower growth rate would aid in proper folding

of the GlpA polypeptide but no significant difference was observed. Only co-expression of GlpC with GlpA as a single polycistronic mRNA [pGLP90 (*glpACB*) or pGLP92 (*glpACB'*)] appeared to prevent the aggregation of GlpA [Figure 10, Panel A, lanes 3 and 4].

3. Enzymatic Activity of Aerobically Expressed *glpACB*

I examined the expression of anaerobic G3PDH under control of the T7 promoter to see if catalytic activity could be expressed under aerobic conditions and to determine optimal conditions for overexpressing G3PDH. I compared the efficiency of the plasmid-encoded thermoinducible T7 RNA polymerase to the *lac* inducible chromosomal T7 RNA polymerase for expression of anaerobic G3P dehydrogenase. Both BL21(DE3) and JM83/pGP1-2 were transformed with pGLP90 (*glpACB*), grown aerobically and induced as required.

Table 4 lists the G3PDH activities of cellular fractions from cells grown under aerobic conditions with temperature or IPTG induction. An increase of G3PDH activity was observed using JM83/pGP1-2/pGLP90 (*glpACB*) over the background strain JM83/pGP1-2. A similar increase in activity was seen with aerobically grown cells under IPTG induction of the T7 RNA polymerase [BL21(DE3)/pGLP90 (*glpACB*)]. In both strains, more than 85% of the activity was seen in the cytoplasm. I expected that pGLP92, encoding the GlpAC dimer, would exhibit a similar increase in enzymatic activity as it had previously been shown that the isolated enzyme is composed of the GlpAC subunits (Schryvers & Weiner 1982). Although increased G3PDH activity was observed in strain BL21(DE3)/pGLP92 (*glpACB'*) [Table 4: 2.13 U/mg], the lack of increased G3PDH activity in JM83/pGP1-2/pGLP92 (*glpACB'*) cellular fractions using the T7 expression system was unexpected [Table 4; 0.03 U/mg for both cellular fractions]. The unexpected result was reproducible and was found with several independent constructs of the plasmid and freshly transformed cells. The GlpA and GlpC subunits were being expressed as determined by [^{35}S]-methionine labelling [Figure 10]. As expected, no enzymatic activity was seen with GlpA (pGLP91), GlpC (pGLP95) or GlpB (pGLP93) alone, nor for GlpCB (pGLP97).

I also attempted to express G3PDH activity using BL21(DE3) or JM83/pGP1-2 transformed with both pGLP91 [*glpA*] and pGLP97 [*glpCB*]. A functional enzyme was marginally reconstituted in either host strain as seen in Table 4. G3PDH activity was observed for cells grown on Enriched medium or M9 supplemented medium. However,

the activity was only one-sixth [0.30 U/mg in the cytoplasmic fraction] that observed with pGLP90 (*glpACB*) or pGLP92 (*glpACB'*) [for BL21(DE3)], where the genes were on one plasmid or transcribed as a single polycistronic message. Again, much of the activity [85%] was found in the cytoplasmic fraction.

B. Overexpression of *glp* Genes Using Anaerobic Growth Conditions

The original overexpression of the *glpACB* operon was done in JM83 with anaerobic growth in G/F medium (Cole *et al.*, 1988). Although I was able to express the various *glp* genes under the control of the T7 promoter system, I was unsuccessful in obtaining useable quantities of GlpB to warrant any further studies or attempt purification.

1. Localization of GlpB

The T7 expression and [^{35}S]-radiolabelling studies suggested that GlpB was localized to the membrane fraction. To test whether this was the true localization of GlpB, I examined the distribution of GlpB in the cytoplasmic, membrane and particulate fractions using conventional Yamato preparations of inner and outer membrane fractions (Yamato *et al.*, 1975). JM83/pGLP1 (*glpACB*) cells, anaerobically grown in large [20 l] G/F cultures, were used as the starting material for cellular fractionation. A protein migrating at 44 kDa, which is consistent with its being GlpB, was associated with the inner membrane fraction [Figure 13, lane 2]. The 44 kDa band was not visible in the electrophoretograms of the outer membrane fractions of JM83/pGLP1 cells [Figure 13, lane 4]. The 44 kDa band had not been observed during purification of the soluble GlpAC dimer, which would have suggested a cytoplasmic location of the GlpB polypeptide (Schryvers & Weiner, 1981). Host strain JM83 cells, without the plasmid pGLP1, did not show any significant enrichment of the GlpB polypeptide in the inner membrane or outer membrane fractions [Figure 13, lanes 1 and 3, respectively]. Although the data are consistent with GlpB being associated with the inner membrane fraction of the cells, a location of GlpB cannot be conclusively assigned without doing more experiments. The identity of the 44 kDa band should be confirmed by amino acid sequence analysis or by specific reactivity with antibodies raised against this polypeptide or a synthetic peptide designed from the GlpB sequence. As well, antibodies raised against FrdC and FrdD, which are integral inner membrane proteins (Condon & Weiner,

1988), could be used to confirm the inner membrane fraction as such. It appeared that the Yamato procedure had been conducted properly for the presence of the outer membrane porins (Nikaido & Vaara, 1987) were only observed in the outer membrane fraction and are quite distinctive as prominent proteins in the outer membrane fraction. Once again though, antibodies specific for the porins should be tested.

Using the Yamato enriched fraction of GlpB, I attempted to solubilize the polypeptide from the membrane by a variety of ionic and nonionic detergents [Section II.B.11a]. Representative results of some of the various treatments are shown in Figure 14. Treatment with Triton X-100, a nonionic detergent which is typically used to solubilize integral membrane proteins (Thomas & McNamee, 1990), did not appreciably solubilize GlpB even at a concentration of 4 %. Only Sarkosyl, at 2 %, was efficient at solubilizing GlpB, with 2 % cholic acid to a lesser degree [Figure 14]. This method of treatment was not further investigated for EPR experiments suggested that the treatment was detrimental [Section IV.B2]. As a preliminary test to determine whether GlpB may be associated with the membrane by palmitic acid linkages with the Cys-Cys-Gly motifs [as described in Chapter I], the inner membrane preparation was treated with hydroxylamine, pH 9.0. This treatment is known to release palmitic acid linked to cysteine residues in proteins by thioester bonds (deVetten & Agre, 1988). Treatment with 0.4 or 0.8 M hydroxylamine did not solubilize GlpB from the inner membrane.

2. Enzymatic Activity by Anaerobic Expression of *glpACB*

I also examined the expression of G3PDH activity following anaerobic induction of the operon. Table 5 lists the G3PDH activity measurements of JM83/pGP1-2 and BL21(DE3) transformed with the various *glp* constructs [pGLP90 series]. The cells were anaerobically grown in G/F medium, and cellular fractions prepared as described in Materials & Methods. BL21(DE3)/pGLP90 (*glpACB*) showed a dramatic increase of G3PDH activity [5.79 U/mg] over the respective background strain, while JM83/pGP1-2/pGLP90 showed a slightly lower specific activity [3.31 U/mg]. Both strains showed greater increases in activity with anaerobic induction than with aerobic T7 induction of the *glp* genes [Table 4]. In contrast to the equivalent activity seen in aerobic BL21(DE3) transformed with pGLP90 (*glpACB*) or pGLP92 (*glpACB'*) [Table 4], there was less overexpression of pGLP92 during anaerobic growth compared to pGLP90 [1.16 vs. 5.79 U/mg, respectively]. Once again, minor activity was observed with pGLP92 (*glpACB'*) in JM83/pGP1-2 [0.28 U/mg]. As well, no activity was detected for

amplification of *glpA* (pGLP91) alone, as expected. Anaerobic growth expression was not tested for *glpC* (pGLP95), *glpB* (pGLP93), *glpCB* (pGLP97) or complementation of *glpA* (pGLP91) with *glpCB* (pGLP97) as the various constructs are not under control of the endogenous *glp* promoter.

C. Discussion

I have examined and compared the expression of anaerobic G3PDH under both aerobic and anaerobic growth conditions and in several host strains. Visual identification of the polypeptides on SDS-polyacrylamide gels, as well as anaerobic G3PDH activity, was used to compare expression. *E. coli* K38 has been used by many investigators to express proteins in conjunction with the T7 RNA polymerase/promoter system (Tabor & Richardson, 1985). Unfortunately, the Glp polypeptides were very poorly expressed [^{35}S-methionine labelling] under T7 RNA polymerase in this host although the identical plasmid constructions expressed well in *E. coli* JM83/pGP1-2 and in BL21(DE3). This was unexpected as the G3PDH activity was similar in K38 and JM83 grown under anaerobic conditions. G3PDH is positively induced by the FNR protein (Kuritzkes *et al.*, 1984) and is repressed by the GlpR repressor (Lin & Kuritzkes 1987) but it is unlikely that either of these proteins would modulate T7 RNA polymerase dependent transcription. Thus it is not clear why G3PDH was poorly expressed under T7 control in K38.

I compared the expression of the Glp subunits using two different T7 systems; the pGP1-2 encoded T7 RNA polymerase under λ cI$_{857}$ control (Tabor & Richardson, 1985) and the chromosomally encoded T7 RNA polymerase under *lac* regulation (Studier & Moffatt, 1986). My results indicated that both systems were equally effective in expressing anaerobic G3PDH [pGLP90 or *glpACB*]. I also compared the expression of G3P dehydrogenase under anaerobic induction of the endogenous *glp* promoter to the inducible T7 promoter systems grown during aerobic conditions. I found that whereas both the anaerobic and aerobic systems gave dramatic amplification of the activity, anaerobic expression was two to three fold better than aerobic induction. Anaerobic conditions may facilitate efficient assembly of the cofactors and the production of the subunits may be under more defined regulation during the slower anaerobic growth conditions. Recall that the anaerobic growth of cultures was carried out over 24 - 48 hr whereas aerobic expression was conducted for 2 hr. Activity measurements still indicated that anaerobic G3PDH can be expressed, assembled and associated with flavin

cofactors under aerobic conditions. This is in agreement with the results of Kuritzkes *et al.* (1984) using a β-galactosidase fusion system [ϕ(*glp-lac*)] in which the *glpA* gene was expressed aerobically. Kuritzkes *et al.* (1984) also studied the effect of an *fnr* mutant allele on anaerobic ϕ(*glpA-lac*) expression and demonstrated that the mutant allele impeded induction of the fusion operon by about 1/3 under anaerobic conditions. The two to three fold increase in expression during anaerobic conditions which I observed with the T7 expression studies reported herein [as compared to aerobic] may reflect the maximal *glpACB* induction with ArcA repression of *glpD* and FNR activation of *glpACB* (Compan & Touati, 1994).

When GlpA was expressed in the absence of GlpC [pGLP91], it accumulated as an inclusion body in the cytoplasm. Analysis by fluorescence showed weak incorporation of FAD, the flavin cofactor associated with GlpA (Schryvers & Weiner, 1982), but much of the cofactor could have been lost during preparative handling as it is noncovalently bound. Perhaps, the hydrophobic regions of GlpA which would normally be involved in interpeptide association with GlpC, caused the insoluble aggregation of the GlpA polypeptides in the absence of GlpC. However, I observed little solubilization of GlpA during co-expression of the two genes [*glpA* and *glpC*] on separate plasmids (pGLP91 and pGLP97). Expressed on its own, GlpA formed misfolded aggregates. Co-expression with GlpC as a polycistronic message [pGLP90 or pGLP92] did appear to help stabilize GlpA into its proper soluble state.

Many investigators are actively studying the mechanism and manner of how proteins fold, and why overexpression causes some overexpressed proteins to accumulate as inclusion bodies yet allows other polypeptides to fold properly (Creighton, 1990; Richards, 1991; Allewell, 1993). Further support for the difference of protein folding is seen with the overexpressed GlpC polypeptide in contrast to GlpA. Overexpressed GlpC was soluble as expected from the cellular location of the polypeptide as determined by the purification of the soluble dimer (Schryvers & Weiner, 1982). When both subunits were expressed together on one plasmid [pGLP90 (*glpACB*) or pGLP92 (*glpACB'*)] the solubility of GlpA was enhanced, indicating that GlpC may serve a chaperone-like role in addition to its catalytic function. It was interesting to see that expression of the two genes, *glpA* and *glpC* onto separate plasmids [pGLP91 and pGLP97, respectively] did not result in assembly of a functional enzyme to levels observed with single plasmid expression. This was evident not only from the G3PDH activity measurements but as well from the [^{35}S] -radiolabelling and relative band intensities. Relative band intensities of GlpC and GlpB as compared to GlpA

suggested a weaker expression of GlpCB as compared to GlpA [Figure 10, lane 10]. GlpA still appeared to aggregate as the corresponding polypeptide band on the gel was found in the cellular debris or low speed pellet fraction [Figure 10, Panel A, lane 11]. It appears that translation of polycistronic mRNA, *glpAC*, is needed within the cell for formation of a functional dimer, as evidenced from the lesser degree of reconstitution of G3PDH activity during complementation of pGLP91 [*glpA*] with pGLP97 [*glpCB*] compared to both genes [*glpA* and *glpC*] on one plasmid [pGLP90 or pGLP92].

Expression of GlpB as a single membrane-associated 44 kDa polypeptide was established by the [^{35}S] -radiolabelling during the T7 expression studies. This apparent localization was demonstrated when *glpB* was coexpressed with *glpC* and the division of the two polypeptides to their respective subcellular fractions occurred. The labelling studies suggested that GlpC was not required in a chaperone-like role for GlpB stability as it was for GlpA. GlpB appeared to be consistently located to the membrane fraction whether GlpC was present or not. Results from studies with Yamato membrane preparations using cells overexpressing the *glpACB* operon [JM83/pGLP1] suggested that GlpB is an inner membrane associated protein. The 44 kDa band was not present in the outer membrane fraction [Figure 13, lane 4], nor was the band observed in the cytoplasmic fractions during these experiments nor during the purification of the GlpAC dimer (Scryvers & Weiner, 1981). However GlpB exhibited unusual behavior it its inability to be solubilized by conventional detergents used for solubilization of other inner membrane proteins [i.e. Triton X-100 for FrdCD (Cole *et al.*, 1985)]. Perhaps it is for this reason, as well as poor staining with Coomassie blue stain that the presence of GlpB was undetected until the cloning and sequencing of the operon (Cole *et al.*, 1988). Alternatively, the *glpB* expression may be weaker than that of *glpA* or *glpC*, and hence results in lesser quantities of GlpB than GlpA or GlpC. The proposed weaker expression of *glpB* could be due to the overlap of the stop codon of *glpC* with the ATG initiator codon of *glpB*, thus restraining the coding potential of *glpB* (Cole *et al.*, 1988). This codon overlap scenario also occurs at the *glpA* and *glpC* interface and does not appear to affect translation. Future analysis of the various *glpACB* genes is recommended utilizing an expression vector carrying the endogenous *glp* promoter and FNR control regions, with a 'universal ribosome binding site' (Balbas & Bolivar, 1991). This may allow for quantitative measurements on the translation of the individual subunits to be conducted. Recall that with the *unc* operon [F_0-F_1 ATPase], the expression of the individual genes must rise and fall three times from one end of the operon to the other and the control appears to be largely post-transcriptional [differential

translation initiation] (Brusilow, 1993). The level of transcription of the various genes in the *glpACB* operon has not been investigated as yet, and may provide further clues to the difference in expression.

I expected that bacteria harboring a plasmid which only encodes *glpAC* [pGLP92] would express similar levels of enzyme activity compared to *glpACB* [pGLP90)], as the catalytic activity resides in the GlpAC dimer. However, as the data in Tables 4 and 5 indicate, JM83 harboring plasmid pGLP92 (*glpACB'*) did not express G3PDH activity. This was repeatedly observed with different constructs of pGLP92. Both the GlpA and GlpC polypeptides were synthesized in JM83 as indicated by [^{35}S]-methionine labelling experiments. The pGLP92 plasmid resulted in limited expression of G3PDH in BL21(DE3) grown anaerobically as compared to the activity levels seen with anaerobically grown BL21(DE3)/pGLP90. BL21 is an *E. coli* B strain, carries the *lon* and *ompT* mutations and thus lacks proteases known to degrade some polypeptides (Studier *et al.*, 1990). The protease La [*lon* gene] is essential for the degradation of most abnormal proteins and certain normal short-lived polypeptides (Chung, 1993). Perhaps, in a *lon*$^{+}$ background, GlpB may be necessary for stabilization of the GlpAC dimer. Once formed however, GlpB is evidently not required to maintain stability of the enzyme since the functional catalytic dimer can be readily purified (Schryvers & Weiner, 1982). A similar phenomena of association is observed with the fumarate reductase complex. If FrdC and FrdD are translated from separated plasmids, they do not form a functional anchor complex although they are synthesized and migrate to the membrane (Condon & Weiner, 1988). Thus, in the absence of full length GlpB [i.e. expression from pGLP92], the GlpAC dimer may be more susceptible to degradation, less accumulation of the polypeptides and hence the lower levels of observed enzymatic activity. In a *lon*$^{-}$ background [BL21(DE3)], the lack of the La protease may account for nondegradation and hence enhanced activity.

The results of the T7 expression studies provided clear indications that an enzyme that is normally expressed during controlled anaerobic expression could be overexpressed during rapid aerobic growth. The enzymatic activity measurements gave positive indication that the cell was able to assemble the polypeptides correctly and also incorporate the appropriate cofactors to create a functional enzyme. GlpA on its own localized to the particulate fraction, but when *glpC* was on the same plasmid as *glpA*, GlpC acted to enhance the solubility of GlpA, consistent with the soluble nature of the dimer. The functional assembly of the catalytic dimer appeared partially dependent upon a full length GlpB polypeptide as suggested from the difference in enzymatic activity in

the different background strains and the presence of the full length operon. Although the aerobic T7 expression system was able to effectively express the anaerobic G3PDH, anaerobic expression of the enzyme still appeared to be better, as activity measurements were slightly higher [2 - 3 fold]. Furthermore, the T7 system was useful for positive identification of the *glpACB* genes with the corresponding GlpACB polypeptides, but only GlpA was produced in significant levels to be clearly observed on Coomassie blue stained SDS-polyacylamide gels. It was necessary to resort to anaerobic expression of the *glp* genes with the endogenous *glp* promoter in order to produce enough GlpB to be able to localize the polypeptide to the inner membrane of *E. coli*.

The role of the GlpB subunit has been an enigma. Kuritzkes *et al.* (1984) showed by genetic means that GlpB participated in membrane association of GlpAC as did studies by Cole *et al.* (1988). However, the need for GlpB in anaerobic electron transport is not clear. The next chapter describes the investigation of this question.

FIGURE 9. Autoradiogram of [^{35}S]-Methionine Labelling of *glpACB* Genes in *E. coli* strains K38 and JM83. Samples were prepared, subjected to 12 % SDS-PAGE and autoradiographed as described in Materials & Methods. In the lane assignments, the genes carried on the pGLP90 series plasmid are listed in the brackets [i.e pGLP90 expresses *glpACB*]. Lane 1, K38/pGP1-2 [no *glp* genes]; lane 2, K38/pGP1-2/pGLP90 [*glpACB*]; lane 3, JM83/pGP1-2/pGLP94 [*glpB'*]; lane 4, JM83/pGP1-2/pGLP93 [*glpB*]; lane 5, JM83/pGP1-2/pGLP90 [*glpACB*]; lane 6, JM83/pGP1-2 [no *glp* genes]. The purified GlpAC dimer and the molecular weight markers were run in adjacent lanes [not shown], and their positions were as follows: The positions of the purified GlpAC dimer subunits are indicated on the right side of the panel, as well as the expected position of the 44 kDa GlpB band and the GlpB truncate (GlpB'). Arrows at left indicate molecular weight markers and from the top of the panel downward are: rabbit muscle phosphorylase b, 97,400; bovine serum albumin, 66,200; ovalbumin, 45,000; carbonic anhydrase, 31,000.

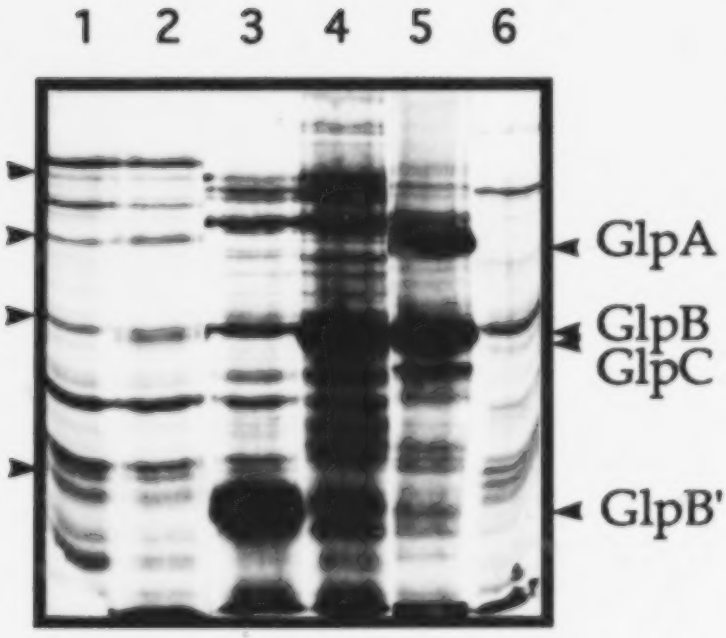
1 2 3 4 5 6
GlpA
GlpB
GlpC
GlpB'

FIGURE 10. Autoradiogram of the Cytoplasmic and Particulate Fractions of [^{35}S]-Methionine Labelled Cells. The various pGLP90 plasmids [refer to Table 2] were transformed into JM83/pGP1-2 and the samples were prepared [Section II.B.6a], subjected to 7.5 % SDS-PAGE and autoradiographed as described in Materials & Methods [Section II.b.13]. Panel A and Panel B show the cytoplasmic and particulate fractions, respectively. As in Figure 9, the genes expressed from each of the pGLP90 series plasmids are listed in the brackets following the plasmid number, while the controls in lanes 1 and 2 do not express any of the *glp* genes. Lane 1, JM83/pGP1-2 [no rifampicin]; lane 2, JM83/pGP1-2 [rifampicin added]; lane 3, JM83/pGP1-2/pGLP90 [*glpACB*]; lane 4, JM83/pGP1-2/pGLP92 [*glpACB'*]; lane 5, JM83/pGP1-2/pGLP91 [*glpA*]; lane 6, JM83/pGP1-2/pGLP95 [*glpC*]; lane 7, JM83/pGP1-2/pGLP93 [*glpB*]; lane 8, JM83/pGP1-2/pGLP97 [*glpCB*]; lane 9, JM83/pGP1-2/pGLP94 [*glpB'*]; lane 10, JM83/pGP1-2/pGLP91 [*glpA*]/pGLP97[*glpCB*]. Lane 11 in Panel A shows the cellular debris fraction of JM83/pGP1-2/pGLP91/pGLP97 [*glpA/glpCB*]. The positions of GlpA [62 kDa] and GlpC [43 kDa] are indicated on the right side of each panel, which were run in an adjacent lane. An arrow indicating the apparent position of GlpB [44 kDa] is also indicated for reference. Arrows at left indicate molecular weight markers and from the top of the panel downward are: rabbit muscle phosphorylase b, 97,400; bovine serum albumin, 66,200; ovalbumin, 45,000; carbonic anhydrase, 31,000. The position of the truncated GlpB polypeptide is indicated in Panel B, lane 4 with an arrow immediately adjacent to the band.

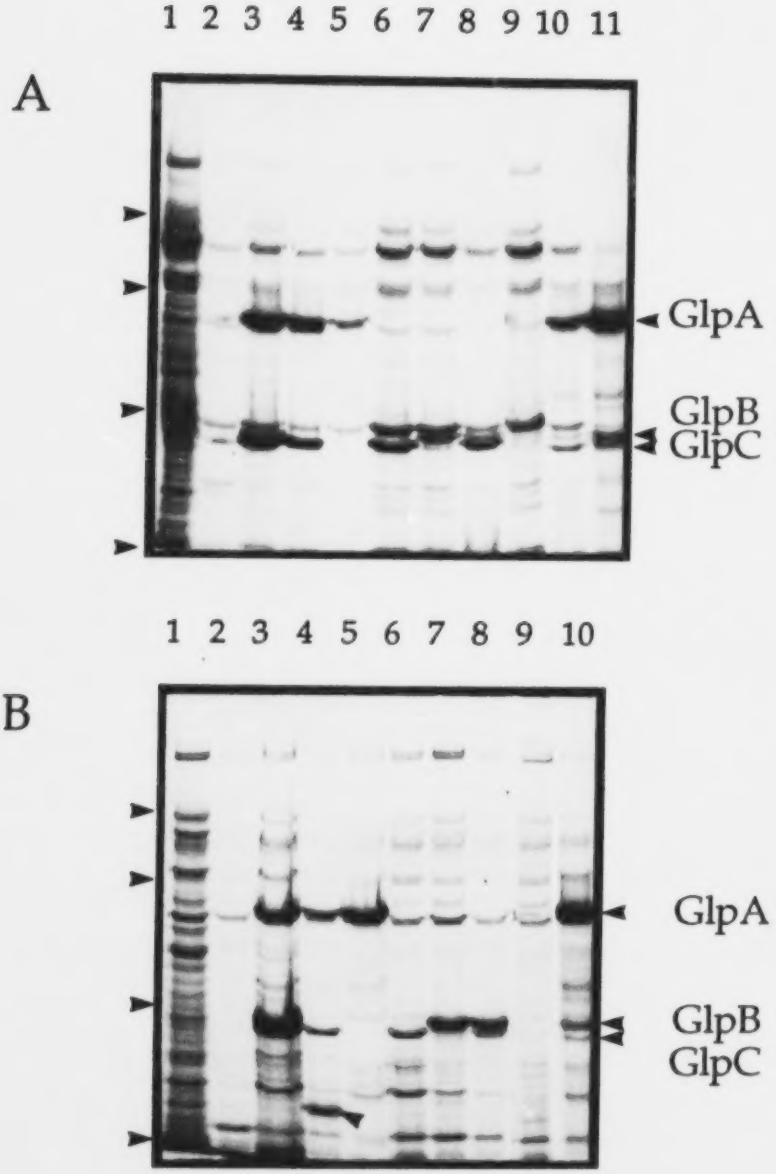
1 2 3 4 5 6 7 8 9 10 11
A
GlpA
GlpB
GlpC
1 2 3 4 5 6 7 8 9 10
B
GlpA
GlpB
GlpC

FIGURE 11. Electron Micrographs of JM83 Cells Overexpressing GlpA. Panel A shows JM83/pGP1-2/pGLP91 cells and Panel B shows the control background JM83/pGP1-2 cells. The thin sections of the cells were prepared by R. Bradley as described in Materials & Methods, and analyzed by electron microscopy and photographed by Dr. D. Scraba. Panel A magnification is 97,800 X and Panel B magnification is 67,000 X. The inclusion body or aggregation of GlpA is shown by the arrow in Panel A.

A

B

FIGURE 12. Analysis of GlpA Inclusion Body Preparation. BL21(DE3)/pGLP91 cells were prepared and analyzed as described in Materials & Methods. The samples were prepared [refer to Section II.B.12] and subjected to 10 % SDS-PAGE, and stained with Coomassie blue stain as described in Materials & Methods. Lane 1, purified GlpAC dimer, 10 μg; lane 2, Chymotrypsin digest of purified GlpAC dimer [TCA precipitated]; lane 3, Enriched GlpA preparation, 15 μg; lane 4, Chymotrypsin digest of enriched GlpA fraction [TCA precipitated]. The positions of GlpA and the peptide fragment thought to arise from GlpA [GlpA'] are indicated on the right of the panel.

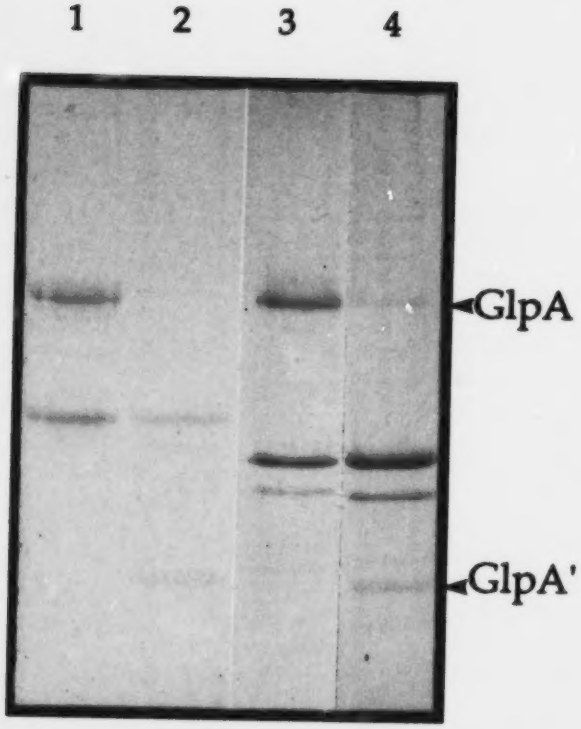
1
2
3
4
GlpA
GlpA'

TABLE 4

G3P Dehydrogenase Activity # from T7 Promoter During Aerobic Expression

Plasmid§	Cellular Fraction	BL21(DE3) [U/mg]+	JM83/pGP1-2 [U/mg]
None	Cytoplasmic	ND*	0.03
	Particulate	ND	0.02
pGLP90 [ACB]	Cytoplasmic	1.80	1.94
	Particulate	0.16	0.34
pGLP91 [A]	Cytoplasmic	ND	0.03
	Particulate	ND	0.03
pGLP92 [AC]	Cytoplasmic	2.13	0.03
	Particulate	0.27	0.03
pGLP93 [B]	Cytoplasmic	ND	0.02
	Particulate	ND	ND
pGLP95 [B]	Cytoplasmic	ND	0.02
	Particulate	ND	ND
pGLP97 [CB]	Cytoplasmic	ND	0.02
	Particulate	ND	ND
pGLP91/97 [A/CB]	Cytoplasmic	0.30	0.30
	Particulate	0.08	0.08

\# Preparation of cellular fractions in *E. coli* strains BL21(DE3) and JM83/pGP1-2 transformed with the various pGLP90 plasmids and determination of G3PDH activity was as described in Materials and Methods.

§ Letters in the brackets following the plasmid number indicate the *glp* genes expressed from the respective plasmid.

*ND Not Detectable

\+ Specific activity expressed in units (U) per milligram (mg) of protein . [One unit of activity is defined as 1 µmole of MTT reduced per minute].

FIGURE 13. Membrane Association of GlpB. The Yamato inner and outer membrane fractions of JM83 and JM83/pGLP1 (which overexpresses *glpACB*) were prepared [Section II.B.10] and the samples were subjected to 7.5 % SDS-PAGE and stained in Coomassie blue as described in Materials & Methods. Lane 1, JM83 cytoplasmic membrane fraction [30 µg]; lane 2, JM83/pGLP1 cytoplasmic membrane fraction [30 µg]; lane 3, JM83 outer membrane fraction [40 µg]; lane 4, JM83/pGLP1 (*glpACB*) [40 µg]; lane 5, purified GlpAC dimer [10 µg]; and lane 6, molecular weight markers [20 µg]. The location of the GlpA [62 kDa] and GlpC [43 kDa] subunits [corresponding to the bands in lane 5] and the expected location of the GlpB [44 kDa] subunit are indicated on the right side of the panel. The molecular weight markers [lane 6], from the top of the panel down, are: rabbit muscle phosphorylase b, 97.4 kDa; bovine serum albumin, 66.2 kDa; ovalbumin, 45.0 kDa; carbonic anhydrase, 31.0 kDa; soybean trypsin inhibitor, 21.5 kDa.

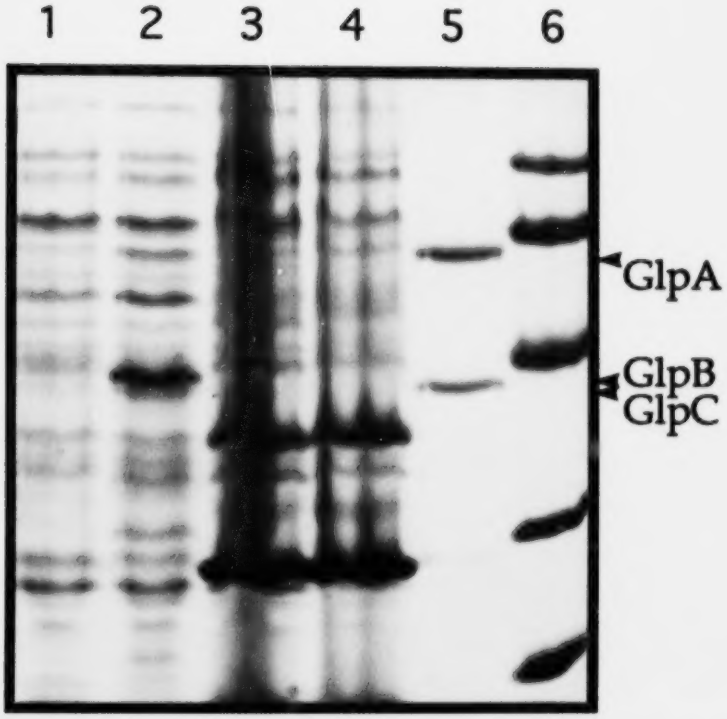
1
2
3
4
5
6
GlpA
GlpB
GlpC

FIGURE 14. Solubilization of GlpB from the Cytoplasmic Membrane by Detergents. The samples were prepared, subjected to 10 % SDS-PAGE and the gels were stained with Coomassie blue as described in Materials & Methods. Panel A and Panel B show the soluble and membrane [pelleted] fractions, respectively. Panel A: lane 1, purified GlpAC dimer; lane 2, 2 % DDAPS; lane 3, 2 % Thesit; lane 4, 2 % cholate; lane 5, 2 % n-octylglucoside; lane 6, 2 % Triton X-114; lane 7, 2 % Sarkosyl; lane 8, 2 % CHAPS; lane 9, 4 % Triton X-100; lane 10, 2 % Triton X-100; lane 11, 1 % Triton X-100; lane 12, Yamato inner membrane starting preparation. Panel B: lane 1, purified GlpAC dimer; lane 2, 1 % Triton X-100; lane 3, 2 % Triton X-100; lane 4, 4 % Triton X-100; lane 5, 2 % CHAPS; lane 6, 2 % Sarkosyl; lane 7, 2 % Triton X-114; lane 8, 2 % cholate; lane 9, 2 % Thesit; lane 10, 2 % DDAPS; lane 11, 2 % n-octylglucoside; lane 12, Yamato inner membrane starting preparation. The arrow at the right of each panel indicates the expected position of the GlpB [44 kDa] polypeptide.

A

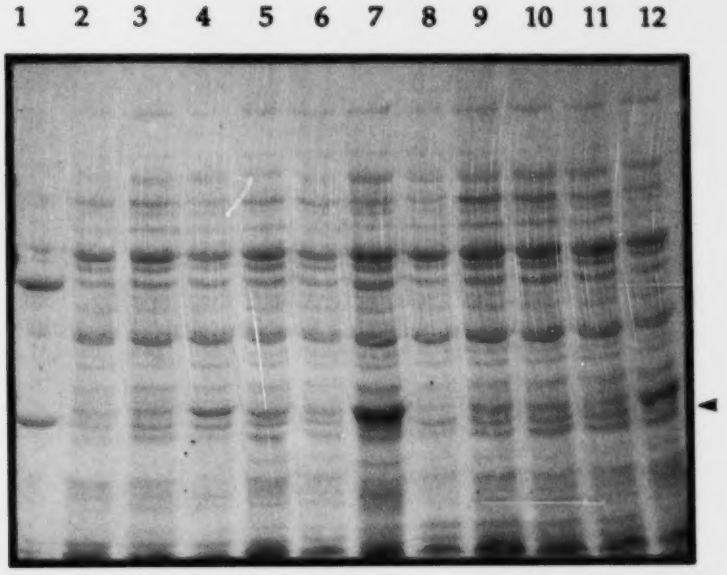

B

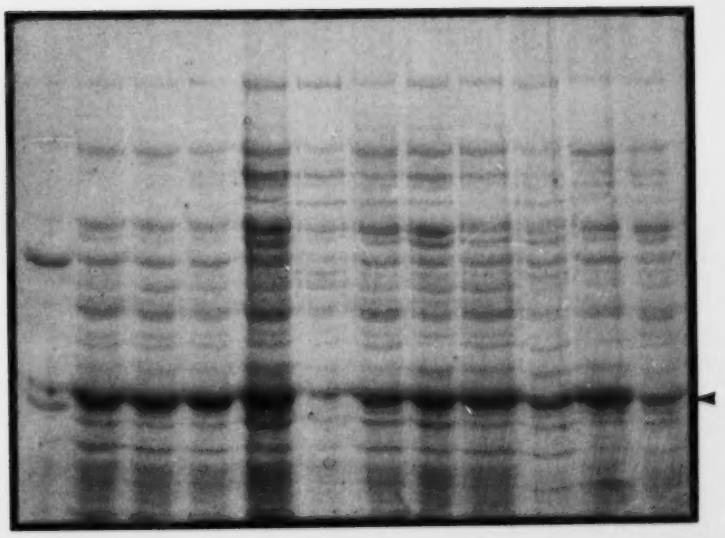

TABLE 5

G3P Dehydrogenase Activity[#] from *glp* Promoter During Anaerobic Expression

Plasmid[§]	Cellular Fraction	BL21(DE3) [U/mg][+]	JM83/pGP1-2 [U/mg]
None	Cytoplasmic	0.03	0.03
	Particulate	0.03	0.02
pGLP90 [ACB]	Cytoplasmic	5.79	3.31
	Particulate	0.89	0.88
pGLP91 [A]	Cytoplasmic	0.03	0.03
	Particulate	0.03	0.03
pGLP92 [AC]	Cytoplasmic	1.16	0.28
	Particulate	0.34	0.06

\# G3PDH activity was determined as described in Materials & Methods.

§ Letters in brackets following the plasmid number indicate the *glp* genes which are expressed for each of the respective plasmids.

\+ Specific activity expressed in units (U) per milligram of protein [One unit of activity is defined as 1 μmole of MTT reduced per minute].

Note: pGLP93, 95, and 97 do not carry an endogenous *glp* promoter and hence were not included in this study.

CHAPTER IV. PHYSIOLOGICAL ROLE OF GLPB

Kistler *et al.* (1969) originally reported the existence of an anaerobic L-α-glycerophosphate dehydrogenase of *Escherichia coli*. The dehydrogenase was characterized as a soluble enzyme in contrast to the membrane-associated aerobic G3PDH [*glpD*]. Maximal activity of the anaerobic dehydrogenase was observed only in the combined presence of exogenous FAD and FMN, whereas GlpD did not require added flavins. They originally reported the importance of the soluble dehydrogenase for anaerobic catabolism of glycerol and G3P, particularly when fumarate served as a hydrogen acceptor. Further studies by Lin's group (Miki & Lin, 1973) went on to show that anaerobic G3PDH and fumarate reductase constitute a functional complex which could catalyze dehydrogenation of G3P at the expense of fumarate without any added cofactor. The coupling activity exhibited high sensitivity to low concentrations of detergent, suggesting disruption of the membrane disassociated the functional complex. As well, reconstitution of the coupling activity was not possible with mixing of extracts containing the respective enzymes. These studies were among the first to describe that the two enzymes participate in an induced respiratory chain during anaerobic growth. However, because of the soluble nature of the dehydrogenase, it was not clear whether the dehydrogenase was structurally associated with the reductase as a complex, whether the dehydrogenase interacted with an intermediate membrane bound component or whether functional association was a transitory contact. These concerns were again addressed when the dehydrogenase was purified as a catalytic dimer (Schryvers & Weiner, 1982) and although Kuritzkes *et al.* (1984) provided some evidence that the anaerobic dehydrogenase may associate with a membrane polypeptide, the identification of this polypeptide was not clear. As mentioned, the polypeptide encoded by the third open reading frame, *glpB*, was assumed to be the membrane polypeptide which would associate with GlpAC based on Kuritzkes *et al.* (1984) genetic studies. The role of the third polypeptide, GlpB in the electron transport function of the anaerobic G3PDH complex was still in question. Based on the amino acid sequence of GlpB and the presence of the conserved ferredoxin cysteine motif for [Fe-S] clusters (Cole *et al.*, 1988) it is proposed that GlpB passes on the reducing equivalents from the GlpAC dimer to fumarate reductase via these proposed [Fe-S] clusters.

To investigate the physiological role of GlpB, I addressed two main questions: 1) Is GlpB essential for anaerobic growth? and 2) Does the polypeptide exhibit a redox center which may be involved in electron transfer? To investigate the first question, I

adopted the following approach. I complemented a mutant background strain, deficient in *glpACB* and unable to grow anaerobically on G3P/F, with various recombinant plasmids carrying genes of the *glpACB* operon. The mutant strain transformed with each of the plasmids was then tested for anaerobic growth on G3P/F. G3P/F was the medium of choice as maximum induction of the *glpACB* operon occurs when the cell grows on glycerol or G3P and fumarate [refer to section I.C.2a or I.D.1]. To address the second question, I used EPR spectroscopy to investigate the presence of a paramagnetic center. The EPR studies described in this chapter were conducted chronologically after the studies done with the full length GSTGlpB fusion studies [refer to Chapter V], as well as in conjunction with the EPR studies described in Chapter VI. The results are reported within this chapter though, for their contribution to the elucidation of the physiological role of GlpB.

In this chapter, I discuss some of the experiments which were conducted to address the questions put forth. Using a combination of plasmid complementation and EPR spectroscopy, I have shown that GlpB is an essential membrane protein which participates in oxidation-reduction reactions by transferring electrons from GlpAC to fumarate reductase. I have identified the presence of paramagnetic redox centers within GlpB, which are reduced by the artificial reductant dithionite, as well as the physiological substrate, G3P, and are oxidized by the physiological oxidant of the complex, fumarate.

A. Complementation Studies With MERV84

My aim was to express various combinations of the *glpACB* genes in a Δ*glpACB* genetic background in order to investigate if GlpB was essential for anaerobic growth with G3P. My initial studies were carried out in *E. coli* SH173, a strain deleted for both the *glpACB* operon and the *glpTQ* operon [necessary for G3P transport] (Ehrmann *et al.*, 1987). SH173 was unable to grow anaerobically on G3P/fumarate medium at incubation times up to 36 hr, whereas the parent MC4100 reached stationary phase in 36 hr. SH173, however, was able to grow anaerobically on G/F medium [Figure 15]. Enzyme assays indicated that the cells indeed lacked anaerobic G3PDH and aerobic G3PDH was not expressed. The growth was traced to the induction of a bypass pathway [refer to Figure 3] in which glycerol dehydrogenase [*gld* (Tang *et al.*, 1979); *gldA* (Truninger & Boos, 1994)] was expressed, although at very low levels [0.02 U/mg]. The kinase [GlpK] was replaced by the NAD^+ linked dehydrogenase as the first enzyme for glycerol dissimilation with the generation of NADH. Oxidation of NADH

not only ensures a supply of oxidant for NAD^+ requiring oxidation reactions, but can also generate a Δp.

1. GlpB is Required for Growth

Both aerobic and anaerobic G3P dehydrogenases can participate in the transfer of reducing equivalents from G3P to nitrate (Miki & Lin, 1975). Nitrate reductase is able to utilize both quinones, ubiquinone [predominant at high oxygen levels] and menaquinone [low oxygen]. Menaquinone is the only quinone species present during fumarate respiration. Anaerobic growth on glycerol and nitrate can be accomplished with either *glpD* or *glpA* though it is generally accepted that mutants missing anaerobic G3PDH do not grow anaerobically on either glycerol or G3P with fumarate as the hydrogen acceptor (Lin & Kuritzkes, 1987). G3P/F was the medium of choice for the growth experiments, in order to minimize a possible contribution of growth due to the expression of *glpD* on G3P/nitrate and to have maximal expression of the *glpACB* operon. As the original aim was to determine which subunits of anaerobic G3PDH were essential for growth, a background strain unable to support anaerobic growth on G/F or G3P/F was necessary. To overcome interference associated with the secondary growth pathway [*gld*], I constructed a double mutant [MERV84], lacking both the *gld* and *glpACB* pathways, by bacteriophage P1 transduction of a transposon insertion in the *gld* gene [*gld*::Tn10 mutation] from *E. coli* DLT242 into SH173 [Section II.B.3]. *gld* appears to be closely linked to glycerol kinase, *glpK*, and DLT242 is Δ*glpK gld*::Tn10. All the *gld*$^+$ transductants, including MERV84, were *glpK*$^-$. MERV84 was unable to grow anaerobically on G/F or G3P/fumarate media [Figure 15]. To carry out the complementation studies I transformed MERV84 with a set of plasmids carrying both the *glpTQ* operon and appropriate fragments of the *glpACB* operon [pGLP1 (*glpACB*), pGLP15 (*glpA*), and pGLP20 (*glpACB'*)]. The bacteriophage T7 promoter plasmids [pGLP90 series] described in Chapter III were not utilized as these plasmids were deficient in *glpT*. Reintroduction of the G3P transport activity, *glpT*, along with *glpACB* (MERV84/pGLP1) restored logarithmic growth on anaerobic G3P/fumarate media within 22 hours [similar behaviour as wild type - MC4100 and DLT242]. After a lag of 36 hr MERV84/pGLP20 started to grow [Figure 15] as did MERV84/pGLP15 after 52 hr. The long lag phases observed with the growth of MERV84/pGLP15 and MERV84/pGLP20 were indicative of a bacteriostatic culture or time period in which some metabolite must build up within the cell before the cell can utilize the compound to

grow.

2. *glpX* Does Not Complement MERV84

As activity measurements in SH173 suggested the induction of glycerol dehydrogenase, I obtained two plasmids from Dr. Boos [Frankfurt, Germany] which contained the coding region of the *glpX* gene (Truniger *et al.*, 1992); pVT13 and pVT14. Recall that *glpX* is a gene encoding a 40 kDa polypeptide of unknown function and is located in an operon with *glpFK* [refer to Section I.D]. pVT13 carries a *glpK*$^-$ *glpX*$^+$ region while pVT14 carries *glpK*$^+$*glpX*$^+$ in the opposite orientation. Although Truniger reported that she had as yet been unsuccessful in being able to detect glycerol dehydrogenase activity with either pVT13 or pVT14, I considered the possibility that it may require the appropriate background strain to exhibit expression [i.e. as I observed with K38 *vs.* JM83 in the T7 labelling experiments, Section III.A.1a]. I transformed both plasmids into MERV84 and DLT242 and tested for growth on G/F and G3P/fumarate media. The results are shown in Figure 16. My growth experiments agree with V. Trunigers' assessment that pVT13 and pVT14 are unable to complement a *gld*$^-$ background. Growth was observed in DLT242/pVT14 on G/F but this was as expected as pVT14 carries *glpK* and DLT242 is *glpA*$^+$. The experiments were conducted prior to the recent report by Truniger & Boos (1994) that *glpX* was indeed not glycerol dehydrogenase, but the enzyme instead was encoded for by the *gldA* gene at 89.2 min [not 88.6 minutes; *glpX*]. My complementation growth studies with *glpX* confirmed their studies. Interestingly, the *gldA* gene is cotransducible with *glpFKX*, with a frequency of 31 % (Truniger & Boos, 1994). Although the function of *glpX* is unknown and may not be directly involved with glycerol dehydrogenase, the expression of *glpX* may be essential to glycerol metabolism when the cell is in a stressed condition as in the SH173 mutant background. Hence, the presence of *glpX* should be considered in growth experiments with glycerol dehydrogenase or the G3P dehydrogenases.

B. GlpB Exhibits a Paramagnetic Center

1. EPR Visible Center Exhibited in the Reduced State of Whole Cells

As described in the Introduction of the thesis, electron paramagnetic resonance spectroscopy is a useful technique for the study of [Fe-S] centers in biological systems.

Whole cells of JM83 with and without the plasmid pGLP1 [*glpACB*] were grown anaerobically in G/F medium and harvested [aerobically] as described in Materials & Methods. EPR spectra of whole cell samples of JM83 and JM83/pGLP1 reduced with 2.5 mM dithionite are shown in Figure 17, Panel A. The reduced spectrum of the host JM83 was primarily of the fumarate reductase [iron-sulfur] Center 1 signal [major peaks at g = 2.03 and a peak-trough at around g = 1.94] (Johnson *et al.*, 1985; 1988). The spectrum of JM83/pGLP1 [*glpACB*] was a composite of G3PDH and fumarate reductase. To determine the effect of the overexpression of the *glpACB* operon, a difference spectrum of the JM83/pGLP1 spectrum minus the JM83 spectrum is also shown in Figure 17. The contribution of the signal from overexpression of GlpACB showed features in the g = 2 region [g values of 2.00, 1.96 and 1.88], suggesting the presence of iron-sulfur centers although definitive characterization of cluster type is discussed in Chapter VI. No major features attributable to GlpACB overexpression were observed in the oxidized state of the cells. Although the purified GlpAC dimer was reported to contain nonheme iron (Schryvers & Weiner, 1981), no signal was observed in the reduced state with the GlpAC preparation [this was determined during the GSTGlpB fusion study experiments - Section V.A.6]. The lack of a signal associated with the dimer would suggest that the signal observed with the analysis of cells overexpressing the operon is due to the presence of the GlpB polypeptide. Whole cell samples of JM83 transformed with pGLP15 [*glpA*] or pGLP20 [*glpAC*] and reduced with dithionite were also analyzed [refer to Figure 49, Chapter VI]. The spectra exhibited features predominant of the fumarate reductase center 1, as was previously seen with the reduced spectra of JM83 whole cells [Figure 17]. Although there were slight changes from the *glpA* only case [pGLP15], the reduced spectrum for expression of JM83/pGLP20 [*glpAC*] still resembled the JM83 spectrum and did not show any definitive characteristic features of JM83/pGLP1 [*glpACB*] expression. It is not likely that the overexpression of GlpA or GlpAC resulted in the formation of proteins devoid of normally occurring iron sulfur centers. Lack of the centers due to overexpression of the subunits would then be expected with overexpression of the full operon, and this was not the case. The features of the reduced signal of JM83/pGLP1 [*glpACB*] cells over the background JM83 cells are thus attributed to the GlpB polypeptide.

SH173 ± pGLP1 whole cells were also reduced with dithionite and analyzed by EPR. Similar spectra to those observed with the JM83 host cells were observed but the intensity of the signal was weaker.

A large contribution of fumarate reductase [Fe-S] center 1 was seen in the

background of JM83 and JM83/pGLP1. It was hoped that analysis of strain MI1443, which carries a Δ*frd*, would aid in deconvoluting the spectra associated with the *glp* center(s). MI1143 cells were grown anaerobically in glucose/peptone media. There was a signal associated with the dithionite reduced MI1443/pGLP1 whole cells spectrum with g-values similar to the signal observed with JM83/pGLP1 [Figure 18], but growth and expression were poor for proper characterization of the spectra.

2. Analysis of Membrane Fraction

As GlpB is a membrane bound polypeptide, further characterization of the signal was attempted using membrane fractions of JM83/pGLP1 cells. The crude membrane fractions were isolated and analyzed as described in Materials & Methods. Figure 17, Panel B shows the EPR spectra of the dithionite reduced crude membrane fractions of JM83 and JM83/pGLP1, as well as the difference spectrum [JM83/pGLP1 minus JM83]. There was a significant change in the lineshape of the GlpB reduced signal upon breakage of the cells. The signal for GlpB was similar to the whole cell spectrum with g values still around 2.00, but altered with peaks at g = 2.00 and 1.98 and troughs at g = 1.94 and 1.88. Samples prepared from Yamato inner membranes of JM83/pGLP1 cells were also prepared and analyzed with very similar spectra obtained as for crude fractions, but the contribution of GlpB being more enriched [Figure 19; ~ 3400 gauss]. In conjunction with the GlpB detergent solubilization studies [refer to Section III.B.1], I investigated whether detergent solubilization of the GlpB polypeptide from the membrane would alter the paramagnetic center. As it was observed that Sarkosyl and cholic acid [at 2 %] yielded some degree of solubilization, the soluble fractions of these detergent treated samples were analyzed by EPR. The spectra obtained showed a significant loss of the features attributed to GlpB [Figure 19], confirming that significant denaturation had occurred. It was because of this result that further studies using detergent solubilized fractions were not conducted.

C. G3P reduction of GlpB

The ability of the physiological substrate, G3P, to produce a similar reduced state signal was tested as described in Materials & Methods and the resulting spectra are shown in Figure 20. Reduction of JM83/pGLP1 cells by G3P [Spectrum b] exhibited a similar signal to that observed with the dithionite reduced sample [refer to Figure 17,

Panel A]. This indicated that the physiological substrate, G3P, was a reductant for the GlpB iron-sulfur centers. Other electron donors such as formate [Spectrum c] and lactate [Spectrum d] were also tested but the observed spectra appeared similar to that seen with JM83 cells [Spectrum a]. Importantly, incubation with the electron acceptor fumarate altered the signal to one representative of the oxidized state [Spectrum e], suggesting that the GlpB paramagnetic centers are intermediary between the primary electron donor and the terminal electron acceptor. The oxidized signal of JM83/pGLP1 cells treated with fumarate [spectrum e] exhibited features representative of the diminution of the fumarate reductase Center 1 spectral features and the appearance of the sharp peak at g = 2.02 with a trough immediately upfield, characteristic of the oxidized [3Fe-4S] center 3 of fumarate reductase (Johnson *et al.*, 1985; 1988).

D. Discussion

In a series of experiments, I examined the physiological role of GlpB, the third polypeptide of the anaerobic G3P dehydrogenase operon, by a combination of genetic complementation and biophysical analysis. Initially, I examined the requirement for the *glpB* gene product for restoration of anaerobic growth on G3P in a strain lacking the entire *glpACB* operon. Growth was only restored when all three of the genes *glpAC* and *B* were present and expressed. As well, the growth curve was similar to that observed in wild type cells, with short lag times and a stationary phase being reached within 22 hours. The essential requirement for GlpB suggested that GlpAC, which has the observed catalytic activity *in vitro*, was unable to funnel the electrons from the oxidation of G3P in a productive manner to the menaquinone pool in the absence of GlpB.

It was necessary to carry out the growth experiments in a strain lacking the NAD^+-dependent glycerol dehydrogenase because I found that under the selective conditions used, a bypass pathway was induced permitting anaerobic growth on glycerol independent of GlpACB [refer to Figure 3]. In cells overexpressing only GlpAC [MERV84/pGLP20] I consistently observed anaerobic growth after a lag of 36 hr even though glycerol dehydrogenase was inactive. The source of this growth was unclear but it may have resulted from selection of mutants with an alternate electron acceptor for GlpAC. The aerobic G3PDH [GlpD] may have become functional under these stressed anaerobic growth conditions, although activity was negligible. It is possible that the dalayed growth of the strain MERV84/pGLP20 resulted from a balance between plasmid or protein overexpression toxicity and dependence on G3PDH oxidation for growth, but

is unlikely as negligible G3PDH activity was detected. Most likely, the observed growth was due to the induction of a rescue metabolic pathway of a G3P product. Although no viable counts on the cell culture were conducted, the culture may have been bacteriostatic, until a particular metabolite accumulated, which may have induced the rescue pathway. This would also explain the observed growth properties of MERV84/pGLP20 and MERV84/pGLP15 after extremely long lag periods of 30^{+} hours.

Although the glycerol dehydrogenase [*gld*] pathway is a minor bypass to allow growth on glycerol, it was originally reported to be weakly expressed in wild type strains (Asnis & Brodie, 1952). Also, the dehydrogenase was induced during aerobic conditions [i.e. *glpK glpD glpR* mutant that regained its ability to grow on glycerol (St. Martin *et al.*, 1977; Tang *et al.*, 1979)]. It is thus interesting to have observed growth in SH173 due to the induction of glycerol dehydrogenase during anaerobic growth. In reporting the identification of *glpX*, Truniger *et al.* (1992) could not determine a function. They showed that *glpX* encoded a 40 kDa protein, which matched the 39 kDa apparent size as analyzed by SDS-PAGE reported previously for glycerol dehydrogenase (Tang *et al.*, 1979). Further comments by Truniger *et al.* (1992) suggested a mutant was required that expressed *glpX* in the absence of glycerol kinase in order to test for the role of GlpX in glycerol metabolism. The role of *glpX* is perplexing, particularly with the identification of the *gldA* gene at 89.2 minutes encoding for glycerol dehydrogenase (Truniger & Boos, 1994). The expression of *gldA* was dependent on strain background and was maximally expressed during stationary-phase growth. The expression studies of *gldA* were conducted with aerobic growth conditions, and the authors (Truniger & Boos, 1994) suggested that the *gldA* pathway for the utilization of glycerol under anaerobic conditions did not exist in *E. coli*. The results of my studies were contrary to these findings as my growth experiments, where the induction of glycerol dehydrogenase was observed, were carried out in glycerol media during anaerobic growth. Perhaps *glpX* in some way modulates the expression of *gldA* during anaerobic growth. In SH173, a copy of the *glpX* gene and the *gldA* gene are present, and hence the induction of glycerol dehydrogenase during anaerobic growth on glycerol can occur. In MERV84, both genes have been replaced by the respective mutations from DLT242 by P1 transduction, and hence lack of the ability to grow anaerobically on glycerol. Growth was not restored with the pVT13 [*glpX*] plasmid, as the *gldA* mutation was still present in the strain. It would be necessary to independently test whether the isolated *gldA* gene would restore growth of MERV84 during anaerobic growth or whether *glpX* as well was required. The presence of the *gldA* gene offers further evolutionary

speculation as to why *E. coli* would have such duplication or minor variance of a number of genes which perform the same or similar functions within the cell. Perhaps *gldA* and *glpX* only manifest themselves when the other *glp* genes are severely compromised or increase the normal expression of the *glp* genes by some unknown mechanism.

The interaction of some primary dehydrogenases with the cytoplasmic membrane is a poorly understood phenomenon whereas the terminal oxidases and reductases of electron transfer chains have clearly identified membrane anchor domains and all subunits are firmly associated with the membrane (Hederstedt & Ohnishi, 1992; Hosler *et al.*, 1993; Weiner *et al.*, 1992). In the case of proline dehydrogenase, the catalytic subunits were found in the cytoplasm. Upon reduction, proline dehydrogenase associated with an acceptor in the membrane to pass its reducing equivalents to the quinone pool (Wood, 1987). With other electron transport chain coupled dehydrogenases, a membrane association has been observed but the nature of this interaction was not clear. For example, GlpD, was shown to be membrane-associated and required lipid for activity (Schryvers *et al.*, 1978), yet examination of the inferred amino acid sequence did not identify any transmembranal α-helical segments (Austin & Larson, 1991). D-Lactate dehydrogenase (D-LDH) interacts with the cytoplasmic membrane, requires detergent, yet has no lengthy stretches of hydrophobic amino acids. D-LDH apparently interacts with the membrane via several separated structural elements (Sun *et al.*, 1993). I have shown that the GlpAC dimer transfers its reducing equivalents to the terminal reductase via GlpB, perhaps in a manner analogous to proline dehydrogenase, although I have not been able to distinguish a difference in binding of the dimer to the membrane associated with a change in redox state. Although GlpAC is found in the cytoplasm of broken cells, it may be associated with the membrane and GlpB in intact cells. Recall from the T7 labelling/expression studies [Section III.B.6a], a weak GlpB band was observed in the soluble fraction, and as well GlpA and GlpC were observed in the particulate fraction. These observations may indicate some interaction of the polypeptides or may just reflect carryover of material during handling. The observed changes in the EPR spectral properties upon lysis of the cells suggested that a structural change had occurred within the protein and further supports the idea that the Glp polypeptides are interacting.

Kuritzkes *et al.* (1984) had obtained genetic evidence from genetic fusions studies for an additional subunit which they proposed would anchor the catalytic dimer. Although an additional subunit was identified when the DNA sequence of the operon became available, the role of this polypeptide as an anchor has not been substantiated

(Cole *et al.*, 1988). My inability to confirm an anchor function may reflect conformational changes associated with cell lysis but it is also possible that the interaction between GlpAC and GlpB is transient. My results do support the localization of GlpB to the cytoplasmic membrane and hence the subunit is suitably located to interact with the menaquinone pool.

The presence of highly conserved ferrodoxin type iron-sulfur binding motifs in GlpB led me to investigate the EPR properties of the protein. The enzyme exhibited iron-sulfur like signals which were paramagnetic in the reduced state at temperatures near 20 K. The functional role of GlpB in electron transfer was confirmed. The EPR centers became paramagnetic upon reduction with either an artificial electron donor or the physiological donor, G3P. Other electron donors such as lactate or formate were without effect indicating that GlpB reduction is specific to G3P and was not simply reflecting equilibration of reducing equivalents in the membrane (Rothery & Weiner, 1991). Importantly the centers were oxidized by addition of the electron acceptor, fumarate. Together these results indicate that GlpB is a participant in the electron transport path.

The participation of the paramagnetic centers is important in the understanding of the electron pathway within the G3PDH/fumarate reductase complex. The initial characterization of the centers is discussed in the next chapter.

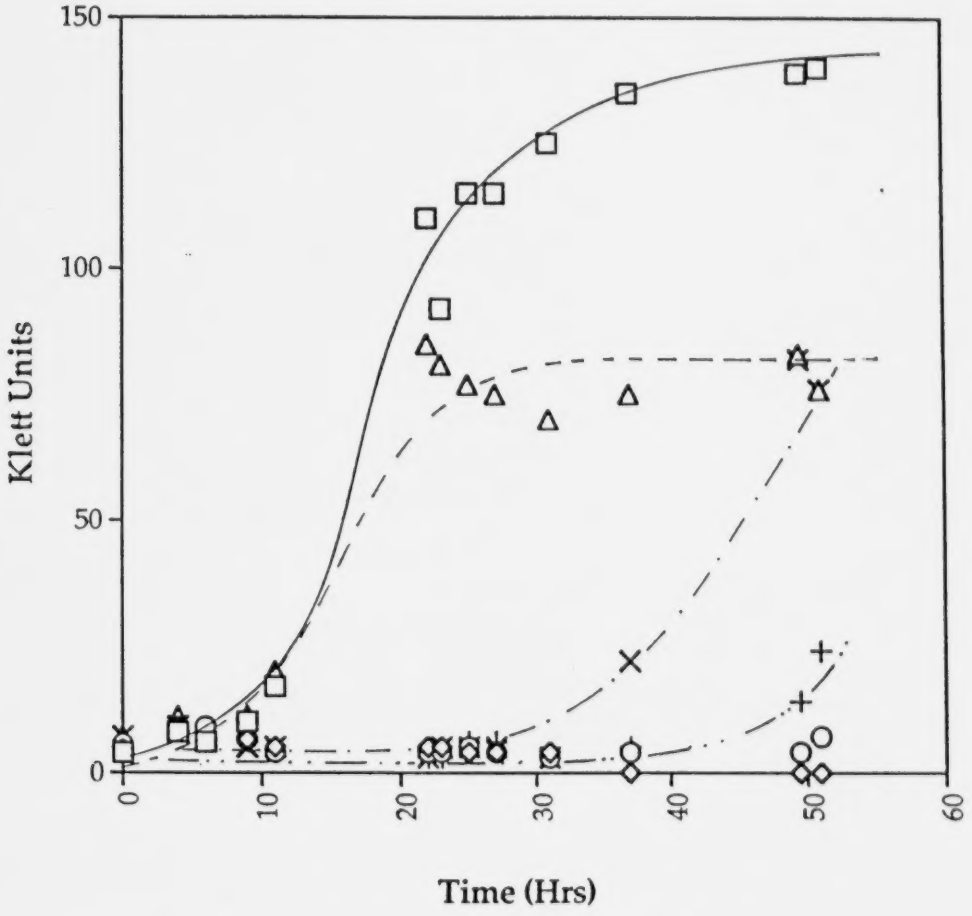

FIGURE 15. Complementation of MERV84 with *glp* Genes. Cultures containing SH173 or MERV84 were grown on glycerol/fumarate (G/F) medium and MERV84 cells alone or harboring plasmids pGLP1, pGLP15 and pGLP20 were grown in 160 ml Klett flasks, anaerobically at 37°C in G3P/fumarate (G3P/F) medium. The turbidity was followed in a Klett Summerson colorimeter equipped with a No. 66 filter. Symbols: □, SH173 (G/F); ◇, MERV84 (G/F); O, MERV84 (G3P/F); Δ, MERV84/pGLP1 [GlpACB]; X, MERV84/pGLP20 [GlpAC]; +, MERV84/pGLP15 (GlpA).

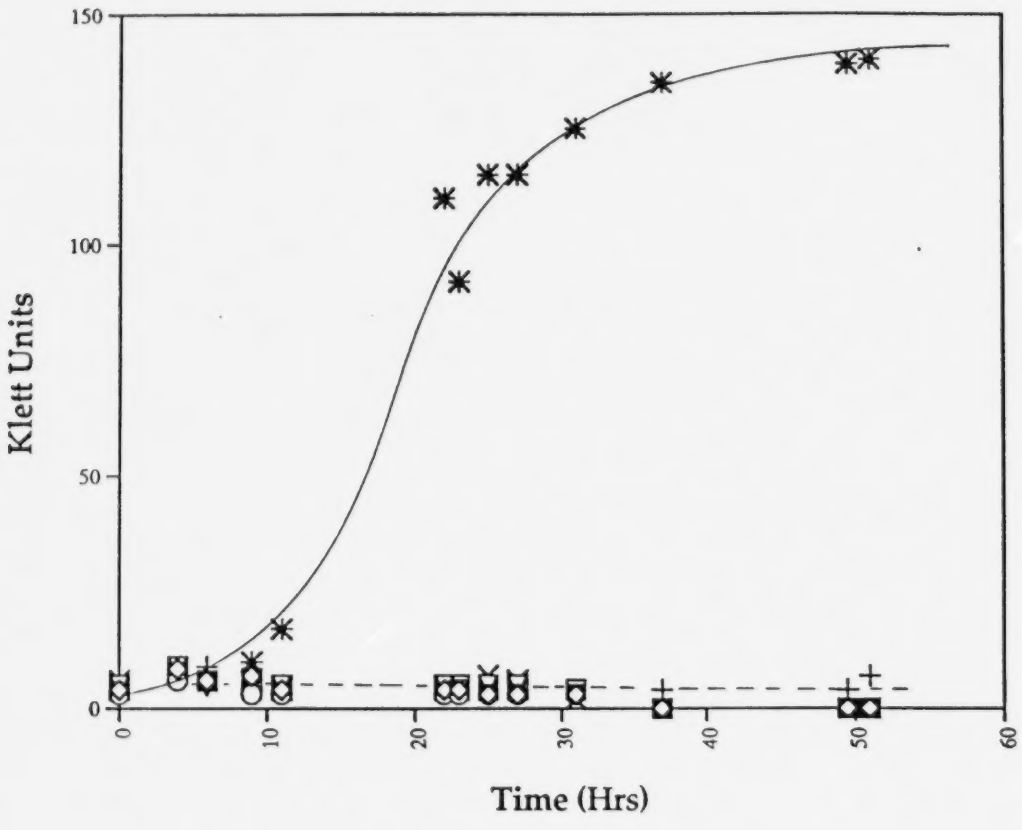

FIGURE 16. *glpX* Does Not Complement MERV84. Cultures containing MERV84 harboring plasmids pVT13 and pVT14 were grown on glycerol/fumarate (G/F) or G3P/fumarate (G3P/F) medium in 160 ml Klett flasks at 37°C. The turbidity was followed in a Klett Summerson colorimeter equipped with a No. 66 filter. Symbols:◇, MERV84/pVT13 [*glpX*] (G/F); O, MERV84/pVT14 [*glpKX*] (G/F); ✱, SH173 (G/F); □, MERV84 (G/F); +, MERV84 (G3P/F); ▽, MERV84/pVT13 (G3P/F); X, MERV84/pVT14 (G3P/F).

FIGURE 17. EPR Spectra of the Paramagnetic Center of JM83/pGLP1 at 20 K.
Panel A: EPR spectra of whole cells reduced with 2.5 mM dithionite. Spectra (a) JM83/pGLP1 cells; (b) JM83 cells; and (c) Difference spectra of spectrum (a) - (b). g-values are as indicated. Samples were prepared and spectra were recorded as described in Materials & Methods.
Panel B: EPR spectra of crude membranes reduced with 2.5 mM dithionite. Spectra (a) JM83 cells; (b) JM83/pGLP1 cells; and (c) Difference spectra of spectrum (b) - (a). g-values are as indicated. Samples were prepared and spectra were recorded as in Panel A. Asterisks are used to indicate the features attibuted to the *glpACB* overexpression.

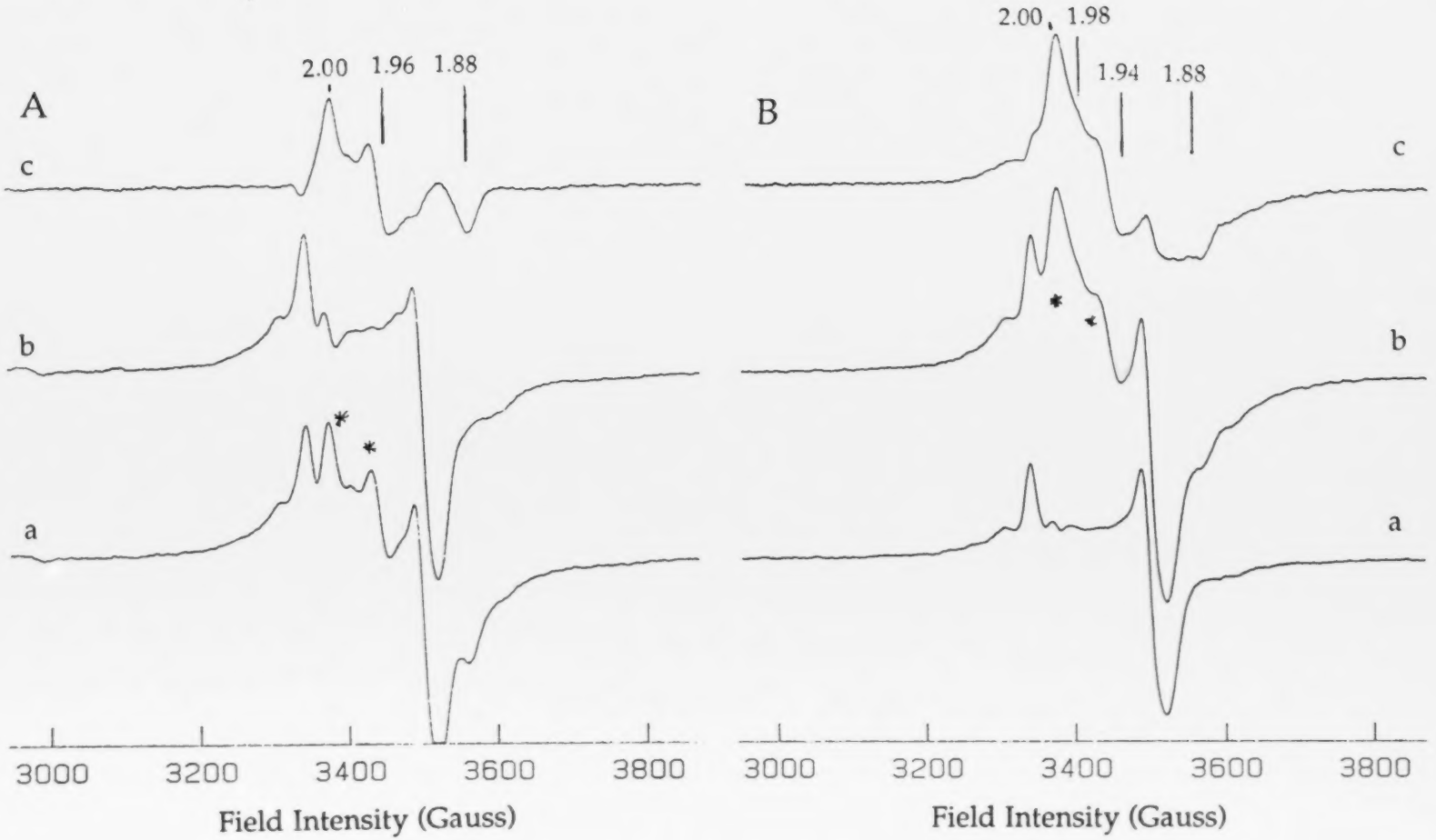
A
2.00
1.96
1.88
c
b
a
3000
3200
3400
3600
3800
Field Intensity (Gauss)
B
2.00
1.98
1.94
1.88
c
b
a
3000
3200
3400
3600
3800
Field Intensity (Gauss)

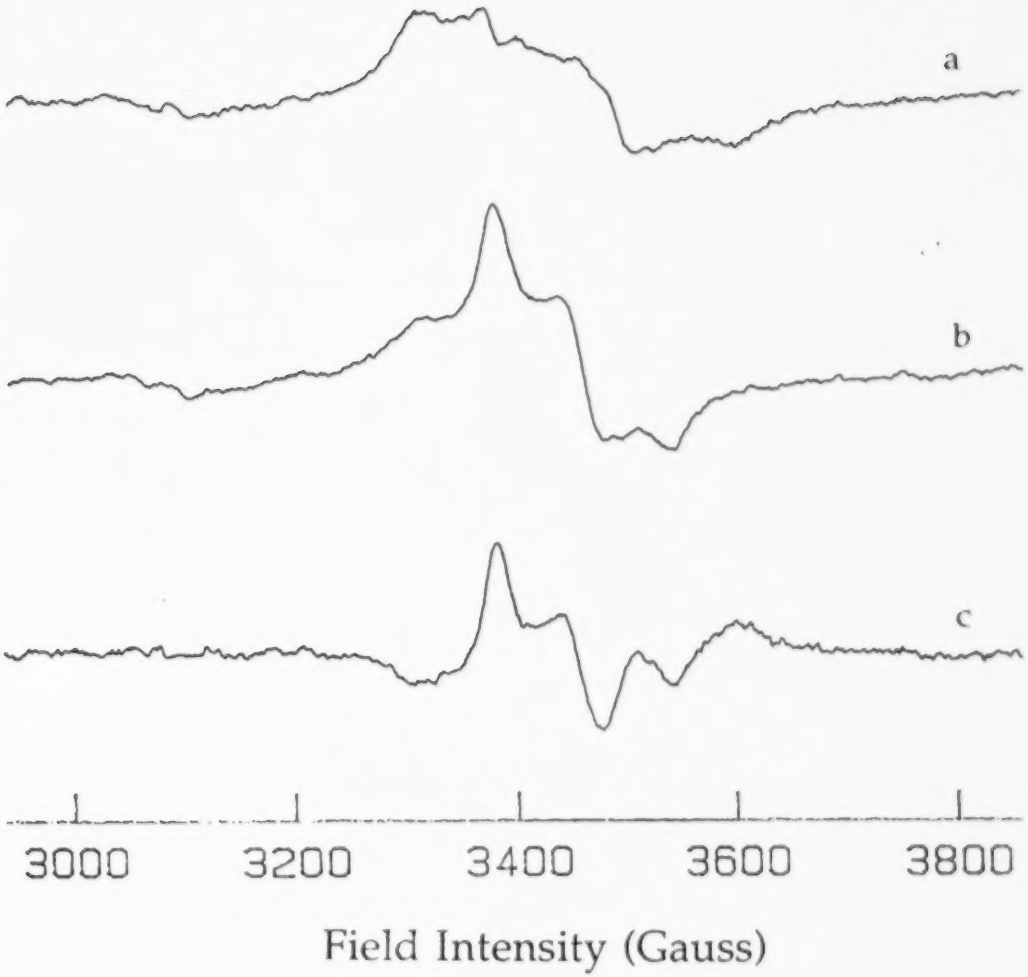

FIGURE 18. EPR Spectra of Whole Cells at 20 K of GlpACB in MI1443 [*frdABCD*$^-$]. The whole cell extracts were reduced with 2.5 mM dithionite as described in Materials & Methods. Spectra (a) MI1443 cells; (b) MI1443/pGLP1 cells; and (c) Qualitative difference spectrum of spectrum (b) - (a). Samples were prepared and spectra were recorded as described in Materials & Methods.

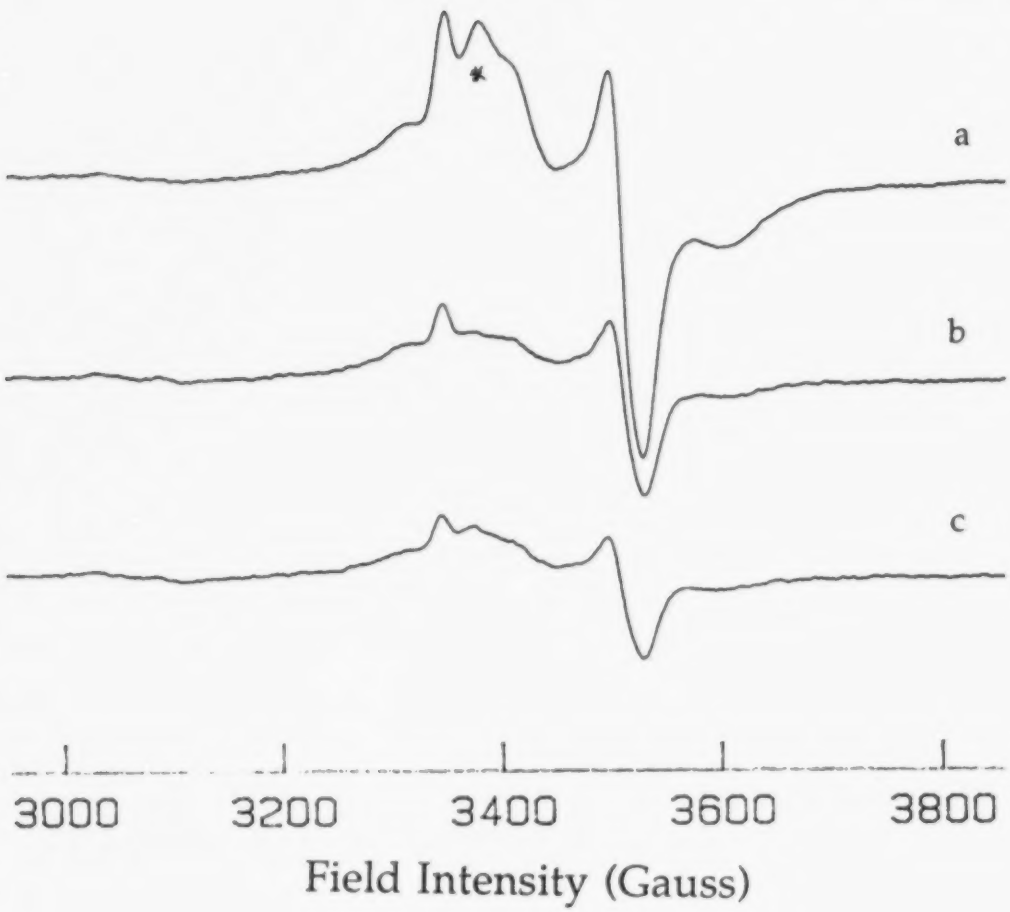

FIGURE 19. EPR Spectra at 20 K of Yamato Inner Membranes of JM83/pGLP1. The inner membranes of JM83/pGLP1 cells grown on glycerol/fumarate medium were prepared and solubilized with detergent as described in Materials & Methods. The detergent soluble fractions as well as the inner membranes prior to treatment with detergent were reduced with 2.5 mM dithionite. Spectra (a) Pretreated inner membranes; (b) 2 % Sarkosyl treated soluble fraction; and (c) 2 % cholate treated soluble fraction. Samples were prepared and spectra recorded as described in Materials & Methods. The spectra were normalized for tube calibration. An asterisk indicates the features of the spectrum as discussed in the text.

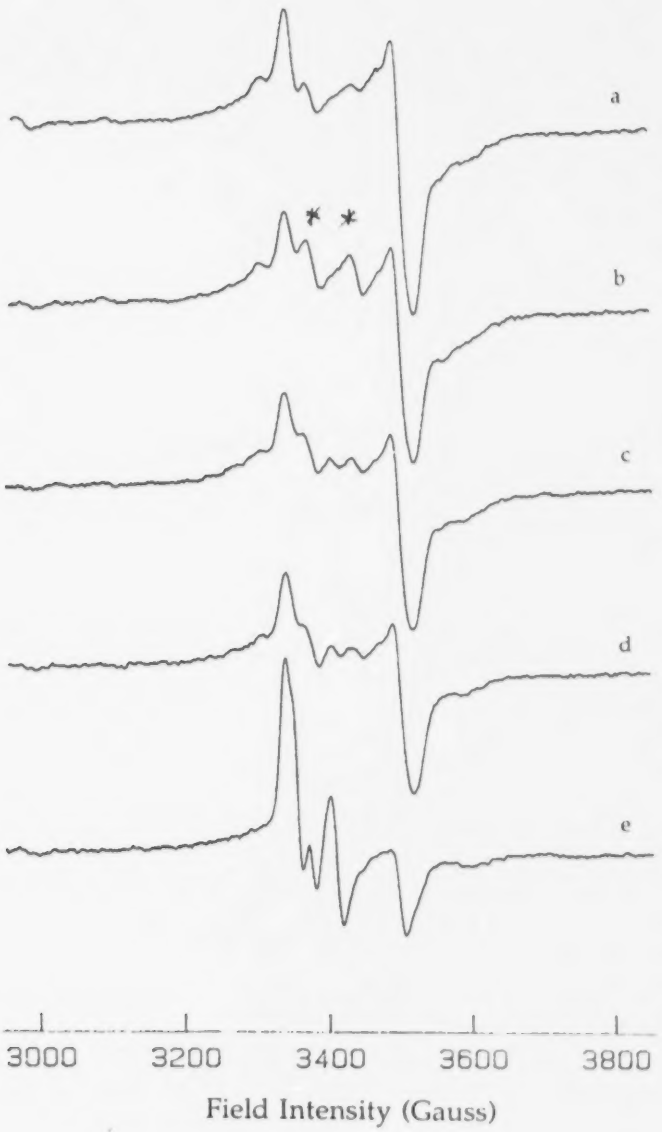

FIGURE 20. EPR Spectra at 20 K of Whole Cells Incubated with Physiological Substrates. Spectrum (a) JM83 reduced with 20 mM G3P; (b) JM83/pGLP1 reduced with 20 mM G3P; (c) JM83/pGLP1 reduced with 20 mM formate; (d) JM83/pGLP1 reduced with 20 mM lactate; and (e) JM83/pGLP1 oxidized with 25 mM fumarate. Samples were prepared and spectra recorded as described in Materials & Methods. The spectra were normalized for tube calibration. An asterisk indicates the features of spectrum b which are attributed to the reduction of the Glp paramagnetic center.

CHAPTER V. ANALYSIS OF GLPB REGIONS BY GST FUSIONS

The amino acid sequence of GlpB (Cole *et al.*, 1988) predicted several interesting motifs as previously described [Section I.D.2e]. Figure 21 is a schematic of the various motifs of GlpB. The focus of the last chapter was the discussion of the importance of GlpB for growth of the cell during anaerobic growth and the presence of a paramagnetic center as originally proposed from the presence of the *Clostridium*-like Fd cysteine motifs in the amino-terminal region. The presence of the various histidines scattered throughout the mid section of the GlpB sequence was interesting as histidines are known to bind *b*-type hemes which interact with the quinone pool in the membrane. Based on structural similarities which exist in the sequence of hydrophobic segments which bind the cyt *b* hemes (Degli Esposti, 1989), H_{167} was predicted to have a strong potential to act as a heme binding ligand, while H_{97}, H_{133} and H_{175} were of low potential. Two histidines are generally required to bind a *b*-type heme. Also in the sequence of GlpB was the sequence $CX_2CX_{11}CXH$ which may be a potential metal binding domain or involved in coordination of a [2Fe-2S] cluster in the carboxy terminal end of the polypeptide. These various motifs offer intriguing possibilities for electron transfer within the polypeptide as well as the electron transfer pathway to the quinone pool. Furthermore, the Cys-Cys-Gly motifs may provide a mechanism for membrane attachment of the polypeptide, as there are no obvious transmembrane segments within the sequence.

The studies described to this point in the thesis have demonstrated the apparent localization of the GlpB polypeptide to the inner membrane and the failure to purify the polypeptide without changes to the redox center. To conduct more quantitative biophysical and biochemical studies with GlpB, especially to determine which regions of the polypeptide were important for function, I overproduced and purified the polypeptide by an alternative method from those previously described. The alternate method I employed was the use of the plasmid expression vector pGEX-3X to construct fusion polypeptides with the carboxy terminus of the *Schistosoma japonicum* Sj26 glutathione S-transferase (GST) protein (Smith & Johnson, 1988) and GlpB. The GST fusion system was used as it provided a rapid means of overexpression and affinity purification of the protein. Conditions used for solubilization of the fusion protein, such as addition of detergents in the buffers, have shown that the detergents do not disrupt binding to glutathione-agarose (Smith & Johnson, 1988). The construction, expression, purification and spectral properties of two GSTGlpB constructs, namely the full length

fusion protein and a second construct which contains approximately the first third of the GlpB polypeptide are described in this chapter.

A. Full Length GSTGlpB [Expression of pGLP100]

1. Expression of GSTGlpB

To obtain large quantities of GlpB, I constructed a fusion protein with glutathione S-transferase using the pGEX-3X expression vector as described in Materials & Methods. The recombinant plasmid pGLP100 carried the entire *glpB* coding region as an in-frame fusion to the carboxy terminus of GST. The DNA construct was under control of the *E. coli* synthetic *tac* promoter and was inducible by IPTG. It was transformed into *E. coli* strain BNN103, which was *lon*$^-$ like BL21(DE3). Large quantities of a protein, migrating on SDS-polyacrylamide gels at 64 kDa, were produced in cells transformed with pGLP100, grown on LB medium at 37°C and induced with IPTG [Figure 22, Panel A, lane E], but not when IPTG was omitted [lane D]. Neither plasmid-free BNN103 nor BNN103/pGEX-3X produced a major protein migrating at 64 kD [lanes B & C]. BNN103/pGEX-3X overexpressed GST [lane C; 26 kDa] as expected. It was concluded that the 64 kDa-protein was the expected GSTGlpB fusion protein.

Similar expression of the fusion protein was observed in cells induced at temperatures between 20°C and 37°C [see below]. Expression was unaffected by the addition of magnesium, iron or calcium to the medium.

2. Localization of GSTGlpB

The subcellular localization of GSTGlpB was monitored by densitometric analysis of Coomassie blue stained SDS-PAGE gels following French Press cell lysis of the cells and differential centrifugation of the cellular extract. The cytoplasm, of cells induced at 37°C, contained a small amount of GSTGlpB accounting for ~ 6 % of soluble protein [Figure 22, Panel A, lane F]. GSTGlpB was the major protein [40 %] of the 6 000 xg particulate cellular debris fraction [lane G]. Thus, despite the highly soluble nature of the GST polypeptide alone (Smith & Johnson, 1988), the fusion of the GlpB polypeptide to the GST polypeptide resulted in a less soluble protein than GST alone. Increased solubilization of the fusion protein was achieved by the addition of 1 % Triton

X-100 to all buffers. The large percentage [40 %] of GSTGlpB in the particulate cellular debris fraction suggested that the fusion protein, overproduced at 37°C, accumulated as insoluble inclusion bodies. Similar results were seen when cells were grown at 30°C. Induction at lower temperatures [20°C] has been shown to limit the formation of inclusion bodies for some proteins (Chalmers *et al.*, 1990). As shown in Figure 22, Panel A, I was able to express GSTGlpB efficiently at 20°C and at this temperature the GSTGlpB was 10 % of the total soluble fraction [lane H] while only being 6 % of the particulate fraction [lane I].

3. Affinity Enrichment

To enrich for GSTGlpB, I applied the soluble fraction [at 6 000 xg] to a glutathione agarose affinity chromatography column. With this fractionation step I obtained enriched GSTGlpB suitable for EPR investigation. As I did not have an enzymatic assay for GSTGlpB, I estimated the purification and recovery by semi-quantitative densitometer analysis of Coomassie blue stained PAGE gels [Figure 22, Panel B] and by relative EPR signal heights. The enrichment for the fusion protein from the starting material [Figure 22, Panel B, lane 3] was three to four fold as the GSTGlpB polypeptide was 30 - 40 % the final concentrated fraction [lane 4]. This enrichment step was efficient and resulted in equivalent purification from the soluble fraction obtained at 20°C, 30°C or 37°C. In the final Amicon filtration concentration stage of the purification, the fusion protein was observed to adhere to the membrane filter and required numerous washings to remove it from the membrane. This suggested atypical properties or aggregation of the GSTGlpB fusion protein.

4. Site Specific Cleavage with Factor X_a

It was my intent to cleave GlpB from the fusion protein by utilizing the unique human Factor X_a cleavage site [Ile-Glu-Gly-Arg] engineered in the fusion site. I conducted the cleavage reaction as described in Materials & Methods and monitored Factor X_a cleavage over a 12 hour time course at 20°C. This was done by electrophoresis of the samples taken at various time points during the cleavage reaction, on SDS-polyacrylamide gels. The GlpB band could only be observed on the gel at samples taken at 1 - 3 hours. By 4 hours significant degradation was seen which increased with further incubation. I monitored cleavage at a reduced temperature [4°C] as

well as in the presence of 1 mM DTT. Increased stability of the cleaved GlpB was seen after 16 hours incubation at 4°C, but the intensity of the GST polypeptide was still greater than the GlpB polypeptide, not the expected 1:1 molar ratio. Furthermore, EPR spectral properties of the cleaved GlpB were significantly diminished [refer to Figure 24 and 32]. The addition of purified GlpAC dimer [GSTGlpB:GlpAC 1:1] did not alter the cleavage reaction or stability of GlpB. I was not able to accumulate sufficient stable quantities of GlpB for biophysical analysis and used the full length fusion protein for further studies.

5. Visible Spectroscopy

Cells transformed with pGLP100 and grown after induction with IPTG were dark brown in appearance. The partially purified preparation of GSTGlpB showed a slight orange-brown color. A visible absorption spectrum is shown in Figure 23 [Panel A, spectrum b]. Purified GST alone did not show any tinge of color [spectrum a]. The GSTGlpB spectrum was similar to other iron-sulfur proteins as the spectrum is very broad and featureless. An obvious peak was observed at 416 - 418 nm , with slight shoulders at ~ 460 nm and ~ 560 nm. Upon the addition of dithionite, there was a marked bleaching of the entire spectrum [spectrum c]. A truncated GSTGlpB' fusion protein was also constructed and produced [refer to Section II.B.7] and similar visible spectra were recorded for the truncated GSTGlpB' protein preparation [shown in Figure 23, Panel B]. The spectral results as well as other experiments condcuted with the GSTGlpB' fusion protein are described later in this chapter [Section V.B].

6. EPR Spectral Analysis of GSTGlpB

The EPR spectral studies for the full length GSTGlpB were carried out by Dr. Richard Rothery, a research associate within the lab. Investigation of the reduction time course studies, effect of methyl viologen and pH were conducted by myself with the help of Professor Richard Cammack of King's College, London, UK while he was visiting our laboratory in February of 1992. Redox potentiometry of 'washed membrane' preparations were also conducted by myself [refer to Section II.B.17c].

EPR spectra recorded between 8.2 and 80 K of reduced GSTGlpB are shown in Figure 24, Panel A. Similar to that seen with JM83/pGLP1 whole cells difference spectra [refer to Figure 17], the reduced protein exhibited a strong signal in the $g = 2$

region, with peaks at g = 2.00 and 1.98, and troughs at g = 1.94 and 1.88. No major features were observed in the oxidized protein [Figure 24, Panel B, spectrum c] or in the oxidized [spectrum a] or reduced state [spectrum b] of the GST polypeptide alone. Incubation of GSTGlpB with a 1:1 molar ratio of GlpAC purifed dimer with G3P did not reduce the GSTGlpB [spectrum d]. This experiment indicated that GlpAC does not contain a paramagnetic center as proposed (Schryvers & Weiner, 1981) for reduction of the center would be expected with the addition of the physiologic substrate, G3P. This is contrary to the reduction of the centers as observed with addition of G3P to the cellular preparation from JM83/pGLP1 [Figure 20]. As no reduction of the GSTGlpB centers was observed, this suggested that the GlpAC dimer was not interacting with GlpB. Even if G3P had been converted to DHAP, with the reducing equivalents taken up by the GlpAC dimer, the electrons did not appear to pass on to the GlpB subunit as reduction of the paramagnetic centers in GSTGlpB did not occur. If there was a paramagnetic center associated with GlpAC, additional features would have been observed in the EPR signal. The spectrum of GlpAC did not have any features indicative of a [Fe-S] center.

Studies of the partially purified GSTGlpB indicated instability of the protein below pH 8.0. The enriched fusion protein preparation was subjected to a pH study as described in Materials & Methods, with the samples adjusted to the various pH levels with the 'cocktail buffer'. The GSTGlpB exhibited a preference for more alkaline conditions; at pH 9.0 the amplitude of the signal was greater than at pH 7.0 [Figure 25, spectra a and c, respectively].

Addition of methyl viologen can enhance the reduction of a [Fe-S] center by dithionite due to more efficient mediation with the redox center. In the presence of methyl viologen [5 μM], with dithionite, [pH 8.0] there was rapid loss of the signal [Figure 25, spectrum d and e].

a) EPR Signals of Whole Cells, Soluble and Particulate Fractions

Spectra of samples taken from the various fractions of the enrichment procedure are shown in Figure 26. It is clear that the major EPR detectable species present in IPTG induced whole cells harboring pGLP100 was GSTGlpB [spectrum d]. The Triton X-100 insoluble, French pressure cell lysate [low speed particulate fraction; spectrum c] also contained concentrations of GSTGlpB comparable to those found in the cells. The Triton X-100 soluble fraction, used for affinity enrichment, exhibited similar spectral features in the reduced state [spectrum b]. All fractions gave qualitatively similar signals

as observed for the partially purified [30 - 40 %] fusion protein sample [spectrum a]. Lowering the cell growth and induction temperature did not produce a qualitative or quantitative improvement in the GSTGlpB spectra described above, nor did the addition of iron, calcium and magnesium.

b) Time Course of Reduction

A time course of reduction of partially purified GSTGlpB following addition of 7 mM dithionite, was carried out at pH 8.0 [Figure 27]. The EPR signal appeared after brief [10 sec] reduction, reaching maximum intensity within 250 seconds, and then it diminished to about 60 % of its original height after 3600 seconds.

c) Temperature and Microwave Power Dependence of the GSTGlpB EPR signal

The temperature dependence of the GSTGlpB EPR signal is illustrated in Figure 28, Panel A [representative spectra are shown in Figure 24]. The intensity of the signal reached a maximum [at 2 mW] at around 16 K. Figure 27, Panel B shows the Curie Law temperature dependence of the signal in the 18 - 80 K range, which is usual for a S = 1/2 species. In order to further characterize the GSTGlpB EPR signal, the effect of temperature on the power for half saturation [$P_{1/2}$] was examined. Figure 29, Panel A shows the saturation profiles of spectra recorded at 14, 16, 20, and 24 K. As the GSTGlpB fusion protein was considered more pure than preparations of other cellular fractions such as in the analysis with JM83/pGLP1 fractions, the data was fitted to the empirical equation of Rupp *et al.* (1978) with $P_{1/2}$ values of 3, 18, 50, and 100 mW, respectively. The curvature of the saturation profiles showed a slope factor, b, of less than one. This implied some heterogeneity in the spectrum, consisting of components having the same lineshape but with different relaxation rates. Figure 29, Panel B shows the effect of temperature on the $P_{1/2}$ of the GSTGlpB signal. Between 8 and 16 K the $P_{1/2}$ followed an apparent T^{11} dependence; above 16 K, the GSTGlpB showed a T^5 dependence. Known relaxation mechanisms follow alternate temperature dependence relationships (Blum *et al.*, 1983).

d) Redox Potentiometry of the GSTGlpB

GSTGlpB has proven to be refractory to potentiometric analyses. Preliminary

redox titrations carried out at pH 7.0 on preparations from cells harboring the pGLP100 plasmid or with purified GSTGlpB at pH 8.0 were unsuccessful. In these titrations, the protein was very susceptible to cluster damage due to overreduction. As the GSTGlpB fusion protein was more stable at alkaline pH, titrations were also attempted at pH 9.0. Although I was able to see stable EPR signals from redox titrations from the 'cell debris and microinclusion body' preparation described in the Materials and Methods, the titrations resulted in an estimated E_m to be around - 432 mV at pH 9.0 with an unusually high *n* [~2.0 - 3.0] value [Figure 30]. In these titrations, the GSTGlpB signal appeared as a single phase, with no lineshape changes observed during the titration, similar to that seen with the redox attempts with JM83/pGLP1. 'Washed' membranes at pH 9.0 were also used for redox potentiometry. Representative spectra are shown in Figure 31. Again, overreduction of the clusters by dithionite caused a decrease in signal amplitude, due to destruction of the clusters with hysteresis of the oxidation curve from the reduction curve. Once again, the titration was very rapid, with no intermediate species observed, indicative of one cluster [Figure 31, Panel B]. The midpoint potential though was estimated to be ~ - 465 mV with n = 1.0, but as significant cluster damage occurred, these results were unreliable.

7. Other Studies

a) Activity Measurements

The GlpAC dimer catalyzes G3P oxidation and this activity can be measured using artificial electron mediators (PMS) and a tetrazolium dye (MTT) to trap the reducing equivalents (Cole *et al.*, 1988). GSTGlpB was added to the assay to determine if by some association with the dimer *in vitro*, a decrease in activity would be observed as a reflection of channeling the transfer of the reducing equivalents away from the artificial acceptor. Addition of GSTGlpB protein to the assay mixture did not exhibit any change in activity [3.8 U/mg ± GSTGlpB]. Similar activity was measured when GST alone was added, which suggested that neither the GST domain nor the GlpB domain interacted with GlpAC *in vitro*. Although a reducing environment should be present with excess substrate present, no interaction with GlpAC could be inferred. Substitution of the quinone analog, DMN, for PMS dramatically reduced the observed activity [0.02 U/mg], but this may be due to DMN being an inappropriate mediator to the tetrazoliun dye, MTT as subsequent addition of PMS restored the measured activity [3.6 U/mg].

b) Nonheme Iron and Acid Labile Sulfide Determinations

To aid in the characterization of the type of center present in GlpB, I attempted to quantitatively determine the amount of nonheme iron and acid labile sulfur. As previously mentioned, it was deemed futile to attempt these determinations with JM83/pGLP1 samples as GlpB was not in any pure state. It was believed that the GSTGlpB preparation was amenable to this type of quantitative analysis. The experiments were carried out as described in Materials and Methods. The nonheme iron determination gave a value of 0.16 mol Fe/mol of protein, which was an underestimation. The amplitude of the reduced EPR signal from purified protein [Figure 24] suggested a greater quantity of non-heme iron. Unreliable results were also obtained with the acid labile sulfide analysis as I was unable to obtain a linear standard curve with the methodology. Possible reasons for not obtaining accurate values are described in the upcoming discussion [Section C].

B. The Amino Terminal GSTGlpB Truncate [Expression of pGLP101]

To further investigate whether the paramagnetic center observed in GlpB was due to the Fd-like motifs in the amino-terminal region of the GlpB polypeptide, a truncated GSTGlpB fusion was constructed [refer to Materials & Methods and Figure 21]. The pGLP101 plasmid encoded the *gst* gene with the first 370 nucleotides of the *glpB* gene, corresponding to the first 123 residues of the GlpB polypeptide. This region encompassed the Fd [Fe-S] motifs. As the fusion lacked the regions proposed to contain an amphipathic helix, the Cys-Cys-Gly residues which may be involved in membrane attachment, and the proposed metal binding or [2Fe-2S] domain in the carboxy terminal end of the polypeptide, I had hoped to gain insight into the importance of these regions as well. Some investigators speculate that various fragments of a whole polypeptide are all that is required to maintain a certain structural motif or binding of a ligand [i.e. an iron-sulfur cluster]. If this is so, the amino terminal region may be all that was required for housing the [Fe-S] clusters of GlpB.

1. Characteristics of GSTGlpB'

As in the full length fusion, the strain BNN103 was essential in order to obtain

the appropriate size of fusion protein [~ 40 kDa]. Contrary to the full length protein, the truncated fusion polypeptide was more soluble as addition of detergent in the buffers did not visually appear to alter the amount of the fusion protein in the soluble fraction.

The GSTGlpB' was enriched as before on the glutathione affinity column. The enriched truncated protein exhibited the same orange-brown color as the full length fusion protein and the visible absorption spectrum [Figure 23, Panel B, spectrum a] was similar to that obtained previously for the full length GSTGlpB [Figure 23, Panel A, spectrum b]. The spectrum was once again broad and featureless, with bleaching upon reduction with dithionite. The concentrated protein did not adhere to the Amicon filter.

2. EPR Spectral Analysis

Whole EPR spectra at 20 K were recorded for purified GSTGlpB' reduced with 2.5 mM dithionite [Figure 32, spectrum a]. The spectrum had a high noise to signal ratio, indicative of minimal amounts of the redox species which suggested that the [Fe-S] clusters were not present in most molecules. This was most likely due to the lack of assembly of the clusters or cluster destruction during preparation and handling. Following Factor X_a cleavage, and separation of the GST from the GlpB' polypeptide by affinity chromatography, the eluted GlpB' fraction was also examined by EPR [spectrum c] and compared to cleaved GSTGlpB [spectrum b]. The intensity of the signal was quite weak in all three cases, but the general lineshape was very similar. The precleaved GSTGlpB' [spectrum a] showed a similar spectrum to the cleaved GSTGlpB spectrum, which suggested the loss of the redox species. Again, this was probably due to poor assembly of the cluster, as in the case of the truncated fusion, or cluster destruction for the full length fusion. Cleavage of the truncated fusion with Factor X_a further diminished the signal [spectrum c]. The spectra do not compare to the prominent signal seen in the fractions of full length fusion [Figure 26] which suggested better expression and assembly of the clusters in the full length fusion.

3. Nonheme Iron Stain

A specific stain for the qualitative indication of nonheme iron containing proteins was developed by Leong *et al.* (1992). It involved nondenaturing gel electrophoresis of the samples in question, stained in a 100 mM potassium ferricyanide solution, with development in a 10 % methanol/10 % trichloroacetic acid solution. Purified aliquots of

GSTGlpB and the truncated GSTGlpB' were loaded onto the 10 % polyacrylamide gels lacking SDS, and electrophoresed. Purified ferredoxin [Sigma] at varying amounts, 5 - 50 µg, were used as positive controls and purified GlpAC dimer was also run on the gel. Upon color development, a weak blue band was observed in the control lanes [> 20 µg], as well as for the two GSTGlpB samples [but less intense]. The GSTGlpB lanes however had the band in the loading well and not in the gel front which suggested aggregation of the polypeptide. A small amount of Triton X-100 was added to the samples, gel and buffers in the hopes of improving solubilization, but the fusion protein samples remained in the gel wells. The GlpAC lane did not show any color development. As this method for the detection of nonheme iron containing proteins resulted in a weak presentation of the data, a more quantitative means should be employed in the future.

C. Discussion

Evidence for the structure and role of GlpB has been difficult to provide because of the intractable nature of GlpB. Analysis has suffered from the poor expression of GlpB, from its tendency to aggregate and from its susceptibility to neutral and acid pH. I have overcome some of the difficulties by producing GlpB as a fusion protein with glutathione S-transferase. The overproduction and accumulation of the fusion protein was dependent on expression in BNN103, which is a La protease deficient strain [*lon*$^-$]. The requirement of a *lon*- strain for efficient accumulation of GlpB supported the idea that GlpB required its membrane location or coexpression with GlpAC for proper structure and when not in this form, is rapidly degraded in a *lon*$^+$ strain. It is possible that overproduction of the GSTGlpB resulted in too much protein for the cell to be able to correctly assemble the polypeptide. It has been shown in other systems, particularly fumarate reductase, that the cell is able to accommodate the overproduction of membrane proteins by increasing the amount of membrane material in the form of intracellular organelles with proper assembly of enzyme subunits (Weiner *et al.*, 1984). Furthermore, the cell accommodated the increased necessity of iron as the [Fe-S] centers were formed prior to aggregation of the polypeptides. This was suggested from the presence of the reduced signal in each of the cellular fractions.

A portion of the overproduced fusion protein was soluble in nature. The solubility was maximized by expressing the protein at reduced temperatures and inclusion of detergent in the resuspension buffer. The soluble fusion could be partially

purified by glutathione affinity chromatography in sufficient quantities for biophysical analysis. Although only a 3 - 4 fold enrichment of the protein was achieved, this was a significant improvement over previous attempts with JM83/pGLP1 preparations. As partial purification was obtained, this suggested that the GSTGlpB fusion possessed a properly folded GST-active site capable of binding glutathione affinity agarose and hence I was able to overcome one of the major limitations of the GST-fusion protein system (Hartman *et al.*, 1992). Although a unique Factor X_a cleavage site was present in the GSTGlpB fusion and I was able to get efficient cutting, I was not able to take advantage of this as the released GlpB was rapidly degraded. The GlpB polypeptide was not stabilized by inclusion of GlpAC in the cleavage reaction, but it is possible that inclusion of detergent in the cleavage reaction may have stabilized GlpB. Efficient cleavage of GST did suggest though that proper folding of the Factor X_a cleavage site was also maintained. Nonetheless it was possible to carry out EPR analysis of GSTGlpB in intact cells and subcellular fractions.

1. Characterization of Paramagnetic Center

The visible absorption spectra suggested the presence of [Fe-S] centers. The spectra were broad and featureless with bleaching upon reduction with dithionite. I have examined the EPR properties of the reduced GSTGlpB in partially purified preparations, in whole cells, and in inclusion bodies. I have shown that GSTGlpB exhibited a signal in its reduced state and this signal was not present in GST preparations. The amplitude of the reduced signal exhibited optimal behavior at alkaline pH and with short times of dithionite reduction. Although methyl viologen is generally used as a mediator for EPR spectral studies (Cammack & Watts, 1994), it appeared to diminish the GSTGlpB signal. This was atypical as methyl viologen usually enhances reduction with dithionite. The observed behaviour was perhaps due to the apparent sensitive nature of the GlpB clusters to alternative substrates and environments. It is not uncommon for some mediators to negatively effect the redox species (Dutton, 1978) and in the case of GlpB, this appeared to be so. Although dithionite was a useful reductant, GlpB also appeared subject to a threshold reduction capacity, as prolonged incubation times with dithionite as well as excess dithionite appeared to destroy the clusters. Care was taken to prepare fresh dithionite solutions and maintain the system under anaerobic conditions, but as the oxidation products of dithionite are highly acidic (Dutton, 1978), this may have contributed to cluster damage. A comparable effect of decreasing signal amplitude was

observed at neural pH *vs* the more favored alkaline pH. Despite attempts to fully characterize the [Fe-S] using the GSTGlpB fusion protein, as before, I have been unable to determine the cluster type unequivocally on the basis of these fusion studies.

The lineshape of the reduced GSTGlpB signal can be interpreted [based on R. A. Rothery's analysis] as arising from a single, non-interacting species with $g_z = 2.00$, $g_y = 1.96$, and $g_x = 1.88$. The g_z value was unusual for a [4Fe-4S] cluster, as these clusters usually have g_z at around 2.04 - 2.07 (Guigliarelli *et al.*, 1985; Elliott & Ljungdahl, 1982; Thomson *et al.*, 1981). Unusual g values have been reported for [4Fe-4S] clusters, such as the cluster present in lactyl-CoA dehydratase (Kuchta *et al.*, 1986). Alternatively, it was possible that GSTGlpB contained a proposed [2Fe-2S] cluster, but the actual g values did not resemble other [2Fe-2S] clusters. Jollie & Lipscomb (1991) characterized purified formate dehydrogenase from *Methylosinus trichosporium* OB3b by EPR and identified a cluster, Center 1 in their nomenclature, having $g_z = 1.995$, $g_y = 1.951$, and $g_x = 1.909$ which they assigned to a [2Fe-2S] cluster. The GSTGlpB signal had much broader linewidths for $g_{x,y,z}$ than that reported for the *Methylosinus* Ob3b system. Another possibility was that the center in GlpB may be a dinuclear iron-oxo center, similar to that exhibited in Methane monooxygenase (Cammack, 1991). Like the *M. trichosporium* [2Fe-2S] center, all three g values are below two in methane monooxygenase, but the cluster in this protein contains oxygen as a bridging ligand between the two iron atoms. However, the cluster reversibly loses its EPR spectrum upon reduction and this transition takes place at potentials (Liu & Lippard, 1991) much higher than the redox transitions reported herein for GSTGlpB. It is therefore unlikely that GSTGlpB contains a dinuclear iron-oxo center.

As proposed from sequence homology, an alternative interpretation of the EPR signal of reduced GSTGlpB was that it arose from interactions between two reduced [4Fe-4S] clusters. Recall that EPR spectra of fully reduced 2[4Fe-4S] Fds have major peaks at around $g = 2$ which arise as a result of the spin-spin interactions between the two paramagnetic [4Fe-4S] clusters (Mathews *et al.*, 1974; Prince & Adams, 1987). However, these Fd spectra also contain additional features in the 'wings' which are absent from the spectra of GSTGlpB, but were observed in the anaerobically prepared JM83/pGLP1 whole cell spectra. As well, the absence of a signal from isolated half-reduced iron-sulfur clusters suggested it is unlikely that the lineshape of the GSTGlpB signal was due to an interacting 2[4Fe-4S] system.

The temperature dependence of the GSTGlpB signal was similar to that observed for [4Fe-4S] clusters such as those found in the eight-iron *C. pasteurianum* and

Chromatium D Fds (Rupp *et al.*, 1978). EPR signals from these Fds reach maximum intensity at around 19 and 10 K, respectively. The amplitude of the GSTGlpB reduced signal reached a maximum intensity at around 16 K [Figure 28], and had significantly decreased in intensity at temperatures above 70 K. This temperature dependence was quite unlike that found for the 1Fe center of rubredoxin and typical [2Fe-2S] clusters (Rupp *et al.*, 1978). The signals from [2Fe-2S] centers are optimal at temperatures greater than 40 K.

The power saturation behavior of the GSTGlpB signal was unusual. The data did not fit to the saturation profiles at different temperatures [Figure 29 (Rupp *et al.*, 1978)], but in each case the fit assumed a single species with an inhomogeneity parameter, *b*, of 0.85. This value is outside the usual range for this parameter [1.0 - 3.0 (Innes & Brudvig, 1989)], and indicated the presence of multiple components in the saturation profiles of Figure 29. For example, the data at 14 K in Figure 29 fit to two *b* = 1.0 components $P_{1/2}$ values of 1 and 45 mW, respectively. The number of variable parameters involved in multiple component modeling precluded accurate $P_{1/2}$ estimations of the components present in each of the saturation profiles. However, it was concluded from the saturation behavior that there are at least two components with similar/identical lineshapes responsible for the data of Figure 29. This was significant in the context of what would be expected if GSTGlpB exhibited EPR properties similar to those of the 2[4Fe-4S] Fds. In these proteins, two components would be predicted in the saturation profile of the 'fully reduced' protein. Fully reduced 2[4Fe-4S] Fds exhibit saturation profiles with two components: a slowly relaxing component attributable to residual singly reduced Fd; and a fast relaxing species attributable to the doubly reduced Fd (Rupp *et al.*, 1978; Blum *et al.*, 1981).

My preliminary potentiometric studies indicated that the midpoint potential of the GSTGlpB signal is approximately - 450 mV at pH 9. This was within the range predicted for both [2Fe-2S] clusters and [4Fe-4S] clusters. However, the estimated *n* value in these titrations varied from 1 - 3, which was anomalously high. The anomalous n value suggested the estimated E_m and *n* value were artifacts of the preparation used in these studies. The 'cell debris and inclusion body' and 'washed membrane' preparations were most likely not in good redox equilibrium with the bulk phase and the measuring (Pt) electrode. As before, no half reduced species similar to those observed in the 2[4Fe-4S] Fds were observed in the potentiometric studies conducted with the GSTGlpB prepartions. This indicated that if two clusters (*viz.* [4Fe-4S]) were present, one cluster may have a potential too low to be reduced by dithionite or else the midpoint

potentials of the clusters were so close that they were not distinguishable.

2. Determination of Cluster - Analytical Quantitation

The enriched GSTGlpB preparation was used to try to determine the amount of nonheme iron and acid labile sulfur within the protein. The nonheme iron determination used (Brumby and Massey, 1967) was based on a colorimetric assay where the iron was extracted with trichloracetic acid and then complexed with the chelator o-phenanthroline [0.1% w/v]; the complex exhibiting high absorption and measured at 510 nm. In my studies with GSTGlpB, there was very weak color formation. Although the procedure suggested only short incubation times with the chelator, it is known that o-phenanthroline does not react quickly (Malkin, 1973). A longer incubation time of an hour was tried but this did not help in determining a reliable quantitation. A number of factors can influence the assay, namely interference of the iron complexing with phosphate or lack of complete release of the iron and formation of complexes by other divalent metals which may be inadvertently present. These factors all result in a lower estimation of the nonheme iron present.

The acid labile sulfide determination (King & Morris, 1967) was also attempted with the GSTGlpB enriched preparation. The sample was mixed with zinc acetate and NaOH, with the zinc sulfide being absorbed in solution. It was then complexed with a diamine reagent in the presence of ferric chloride, resulting in methylene blue which was measured spectrophotometrically at 670 nm. Again, the results obtained were not reliable as I experienced problems with the assay. The standard curve measured was not reproducible, which suggested a number of variabilities in the procedure. Specifically, although care was taken for minimal release of gas, sulfide may be lost to the gas phase after the addition of the diamine reagent. Also, the assay coupling reaction can again be influenced by the presence of cations. The protein samples should be purified to the highest degree possible. Although the enriched GSTGlpB protein was far less likely to be contaminated by other species than a cellular extract sample, it also proved to be inappropriate for quantitative analysis.

Based on these experiments I could not obtain any information regarding the type of cluster present in GlpB. It should kept in mind though, that although these quantitative methods are usually standard analyses for characterization of [Fe-S] centers, the data obtained are suggestive of the type of cluster present but are not considered reliable or conclusive. Furthermore, a negative result does not assure absence of labile

sulfide or nonheme iron (Beinert, 1983). Despite lack of quantitative values for the nonheme iron and acid labile sulfide present in GlpB, the qualitative presence of nonheme iron was suggested with the use of the nonheme iron specific stain. The color development of the characteristic blue band, indicative of non-heme iron, was evident in the lane containing the GSTGlpB and GSTGlpB', but owing to the limitations of the presentation of the data with this staining technique, the amount of nonheme iron could not be quantitated. As no color development was visible in the lane loaded with purified GlpAC dimer, this suggested that the presence of nonheme iron previously reported for the dimer (Schryvers & Weiner, 1981) was not accurate. The absence of an EPR signal with the purified GlpAC dimer also suggested that a [Fe-S] center was not associated with the dimer.

3. Structural Considerations of the GSTGlpB Fusion Protein

It has been considered that the cluster type being observed in the GSTGlpB preparations did not arise from the native form of the protein, and was an artifact of the overproduction and purification techniques reported herein. Such artifacts have been observed in a number of Fds, where a native [4Fe-4S] cluster degrades to a [3Fe-4S] cluster or even a [2Fe-2S] cluster, and this has been observed in bacterial Fds, including *Desulfovibrio africanus* Fd III (George *et al.*, 1985) and *P. furiosus* Fd (Conover *et al.*, 1990). Although I found the same signals in the various cellular fractions of cells overexpressing GSTGlpB, the signal differed slightly from that observed with JM83/pGLP1 [refer to Figure 17]. This suggested that the conformation of the fusion protein was not representative of the physiological state. In comparing the various fractions of GSTGlpB, the three to four fold purification technique employed did not drastically alter the shape of the signal, although there was a large increase in specific intensity. The EPR spectral properties of the protein were similar in all fractions tested, surprisingly even in the low speed particulate fraction. This suggested that aggregation into inclusion bodies did not modify the assembly of the [Fe-S] clusters and that assembly of the clusters preceded aggregation. It further suggested that proper folding of the fusion protein occurred, and that aggregation may have been primarily caused by the interaction of the proposed amphipathic helices, and not improper folding attributed to the cause of inclusion bodies (Bowden *et al.*, 1991).

From preliminary studies conducted on the GSTGlpB fusion protein, the amplitude of the EPR reduced signal appeared to be greater at pH 9.0 than at neutral pH.

Originally this was believed to be due to the high stability of glutathione S-transferases to alkaline conditions (Simons & VanderJagt, 1977). It suggested that the GST domain had some sort of stabilizing effect on the GlpB domain, for upon cleavage with Factor X_a, the GlpB centers were lost [by EPR analysis], perhaps by a drastic change in conformation of the polypeptide. This preference for alkaline pH was observed as well in JM83/pGLP1 preparations and thus discounted the effect of the GST domain. Furthermore, if the glutathione binding domain as well as the Factor X_a cleavage site were accessible, this would suggest that there was not much interaction with the GlpB domain. The stability of GlpB appeared to be strongly dependent upon conformation, and as suggested previously, may require either membrane association and/or interaction with GlpAC. GlpB contained a large percentage of charged residues with a calculated net charge of +10 at pH 7.0. As it is important that a charged residue within a protein interior have a suitable partner for ionic interaction, in alkaline pH, the conformation of the [Fe-S] cluster coordination may be optimal due to fewer unbonded positive charges.

Although the GSTGlpB reduced [Fe-S] exhibited a rhombic spectrum similar to that seen in the difference spectrum with JM83/pGLP1 [Figure 17], the lineshapes of the two samples were distinct. The subtle features of the *Clostridium*-like signal seen in JM83/pGLP1 may be due to the proper conformation of the clusters in the presence of the GlpAC dimer. Addition of purified GlpAC dimer to a preparation of GSTGlpB did not result in changes to the observed GSTGlpB signal, but perhaps the GST domain was interfering with sites of interaction. Attempts were made to use cleaved GlpB, but as reported, I experienced rapid degradation of GlpB in the absence of GST. The addition of GlpAC to the cleavage reaction did not act to stabilize GlpB. Addition of reducing agents did not enhance association. This suggested that the membrane association of GlpB was crucial for its stability and proper conformation. If this is the case, the presence of detergent may have provided stability to GlpB, but this was not further pursued due to my reliance of characterization of the native form of the polypeptide during anaerobic expression with the other subunits of the enzyme.

4. The N terminal Region Appears to Hold the Paramagnetic Center of GlpB

A truncated fusion was constructed to help answer some questions posed regarding the various regions of GlpB. GSTGlpB' was constructed fusing the first third of the GlpB polypeptide to the GST domain. This amino terminal end housed the ferredoxin cysteine motifs, but lacked the regions assumed to localize GlpB to the

membrane. Furthermore, the potential heme binding histidines and the carboxy metal binding motif were absent in the truncated construct.

The visible absorption and EPR spectroscopy results suggested that the amino terminal portion of GlpB offered the [Fe-S] cluster coordinating residues. There was not much difference between the visible absorption spectrum and that of the full length fusion protein] though both were broad and relatively featureless. Upon reduction with dithionite, similar significant bleaching of the spectrum was observed.

Evidence for the presence of [Fe-S] in the GSTGlpB' fusion protein was poor. The EPR reduced spectra exhibited weak signals [Figure 32] and were not similar to the intense signal observed with the full length GSTGlpB [Figure 26]. Instead, the spectra resembled that obtained with Factor X_a cleaved GSTGlpB, and what appeared as subsequent degradation of the clusters. Similar spectra with both preparations strongly suggested improper cluster coordination. In the case of full length GlpB, this appeared to be due to improper conformation of the polypeptide removed from the membrane environment. For the truncated GSTGlpB', the absence of the latter two thirds of the polypeptide may have destabilized the cluster due to removal of key regions of the polypeptide for membrane attachment or alternatively, residues essential for cluster coordination. Thus, I cannot conclude from these studies whether or not the ferredoxin like motifs in the amino terminal regions are the sole ligand domains for the observed [Fe-S] cluster in GlpB.

My original aim was to construct a series of other fusion constructs with the other regions of GlpB, namely the carboxy terminal end and the central histidine region of the protein. The results of the N-terminal fusion however suggested that in analysis of the redox species within GlpB, proper conformation and assembly was essential. The use of the GST fusion system, although producing usable quantities of GlpB, did not appear to produce a protein representative of its true physiological state. There was much uncertainty with the results obtained, namely the characterization of the [Fe-S] cluster as well as the midpoint potential. These studies did confirm the presence of [Fe-S] centers within GlpB, with $g_z = 2.00$, $g_y = 1.96$, and $g_x = 1.88$, but the type of cluster was inconclusive. Despite anomalous behaviour of the GSTGlpB center, these studies suggested: 1) the clusters are sensitive to environmental effects, particularly destruction by over reduction with dithionite; 2) the clusters favor alkaline conditions as observed with expression in JM83/pGLP1; and 3) the [Fe-S] center was formed prior to aggregation of the fusion protein. Based on the unreliability of the system for proper analysis of the redox species within GlpB, I felt it unproductive to investigate the other

regions of GlpB with the fusion system.

The next chapter of this thesis discusses the characterization of the paramagnetic center as studied in cells overexpressing the *glpACB* operon under control of the endogenous anaerobic promoter and anaerobic growth conditions.

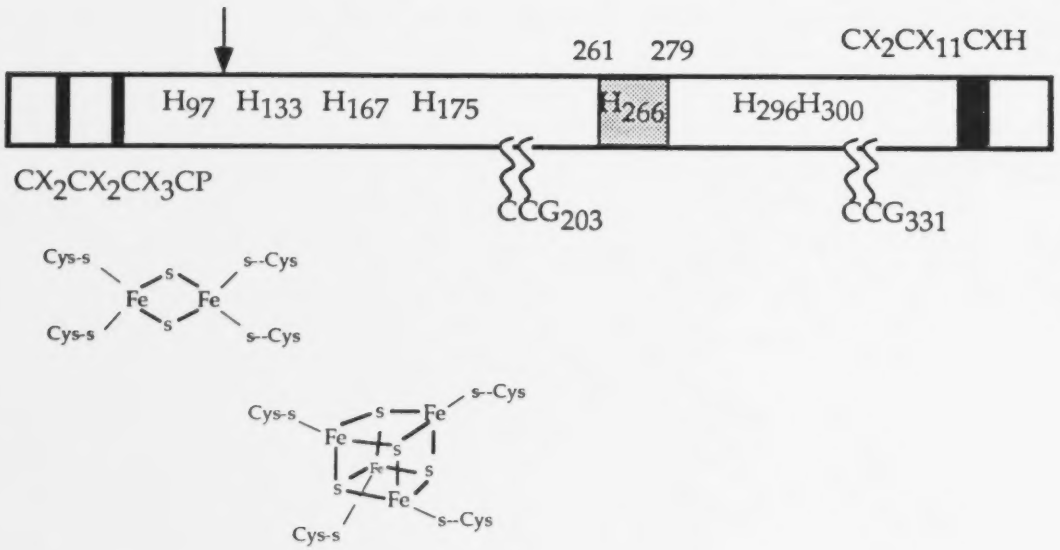

FIGURE 21. A Schematic Illustrating Interesting Residues or Regions of GlpB. Refer to Figure 4 for amino acid sequence. The features represented are: 1) Ferredoxin-like cysteine motifs in the amino terminal region, usually coordinating [4Fe-4S] clusters, but may also act as ligands for the proposed [2Fe-2S] cluster; 2) Histidine residues at the designated positions in the sequence which may act as heme-binding ligands for a cyt *b* (Degli Esposti, 1989); c) Cys-Cys-Gly motifs at positions 201-203 and 329-331, which may act as attachment sites to the membrane by fatty acid linkages; d) an amphipathic helix from residues 261-279; and e) the cysteine motif in the carboxy terminal end which may coordinate a [2Fe-2S] cluster or alternatively a metal-binding site. The arrow near the left of the diagram shows the approximate position of the truncated GST construct [pGLP101].

FIGURE 22. Electrophoretic Gels of Expression, Localization and Affinity Enrichment of GSTGlpB from BNN103. The samples were prepared as described in Materials and Methods and subjected to 10 % SDS-polyacrylamide gel electrophoresis.

Panel A. Expression and Localization: Lane A, Molecular weight markers from the top are: rabbit muscle phosphorylase b, 97,400; bovine serum albumin, 66,200; ovalbumin, 45,000; bovine carbonic anhydrase, 31,000; soybean trypsin inhibitor, 21,500. Lane B, whole cell extract of BNN103 (15 µg); lane C, whole cell extract BNN103/pGEX-3X (16 µg); lane D, whole cell extract BNN103/pGLP100, no IPTG induction (19 µg); lane E, whole cell extract BNN103/pGLP100, with IPTG induction (11 µg); lane F, BNN103/pGLP100 cytoplasmic fraction (18 µg); lane G, BNN103/pGLP100 particulate fraction (30 µg); lane H, BNN103/pGLP100 cytoplasmic fraction (18 µg); lane I, BNN103/pGLP100 particulate fraction (10 µg). Lanes B - G cells grown and induced at 37°C and lanes H & I, cells grown at 37°C and induced with IPTG at 20°C. The positions of GST and GSTGlpB are indicated with arrows shown.

Panel B. Affinity Purification: Lane 1, BNN103/pGLP100 lysed cellular fraction (20 µg); lane 2, BNN103/pGLP100 low speed particulate fraction (30 µg); lane 3, BNN103/pGLP100 cytoplasmic fraction - starting material for affinity purifcation (30 µg); and lane 4, Enriched fraction of GSTGlpB (15 µg). The position of the GSTGlpB fusion protein is indicated at the right of the panel. The molecular weight markers were run in an adjacent lane, and are indicated on the left side of the panel from the top of the panel:.rabbit muscle phosphorylase b, 97,400; bovine serum albumin, 66,200; ovalbumin, 45,000; bovine carbonic anhydrase, 31,000; soybean trypsin inhibitor, 21,500.

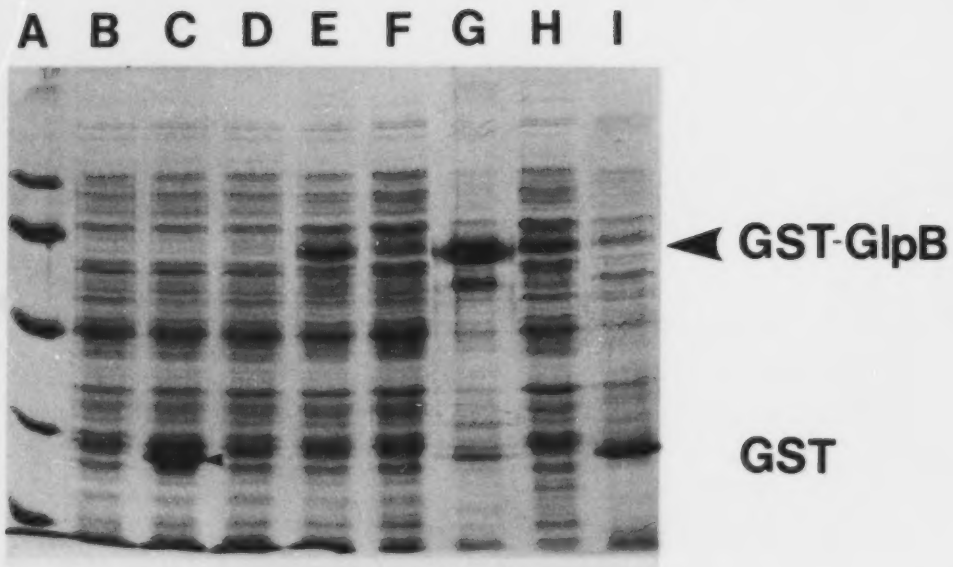
A B C D E F G H I
GST-GlpB
GST

B

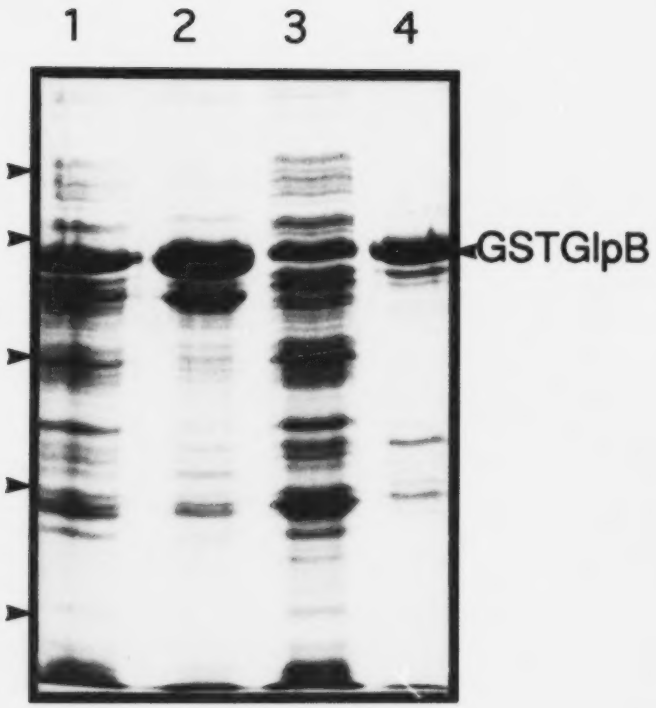

FIGURE 23. The Visible Absorption Spectra of GSTGlpB and GSTGlpB'. Enriched GSTGlpB [1.5 mg/ml] and GSTGlpB' [2 mg/ml] were used for the analysis, with 50 mM Tris-HCl/ 5 mM glutathione, pH 8.0 as the blank. The spectra were measured at room temperature with the Varian DMS100 Spectrometer. Panel A: Spectrum (a), purified GST [1 mg/ml]; spectrum (b), GSTGlpB before treatment; and after treatment with 1 mM dithionite [spectrum (c)]. Panel B: Spectrum (a), enriched GSTGlpB', before; and after treatment with 1 mM dithionite [spectrum b].

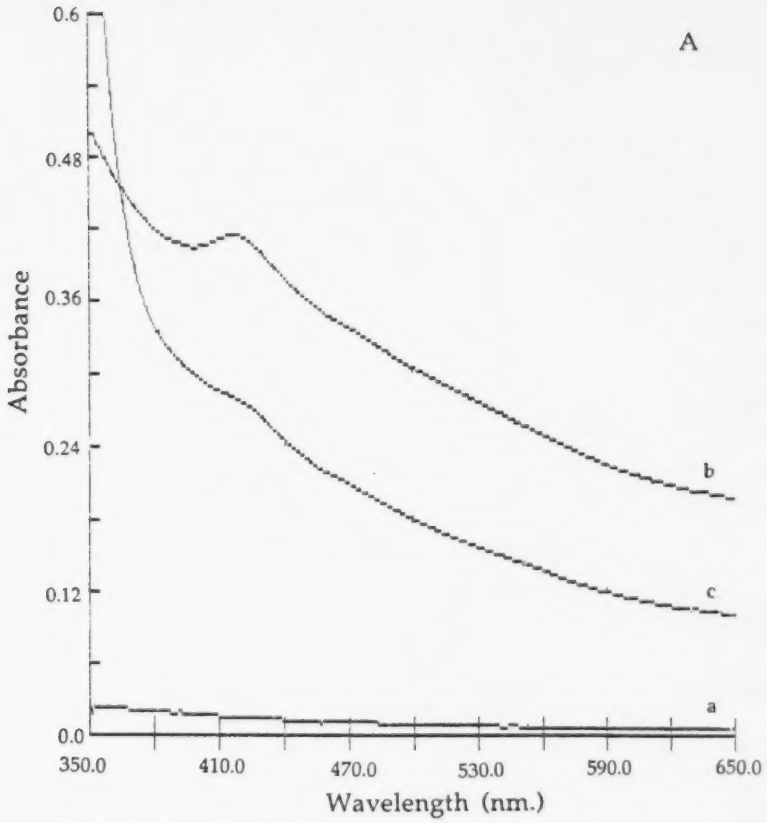
A
0.6
0.48
0.36
0.24
0.12
0.0
Absorbance
b
c
a
350.0
410.0
470.0
530.0
590.0
650.0
Wavelength (nm.)

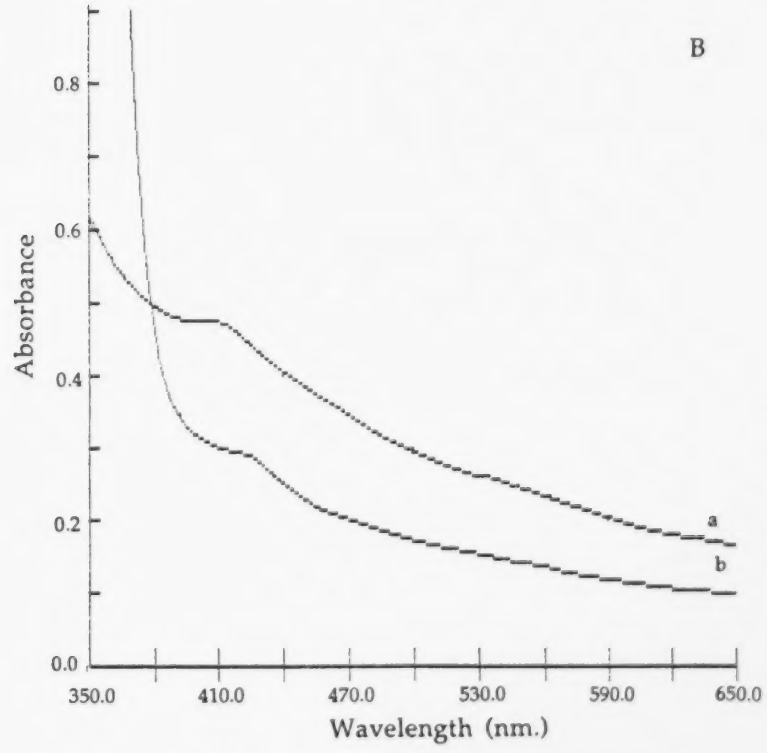
B
0.8
0.6
0.4
0.2
0.0
Absorbance
a
b
350.0
410.0
470.0
530.0
590.0
650.0
Wavelength (nm.)

FIGURE 24. EPR Spectra of Enriched GSTGlpB Fusion Protein.

Panel A: The purified GSTGlpB sample was prepared as described in Materials & Methods, except 7 mM dithionite was used. The spectra were recorded at various temperatures, as illustrated, between 8.2 K - 80 K, and the receiver gain was 4 X 10^4 with power at 2 mW [20 dB]. The g values are as highlighted.

Panel B: The purified GST and GSTGlpB samples were prepared as described in Materials and Methods, except 7 mM dithionite, 20 mM G3P or 1 mM potassium ferricyanide was used as indicated. The spectra were recorded at 12 K, receiver gain was 1 X 10^5, and power at 20 dB. Spectrum (a) Purified GST oxidized with potassium ferricyanide [1X]; spectrum (b) Purified GST reduced with 7 mM dithionite [1X]; spectrum (c) Purified GSTGlpB oxidized with potassium ferricyanide [0.5X]; and spectrum (d) Purified GSTGlpB incubated for 15 minutes with a 1:1 molar ratio of purified GlpAC dimer with the addition of 20 mM G3P [0.5X]. A g = 2.0 value is shown for comparison of features with Panel A spectra.

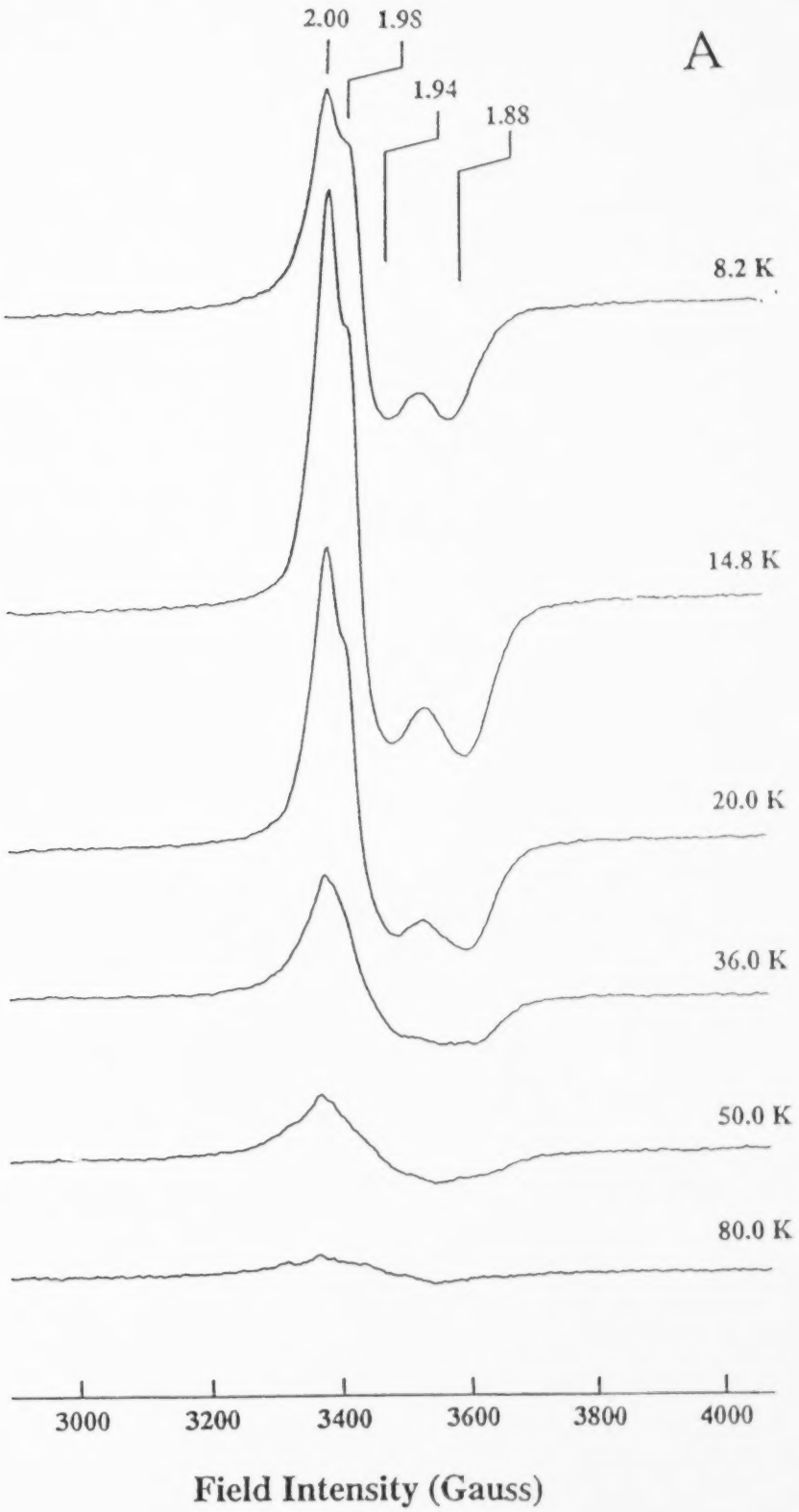
2.00
1.98
1.94
1.88
A
8.2 K
14.8 K
20.0 K
36.0 K
50.0 K
80.0 K
3000
3200
3400
3600
3800
4000
Field Intensity (Gauss)

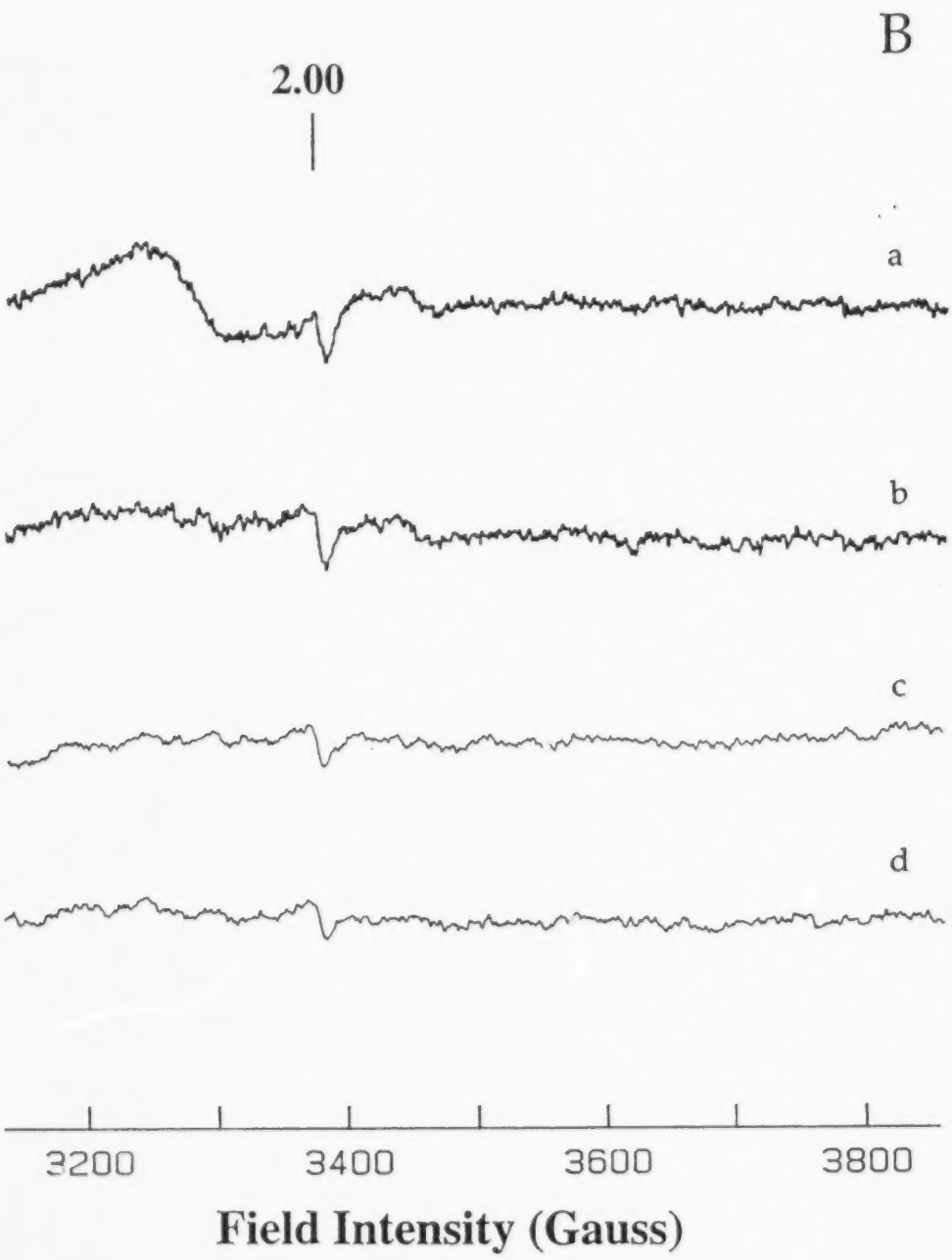
B
2.00
a
b
c
d
3200
3400
3600
3800
Field Intensity (Gauss)

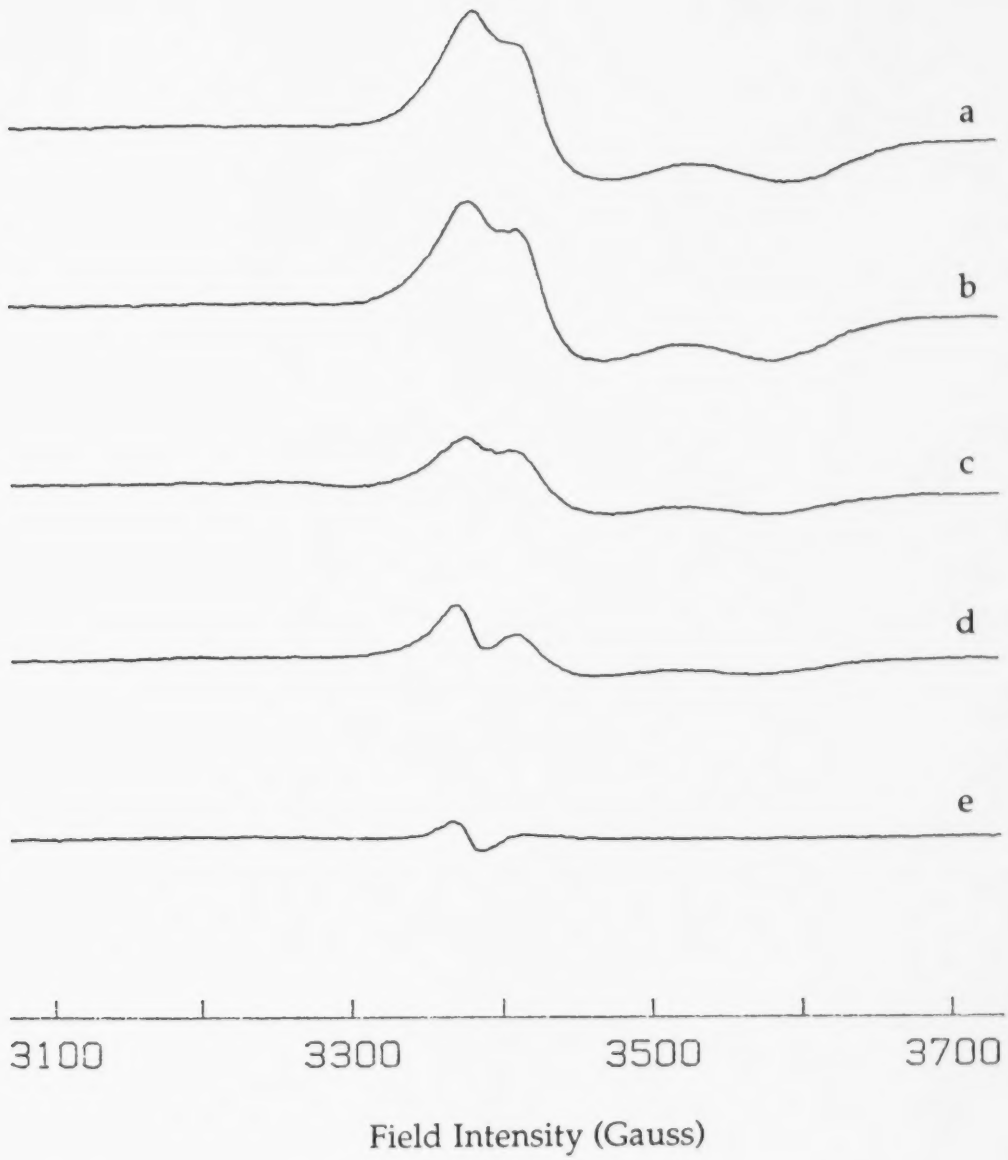

FIGURE 25. Effect of pH and Methyl Viologen on the Reduced EPR Spectra of GSTGlpB. Samples were prepared by addition of 10 µl of a 0.45 M 'cocktail buffer mix' [EPPS/MOPS/CHES] at appropriate pH levels to the purified GSTGlpB fusion protein [3.5 mg/ml]. Spectrum (a) pH 9.0; (b) pH 8.0; and (c) pH 7.0. 5 µM methyl viologen was added after dithionite to a sample of purified GSTGlpB [pH 8.0], and incubated for 1 minute [spectrum d] or ten minutes [spectrum e]. Spectra were recorded at 12 K, 20 mW [10 dB] with a receiver gain of 1.6 X 10^5 and corrected for tube calibration.

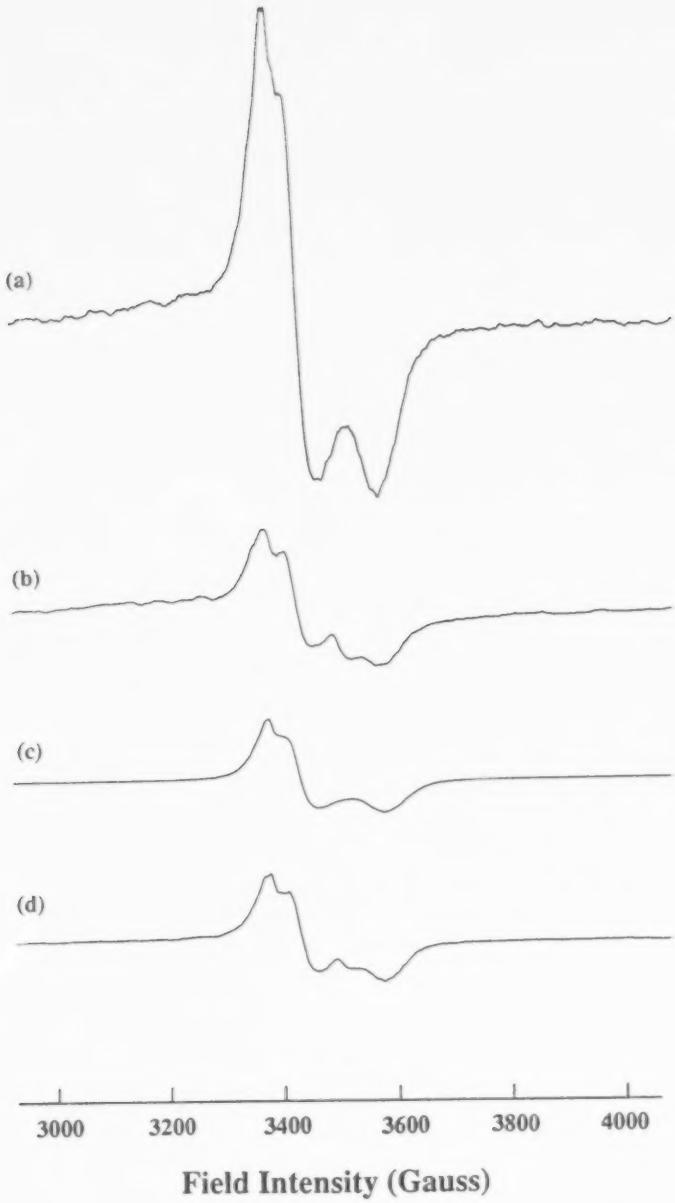

FIGURE 26. EPR Signals of the Various Cellular Fractions of BNN103/pGLP100. The cells were grown at 37°C and shifted to 30°C upon induction with IPTG. Samples were prepared as described in Materials & Methods, except reduced with 5 mM dithionite. Spectra were recorded at a temperature of 12 K and a receiver gain of 5×10^4 (d) or 1×10^5. Spectrum (a) Purified GST-GlpB; (b) low speed soluble fraction (column loading); (c) low speed particulate fraction; and (d) Whole cells. Spectra have been corrected for tube calibration, protein concentration and receiver gain.

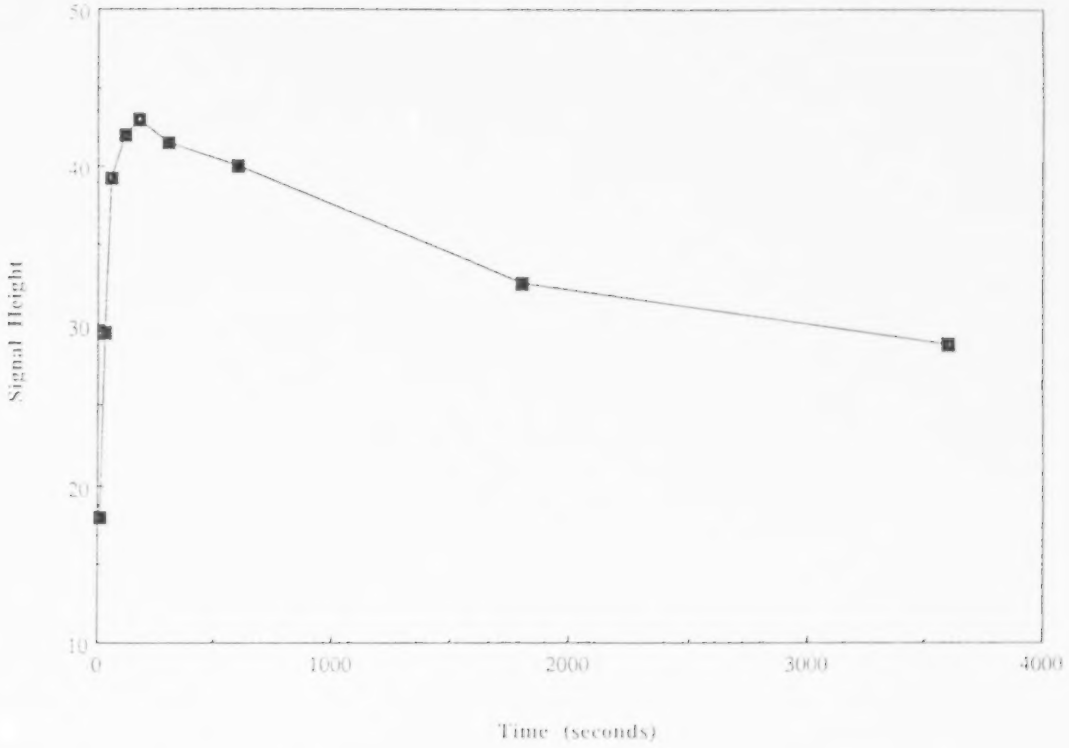

FIGURE 27. Time Course Study of Reduction with Purified GSTGlpB. The purified fusion protein was from BNN103/pGLP100 cells grown at 37°C and shifted to 20°C upon IPTG induction. Spectra were recorded as listed in Figure 49, but at 20 K and receiver gain 1 X 10^5. The amplitude of the derivative was measured for each and plotted as a function of the time of dithionite reduction (sec) [7 mM dithionite] prior to freezing.

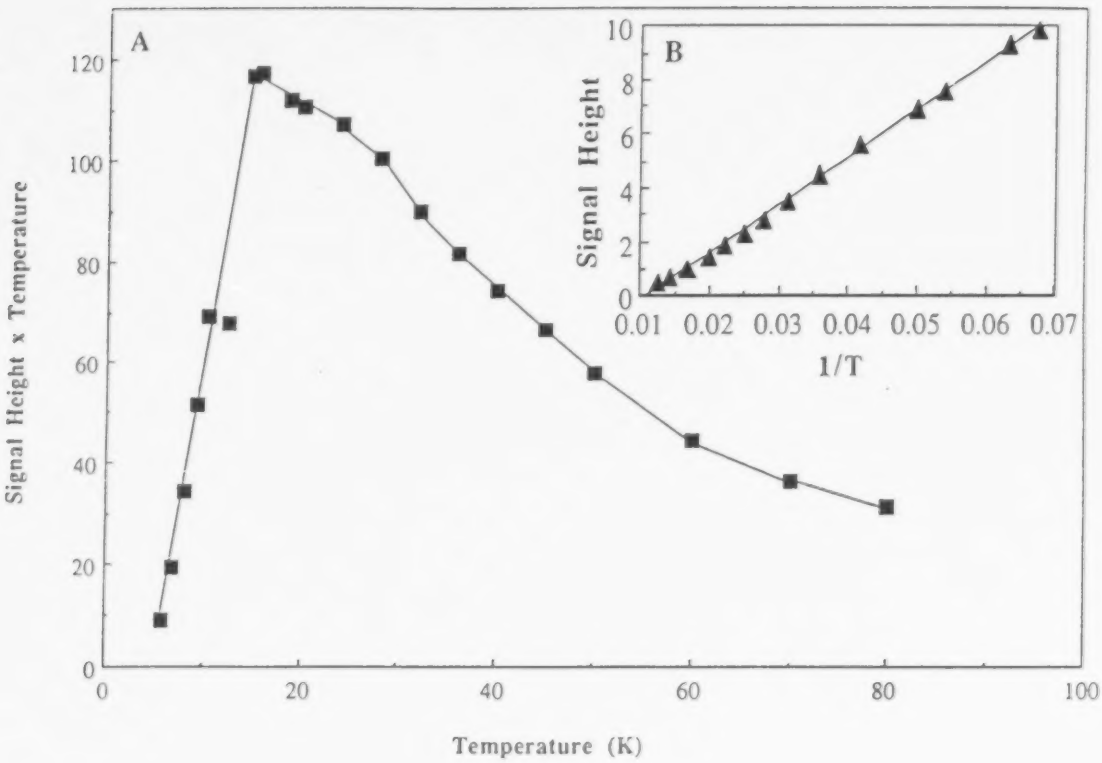

FIGURE 28. Temperature Dependence of GSTGlpB Purified Fusion Protein. The EPR spectra were those recorded for Figure 24. Panel A is a plot of [signal height * temperature] as a function of temperature, K. Optimal temperature for recording of spectra is 16 K. Panel B shows the Curie law (1/T) temperature dependence of the EPR signal between 18 - 80 K.

FIGURE 29. Microwave Power Saturation Behavior of Purified GSTGlpB. Panel A is a plot of [signal amplitude (S)/Microwave power ($P^{0.5}$)] as a function of the power, P (mW). Curves represent power saturation behavior at different temperatures: 14 K, •; 16 K, ■; 20 K, ▲; 24 K, +. Panel B shows the power at half saturation, $P_{1/2}$, (mW) behavior as a function of temperature (K).

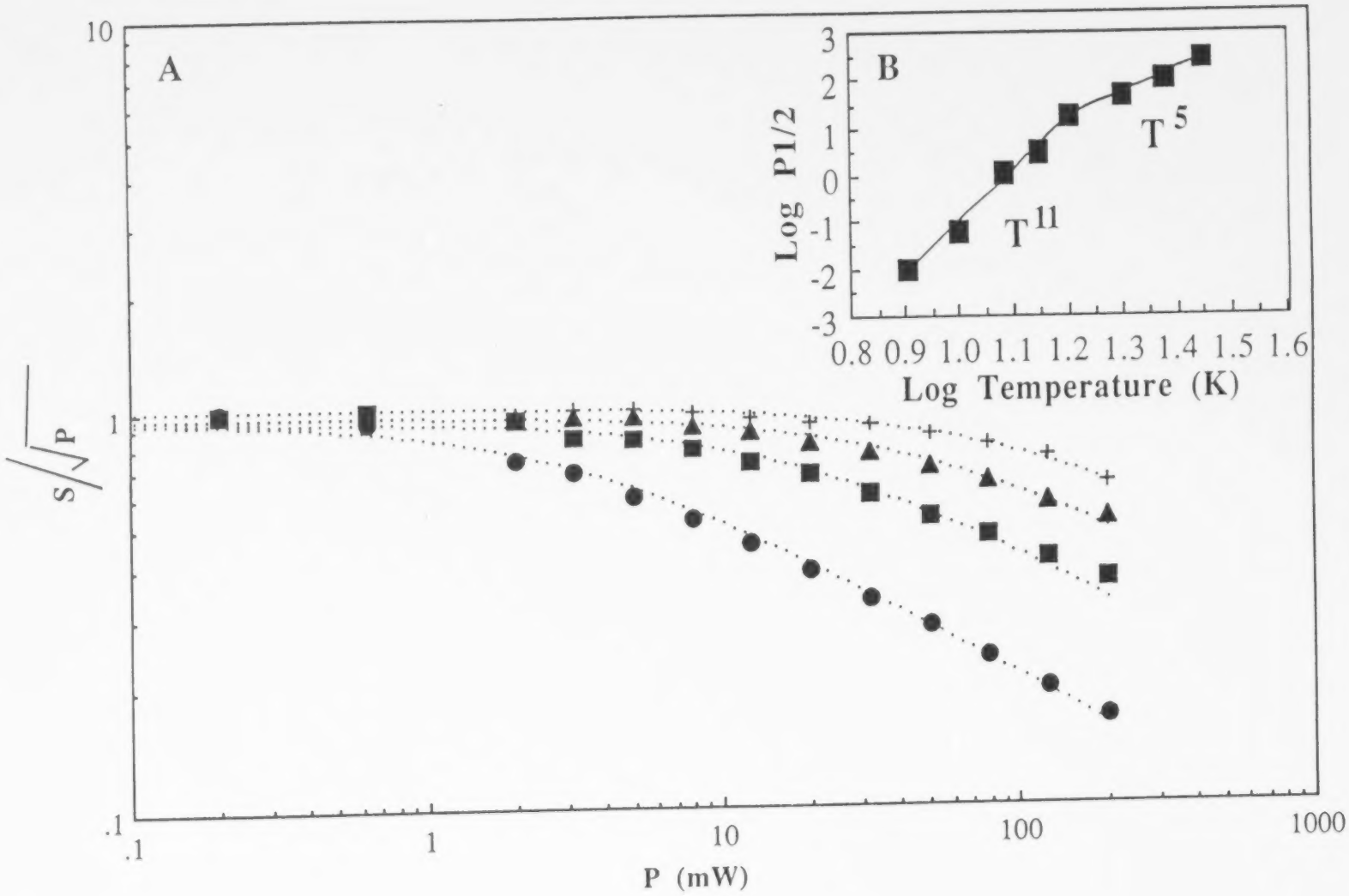
A
B
10
1
.1
.1
1
10
100
1000
P (mW)
S/√P
3
2
1
0
-1
-2
-3
Log P1/2
0.8 0.9 1.0 1.1 1.2 1.3 1.4 1.5 1.6
Log Temperature (K)
T 5
T 11

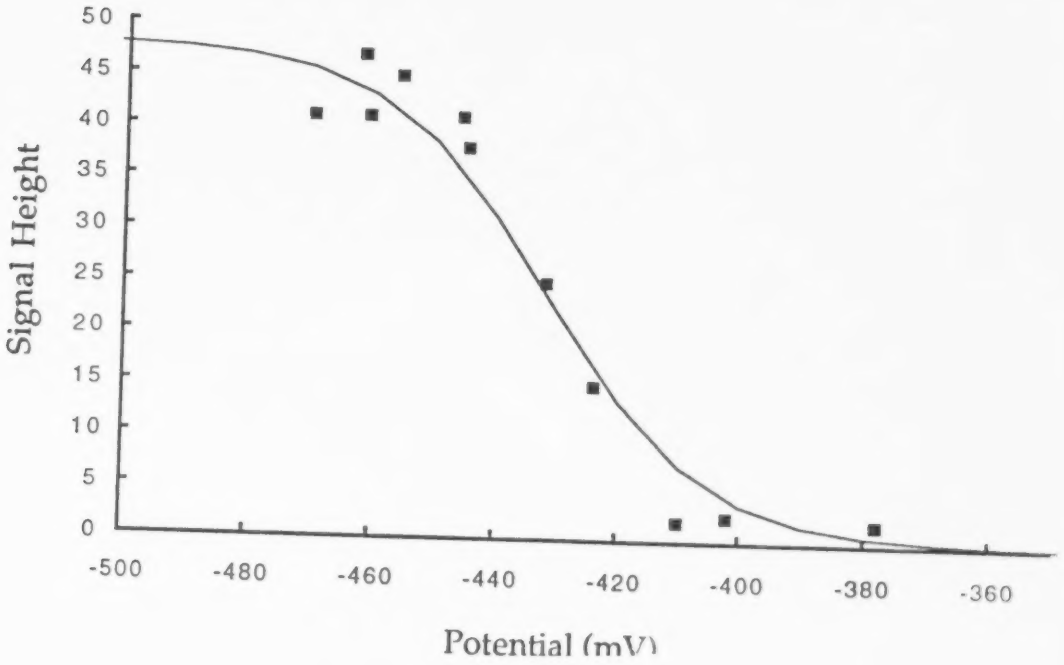

FIGURE 30. Estimation of Midpoint Potential of GSTGlpB Redox Species. Redox potentiometry of a 'cell debris and microinclusion body' preparation was conducted at 25°C as described in Materials & Methods, and spectra recorded at 20 K and a receiver gain of 1 X 10^5. The amplitude of the g = 2.0 peak was measured and plotted as a function of the potential at which the sample was taken. The E_m was estimated to be -432 mV, with an n =2 value. The data points exhibit a steeper slope, which is indicative of a higher n value than shown for the curve calculated from the Nernst equation [solid line].

FIGURE 31. Representative Spectra of GSTGlpB During Redox Titration at pH 9.0. The washed membrane preparation in 100 mM CHES/1 mM EDTA, pH 9.0 buffer was utilized and samples were prepared as described in Materials & Methods. Spectra were recorded as described in Materials & Methods, with a receiver gain at 1 X 10^5 and representative spectra are shown in Panel A. An estimation of the redox potential of -465 mV , n = 1.0 is shown in Panel B. The data points which do not fall on the curve correspond to spectra recorded in the early reducing direction, illustrating the cluster damage associated with overreduction. The Nernst curve [solid line] was matched to the data points taken in the oxidizing and final reducing direction.

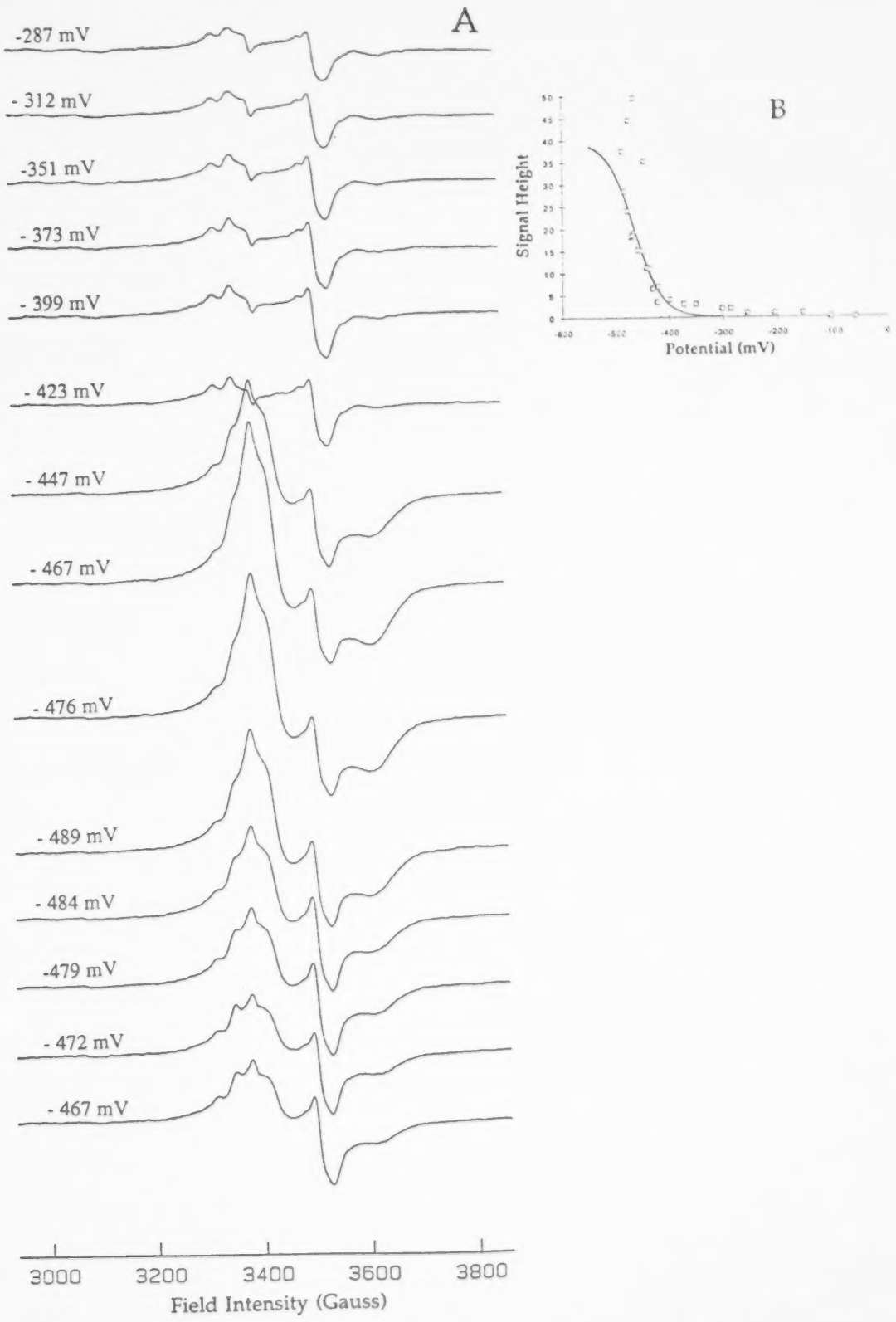
A
-287 mV
- 312 mV
-351 mV
- 373 mV
- 399 mV
- 423 mV
- 447 mV
- 467 mV
- 476 mV
- 489 mV
- 484 mV
-479 mV
- 472 mV
- 467 mV
3000
3200
3400
3600
3800
Field Intensity (Gauss)
B
Signal Height
Potential (mV)

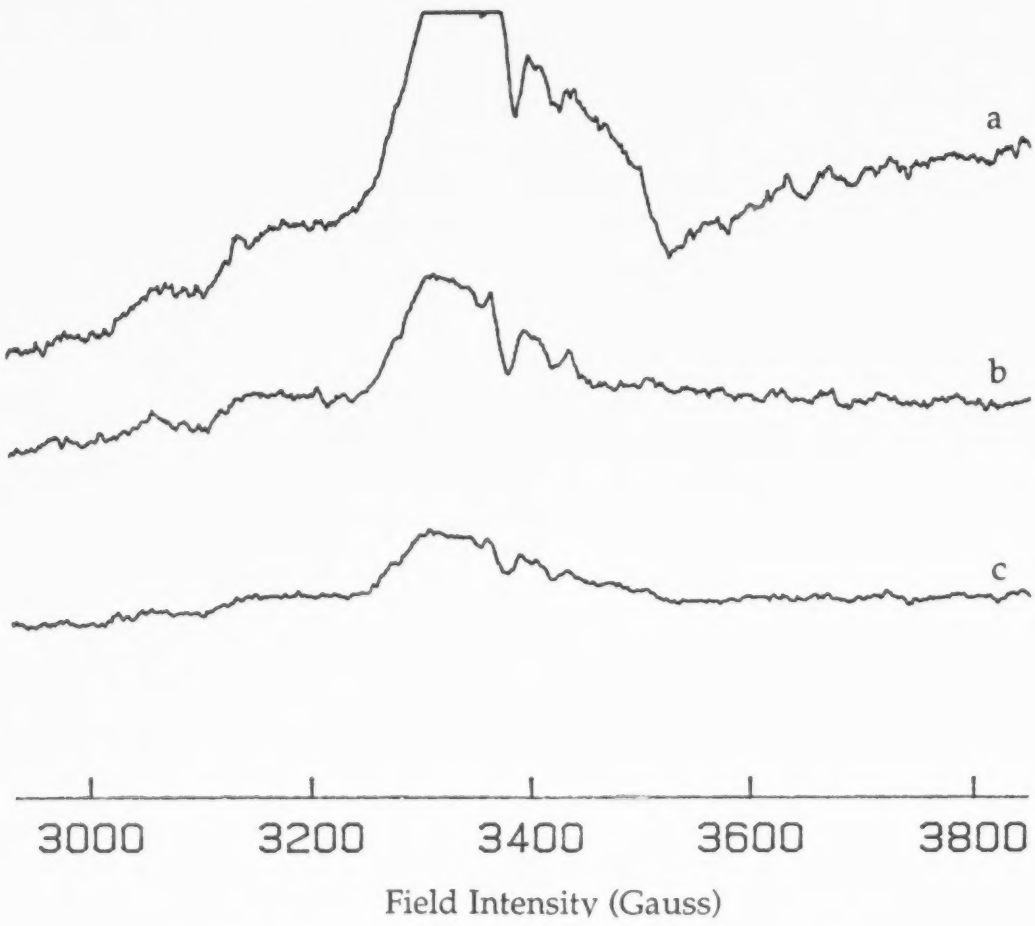

FIGURE 32. EPR Spectra of Purified Truncated GSTGlpB'. Purified GSTGlpB and GSTGlpB' were prepared and EPR reduced samples made as described in Materials & Methods. Spectra were recorded as previously described except at a receiver gain of 5 X 10^4. Spectrum (a) GSTGlpB' [6 mg/ml]; (b) Factor X_a cleaved purified GSTGlpB and concentrated [3.5 mg/ml]; and (c) Factor X_a cleaved purified GSTGlpB' and concentrated [5 mg/ml]. Spectra were normalized for tube calibration and protein concentration.

CHAPTER VI. CHARACTERIZATION OF THE GLPB PARAMAGNETIC CENTER

As described in the previous chapters, GlpB is a membrane bound polypeptide. GlpB contains within its sequence from residues 9 to 20 and 56 to 67 the cysteine motifs [Cys-XX-Cys-XX-Cys-XXX-Cys-Pro] found in *Clostridial*-type ferredoxins. I have shown in the preliminary EPR results [Chapter IV] that GlpB exhibited a paramagnetic signal in the reduced state typical of [Fe-S] clusters. This signal was observed when the cells were reduced with the artificial reductant dithionite or with the physiologic substrate, G3P. Fumarate acted as an oxidant which demonstrated that GlpB participates in the oxidation-reduction reactions from the catalytic dimer GlpAC to fumarate reductase. Using visible and EPR spectroscopic techniques, my aim was to identify the type and number of cluster(s) present within GlpB in an attempt to understand the electron flow through the enzyme. The studies described with the GSTGlpB fusion protein did show that GlpB exhibited a paramagnetic center, but due to the atypical nature of the center, was not assigned to a particular type of cluster.

The finding of a g value of 1.94 in the spectrum supported the hypothesis that the paramagnetic center in GlpB may be an iron-sulfur cluster. This 'classic' feature, observed at low temperature [< 70 K] is indicative of such a cluster (Orme-Johmson, 1973; Cammack, 1991). The identification of iron-sulfur clusters by EPR is not always straightforward (Cammack, 1991). For example, both [2Fe-2S] and [4Fe-4S] clusters typically give "g = 1.94" signals in the reduced states, but these clusters behave differently when analyzed as a function of temperature at which the spectra are recorded. [2Fe-2S] clusters exhibit optimum spectra at higher temperatures [~ 70 K], while [4Fe-4S] clusters are generally observed at lower temperatures [i.e. < 30 K] (Gayda *et al.*, 1979). My efforts concentrated on using the whole cell [JM83/pGLP1] preparations for three reasons: 1) JM83 is an efficient host for overexpression of the *glp* operon as opposed to SH173 or MI1443; 2) the use of crude and purified inner membranes appeared to alter the observed spectrum, thus complicating the characterization; and 3) anomalous results obtained with the GSTGlpB fusion protein. The change of the spectrum from intact cells to membrane fractions could have resulted from a conformational change of GlpB due to lysis of the cells and dissociation of GlpAC from the membrane, or due to the presence of oxygen and disruption of the cluster(s). This chapter discusses the characterization of the paramagnetic center in GlpB. The spectroscopic evidence for the assignment of the GlpB paramagnetic center as a [2Fe-2S]

cluster is summarized.

A. Visible Spectroscopy

JM83 and JM83 harboring plasmids pGLP1, pGLP15, or pGLP20 were anaerobically grown in G/F medium as described in Materials & Methods. The JM83/pGLP1 [*glpACB*] whole cell pellets were a characteristic dark brown color, in contrast to the relatively cream color of JM83 or JM83/pGLP15 [*glpA* only] cells. JM83/pGLP20 [*glpAC*] cells were brownish compared to JM83, but never the color level of cells overexpressing the entire operon. The darker color of JM83/pGLP20 was as expected due to the presence of the flavin cofactors in the GlpA and GlpC subunits. The richness of the dark brown color in the JM83/pGLP1 cell pellet varied with each preparation, but was an early qualitative indication of significant expression and accumulation of GlpB.

In iron-flavoproteins, the absorption spectrum is a combination of the contributions of the flavin and of the iron-sulfide cluster moiety. The flavins are generally observed at 370 and 450 nm. Figure 33 shows the visible absorption spectra of a suspension of JM83/pGLP1 cells without and after treatment with 1.5 mM dithionite or 1.4 mM p-chloromercuriphenylsulfonate (PCMPS). The whole cell suspension prior to any treatment [Panel A/B, spectrum a], exhibited absorption bands which were relatively broad and featureless. An absorption maximum occured in the oxidized form [without addition of dithionite or PCMPS] at 420 nm, with shoulders at 450 - 460 nm and 550 - 560 nm. Addition of dithionite [Panel A, spectrum b] resulted in partial bleaching of the spectrum with a decrease in absorption of the 420 nm peak and of the shoulder at 460 nm. The shoulder at 550 - 560 nm also formed a peak at about 550 - 555 nm upon dithionite reduction. The dithionite reduced spectrum of JM83/pGLP1 whole cells was very similar to that observed with JM83 cells, before and after, treatment with dithionite [Panel C, spectrum a and spectrum b, respectively]. Spectra recorded for JM83/pGLP20 (*glpACB'*) [Panel D] were very similar to that recorded for JM83 whole cells, with increased absorption observed in the 430 - 470 nm region prior to treatment with dithionite [Panel D, spectrum a], but not to the degree observed for JM83/pGLP1 (*glpACB*) whole cells prior to treatment with dithionite [Panel A, spectrum a]. Upon reduction with dithionite, the absorption wavelength peaks of the reduced forms of cytochrome b [α band, 555 -567 nm; β band, 526 - 546; and γ band, 408 - 449 nm (Cramer & Knaff, 1991)] were observed in all of the cell suspensions [Panel A/C/D,

spectrum d]. Treatment of the JM83/pGLP1 cell suspension with a mercurial sulfhydryl reagent, p-chloromercuribenzylsulfonic acid (PCMPS), resulted in a 15 % reduction in spectral absorption [Figure 33, Panel B, spectrum b] which is more than expected due to dilution effects upon addition of PCMPS. The reduction in spectral absorption was enhanced with prolonged incubation [Panel B, spectrum c]. The visible absorption spectra are typical of other iron-sulfur proteins.

B. EPR Spectra of Anaerobically Maintained JM83/pGLP1

Whole cells of JM83 and JM83/pGLP1 were grown anaerobically in G/F medium and prepared as well maintained anaerobic samples [refer to Section II.B.17b]. The EPR samples were reduced with dithionite and spectra recorded at 5 K. Figure 34 shows the reduced spectra of JM83 cells [spectrum a] and JM83/pGLP1 cells [spectrum b] over a wide range of field [field sweep ~ 4000 gauss]. The difference spectrum of the two spectra [spectrum b minus spectrum a] is shown in spectrum c. The main feature of the spectrum in JM83/pGLP1 whole cells was the very prominent signal at ~ 3300 - 3600 gauss, which corresponded to g-values of between 1.88 and 2.05. As mentioned previously, the fumarate reductase signal of center 1 [FR1] was evident in the spectrum observed for the aerobic preparation of JM83/pGLP1 cells [Figure 17, A (a)]. The FR1 signal was also predominantly present in the reduced spectrum of anaerobically prepared JM83 cells [Figure 34, (a)]. FR1 was not a major feature in the reduced spectrum of anaerobically prepared JM83/pGLP1 cells [Figure 34, (b)]. This is shown in the difference spectrum [spectrum c] where the features attributable to *glpACB* overexpression are enhanced. The handling of the JM83/pGLP1 samples within the anaerobic environment may protect the GlpB cluster(s) from any oxidative damage and suggest that the clusters within GlpB may be very labile to oxidative environmental changes. As the intensity of the EPR signal is a measure of the concentration of the species present, there was a definite indication that the signal observed in the JM83/pGLP1 reduced spectrum [spectrum b] was a very strong and prominent signal over the spectrum observed in the background strain JM83 [seen with the difference spectrum]. JM83/pGLP15 [*glpA* only] cells reduced with dithionite exhibited a spectrum very similar to the JM83 reduced spectrum, whereas JM83/pGLP20 [*glpAC*] cells reduced with dithionite exhibited slightly altered spectrum but not defined enough to assign any distinctive features to the spectrum [refer to Figure 49]. It is important to note that the reduced spectra of JM83/pGLP15 and JM83/pGLP20 whole cells exhibited a

major contribution from the FR1 center, despite being handled anaerobically, in contrast to spectra recorded for JM83/pGLP1 which exhibited the strong *Clostridium*-like signal. The difference in the intensity of the reduced signal for JM83/pGLP1 lends support that the paramagnetic center is associated with the GlpB polypeptide, as originally suggested with the GSTGlpB fusion studies.

A narrow field spectrum [field sweep of 800 centered at 3400 gauss] of reduced JM83/pGLP1 whole cells recorded at 20 K is shown in Figure 35. Various g values of the prominent features are also highlighted, with the major features as follows: peaks at 2.00 and 1.97, troughs at 1.95 and 1.90, with shoulders at 2.04, 2.02, 1.92 and 1.88. The spectra resembled that observed for *C. pasteurianum* 2[4Fe-4S] Fd in the reduced state (Mathews *et al.*, 1974; Prince & Adams, 1987) and showed additional features over the simpler rhombic signal shown in Figure 17 [Panel A, spectrum c]. From preparation to preparation of JM83/pGLP1 whole cells, there was a slight variation of the amplitude of the various peaks and troughs observed in the EPR spectra as well as with the overall intensity of the signal. Particularly, the depth of the trough g = 1.90/1.88 appeared to vary as well as the shoulder peak at g = 1.97/8. Variation in the recorded spectra are not unusual due to the anisotropic nature of the molecules within the various samples and the variability of expression and handling.

Whole cells of JM83 and JM83/pGLP1 were subjected to anaerobic lysis in an anaerobic bag by lysozyme/freeze/thaw treatment followed by reduction with dithionite, as described in Materials & Methods. The corresponding spectra are shown in Figure 36. There were no significant changes observed in the spectra recorded for the intact and lysed cell suspensions for both JM83 cells [spectrum a and b, respectively] and JM83/pGLP1 [spectrum c and d, respectively]. This was contrary to the observed spectra exhibited by cells which have undergone aerobic handling and lysis, as shown in the Figure 17. Taking into account the change in amplitude of the signal due to the scaling factor at which the spectra were recorded, a three fold increase in the magnitude of the measured amplitude of the signal was observed for the lysed JM83/pGLP1 cell extract [Figure 36, spectrum d] over intact cells [spectrum c] which reflected the easier accessibility of dithionite for reduction upon lysis. Spectrum d represents an 8-fold increase in intensity of the signal as compared to spectrum a, which again indicates the prominence of the signal associated with GlpB, over the background FR1 center.

Similar spectra were once again obtained with G3P reduction of cells [Figure 37]. A difference spectrum [spectrum c] of JM83/pGLP1 [spectrum b] minus JM83 [spectrum a] again exhibited the rhombic signal observed in aerobically handled cells

[Figure 17].

C. Temperature Dependence of Reduced Spectra

In their paramagnetic state, the iron-sulfur proteins are characterized by a spin-relaxation time strongly dependent upon temperature: the EPR signal is easily saturated at liquid helium temperatures and broadens rapidly at temperatures higher than that of liquid nitrogen (Gayda *et al.*, 1979). Marked differences in the relaxation-temperature behavior have been noted for different centers [i.e. a conspicuous difference exists between the [2Fe-2S] and [4Fe-4S] centers]. The temperature behaviour of a signal can be used in a qualitative way for characterization of the signal. However, the differences are not always sufficient to distinguish conclusively between the two types of centers. (Rupp *et al.*, 1978).

The JM83/pGLP1 intact cell sample, reduced with dithionite, was used for this analysis, as the GlpB signal was clear and intense. Figure 38 shows representative spectra of the sample at 2 mW [20 dB] at various temperatures. The signal was quite pronounced at low temperatures [below 30 K], and with increasing temperatures the features were less defined. Very subtle changes in the lineshape of the signal were noticed such as the g = 1.92 trough becoming more prominent at higher temperatures, but the g-value assignment remained the same. The signal was still visible up to 110 K, although quite diminished.

A temperature dependence of the amplitude of the derivative signal was obtained at three power settings of 20 mW [10 dB], 2 mW [20 dB] and 0.2 mW [30 dB]. Figure 39 shows a plot of the signal height [of the derivative signal] as a function of temperature [Panel A] for the three settings. At 10 dB, two peaks in the temperature profile were observed at 9 and 32 K, and a similar behaviour was seen at 20 dB except at 9 and 25 K. This dual peak behavior was atypical, but suggested an optimum for observing the signal at lower temperatures. At 30 dB, a single peak in the temperature profile was observed at 16 K. Panel B is a plot of signal height * temperature as a function of temperature for the three power settings. This method of presentation corrects for the Curie law transition probability or more simply takes into account various temperature effects. Generally at low temperatures, the signal intensity of an observed EPR signal is decreased by power saturation while at higher temperatures, the signal intensity decreases with the Boltzman factor [1/T; where T is the absolute temperature] and eventually becomes undetectable because the linewidth is greatly increased (Rupp *et al.*,

1978). At 20 mW [10 dB] [Figure 39] the signal for reduced JM83/pGLP1 cells showed a maximum at 55 K though at 2 mW [20 dB], a maximum at 35 K was observed. At 30 dB, the behavior was similar to that seen at the lower temperatures of the other two power settings. This data was indicative of an optimal temperature dependence of the signal at lower temperatures [below 40K], but the persistence of the signal at high temperatures [> 80 K] was unusual and was more indicative of a [2Fe-2S] center.

D. Power Saturation Behavior of JM83/pGLP1 Reduced Signal

In some cases, a greater distinction between the cluster type is observed by analysis of the power saturation behavior at low temperatures [10 - 20 K] (Rupp *et al.*, 1978). The saturation method is based on a series of equations which assume 'homogenous broadening' or simply, the sample contains identical paramagnetic centers which all resonate at the same magnetic field (Rupp *et al.*, 1978). In order to analyze the behavior of the signal intensity [S] as a function of the microwave power [P], a series of EPR spectra are recorded with the power varying from a condition of negligible saturation to one of pronounced saturation. Figure 40 shows representative spectra of JM83/pGLP1 whole cells reduced with dithionite recorded at 20 K at various power settings from 0 to 50 dB [200 mW to 2 μW, respectively]. The spectra were also recorded at 9, 16 and 24 K and were similar to the spectra shown in Figure 40. The amplitude of the peak was measured for each spectrum, and normalized to take into account the various receiver gain settings at which individual spectra were recorded. The data [normalized amplitude (S) divided by the square root of the microwave power (P)] was plotted as a function of P as described in Chapter I and is shown in Figure 41, for the four temperature settings. Plotting $\log[S/\sqrt{P}]$ as a function of log P for each temperature setting resulted in a line which is parallel to the abscissa when the signal was not saturated, but sloped downward toward the abscissa with increasing saturation. At lower temperatures [i.e. 9 K], the signal was easily saturated for the curve sloped down quite readily at low power. The power for half-saturation is given by the intersection of the extrapolated straight-line portions of the data curve. The $P_{1/2}$ values were determined to be 0.006, 0.07, 0.22 and 0.76 mW for 9, 16, 20 and 24 K respectively.

A perturbation of a paramagnetic center may change its saturation behaviour in two ways: by changing the $P_{1/2}$ value or by changing the degree of homogenous broadening (Rupp *et al.*, 1978). In the plot of log $[S/\sqrt{P}]$ against log P, the curve tends to a slope of 0.5b under conditions of saturation, where b is the 'inhomogeneous

parameter'. From Figure 41, b was determined to be 1.09 for the system. This is indicative of an inhomogenous system. (Rupp *et al.*, 1978).

As described in Chapter I [Section I.E.2], the various relaxation mechanisms show different temperature dependence behaviour. Figure 42 shows the effect of temperature on $P_{1/2}$, based on the data presented in Figures 40 and 41. The $P_{1/2}$ followed an apparent T^5 dependence, but approached a T^9 dependence at a higher temperature [24 K].

E. Redox Potentiometry of the GlpB Cluster

1. Aerobically Prepared Cell Suspensions

Original redox potentiometry was carried out with aerobically prepared crude or washed membranes of JM83/pGLP1 cells at pH 7.0 in 50 mM MOPS/5 mM EDTA. Although aerobically handled cells produced an altered spectrum upon cell lysis [Figure 17, Panel B (b)], the features attributable to the GlpB center(s) were still quite evident. A sample of the crude membranes, which was the source material for the titration, reduced with dithionite showed a strong signal very similar to that previously observed [Figure 17, B (b)]. However, once the source material was mixed with the redox mediator dyes in the redox vessel and an EPR sample prepared and analyzed, the redox spectra showed a loss of the g = 2.00 peak, and appeared very similar to JM83 samples only [Figure 17, B(a)]. These changes observed in the spectra with the addition of the redox mediators suggested inadequate mediation or denaturation of protein. JM83/pGLP1 whole cells, washed and resuspended aerobically in 50 mM MOPS/5 mM EDTA, pH 7.0 were also used for titration analysis to avoid changes in the spectra due to aerobic cell lysis. No dramatic changes in lineshape nor in amplitude of signal were observed, which suggested that the redox species was being buffered by endogenous substrates or blocked by poor mediation resulted in poor contact with the measuring electrodes.

2. Anaerobically Prepared Cell Suspensions at pH 7.0

To overcome some of the difficulties mentioned in the previous section, I resorted to anaerobic handling of the JM83/pGLP1 whole cells. Within the anaerobic bag, the cell suspension in 100 mM MOPS/ 5 mM EDTA, pH 7.0, was subjected to

lysozyme/freeze/thaw treatment as described in Materials & Methods, and then injected into the prepared anaerobic redox chamber containing buffer with the dye mediators. Representative spectra recorded at 20 K from the titration are shown in Figure 31. The general lineshape was evident by -140 mV and reduction amplified the signal, but no additional features representative of a second cluster and/or interaction were observed. Following oxidation with potassium ferricyanide, re-reduction of the cell suspension resulted in similar spectra as in Figure 43, but slightly diminished in amplitude which indicated cluster damage. Each spectrum was normalized for tube calibration and receiver gain and the signal amplitude of the g = 2.0 peak to g = 1.90 trough was measured. An estimation of the midpoint potential was determined by plotting the signal amplitude as a function of the potential at which the sample was poised and fitting the data to the Nernst equation (at 25°C). Figure 44 illustrates a representative fit [Panel A], with an estimation of the midpoint potential at - 320 ± 10 mV at pH 7.0 [n = 0.75]. No 'steps' in the curve were observed indicative of a second cluster or midpoint potential. Panel B illustrates the Nernst equation with an n = 1.0 value at a midpoint potential of - 320 mV.

The EPR spectra of the redox titration samples were also recorded with a wide field range [field sweep of 4000 centered at 2100 gauss]. As some Fd signals show features in higher g - values [i.e. g > 4.0], I viewed the poised redox samples to determine if any features became prominent during reduction. Figure 45 shows a representative spectrum poised at - 425 mV. The only evident features are those from the prominent Fd-like signal described previously. All the minor bumps and troughs at higher g-values are present throughout all the spectra recorded and did not vary in amplitude. These results indicated the presence of only one cluster.

3. Anaerobically Prepared Cell Suspension at pH 9.0

The redox titration was also carried out with the cell suspension at pH 9.0 in 100 mM CHES/1 mM EDTA at 25°C. The cell suspension was prepared as previously described for the pH 7.0 titration. The spectra were recorded as previously described in Materials & Methods. Figure 46 shows representative spectra of the titration in the reducing direction from - 257 mV to - 491 mV. Again, the lineshape of the reduced signal was visible at the start of the titration, but the characteristic features previously mentioned became dramatically enhanced upon reduction to lower potentials. The amplitude of the signal of the sample poised at - 491 mV was approximately 13 %

smaller than that at - 482 and - 486 mV, which suggested cluster damage due to over-reduction.

The peak-to-trough amplitude was again measured for each spectrum, and normalized for tube calibration and receiver gain used to record the spectra. The normalized amplitude for each recorded spectrum was again plotted against the redox potential the particular sample was poised at, and the data are shown in Figure 47. An estimate for the midpoint potential in this case was more difficult, for although the system appeared stable during the collection of samples, significant hysteresis was observed upon analysis of the EPR spectra. Panel A shows the estimation of the redox potential to be - 390 mV, n = 0.85 using the data points obtained from the reducing direction [i.e. spectra as shown in Figure 46]. Panel B illustrates the hysteresis effects with an estimated midpoint potential of - 318 mV, n = 0.7 for the spectra recorded in the oxidizing direction. An overall estimate is shown in Panel C with an E_m' of - 355 mV, n = 0.75.

F. Effects of Other Variables on the Signal

In an attempt to characterize the signal further, other conditions were examined, with preparation of the samples within the anaerobic bag.

1. pH

JM83/pGLP1 whole cells were washed and then resuspended in 0.2 M MOPS/EPPS/CHES 'cocktail' buffer, with the respective pH levels adjusted by addition of 5 M NaOH to the cocktail [as described in Materials & Methods]. The samples were reduced with 2.5 mM dithionite [2 min incubation] and spectra recorded as previously described. Figure 48 shows the reduced spectra of the various pH conditions. The g = 1.92 trough was more prominent at lower pH as well as the slight peak at g = 1.98, but these features diminished at more alkaline conditions. A plot of the peak [g = 2.0]-to-trough [g = 1.90] amplitude as a function of the pH [Figure 48, Panel B] exhibited an optimum at pH 9.0.

2. Treatment with Denaturants

The lysed cell extract of JM83/pGLP1 cells was treated with guanidine

hydrochloride [0.35 M final] or urea [0.9 M final], incubated for 10 minutes and then reduced with dithionite. The corresponding spectra, recorded at 20 K, are shown in Figure 49, spectrum a and b respectively. Changes in the lineshape of the signal indicated that the paramagnetic center was disrupted. Furthermore the spectra were similar to that observed with JM83/pGLP15 [*glpA*] and JM83/pGLP20 [*glpACB'*] cell extracts reduced with dithionite [spectrum c and d respectively].

3. Treatment with o-Phenanthroline

o-Phenanthroline is an iron chelator, which is known to disrupt iron sulfur clusters (Orme-Johnson, 1973) and is often used in non-heme iron determination assays (Mortenson & Gillum, 1980). The iron in most ferredoxins reacts slowly with iron chelating agents, but in the presence of denaturants the reaction with iron becomes rapid. EPR samples of the JM83/pGLP1 lysed cell extract were prepared with 65 μM o-phenanthroline [2 hr incubation], or urea [0.8 M] treated [incubated for 10 min] followed by addition of 65 μM o-phenanthroline [incubated for 10 min or two hr]. In each case, reduction with 2.5 mM dithionite [incubated 2 min] followed prior to freezing the sample. The spectra were recorded at 20 K and are shown in Figure 50. The spectra have been normalized for tube calibration and protein concentration. Spectrum a illustrates the maximum amplitude of the signal obtained with the cell suspension diluted with buffer to an appropriate level for comparison with addition of o-phenanthroline [spectrum e]. A 15 % reduction in amplitude is seen. Pretreatment of the cell suspension with urea, as previously seen [Figure 49, spectrum b], caused an alteration of the signal as well as a 17 % decrease in the amplitude of the signal [Figure 50, spectrum b]. An enhanced decrease in the amplitude was seen with further incubation in the presence of o-phenanthroline [spectrum c - 36 %]. This effect was quite significant after a 2 hr incubation [Figure 50, spectrum d - 58 % overall reduction].

4. Treatment with 80 % DMSO

Partially reduced *C. pasteurianum* Fd exhibits an EPR spectrum corresponding to molecules with just one center reduced (Rupp *et al.*, 1978; Sweeney & McIntosh, 1979). The observed spectrum resembles that of the protein in 80 % DMSO (Rupp *et al.*, 1978) where the interaction between the centers is prevented by partial unfolding of the protein (Cammack, 1975). I resuspended JM83/pGLP1 whole cells in 80 % DMSO within the

anaerobic bag and reduced with 2.5 mM dithionite to determine if this would alter the reduced signal observed. The spectrum was recorded as previously described and is shown in Figure 51. There did not appear to be any changes associated with this treatment, indicating only a monocluster for the GlpB paramagnetic center.

G. Effect of Oligonucleotide Site-Directed Mutagenesis on the GlpB Signal

Using site-directed mutagenesis, I have changed each of Cys_{12} and Cys_{59} of GlpB to Ser [herein refered to as C12S and C59S respectively], by introducing nucleotide base substitutions into pGLP90 [refer to Table 4]. These cysteine residues were altered because other investigators have shown that the second cysteine in the Fd-like motif appears to be crucial in the proper folding and coordination of the cluster (Rothery & Weiner, 1991; Werth *et al.*, 1990). The mutations were verified by dideoxy sequencing, and no mutations other than those specified by the mutagenesis oligonucleotides were detected. Furthermore, the pGLP90 plasmid was used as the source for PCR amplification of the *glpACB* operon and analyzed by electrophoresis on agarose gels to ensure that no recombination or change in length of the operon had occurred.

1. Expression of the Mutant GlpB Polypeptides

The expression of the mutant enzymes was verified by SDS-PAGE of the Yamato enriched membrane preparations [Figure 52]. The GlpB band was evident in both of the mutant cytoplasmic membrane fractions [C12S, lane 1; and C59S, lane 2]. As well, G3PDH activity assays were done with the soluble cytoplasmic fractions of JM83 cells transformed with plasmids pGLP90C12S and pGLP90C59S, carrying the mutations, to confirm the expression of the operon. C12S and C59S showed comparable activity to wild type [3.8 and 2.3 U /mg respectively for the two mutants, compared with 3.3 U/mg for wild type pGLP90]. The activity measurements as well as the identification of the mutant GlpB band on SDS-polyacrylamide gels confirmed that the enzymes from the mutant plasmids were expressed and that the mutant enzymes were associated with the cytoplasmic membrane fractions.

2. Visible Absorption Spectroscopy

Whole cells of JM83/pGLP90C12S and JM83/pGLP90C59S were resuspended in 50 mM MOPS/5mM EDTA, pH 7.0 buffer and analyzed by visible absorption spectroscopy. The spectra for each mutant are shown in Figure 53, before [spectrum a] and after [spectrum b] treatment with 1.5 mM dithionite, with Panel A for the C12S mutant and Panel B for the C59S mutant. The C12S spectra, before and after dithionite closely resembled the spectra observed for JM83/pGLP1 wild type cells [Figure 33, Panel A], with broad features throughout the 400 - 500 nm region and an additional shoulder at 530 and 560 nm. The reduction with dithionite showed a decrease in absorbance in these regions. The C59S mutant did not exhibit as intense absorption in the corresponding regions as the C12S mutant and wild type. The spectrum [Panel B, spectrum a] prior to dithionite was very similar to that observed for JM83/pGLP20 whole cells. After addition of dithionite, the spectra in each case resembled that observed for dithionite reduced JM83 and JM83/pGLP1 cells.

3. EPR Spectroscopy

Whole cell EPR samples of the mutants were prepared and recorded as previously described and are shown in Figure 54. During aerobic handling of the cells [Panel A], the two mutants, C12S [spectrum b] and C59S [spectrum c] exhibited spectra similar to that seen with JM83 cells [Figure 36, spectrum a] and not the wild type JM83/pGLP90 cells [Figure 54, spectrum a]. Alternatively, when the cells were prepared under anaerobic conditions [Figure 54, Panel B], the C12S mutant [spectrum b] exhibited a reduced spectra similar to the wild type JM83/pGLP1 cells [spectrum a]. The C59S mutant [spectrum c] reduced spectra still closely resembled JM83 whole cell spectra, without the additional features seen in C12S and wild type. The mutation of C59S of GlpB had major effects on the EPR spectra of the dithionite reduced enzyme. The observed changes, as indicated by astericks, were a loss of the $g = 2.0$ and 1.97 peaks and the deepening of the $g = 1.88$ trough. As mentioned, the spectra were very similar to that seen with JM83 preparations, as well as JM83/pGLP1 cells treated with guanidine hydrochloride [Figure 49, spectrum a]. The same spectrum for C59S was observed irrespective of the type of handling, suggestive of no cluster formation rather than oxidative damage.

For both mutants, the presence of the conversion of a [4Fe-4S] cluster

conversion to a [3Fe-4S] cluster was tested by addition of ferricyanide, an oxidant. Spectra were recorded at 10 K, but there were no special features observed over oxidation of the background JM83 strain [i.e. presence of fumarate reductase FR3 [3Fe-4S] cluster (Johnson *et al.*, 1988)]. It did not appear that a [3Fe-4S] cluster was formed with either mutation of the specified cysteine residues.

JM83/pGLP90C12S cells were used for redox potentiometry. The anaerobically lysed cell suspension was prepared as previously described for wild type preparations [refer to Materials & Methods]. A sample of the suspension was reduced with 2.5 mM dithionite and exhibited a reduced spectrum as observed in Figure 54, Panel B (b). Figure 55, Panel A shows representative spectra from the redox titration. The most distinguishing feature of the spectra poised at lower potential [i.e. - 363 and - 429 mV] was that the spectra no longer resembled the reduced spectrum of anaerobically handled cells [Figure 55, B (b)], but instead resembled that observed for aerobic handling [Figure 55, A (b)]. The g = 2.0 peak for each spectra was used to measure the amplitude of the signal [after normalization for tube calibration and receiver gain] and were plotted against the poised potential at which the sample was taken [Figure 55, Panel B]. A midpoint potential of - 385 mV, $n = 0.65$ was estimated, but due to the alteration of the signal in the presence of the redox mediators, this value was suspect.

H. Spin Quantitation

The EPR spectra can provide quantitative information about the amount of the species present. For an s = 1/2 system, the doubly integrated intensity of the spectrum is proportional to spin concentration, provided that it is measured under nonsaturating conditions (Cammack *et al.*, 1985a). Measurement of the spin concentration is normally done by comparison with a standard and must be corrected for temperature, sample geometry and instrument settings. Using the JM83/pGLP1 whole cell sample prepared anaerobically [same sample as used for temperature and power saturation analysis], the spectra were recorded at 30 dB at 16 and 24 K, where nonsaturating conditions still prevailed for the temperature [refer to Figure 41]. A 1 mM $CuSO_4$ in 10 mM EDTA solution was used as the standard, and spectra recorded at the same temperature and power settings as for the JM83/pGLP1 sample. The derivative signals were integrated twice, with base-line correction prior to each integration. The spectra were integrated over the same sweep width of 1800 gauss, encompasing the full signal of the Cu-EDTA standard. A spin concentration of 61.6 µM was determined for the JM83/pGLP1

samples at 24 K, 30 dB. After correction for sample purity and molecular weight, the number of spins per molecule was estimated as 1.3. This value is only a weak estimate as the value is highly dependent on sample purity and concentration, which cannot be determined to definitive values since whole cells were being utilized for the analysis. Appropriately, highly purified samples are routinely used for quantitation to minimize error. Furthermore, the assembly of the clusters in GlpB may not be 100 % efficient.

I. Discussion

Ferredoxins are low molecular weight, nonheme iron proteins that function as electron carriers in a wide variety of electron transport chains (George *et al.*, 1985). All Fds appear to share an ancestral gene duplication (Bruschi & Guerlesquin, 1988; Fukuyama *et al.*, 1988). Bacterial Fds are generally characterized by their strongly negative potentials and the iron-sulfur cluster that forms part of their reactive center. Although sequence comparisons indicate that the bacterial Fds [generally 4Fe-4S cluster(s) but also 2Fe-2S] and plant Fds [2Fe-2S] are homologous, they are distantly related and differ in their physiochemical properties. GlpB contained within its sequence the 'classic' *Clostridium*-type Fd motif which exemplifies the classical bacterial Fd. The motif contains the pattern of four cysteines and a proline [C-xx-C-xx-C-xxx-CP] that is distinctive of *Clostridial* type Fds. From defined crystal structures (Adman *et al.*, 1976), it is known that the polypeptide chain folds back on itself, so that the fourth cysteine of each half molecule ligates to the [4Fe-4S] cluster of the other half molecule. This would suggest that two centers would always be formed with the double motif, but Orme-Johnson (1973) found during reconstitution experiments of cleaved half-chain ferredoxins that the half-chain molecules could function as primordial Fds [i.e. one cluster only]. Furthermore Fukuyama *et al.* (1988) showed with the determination of the tertiary structure of the [4Fe-4S] Fd from *Bacillus thermoproteolyticus* that the second cluster-binding region of 2[4Fe-4S] clusters corresponds to an α-helix region in *B. thermoproteolyticus*. This lends support for the secondary structure predictions which strongly suggests that the α-helix is generally present in monocluster Fds. The disappearance of the second cluster has been correlated to the presence of only four or six cysteines in the protein [versus the required eight] (Bruschi & Guerlesquin, 1988).

1. Presence of an Iron-Sulfur Center

GlpB exhibited a paramagnetic center visible in the reduced state by EPR analysis. The dark brown color of whole cells overexpressing GlpB, was a qualitative indication for the presence of iron-sulfur centers. Visible absorption spectroscopy offered further support that the center was due to nonheme-iron/acid labile sulfur center(s). The spectra were broad and featureless, with maximum at about 420 nm and a broad shoulder from 420 to 480 nm, which were reduced in intensity with reduction by dithionite or PCMPS [sulfhydryl reagent]. This behavior was typical of iron-sulfur clusters (Mortenson, 1964; Meyer & Moulis, 1981). Although one of the most obvious methods for detection of an iron-sulfur cluster is the presence of non-heme iron [or acid labile sulfur], from laboratory trials with preparations of GlpB, it was deemed futile to attempt a determination with non-pure protein. As described earlier [Chapter IV], solubilization of GlpB with Sarkosyl or cholate resulted in a decrease of the EPR spectral intensity and thus these solublized preparations were not used for further characterization of the GlpB signal. It is also generally regarded that analytical values for iron, sulfide and protein are rarely reliable on their own, and the uncertainty is further compounded by the purity and integrity of the preparation (Cammack, 1991). Upon purification of the GlpAC dimer, it was reported that the dimer contained 2 moles nonheme-iron/dimer and 1 mol of acid-labile sulfur/mole of enzyme (Schryvers & Weiner, 1981), but analysis by EPR indicated the GlpAC dimer did not show any distinctive paramagnetic center in the reduced state [refer to Section V.A.6]. Furthermore, the large contribution of FR1 in the recorded spectra for JM83/pGLP15 [*glpA*] and JM83/pGLP20 [*glpAC*] suggested that the GlpA and GlpC subunits did not have a paramagnetic center associated with them [JM83/pGLP15 and JM83/pGLP20; Figure 37 (c) and (d) respectively]. This is an illustration that the quantitative assays can be very misleading.

The presence of the characteristic EPR g values centered below g = 2.0, the classic "g = 1.94", feature in the reduced signal of JM83/pGLP1 cellular fractions was an indication that the center had a paramagnetic iron associated with it. The GlpB signal had a number of features associated with it as evidenced by the reduced spectra obtained with anaerobically handled whole cells [Figure 35]. The spectrum closely resembled that reported for *Clostridium*-like 2[4Fe-4S] Fds (Mathews *et al.*, 1974; Prince & Adams, 1987; Davasse & Moulis, 1992), with prominent features of peaks at 2.00, 1.97 and two major troughs at g = 1.95 and 1.90. Additional shoulders were present at g = 2.04, 2.02, 1.98 and 1.88 and a dip in the trough at g = 1.92. The additional lines in the

center of the spectrum and in the wings were most likely not true g-factors as demonstrated with multi-frequency [X versus K band] EPR conducted with *C. pasteurianum* Fd (Mathews *et al.*, 1974). In the reduced spectra of JM83/pGLP1 whole cells, the depth of the g = 1.92 dip varied with temperature and preparation. In some preparations, a signal was observed at g = 4.3 [1500 gauss region; Figure 35], but as it was also observed in the background strain, this feature was most likely due to bound ferric ions and most likely represented a minor impurity in the samples. The slight variations in the spectra recorded for various JM83/pGLP1 preparations were not unusual as the lineshapes of *C. pasteurianum* and *Micrococcus lactilyticus* 2[4Fe-4S] spectra have been known to vary with sample conditions (Cammack, 1975). Moura *et al.* (1992) have reported the identification of a 6Fe cluster isolated from *Desulfovibrio desulfuricans*, with g values of 1.97, 1.94 and 1.90 at low temperatures, and g values at 2.02, 1.98 and 1.95 at temperatures above 25 K. There are also additional prominent features in the low field range with resonances in the g = 15.3, 9.8, and 5.4 regions. As the spectra were not similar to that observed for GlpB it is unlikely that GlpB contained a 6Fe cluster. Furthermore, the reduced spectrum of GlpB did not resemble the EPR spectrum of reduced pure polyferredoxin from *Methanobacterium thermoautotrophicum*, a recently isolated and characterized *mvhB* gene product predicted to contain six tandemly repeated *Clostridial* Fd-like domains or 12 [4Fe-4S] clusters (Hedderich *et al.*, 1992).

Analysis of the lineshape of the JM83/pGLP1 signal indicated that it is unlikely to be a [2Fe-2S] cluster. A number of reported spectra for such clusters appear to be axial with g values at 2.03/2 and 1.94, typical of plant type Fds. This is the case with such iron-sulfur proteins as chick kidney Fd (Tang & Henry, 1993), center 1 in *E. coli* fumarate reductase (Johnson *et al.*, 1988), *E. coli* Fd (Knoell & Knappe, 1974; Ta & Vickery, 1992), and pyrazon dioxygenase Fd (Mason & Cammack, 1992), which indicate a typical cluster coordination with cysteine ligands. Rhombic signals, with g values at 1.89, 1.95 and 2.05 have also been reported for spinach Fd [2Fe-2S] clusters (Palmer & Sands, 1966). Although the difference spectrum observed with aerobically prepared JM83/pGLP1 cells [Figure 17 , Panel A (c)] shows slight similarity to the [2Fe-2S] rhombic spectra, the EPR spectrum of spinach Fd does not resemble the anaerobically prepared whole cell reduced sample observed with GlpB [Figures 34 and 35]. Alternatively, some unusual [2Fe-2S] clusters have been reported for various dioxygenases [which are summarized in Mason & Cammack (1992)], but again the GlpB reduced spectra had g values quite different from those listed. Despite the dissimilarity

of the signal observed, the temperature behavior of the GlpB reduced signal does not rule out the possibility that a [2Fe-2S] center was present, as the signal was still observed at high temperatures [> 77K], indicative of [2Fe-2S] centers.

A number of bacteria have Fds with a single [4Fe-4S] cluster, which also give rise to a "g = 1.94" signal in the reduced state. *Bacillus polymyxa* contains a Fd which exhibited a rhombic spectrum of peak values of g = 2.06 and 1.93 with the troughs at 1.91 and 1.88 (Shethna *et al.*, 1971). Fumarase A from *E. coli* also exhibits a rhombic spectrum [g values = 2.03, 1.94 and 1.88] and as well a broad peak at g = 5.4. Unlike the GlpB spectrum which does not shift in values upon addition of substrate, G3P, [Figure 25], the fumarase A spectrum shifts upfield [g = 2.035, 1.92 and 1.815] with the disappearance of the g = 5.4 feature (Flint *et al.*, 1992). A shift with substrate addition is suggestive that the cluster is involved in catalysis [as also observed in bacterial trimethylamine dehydrogenase (Steenkamp *et al.*, 1978)]. The [Fe-S] center(s) in GlpB on the other hand, appear not to be involved in the catalytic mechanism of the enzyme, as there is no shift in the spectrum. This is confirmed by the characterized properties of the purified GlpAC dimer (Schryvers & Weiner, 1981). The [Fe-S] center(s) in GlpB do play a role in the transfer of reducing equivalents to the fumarate reductase complex. Although FrdB of fumarate reductase in *E. coli* also contains a [4Fe-4S] cluster observable in the reduced state (Cammack *et al.*, 1986), the GlpB signal does not resemble the FrdB spectrum. *Pyrococcus furiosus* Fd, which contains a unique [4Fe-4S] monocluster with incomplete cysteinyl coordination [aspartyl ligand substitution] also exhibits a broad rhombic signal in the reduced state with g values of 2.10, 1.87, and 1.80, but undergoes rapid relaxation as the signal is not observable above 15 K (Conover *et al.*, 1990). Although GlpB exhibited a rhombic signal [g values = 2.00, 1.96 and 1.88] in the difference spectra [Figure 17, 37], the spectrum did not appear to resemble other rhombic spectra observed with other [4Fe-4S] clusters, which tend to be skewed to high field [low g values] and thus are almost axial in appearance.

Contrary to the behavior seen with *C. pasteurianum* Fd, GlpB did not exhibit changes in the spectra characteristic of partially reduced species, such as in single cluster reduction. *C. pasteurianum* Fd samples, partially reduced, exhibited a simple rhombic EPR spectrum but as the degree of reduction increased, the shape of the spectrum changed markedly: additional intensity was acquired in the center of the signal and additional structural detail developed throughout the spectrum (Orme-Johnson & Beinert, 1969). Furthermore, the EPR spectrum of *C. pasteurianum* Fd undergoes a sudden change, as DMSO is increased to about 70 %, to a simple axial signal (Cammack, 1975).

The DMSO-treatment signal resembles the partially reduced spectrum of the Fd which is explained by the loss of spin-coupling between the centers. In *C. pasteurianum* Fd, the two clusters or independent centers interact strongly enough to alter their EPR spectra, but not strong enough to alter their redox potentials [- 412 ± 11 mV] (Prince & Adams, 1987). NMR studies have also shown that the midpoint reduction potentials of the two clusters differ by 10 ± 5 mV on 1-electron reduction of the protein (Packer *et al.*, 1975). Further studies to determine whether after the initial 1-electron reduction, the E_{mp} of the unreduced cluster is altered, have shown that cluster-cluster cooperative interaction is not strong enough to be of functional importance in the *C. pasteurianim* Fd (Sweeney & McIntosh, 1979). A sample of *C. pasteurianum* Fd at intermediate reduction exhibits an EPR spectrum composed of two overlapping EPR spectra arising from 1- and 2-electron reduced molecules. The behavior of the Fds from *C. pasteurianum* and *M. lactilyticus* (Mathews *et al.*, 1974) have been suggested to arise from the following: each of the two active centers have essentially identical EPR spectrum. Upon minimal reduction, one of the centers is reduced exhibiting a simple rhombic spectra with g values approximately 2.07, 1.94 and 1.89. As reduction increases, both centers become paramagnetic each with its own simple spectrum, but now these clusters can interact. Hence the EPR spectrum becomes more complex. Two sources of interaction are suggested namely, magnetic dipole-dipole and electrostatic exchange, resulting in the 'spin-coupled system' (Mathews *et al.*, 1974). In GlpB, I was unable to detect the existence of a half-field [1700 gauss] signal which has been shown to be characteristic of a spin-coupled system with both centers having an average g value of 1.94 (Mathews *et al.*, 1974). As well, 80 % DMSO did not alter the signal [Figure 51], suggesting only one cluster was present [i.e. no spin coupling between two centers]. Interestingly, the 2[4Fe-4S] Fd II from *Clostridium thermoaceticum* exhibited an EPR spectrum in its fully reduced state which resembled that observed for partially reduced *C. pasteurianum* Fd [i.e. typical rhombic low potential [4Fe-4S] center with g values of 2.05, 1.92 and 1.89] (Elliott & Ljungdahl, 1982). This would suggest that the complex spectrum observed with two [4Fe-4S] clusters was not present in *C. thermoaceticum*, but integration of the reduced rhombic spectrum can be correlated with the uptake of two electrons for complete reduction of Fd II, although again a single midpoint potential of - 365 mV is measured.

From comparisons with the various respective spectra reported for the numerous [Fe-S] centers, the reduced spectrum of GlpB most resembled the 2[4Fe-4S] signal characteristic of *Clostridium*-like Fds. This was in agreement with predictions from the presence of the Cys motifs within the GlpB sequence. Although no distinction between

the two proposed centers was observed, variances in other systems show that unusual or atypical features arise within the evolutionary well conserved motifs.

2. Oxidation-Reduction Potentiometry

Clostridium-type Fds are distinguished by their low oxidation-reduction potentials [approximately - 400 mV] (Bruschi & Guerlesquin, 1988). As mentioned, the midpoint potentials of the two [4Fe-4S] clusters are within ± 10 mV of each other and are sometimes hard to distinguish. While potentiometric data for the study of several bacterial Fds fit a Nernst equation for which $n = 1$, the number of electrons transferred during reduction, as determined by integrations of EPR spectra and dithionite titration, was shown to be two (Stombaugh *et al.*, 1976). These studies indicate that two different single-electron carriers are present in *Clostridium* Fds as previously implied by the EPR results obtained by Orme-Johnson & Beinert (1969).

Redox titrations with GlpB have been attempted using whole and lysed cell suspensions of aerobically handled preparations, but as mentioned the fumarate reductase FR1 center features predominated and overshadowed the GlpB signal. Perhaps the center(s) within GlpB were highly sensitive to oxidative damage and hence collapsed upon lysis of the cells, thus permitting the prominence of the fumarate reductase signals. After determining that lysis of the cells within the anaerobic bag maintained the same *Clostridium*-like reduced signal, lysed cell suspensions [anaerobic handling] were used for the redox titration and a midpoint potential has been estimated at - 320 mV at pH 7.0 [$n = 0.75$]. During the titrations, re-reduction of the cell suspension resulted in a decrease in the magnitude of the signal indicative of cluster degradation. Only one midpoint potential was observed in the titrations. The failure to observe a distinct second cluster midpoint potential within GlpB may have arisen because the second cluster may have an extremely negative potential and not reducible by dithionite. This is the case in *Azotobacter vinelandii* Fd I (Martin *et al.*, 1990). Sodium dithionite has a E_m at pH 7.0 of - 420 mV, but is a favored reductant as it reacts rapidly (Dutton, 1978). Alternatively, the two midpoint potentials could be so close that they are hard to distinguish. At pH 9.0, a midpoint potential of - 355 mV, $n = 0.75$ was estimated, although significant hysteresis effects were present, despite longer equilibration times and higher redox mediator concentrations. The difference in the two midpoint potentials was not great enough to reflect a dependence on pH. From the Nernst equation, an increase of 59 mV is observed with each decrease in pH unit if protons are also involved in the reduction of

the species [Dutton, 1978].

Problems with hysteresis, cluster destruction by overreduction and variability of signal intensity from preparation to preparation have hindered obtaining a more definitive value. Hysteresis effects are not uncommon and can result from denaturation and/or precipitation of protein (Wilson, 1978). Technical problems associated with poor mediation between the iron sulfur centers and the electrodes may play an important role in the difficulties experienced. The redox 'dye' mediators present in the titration buffer act to indirectly relay electrons from the redox center in GlpB to the electrode, but this mediation may not always be rapid due to the location of the center within the polypeptide. Direct interaction of the electrodes with membrane-bound biological redox components is limited and tends to be slow. The effectiveness of relatively weakly interacting mediators can be improved by increasing their concentration or using multiple mediators (Dutton, 1978), but this did not appear to aid in trials with JM83/pGLP1 cellular fractions. As previously alluded to, another problem may be the presence of an active "endogenous reducing system", namely nonspecific reducing equivalents from stored substrates, as whole cell suspensions are being used. This problem can also be handled by increasing the concentration of the redox mediators and the use of multiple mediators (Dutton, 1978). Also, a common occurrence is the formation of an insulating layer of denatured protein to the metal electrode surface which 'blocks' mediation (Hitchens, 1989). Although care was taken to ensure usage of a clean electrode, once the titration was underway, it was difficult to maintain a clean surface without disruption.

Although most midpoint potentials for ferredoxin-like [Fe-S] centers reported to date are near - 400 mV, there are a few systems with lower potentials (Cammack, 1991). In the study of the low potential iron-sulfur centers of chloroplast photosystem I, photoreduction or the use of hydrogen plus hydrogenase in the presence of methyl viologen is used to reduce the centers [E_m ~ - 530 and - 600 mV] (Malkin & Bearden, 1980). There has also been some considerable effort in recent years to achieve direct and preparative electrochemistry of iron-sulfur proteins using gold, mercury, or platinum electrodes, with the use of 'promoters' which are viologen derivatives (Hitchens, 1989; Park *et al.*, 1991). Although methyl viologen is a low potential mediator [i.e. - 440 mV], its inclusion in initial GlpB redox attempts showed a prominent free radical signal characteristic of the mediator which further complicated analysis of the GlpB system. Hence it was subsequently left out of other redox titrations.

From redox potentiometric analysis, only one midpoint potential was evident in the GlpB system, indicative of one center. At present, the best estimate of the midpoint

potential of the GlpB [Fe-S] center is - 320 mV at pH 7.0. The midpoint potentials of the G3P/DHAP and fumarate/succinate couples, which are the physiological electron donor and acceptor, are - 190 mV and + 30 mV, respectively. The GlpB redox center would thus be competent to transfer electrons between these couples via the intermediate carrier menaquinol [- 80 mV] (Cole *et al.*, 1985; Cammack & Weiner, 1990).

3. Temperature Dependence and Power Saturation Behavior

As briefly mentioned, the optimal temperature to observe the reduced *Clostridium*-type signal was determined to be below 30 K. This is representative of an [4Fe-4S] cluster (Gayda *et al.*, 1979). Contrary to this normal behavior for [4Fe-4S] centers was the persistence of the JM83/pGLP1 signal to higher temperature [> 80 K]. This type of behavior is more typical of [2Fe-2S] centers which do not exhibit the rapid relaxation observed with the [4Fe-4S] clusters. However, in cases where the sample was very concentrated, one in general may observe EPR signals at higher than normal temperatures (Orme-Johnson & Sands, 1973). As well, Payne *et al.* (1993), in their studies with an [4Fe-4S]-type hydrogenase in the parasitic protozoan *Trichomonas vaginalis*, recently reported that the EPR spectrum was detectable at temperatures up to 100 K. In JM83/pGLP1 cellular suspensions, the amplitude of the signal increased as the temperature was lowered from 40 K to 16 K [20 dB] then decreased from 12 K to 5K most likely due to power saturation. The dual optimum peaks seen at 10 and 20 dB are unusual, but when the Curie law transition probability was accounted for [i.e. by plotting signal height * temperature as a function of temperature], an optimal temperature between 30 - 50 K was observed. This behaviour was more representative of a [2Fe-2S] center (Rupp *et al.*, 1978).

The power saturation behavior was also more typical of a [2Fe-2S] center, as the center was easily saturated at low temperatures [< 20 K] (Rupp *et al.*, 1978). Saturation with increasing microwave power of the [2Fe-2S] centers is a reflection of the more efficient electron-spin relaxation in the [4Fe-4S] centers. Relief from power saturation was reflected in a higher value of $P_{1/2}$ as seen at 20 and 24 K with $P_{1/2}$ values of 0.22 mW and 0.76 mW, respectively. Calculation of the slope factor or 'inhomogeneity parameter' was 1.09, which was indicative of an inhomogenous system. Values reported for b are usually between 1.0 [for inhomogeneous broadening] and 2.0 [for homogenous broadening] (Rupp *et al.*, 1978).

A temperature dependence of T^5 was observed for the system [Figure 30]. As

previously described, the known relaxation mechanisms generally yield a temperature dependence of T^2 or T^9 in the temperatures and power settings at which the spectra were recorded [refer to Chapter I]. Blum *et al.* (1983) have observed a similar T^5 temperature dependence for *C. vinosum* High Potential Iron Protein (Hipip), which they attributed to a varying T_2 or spin-spin relaxation time [which normally is considered constant]. From 20 to 24 K, the JM83/pGLP1 system exhibited a temperature dependence more representative of a usual intermediate-temperature T^9 Raman process found in other iron-sulfur proteins [Blum *et al.*, 1983].

4. Environmental Effects on the GlpB [2Fe-2S] Cluster

As we have seen with the T7 expression studies and expression from the endogenous *glp* promoter, elevated expression of *glpACB* can be obtained [Chapter III]. No effects on cell viability were apparent with JM83/pGLP1 as compared with JM83 during the 24 hour anaerobic growth conditions. This suggested that high concentrations of the enzyme are not toxic to the cell. As observed in the assembly of the cofactors into the catalytic dimer with overexpression, the cellular components required for assembly of the [Fe-S] centers and their regulation must be able to effectively respond to the increased demand due to polypeptide overexpression. Furthermore, the overexpression of the entire operon and assembly of the corresponding polypeptides did not appear to be affected by the chromosomal copy of the genes. However, in the overexpression of GlpB alone [as seen with T7 expression studies of pGLP93; *glpB* only] this may not be the case as I observed limited accumulation of the GlpB polypeptide. The extent of overexpression of GlpB appeared to be a major factor in the observed reduced spectra, for in optimal expression, the reduced [difference] spectrum closely resembled that of a *Clostridium*-type 2[4Fe-4S] spectra [Figure 35], and on weaker expression the difference spectrum was more rhombic in appearance [Figure 37]. Both of these spectra were obtained with GlpB handled within the anaerobic bag. This variability in observed reduced spectra is not unique. The [4Fe-4S] cluster in *Clostridium* lysine 2,3-aminomutase exhibited a rhombic signal pattern which varied from sample to sample, presumably owing to slight variations in the purification conditions (Petrovich *et al.*, 1992).

It is known that many [4Fe-4S] clusters of bacterial ferredoxins are sensitive to oxidative damage. As observed in the lysine 2,3-aminomutase, brief exposure to air at some point during the purification rather than maintaining strict anaerobic conditions also

resulted in slight lineshape change of the reduced signal (Petrovich *et al.*, 1992). In other Fd systems [i.e. *P. furiosus* Fd], once isolated under anaerobic conditions, the [4Fe-4S] center was remarkably inert to oxidative degradation (Conover *et al.*, 1990). The change in lineshape due to aerobic handling was quite evident with GlpB though not with another enzyme system studied within the lab, namely DMSO reductase DmsB [4Fe-4S] centers (Rothery & Weiner, 1991). This may be due to the lower midpoint potential of the GlpB center than in DmsB (Cammack & Weiner, 1990). In Chapter IV, the reported spectrum for reduced whole cells of JM83/pGLP1 exhibited a major fumarate reductase FR1 signal, with contributions of the GlpB centers showing features in the middle regions of the spectra, and the difference spectrum exhibiting the rhombic signal discussed. However, in the handling of the cell suspension in the anaerobic bag immediately upon harvesting of the cells, the ferredoxin-like signal was more prominent, even in the difference spectrum [Figure 34, (c)]. The features of the various reported peaks and troughs are the same in the reduced whole cell spectra of both aerobic and anaerobic handled samples, but this was not apparent at first as the intensity of the features was considerably different in the two preparations.

The type of handling was also a variable in the observed reduced spectra of the C12S mutant. Although the general lineshape of the wild type was observed in the spectra of the anaerobically handled preparations, aerobic handling appeared to fully disrupt the cluster as the observed reduced spectrum appeared similar to that of the background JM83 cells. Alternatively, when anaerobically prepared lysed cell suspensions were used in a redox titration, the spectra exhibited the aerobic JM83 type signal with the broadened troughs [Figure 55]. This suggested, that although the cluster in the mutant appeared to be unchanged, subtle differences in the cluster environment may have altered the cluster to become more susceptible to denaturation by the redox mediators in the titration vessel. Alternatively, perhaps the mutant C12S was able to retain a [2Fe-2S] cluster by using a cysteine elsewhere in the GlpB sequence as observed in *Azotobacter* (Martin *et al.*, 1990). As well, structure-function studies with high resolution x-ray crystollography and NMR/EPR studies with *E. coli* [2Fe-2S] Fd have shown that serine can replace cysteine at each of the four cluster attachment sites and still support cluster assembly (Holden *et al.*, 1994). Thus the C12S mutation may have caused structural changes within the protein, but such changes are not clearly indicated by the similarity of the reduced EPR spectrum with wild type. Of course, the possibility also exists that the first half of the ferredoxin cysteine motif is not involved in cluster binding. The C59S mutant, on the other hand, did not appear to exhibit any sign that the

[2Fe-2S] cluster was formed, thus suggesting that this cysteine was involved in coordination of the cluster. This was further supported by the decrease in the visible absorption spectrum in the 420 - 480 nm region which is generally attributed to the nonheme-iron clusters.

Aerobic lysis was shown to alter the GlpB reduced signal. In the anaerobic case, freeze/thaw lysis did not seem to change the spectra [Figure 36]. This suggested that the change in the observed spectrum was most likely due to air contact [oxidative damage] and not to the alternative proposal of the disassociation of GlpAC from the membrane. Perhaps in keeping the lysis suspension anaerobic, the redox environment was maintained and hence no dissociation occurred. As previously mentioned, this association may be similar to that seen with PutA in proline dehydrogenase, which shows association of the protein with the membrane only in the presence of substrate, with coincident flavin reduction and conformational change in the protein stucture (Wood, 1987; Brown & Wood, 1993).

The basis for the differences in oxidation-reduction potentials of the various [Fe-S] is not understood. Although a combination of factors are likely to contribute in modulating the value of midpoint redox potential, the differences depend upon the geometry and electronic properties of the clusters, the interactions with the polypeptide and the general conformation of the protein. These factors are considered to be sufficiently similar in *Clostridium*-type Fds that the redox potentials are the same (Packer *et al.*, 1975). The high potential iron protein in *Chromatium* which contains a [4Fe-4S] cluster [same geometry] exhibits a redox potential about 750 mV higher (Dus *et al.*, 1967), and alternatively *B. polymyxa* [4Fe-4S] cluster has a midpoint potential of -400 mV (Stombaugh *et al.*, 1973). It appears based on the vast difference between these two examples that a detailed analysis of the immediate neighborhood of the cluster is essential in understanding the basis for the midpoint potential within iron-sulfur proteins. Generally, iron-sulfur clusters are surrounded by hydrophobic residues, and a study by Kassner & Yang (1977) suggested that an environment composed of nonpolar amino acid side chains would contribute a redox potential which is negative, while a cluster surrounded by more polar amino side chains would be more positive. X-ray diffraction studies (Adman *et al.*, 1973) and ^{13}C-NMR (Packer *et al.*, 1975) studies introduced the possible involvement of aromatic residues, namely tyrosine or phenylalanine in interactions with the [Fe-S] cluster, as the presence of such a residue seemed to be conserved among the Fds (Malkin, 1973). EPR studies, though, have ruled out the possibility of direct involvement of the aromatic residues neighboring the cluster groups

(Gaillard *et al.*, 1986). Furthermore, some systems appear more susceptible to variations in the potential due to changes in pH [as is observed with JM83/pGLP1], ionic strength, etc. [i.e. *C. acidi-urici* and *C. pasteurianum*]. This is most likely due to the position of the cluster within the polypeptide as those that are buried within a hydrophobic region are most likely shielded from the solvent, while those close at the surface of the polypeptide are more readily exposed and thus more susceptible to environmental perturbations. Langen *et al.* (1992) showed that the potentials in four crystallographically characterized Fds [*Azotobacter vinelandii*, *Peptococcus aerogens*, *B. thermoproteolyticus* and *Chromatium vinosum*] are tuned in part by varying the access of solvent water to the neighborhood of the cluster, but the variations in the redox potential predominate in changes in protein structure in the region of the cluster.

Based on the studies conducted with GlpB, I propose that the [2Fe-2S] cluster was located near the surface of the polypeptide. As described, the center appears very susceptible to oxidative damage and the signal was readily altered [resembling no cluster formation] upon the addition of guanidine hydrochloride or urea. The resemblance of JM83/pGLP20 [*glpACB'*] reduced spectra with that of urea treated JM83/pGLP1 cells suggested that the [Fe-S] clusters may be partially assembled, but the polypeptide was unfolded from its true state. This further suggested that the latter 1/3 of the GlpB polypeptide may play a stabilizing role in cluster formation. Alternatively, guanidine hydrochloride, a chaotropic agent, totally disrupted the cluster as the reduced spectrum was similar to that seen with JM83/pGLP15 [*glpA*] reduced cells. The iron chelator o-phenanthroline, which normally is a very slow reactant with iron in [Fe-S] clusters, had a diminishing effect on the reduced signal, which was enhanced in the presence of urea. The effect was as observed for other nonheme iron-sulfur proteins where the denaturant like urea was present to allow access to the clusters (Malkin, 1973). The amino terminal cysteine motifs of GlpB are surrounded in most by nonpolar, hydrophobic residues [based on speculation of the cluster coordination and protein folding]. Immediately following the first cysteine motif are a number of glycines and prolines which must not only act for the polypeptide chain to fold back on itself for proper cluster coordination, but may also aid in burying the second cysteine motif [i.e potential ligand residues] into a hydrophobic pocket.

In summarizing the data of these EPR studies, the most reasonable assignment of the paramagnetic center within GlpB is likely due to a [2Fe-2S] cluster. The midpoint potential of the cluster was estimated to be - 320 mV. The cluster appeared to be very labile with rapid destruction due to overreduction with dithionite or oxidative damage.

The dependence of the EPR spectrum upon physiochemical factors showed that the cluster was accessible to the solvent matrix and was not buried within a protected hydrophobic pocket. The polypeptide environment thus seemed to play a major role in the coordination of the cluster. Although the GlpB reduced signal closely resembled those reported for 2[4Fe-4S] *Clostridium*-type Fd centers, atypical temperature and power saturation behavior as well as redox characteristics can not allow for a dual cluster assignment. These results do not rule out the possibility that other regions of the GlpB sequence contribute to the observed paramagnetic center. The results also do not rule out the possibility that the paramagnetic center is not a typical [Fe-S] cluster characterized to date, but may reflect a novel type of cluster.

The final chapter of this thesis is an attempt to summarize the results obtained herein, in view of the original thesis objective. Future directions are also discussed.

FIGURE 33. Visible Absorption Spectra of JM83/pGLP1 Whole Cells. Whole cells were resuspended in 50 mM MOPS/ 5 mM EDTA, pH 7.0 and the spectra were measured with the Varian DMS100 Spectrometer equipped with a chamber modified for analysis of particulate matter. The spectra were measured at room temperature using 50 mM MOPS/ 5 mM EDTA, pH 7.0 as the blank buffer.

Panel A: JM83/pGLP1 (*glpACB*) whole cells [6 mg/ml protein concentration] before [spectrum a] and after treatment [spectrum b] with 1.5 mM dithionite; and

Panel B: JM83/pGLP1 before [spectrum a] and after treatment with 75 µl of 20 mM p-chloromercuriphenylsulphonate (PCMPS) in 50 mM MOPS/5 mM EDTA, pH 7.0, and incubated at room temperature for 2 min [spectrum b] and 5 min [spectrum c]. The reference blank contained 1.4 mM PCMPS.

Panel C: JM83 whole cells [5.0 mg/ml protein concentration] before [spectrum a] and after treatment [spectrum b] with 1.5 mM dithionite; and

Panel D: JM83/pGLP20 (*glpACB'*) whole cells [5.5 mg/ml protein concentration] before [spectrum a] and after treatment [spectrum b] with 1.5 mM dithionite.

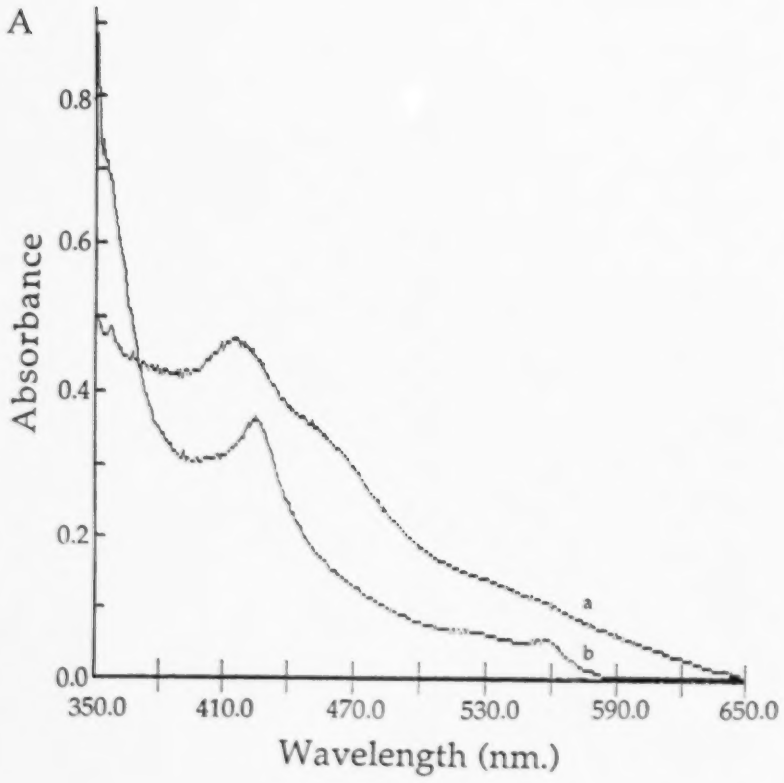
A
Absorbance
0.8
0.6
0.4
0.2
0.0
350.0
410.0
470.0
530.0
590.0
650.0
Wavelength (nm.)
a
b

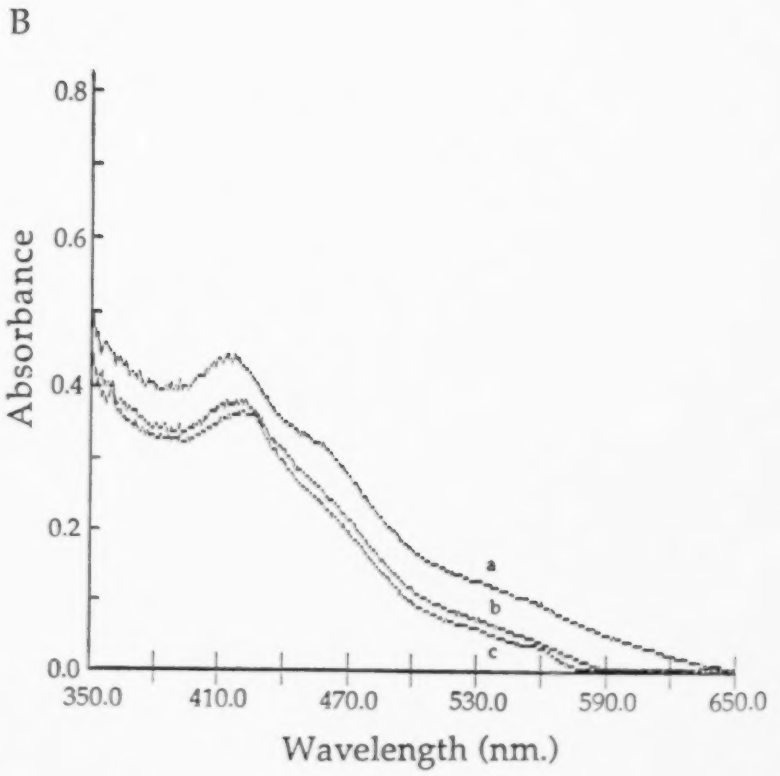
B
Absorbance
0.8
0.6
0.4
0.2
0.0
350.0
410.0
470.0
530.0
590.0
650.0
Wavelength (nm.)
a
b
c

C

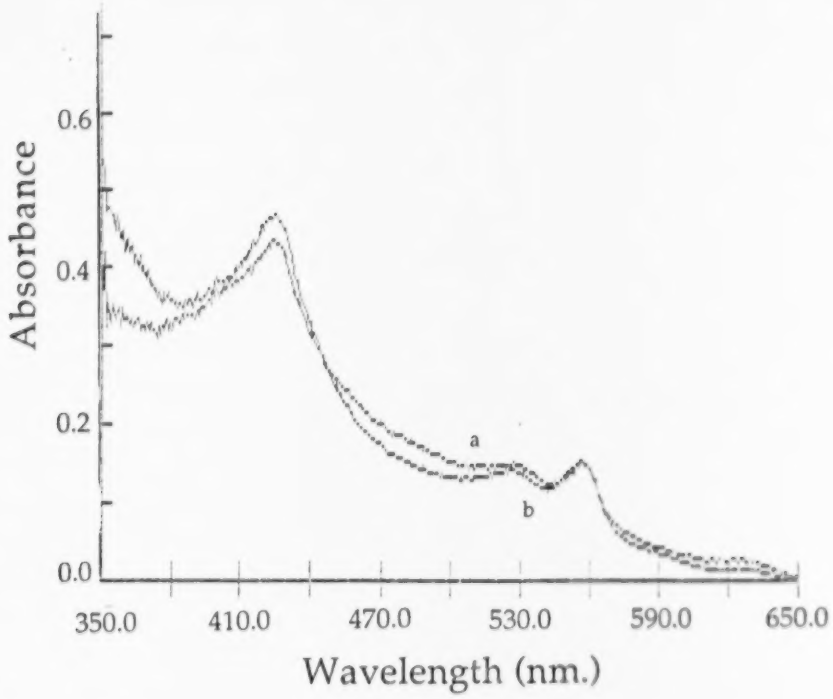
Absorbance
0.6
0.4
0.2
0.0
a
b
350.0
410.0
470.0
530.0
590.0
650.0
Wavelength (nm.)

D

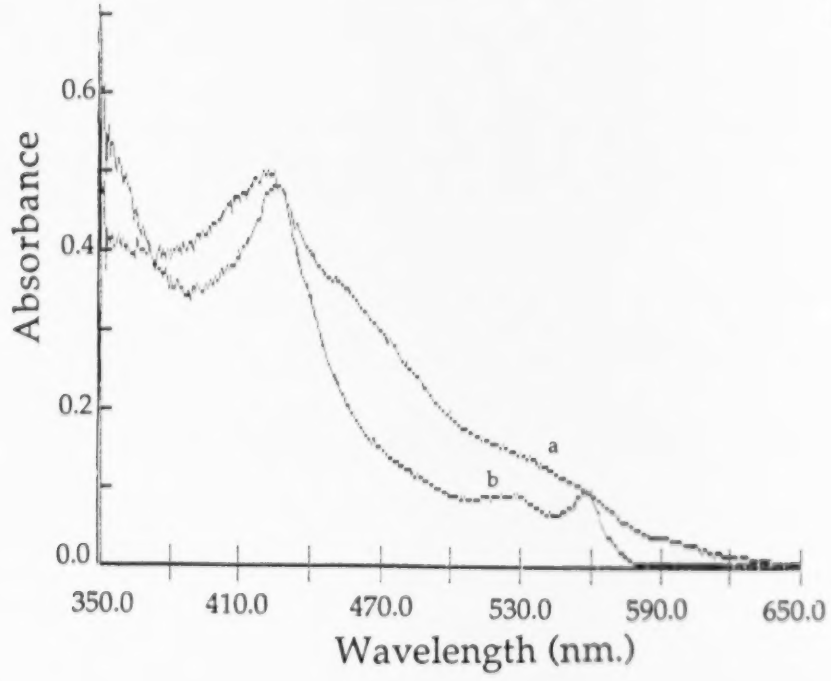
Absorbance
0.6
0.4
0.2
0.0
a
b
350.0
410.0
470.0
530.0
590.0
650.0
Wavelength (nm.)

FIGURE 34. Wide Band EPR Spectra at 5 K of Anaerobically Handled JM83/pGLP1 Whole Cells. Samples of JM83 and JM83/pGLP1 whole cells were prepared and reduced with 2.5 mM dithionite as described in Materials & Methods. Spectra (a) JM83 cells; (b) JM83/pGLP1 cells; and (c) Difference spectrum of spectrum (b) - (a). Spectra were recorded as described in Materials & Methods, except at a temperature of 5 K and a microwave power of 2 mW [20 dB]. The spectra were normalized for protein concentration and tube calibration.

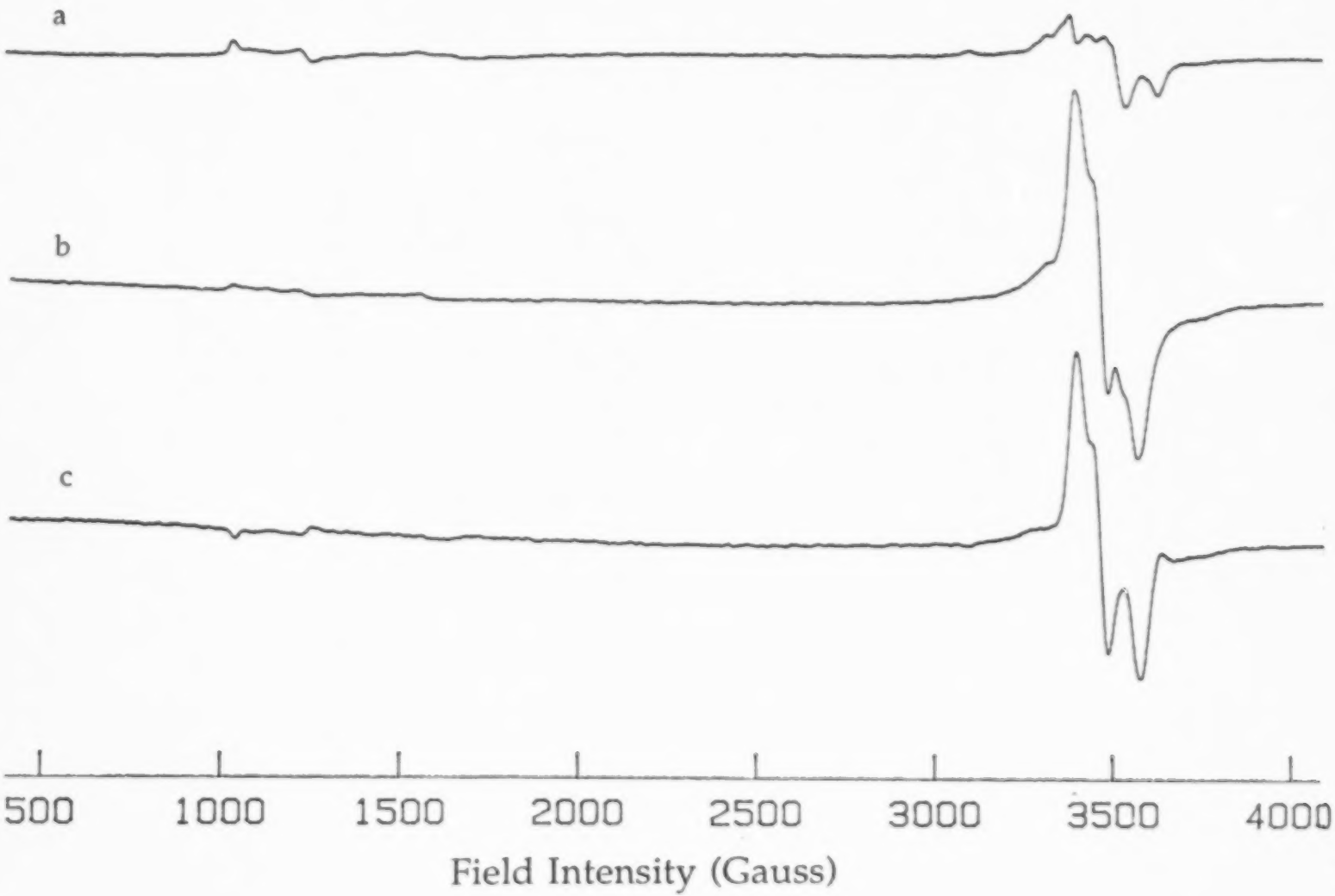
a
b
c
500
1000
1500
2000
2500
3000
3500
4000
Field Intensity (Gauss)

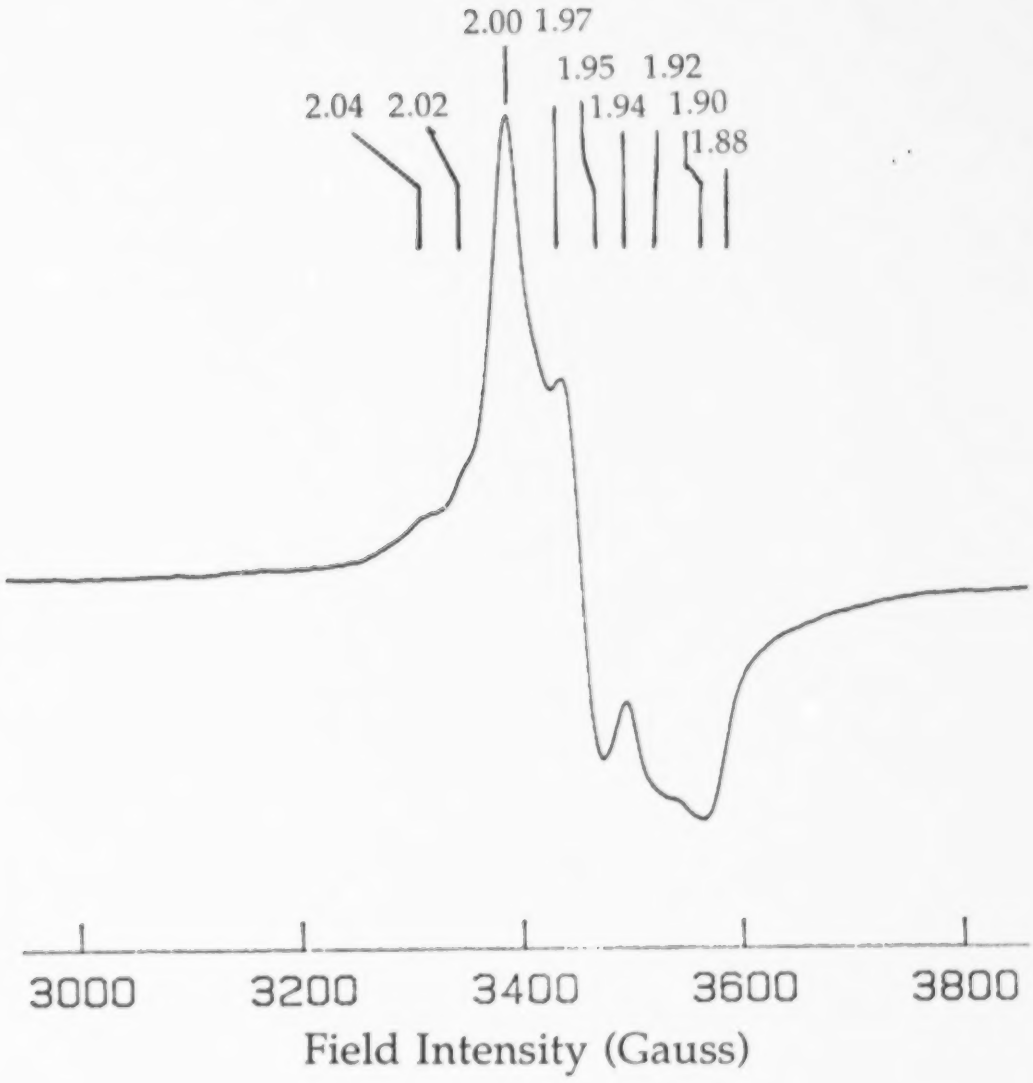

FIGURE 35. A Narrow Band EPR Spectrum at 20 K of Anaerobically Handled JM83/pGLP1 Whole Cells. The EPR sample was that used to record Figure 22, spectrum b. g-values are as indicated. Spectra were recorded as described in Materials & Methods.

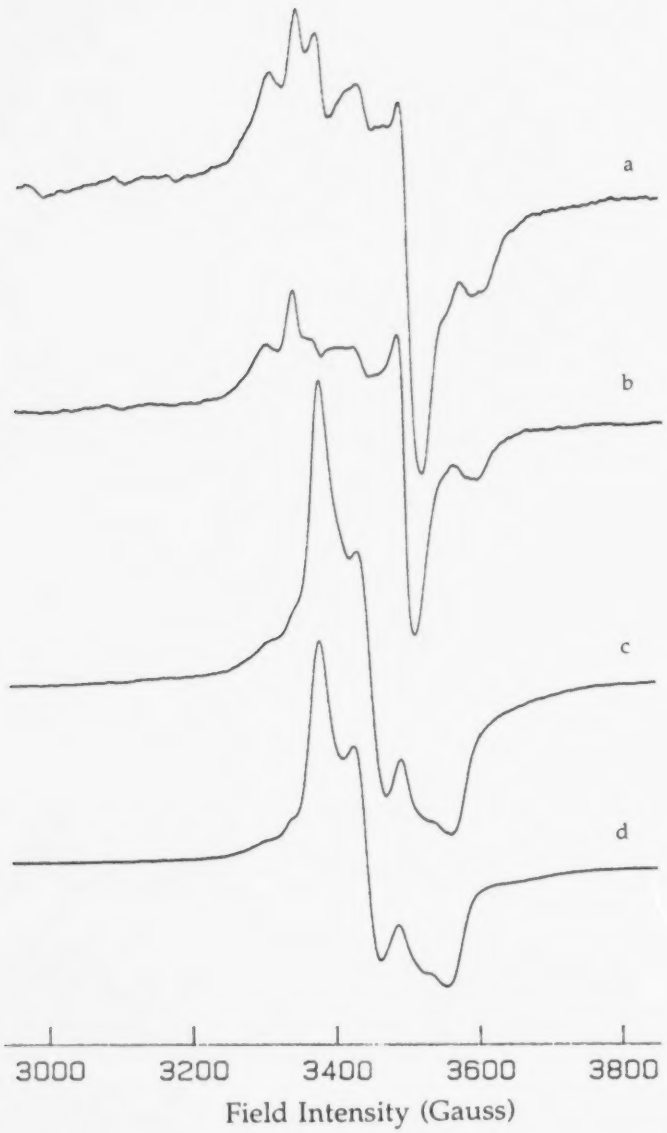

FIGURE 36. EPR Spectra at 20 K of Intact and Anaerobically Lysed Cells. JM83 and JM83/pGLP1 cells were prepared within the anaerobic bag as described in Materials & Methods. The samples were reduced with 2.5 mM dithionite and spectra recorded as previously described. Spectra were normalized for tube calibration, protein concentration and receiver gain and the appropriate scaling factor is also highlighted. A factor of 1X indicates the spectrum was plotted at scale 16; 0.5X, scale 17; 0.25X, scale 18; and 0.125X, scale 19, respectively, noting that an increment in a scale represents a factor of two in the amplitude of the spectrum. Spectra (a) JM83 intact cells [1X]; (b) JM83 lysed cell suspension [0.5 X]; (c) JM83/pGLP1 intact cells [0.25X]; and (d) JM83/pGLP1 lysed cell suspension [receiver gain 2 X 10^4] [0.125X].

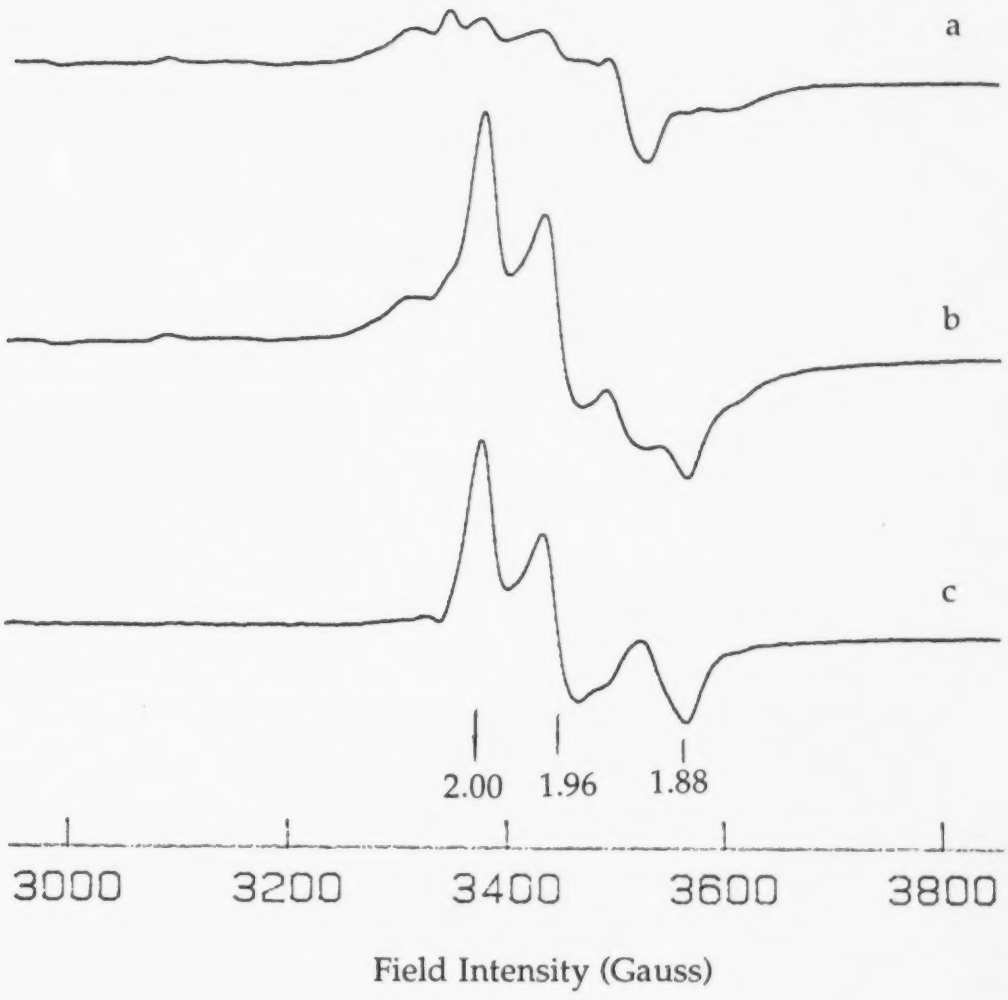

FIGURE 37. EPR Spectra at 20 K of Anaerobically Handled Intact Cells Reduced with G3P. JM83 and JM83/pGLP1 cell samples were incubated with 20 mM G3P for 10 min within the anaerobic bag as described in Materials & Methods. Spectra (a) JM83 cells; (b) JM83/pGLP1; and (c) Difference spectrum of (b) - (a). g-values are as indicated. Spectra were normalized for tube calibration and protein concentration and were recorded as described in Materials & Methods.

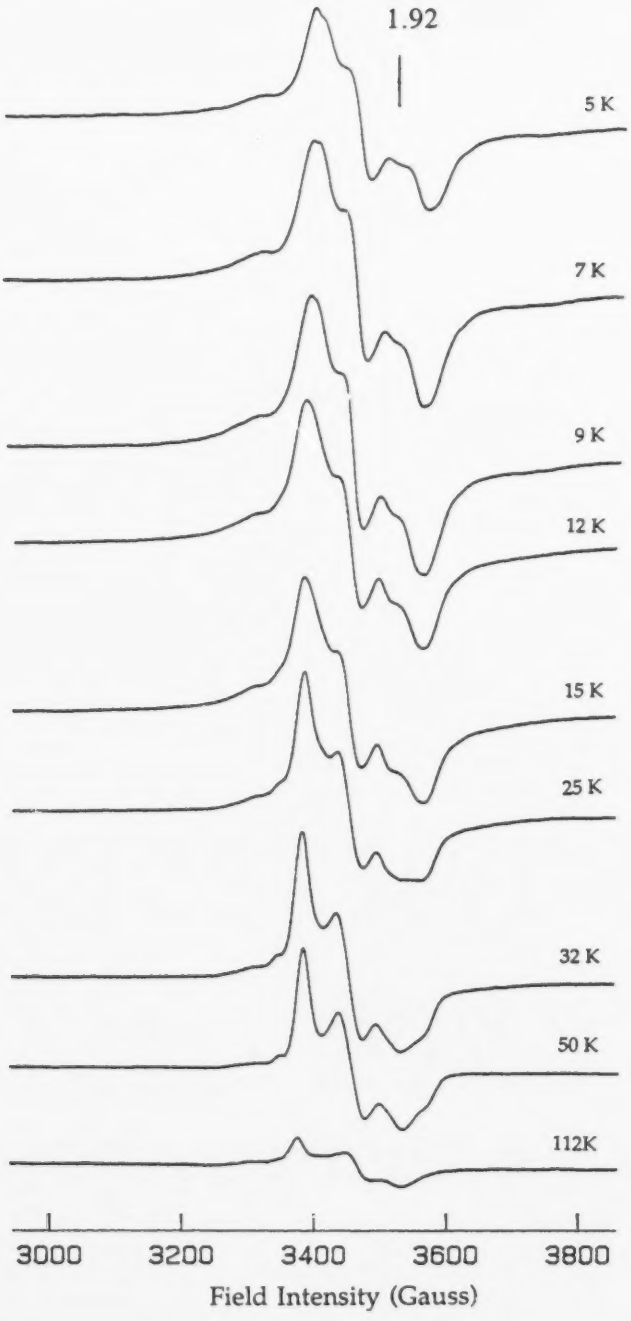

FIGURE 38. EPR Spectra of Anaerobically Prepared JM83/pGLP1 Whole Cells at 20 dB. The sample was treated with 2.5 mM dithionite [same sample as used for wide band scan in Figure 22]. The spectra were recorded at various temperatures, as illustrated, between 5 K - 112 K. Spectra were recorded as described in Materials & Methods, except at 7, 9 and 12 K, receiver gain was 3.2 X 10^4. Spectra were normalized for receiver gain.

FIGURE 39. Temperature Dependence of the Signal Amplitude in JM83/pGLP1 Intact Cells. Representative spectra are as shown in Figure 26 for 20 dB. Similar spectra were recorded at 10 and 30 dB. Panel A is a plot of derivative intensity [signal height] as a function of temperature [K] for the three power settings: ◇, 10 dB; □, 20 dB; ○, 30 dB. Panel B is a plot of [signal height * temperature] as a function of temperature [K], with the symbols as described for Panel A for the three power settings. Signal amplitude is in arbitrary units.

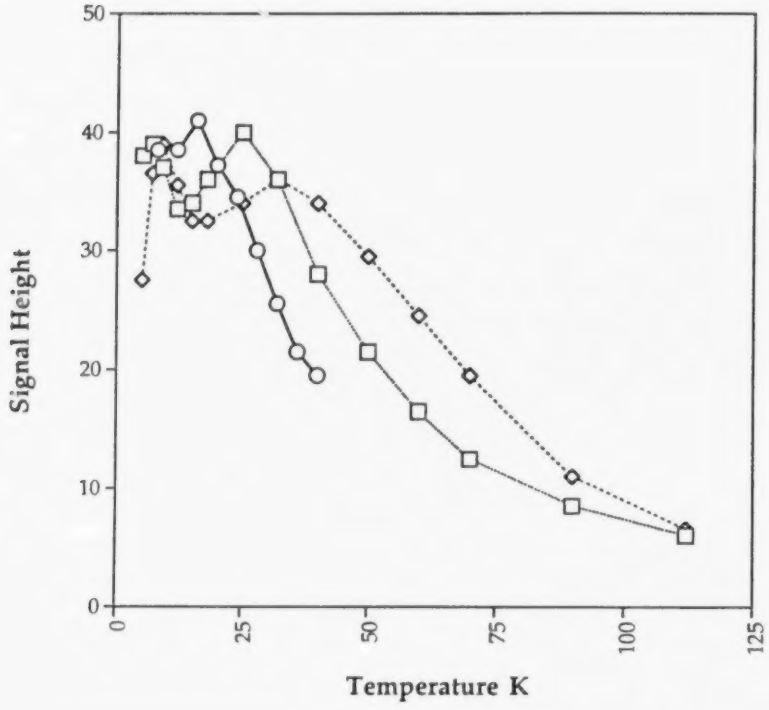
A
Signal Height
50
40
30
20
10
0
0
25
50
75
100
125
Temperature K

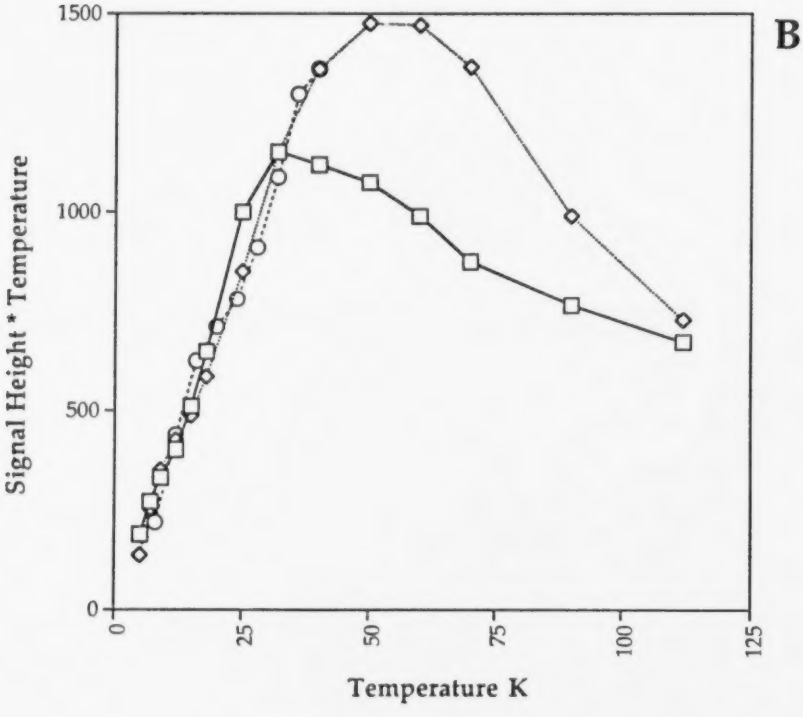
B
Signal Height * Temperature
1500
1000
500
0
0
25
50
75
100
125
Temperature K

FIGURE 40. Representative EPR Spectra of Anaerobically Prepared JM83/pGLP1 Whole Cells at 20 K With Varying Power Levels. The sample used was as for Figure 26. The microwave power was varied from 0 to 26 dB in two dB increments and then from 30 to 50 dB in five dB increments as shown. Similar spectra were recorded at 9, 16 and 24 K. The spectra shown have not been normalized for variation in receiver gain at which the individual spectra were recorded, but such normailizations are included in the calculations for plotting of data in Figure 41.

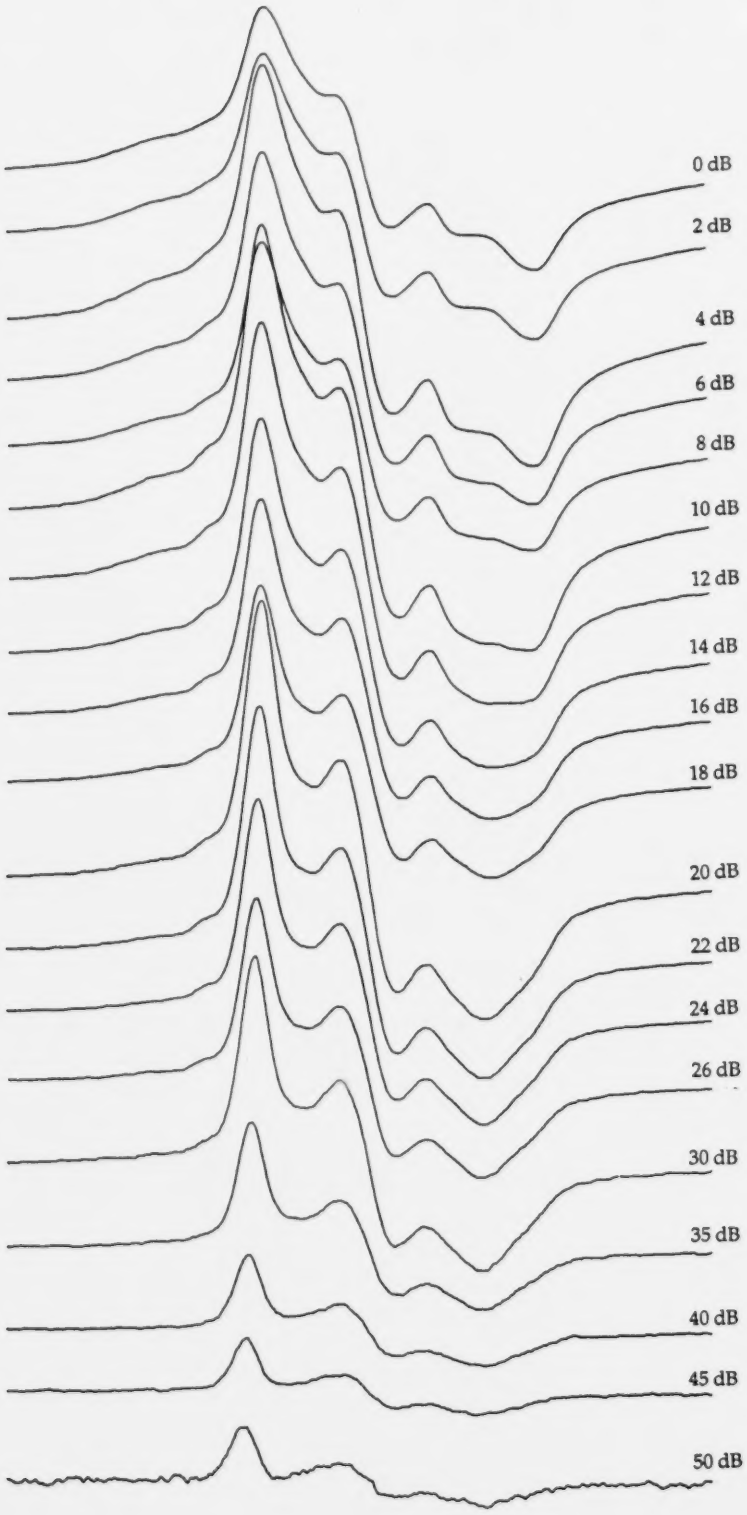
0 dB
2 dB
4 dB
6 dB
8 dB
10 dB
12 dB
14 dB
16 dB
18 dB
20 dB
22 dB
24 dB
26 dB
30 dB
35 dB
40 dB
45 dB
50 dB

FIGURE 41. Microwave Power Saturation Behaviour of JM83/pGLP1 Intact Cells. The sample used was as described in Figure 38. Representative spectra are as shown in Figure 40 for 20 K. Signal amplitude (S)/ [Microwave power (P)]$^{1/2}$ is plotted as a function of the power, P [mW]. Points represent power saturation behaviour at different temperatures: 9 K, Δ; 16 K, O; 20 K,◇; and 24 K,□. The signal amplitude has been normalized for receiver gain. The power at half saturation, $P_{1/2}$, at the various temperatures was determined as described in Chapter I. $P_{1/2}$ values are 0.006 mW, 0.07 mW, 0.22 mW and 0.76 mW for 9, 16, 20 and 24 K, respectively.

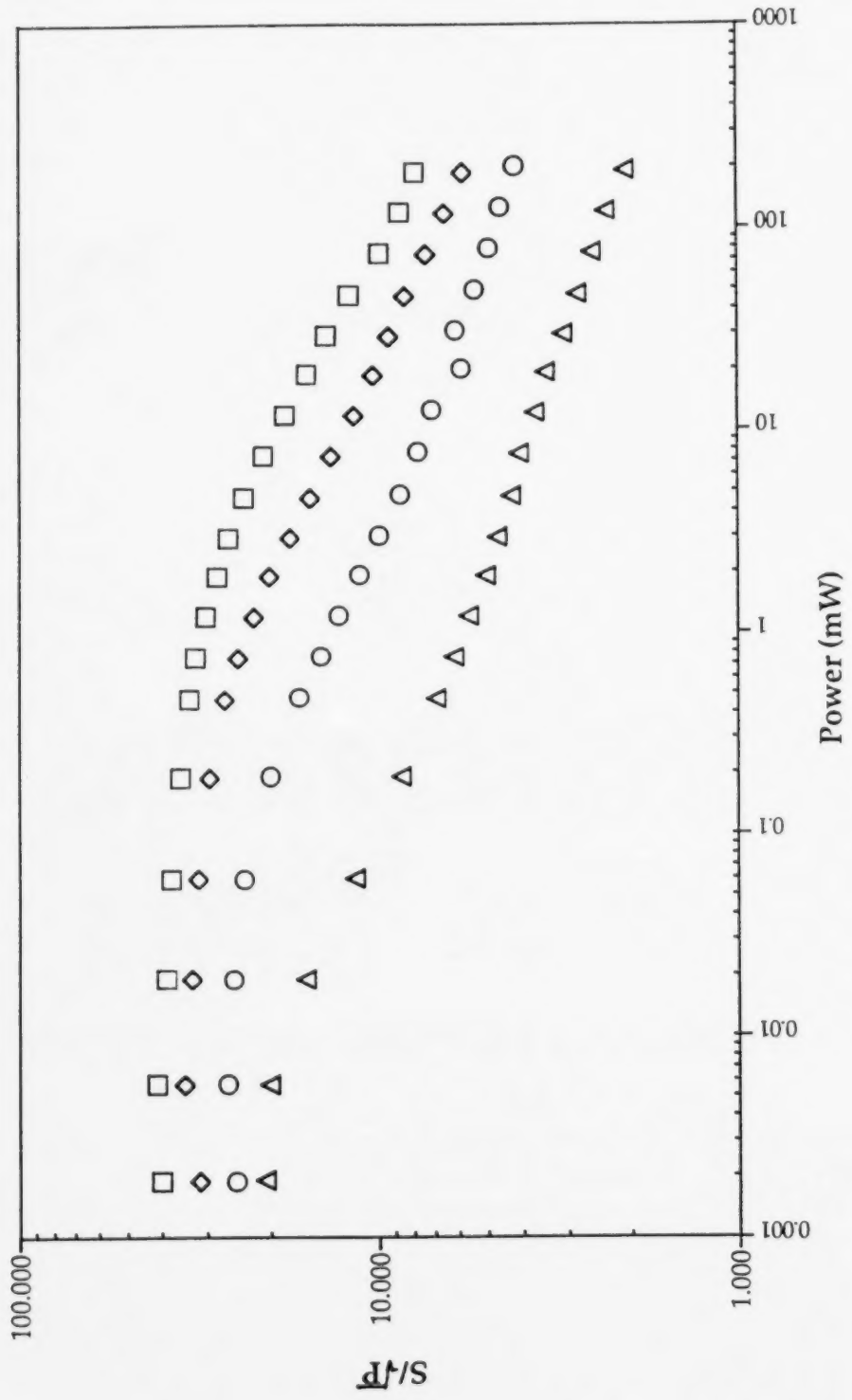
100.000
10.000
1.000
S/√P
0.001
0.01
0.1
1
10
100
1000
Power (mW)

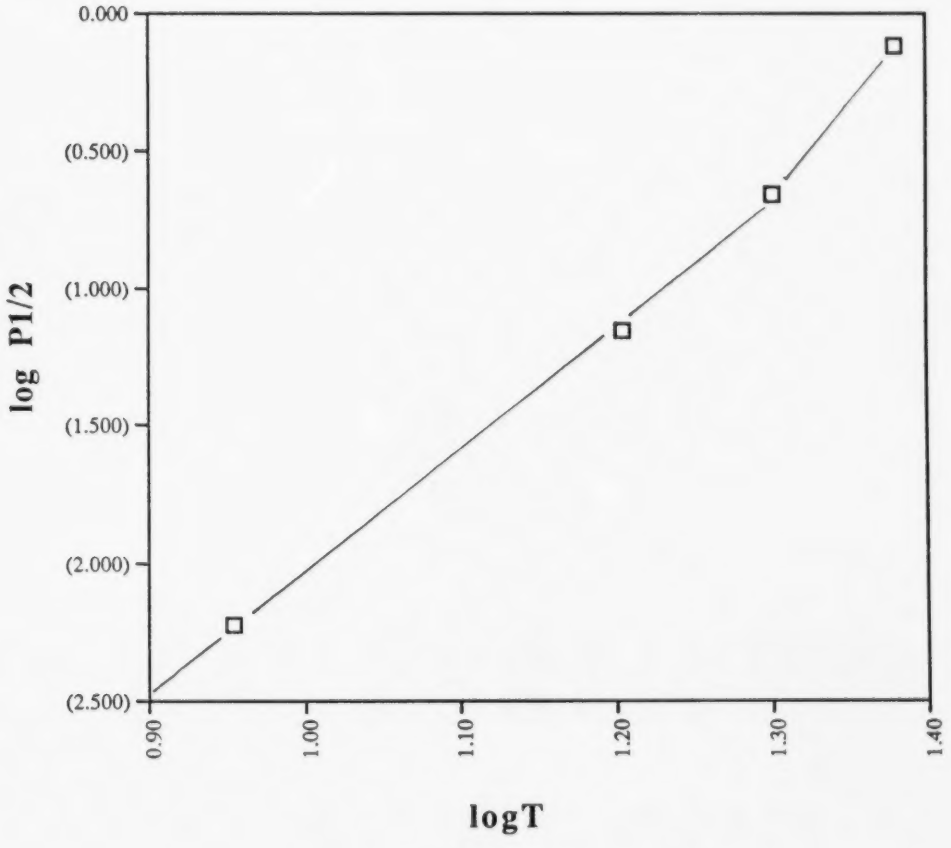

FIGURE 42. Temperature Dependence of Power at Half Saturation. The determined $P_{1/2}$ values [Figure 41] are plotted as log $P_{1/2}$ vs. log T. The slope of the line is representative of the relaxation mechanism of the system showing a temperature dependence of T^5 [refer to Section V.I.3].

FIGURE 43. Representative EPR Spectra of JM83/pGLP1 Anaerobically Lysed Cell Suspension During Redox Titration at pH 7.0. The lysed cell suspension in 50 mM MOPS/5 mM EDTA, pH 7.0, was prepared and used for redox potentiometric analysis as described in Materials & Methods. Spectra were recorded as previously described at 20 K. The poised potential at which each sample was taken at is shown for each spectra, respectively. Spectra were normalized for tube calibration and the appropriate scaling factor is also highlighted. A factor of 1X indicates the spectrum was plotted at scale 16; 0.5X, scale 17; and 0.25 X, scale 18, respectively, noting that an increment in a scale [i.e. scale 16 to 17] represents a factor of two in the amplitude of the spectrum.

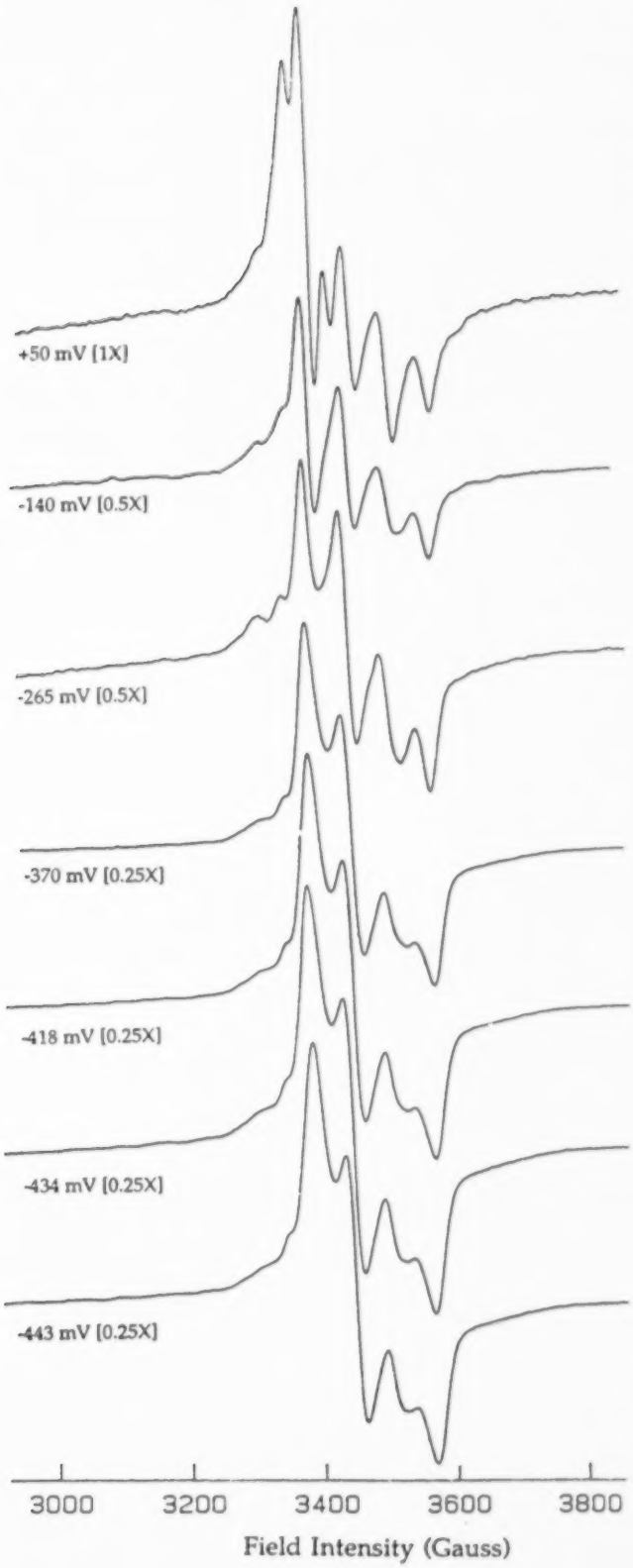
+50 mV [1X]
-140 mV [0.5X]
-265 mV [0.5X]
-370 mV [0.25X]
-418 mV [0.25X]
-434 mV [0.25X]
-443 mV [0.25X]
3000
3200
3400
3600
3800
Field Intensity (Gauss)

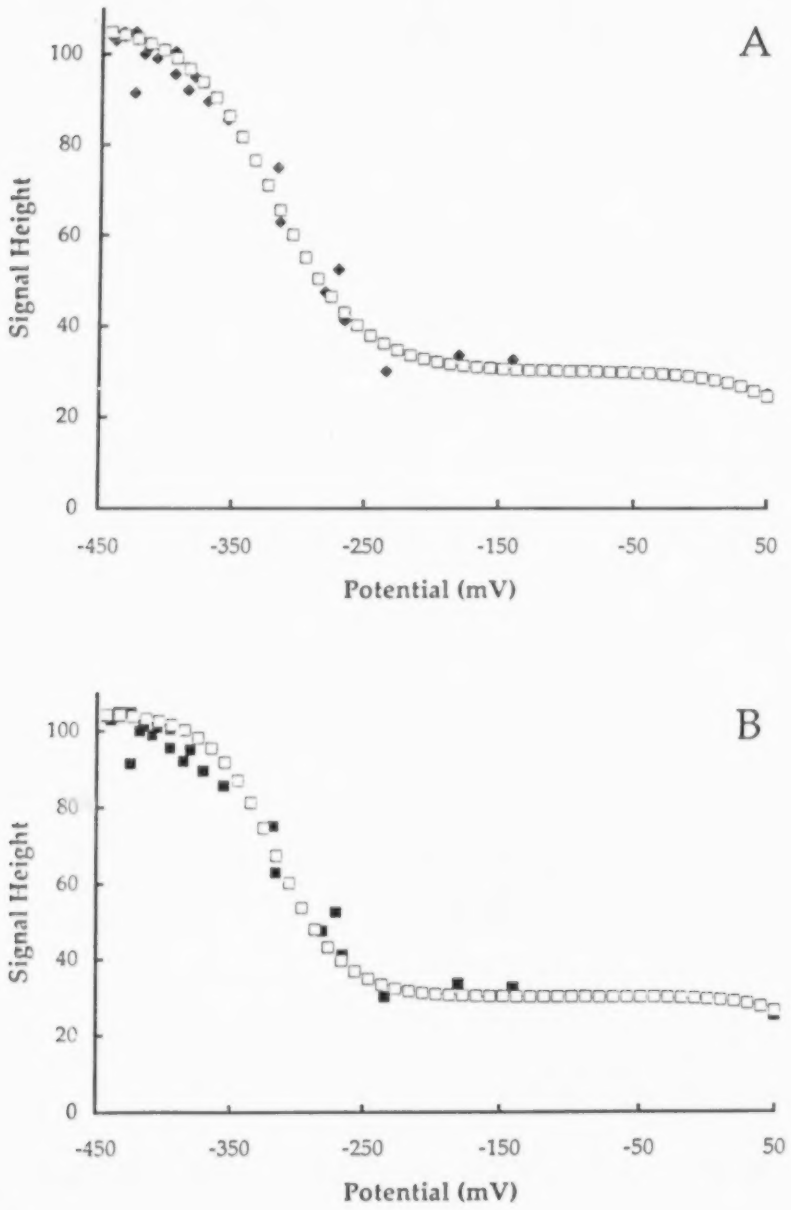

FIGURE 44. Estimation of Midpoint Potential of JM83/pGLP1 signal. The representative spectra used for the analysis are shown in Figure 31. The open symbols represent the calculated values from the Nernst equation used to match the shaded data points. The signal height was measured as the peak-to-trough value for each spectrum. The midpoint potential was estimated at - 320 mV, n = 0.75 [Panel A]. Panel B illustrates the Nernst equation with an n = 1.0 value at a midpoint potential of - 320 mV.

FIGURE 45. A Wide Band EPR Spectrum at 5 K of a JM83/pGLP1 Lysed Cell Suspension Sample Poised at - 425 mV. The sample was one representative of the redox titration for which the data are shown in Figures 31 and 32. The spectrum was recorded as described in Materials & Methods except at 5 K.

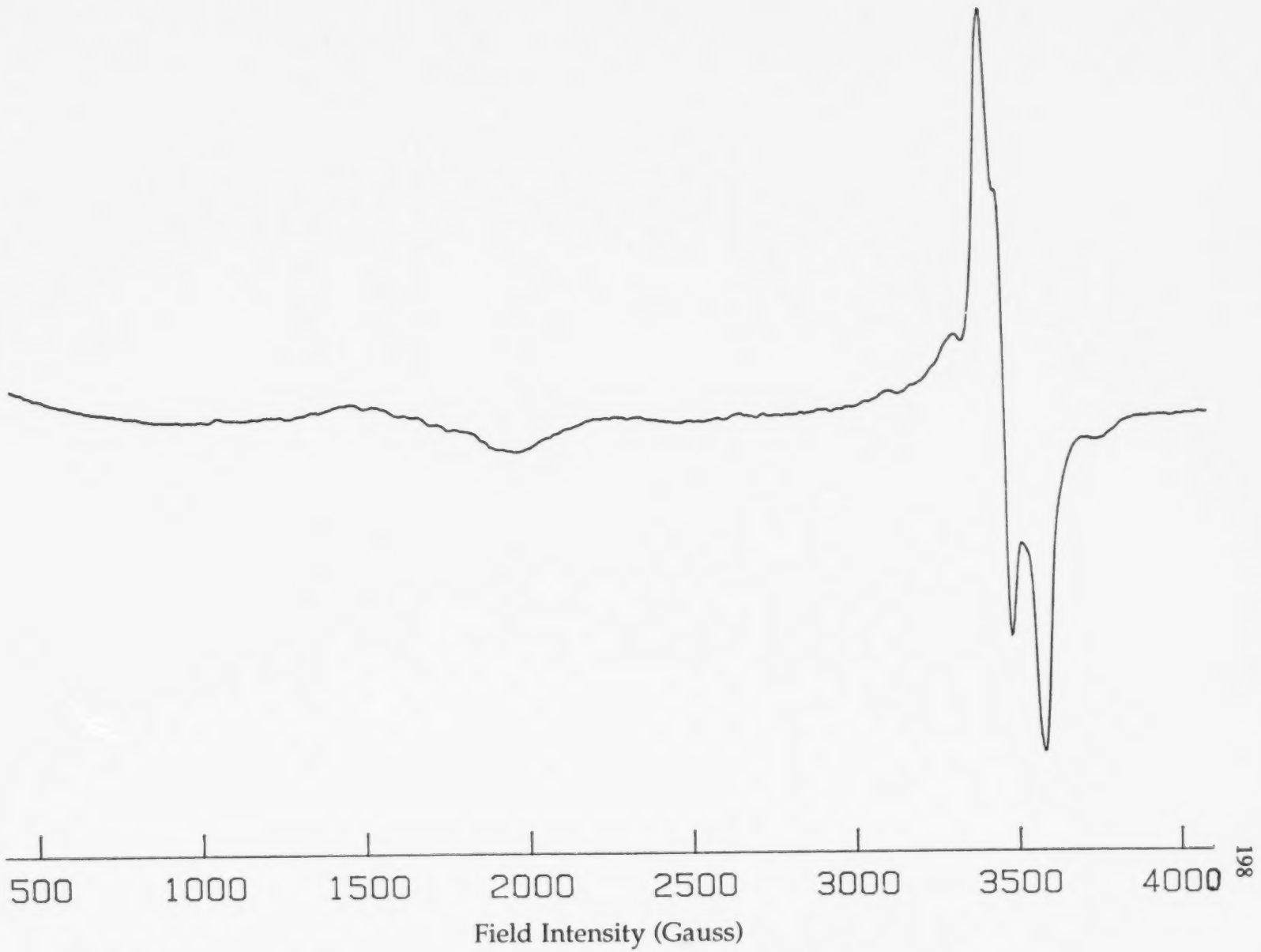
500
1000
1500
2000
2500
3000
3500
4000
Field Intensity (Gauss)

FIGURE 46. Representative EPR Spectra of JM83/pGLP1 Anaerobically Lysed Cell Suspension During Redox Titration at pH 9.0. The lysed cell suspension in 100 mM CHES/1 mM EDTA, pH 9.0, was prepared and used for redox potentiometric analysis as described in Materials & Methods. Spectra were recorded as previously described at 20 K. The poised potential that each sample was taken is as shown for each spectra, respectively. Spectra were normalized for tube calibration and are plotted on an equivalent scale.

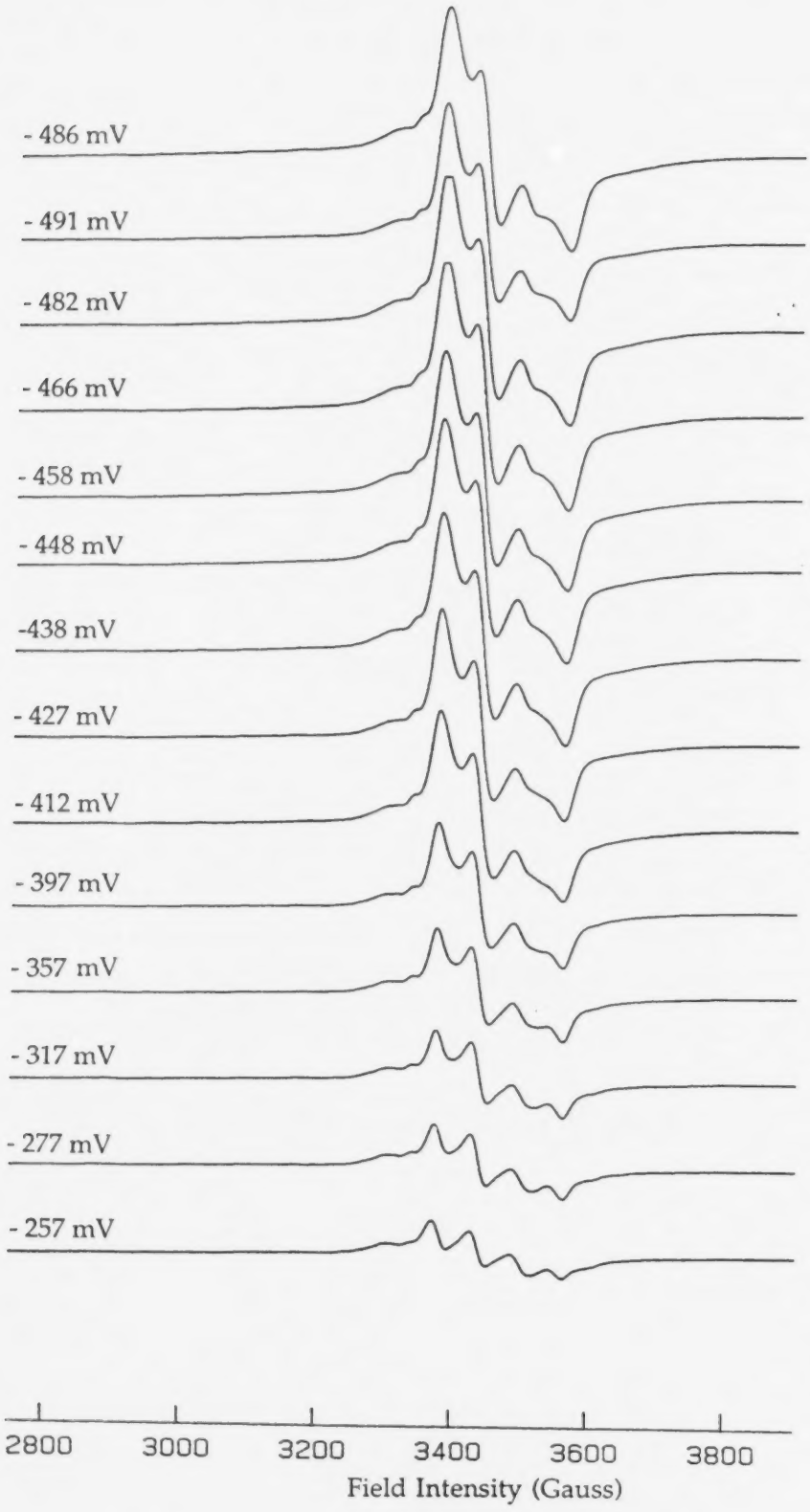
- 486 mV
- 491 mV
- 482 mV
- 466 mV
- 458 mV
- 448 mV
-438 mV
- 427 mV
- 412 mV
- 397 mV
- 357 mV
- 317 mV
- 277 mV
- 257 mV
2800
3000
3200
3400
3600
3800
Field Intensity (Gauss)

FIGURE 47. Estimation of Midpoint Potential of the JM83/pGLP1 Signal at pH 9.0. The representative spectra used for the analysis are shown in Figure 46. The signal height was measured as the peak-to-trough value for each spectrum. The midpoint potential is estimated at: Panel A, reducing direction of data points, - 390 mV, $n = 0.85$; Panel B, oxidizing direction of data points, - 318 mV, $n = 0.7$; and Panel C, all data points, - 355 mV, $n = 0.75$. In each panel the data points are represented by the shaded boxes, while the open boxes are as calculated from the Nernst equation.

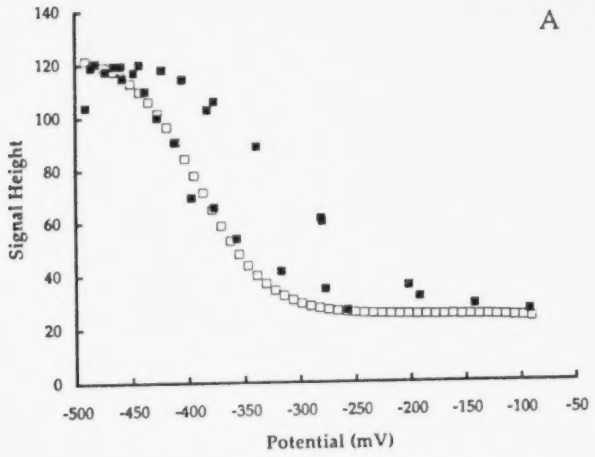
A
Signal Height
140
120
100
80
60
40
20
0
-500 -450 -400 -350 -300 -250 -200 -150 -100 -50
Potential (mV)

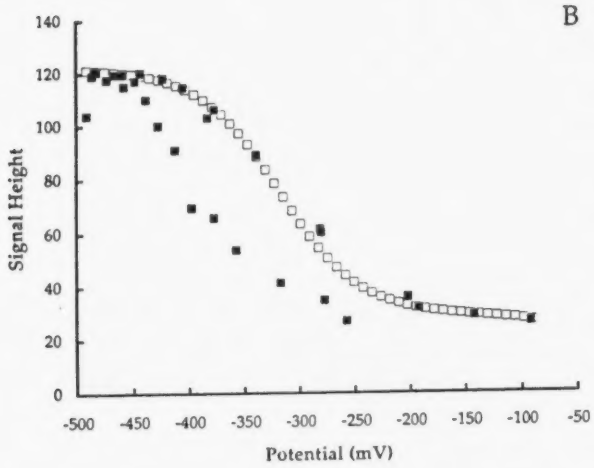
B
Signal Height
140
120
100
80
60
40
20
0
-500 -450 -400 -350 -300 -250 -200 -150 -100 -50
Potential (mV)

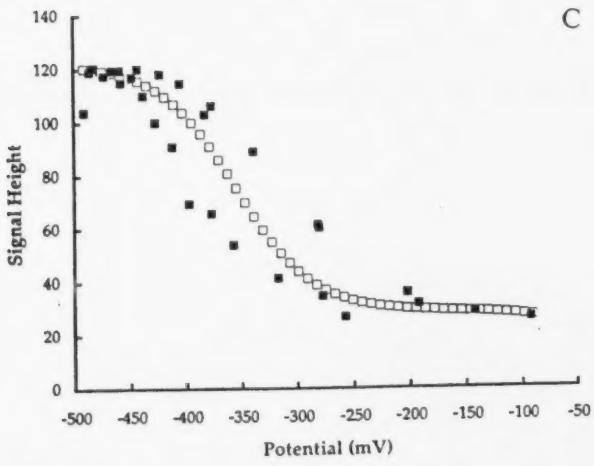
C
Signal Height
140
120
100
80
60
40
20
0
-500 -450 -400 -350 -300 -250 -200 -150 -100 -50
Potential (mV)

FIGURE 48. pH effects on EPR Spectra of JM83/pGLP1 Whole Cells. Anaerobically handled whole cells were prepared at the various pH levels and spectra recorded as described in Materials & Methods. Panel A shows the representative spectra at each of the pH levels indicated. Panel B is a plot of the signal amplitude as a function of the pH. The spectra for pH 9 and 10 were plotted at a scale of 17, while the others spectra, pH 5 - 8 were plotted at scale 16 and hence are an order of magnitude of two smaller in amplitude. The g-values are as indicated.

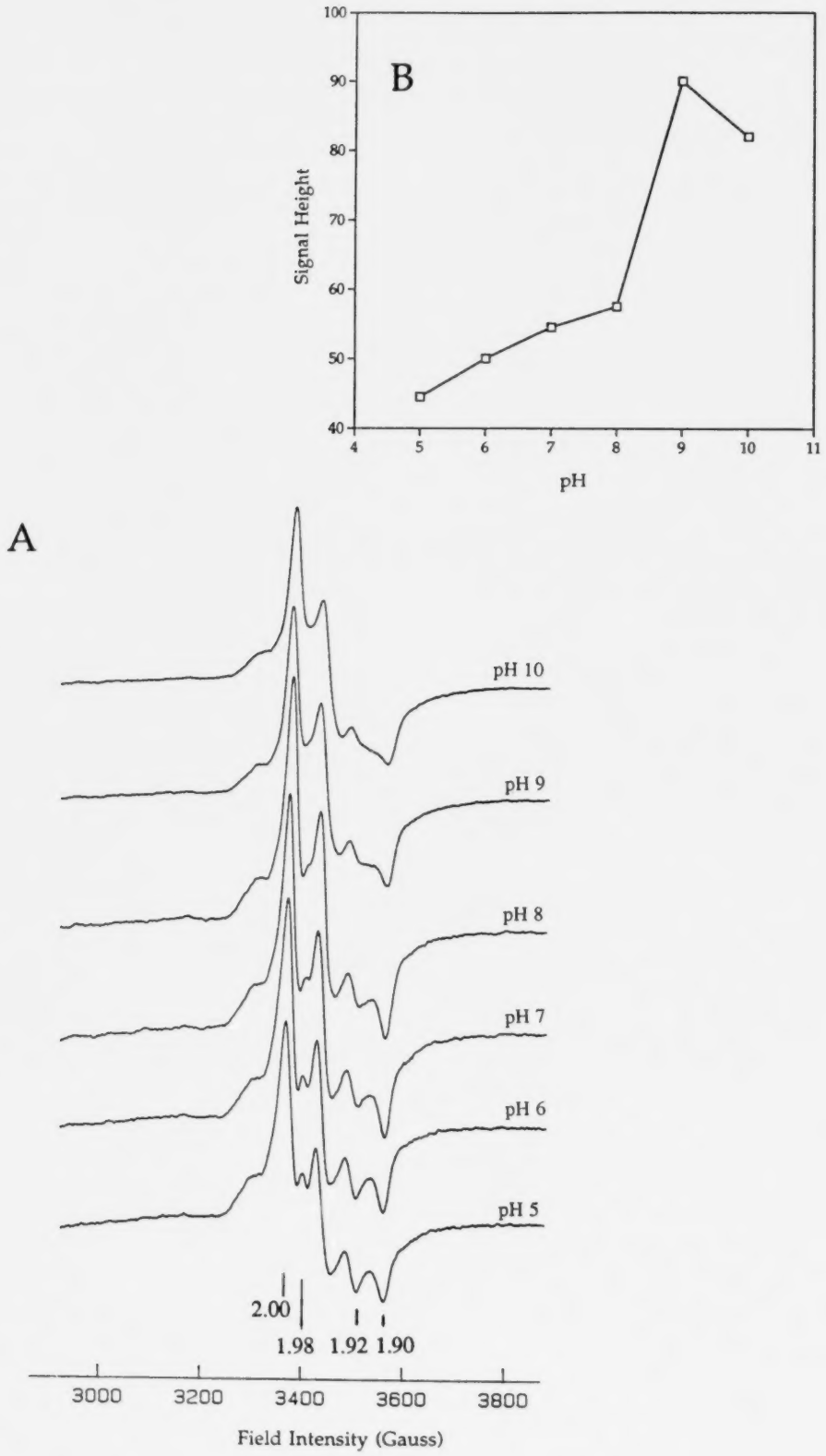
B
Signal Height
100
90
80
70
60
50
40
4
5
6
7
8
9
10
11
pH
A
pH 10
pH 9
pH 8
pH 7
pH 6
pH 5
2.00
1.98
1.92
1.90
3000
3200
3400
3600
3800
Field Intensity (Gauss)

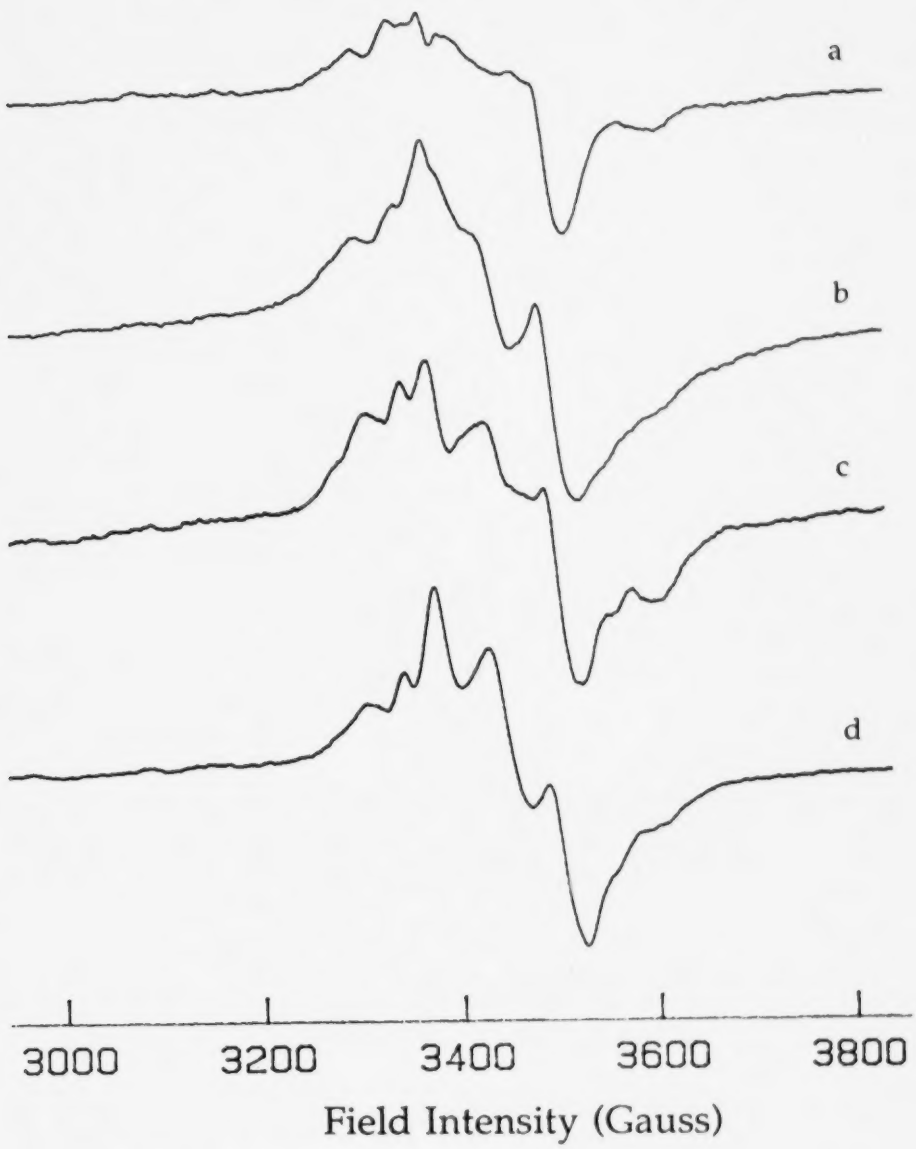

FIGURE 49. Effect of Denaturants on JM83/pGLP1 Lysed Cells. Anaerobically lysed JM83/pGLP1 cells were treated with 0.35 M guanidine hydrochloride or 0.9 M urea for 10 min and then reduced with 2.5 mM dithionite. Lysed cells suspensions of JM83/pGLP15 (*glpA*) and JM83/pGLP20 (*glpAC*) were reduced with 2.5 mM dithionite. Spectra were recorded as described in Materials & Methods. Spectra (a) JM83/pGLP1 (*glpACB*) cells treated with 0.35 M guanidine hydrochloride; (b) JM83/pGLP1 cells treated with 0.9 M urea; (c) JM83/pGLP15 cells; and (d) JM83/pGLP20 cells. Reduced spectrum of untreated JM83/pGLP1 whole cells was as previoulsy shown in Figure 35.

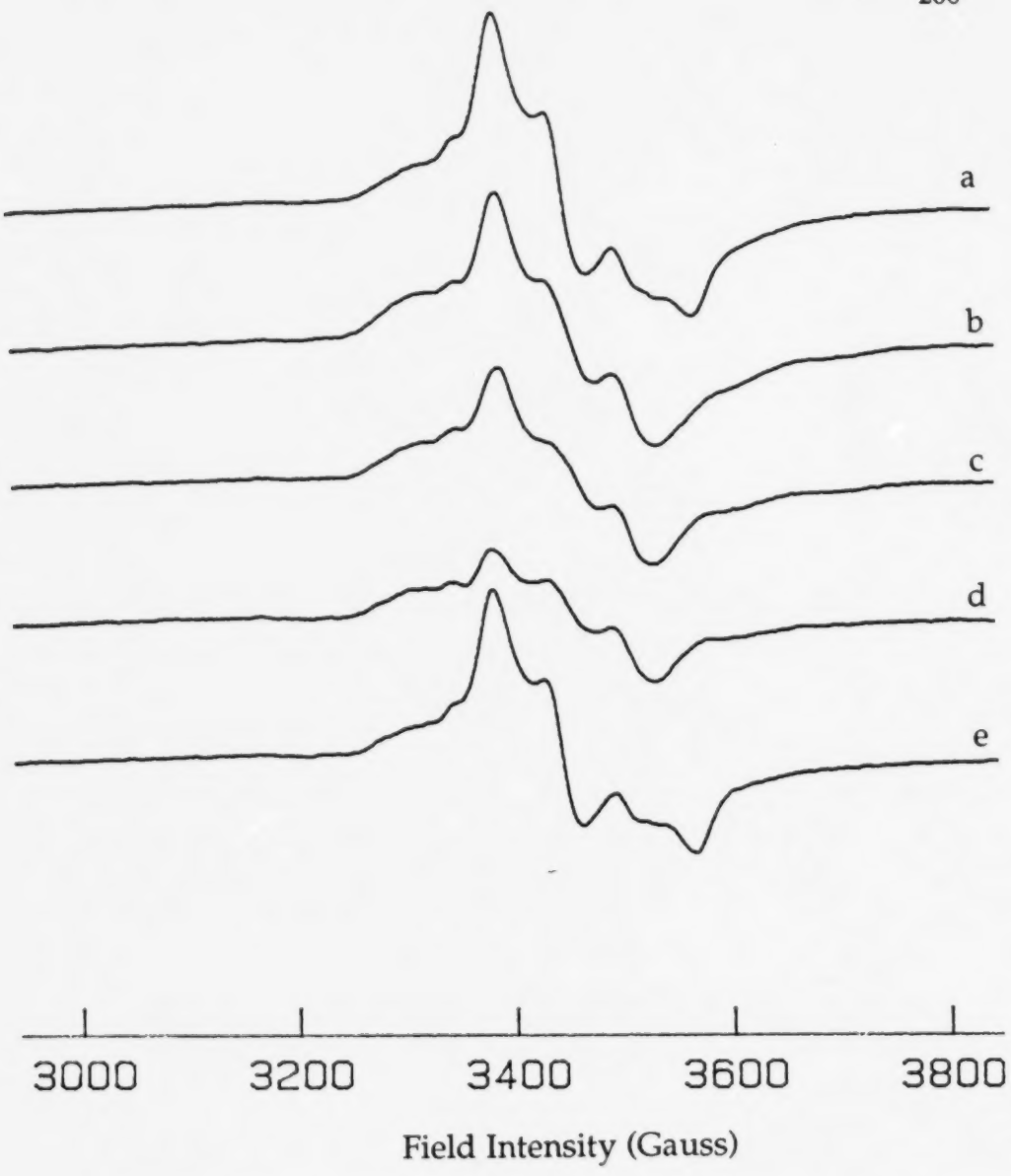

FIGURE 50. Effect of the Iron Chelator o-Phenanthroline on JM83/pGLP1 Lysed Cells. Anaerobically lysed cells were treated with 65 μM o-phenanthroline in the presence and absence of 0.8 M urea. After the designated treatment and incubation period, the cells were then reduced with 2.5 mM dithionite [2 minutes]. Spectra were recorded as described in Materials & Methods. Spectra (a) cells incubated with excess buffer to take into account dilution of reagents; (b) 0.8 M urea [10 minutes]; (c) 0.8 M urea [10 minutes] followed by 65 μM o-phenanthroline [10 minutes]; (d) same as (c) except 2 hour incubation following addition of o-phenanthroline; and (e) 65 μM o-phenanthroline [2 hours]. Reduced spectrum of untreated JM83/pGLP1 whole cells was as previoulsy shown in Figure 35.

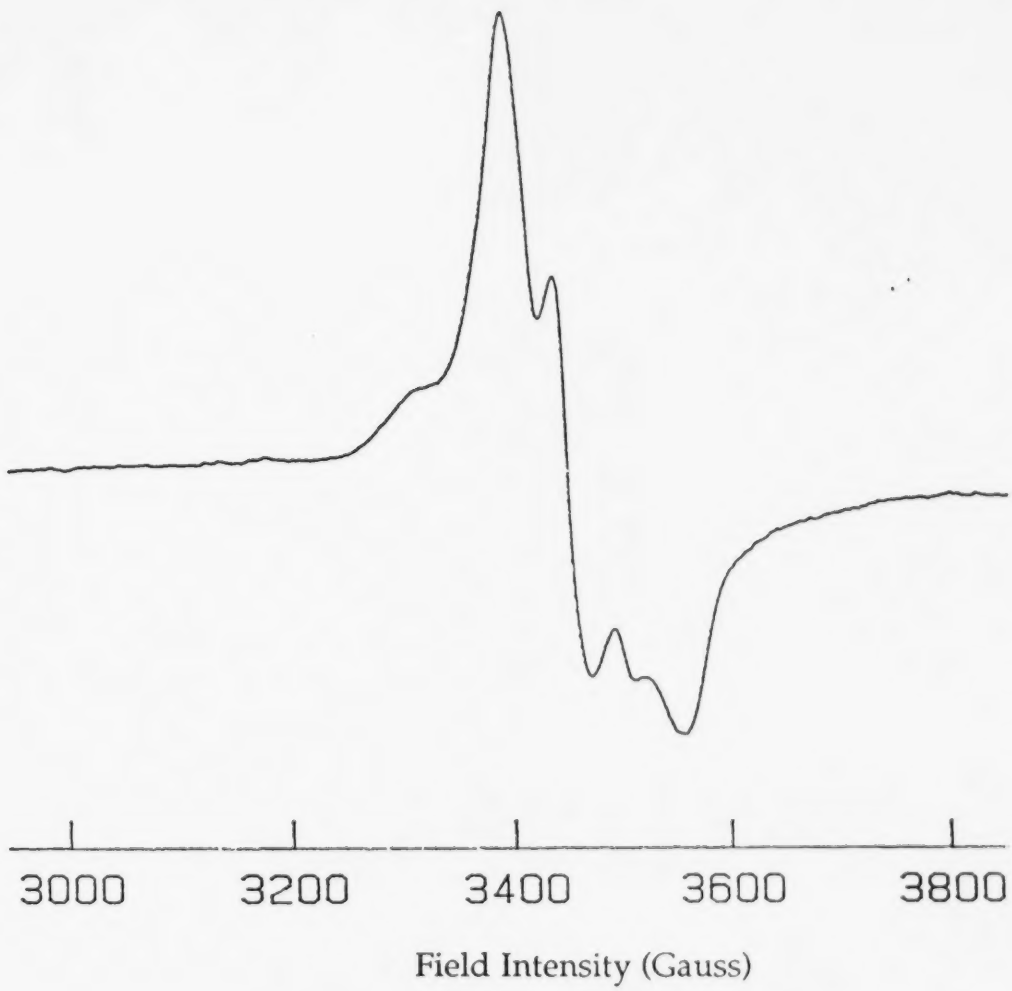

FIGURE 51. EPR Spectrum of JM83/pGLP1 Whole Cells Resuspended in 80 % DMSO. Anaerobically handled whole cells were resuspended in 80 % dimethyl sulfoxide (DMSO) and then reduced with 2.5 mM dithionite. The spectrum was recorded as described in Materials & Methods.

FIGURE 52. Yamato Inner Membranes of JM83/pGLP90C12S and JM83/pGLP90C59S. The samples were prepared as described in Materials & Methods and subjected to 7.5 % SDS-PAGE and stained in Coomassie blue. Lane 1, JM83/pGLP90C12S cytoplasmic membrane fraction [40 µg]; lane 2, JM83/pGLP90C59S cytoplasmic membrane fraction [35 µg]; lane 3, purified GlpAC dimer [10 µg]. The location of the GlpA [62 kDa], GlpB [44 kDa] and GlpC [43 kDa] subunits are indicated on the right side of the panel.

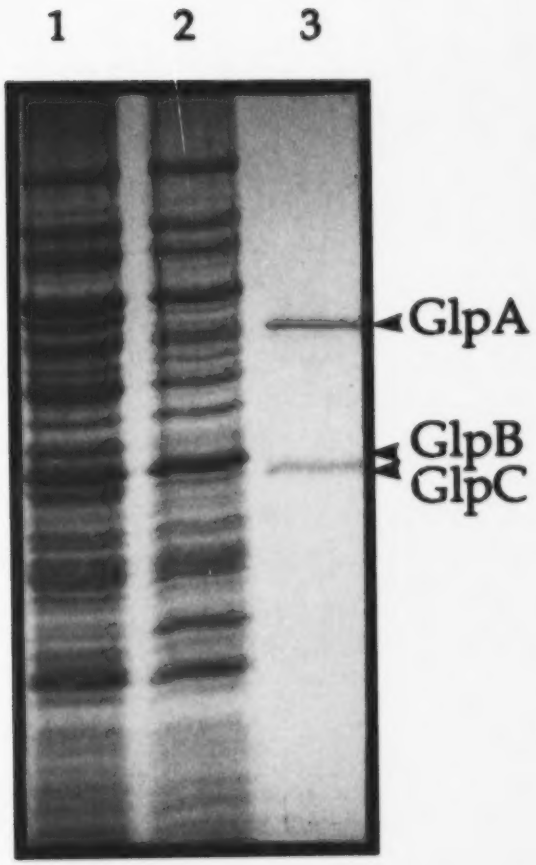
1
2
3
GlpA
GlpB
GlpC

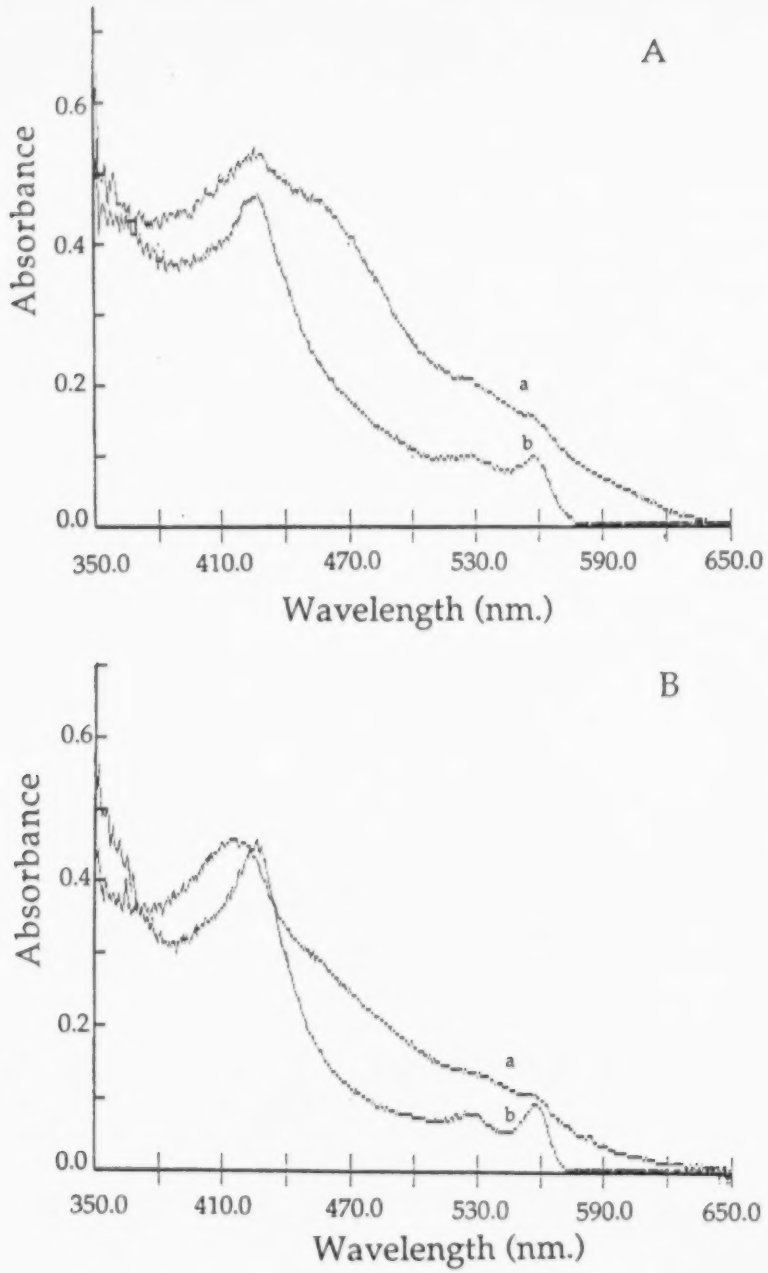

FIGURE 53. The Visible Absorption Spectra of JM83/pGLP90C12S and JM83/pGLP90C59S Mutants. Whole cells were resuspended in 50 mM MOPS/ 5mM EDTA, pH 7.0 and the spectra were measured with the Varian DMS100 Spectrometer equipped with a chamber modified for analysis of particulate matter. The spectra were measured at room temperature using 50 mM MOPS/ 5 mM EDTA, pH 7.0 as the blank buffer. Panel A: JM83/pGLP90C12S whole cells [14 mg/ml] before [spectrum a] and after treatment [spectrum b] with 1.5 mM dithionite; and Panel B: JM83/pGLP90C59S [13 mg/ml] before [spectrum a] and after treatment with 1.5 mM dithionite.

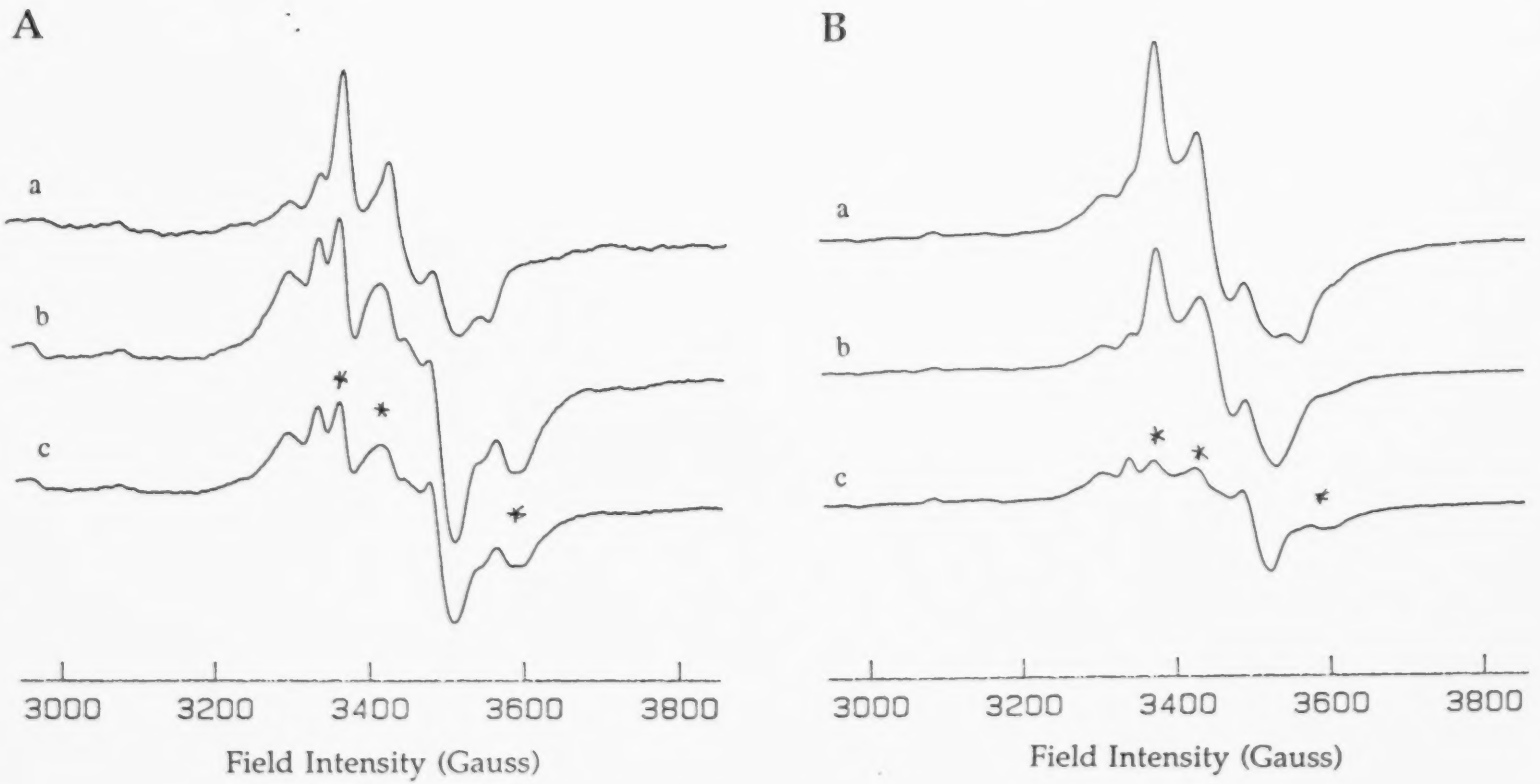

FIGURE 54. EPR Spectra at 20 K of C12S and C59S Mutants. JM83 cells harboring the plasmids pGLP90C12S and pGLP90C59S were handled aerobically and anaerobically as described in Materials & Methods. The samples were reduced with 2.5 mM dithionite and recorded as previously described. Panel A and Panel B show the aerobically and anaerobically handled cell suspensions, respectively. Panel A: Spectra (a) JM83/pGLP90; (b) JM83/pGLP90C12S; and (c) JM83/pGLP90C59S. Panel B: Spectra (a) JM83/pGLP1; (b) JM83/pGLP90C12S; and (c) JM83/pGLP90C59S.

FIGURE 55. Representative EPR Spectra of a Redox Titration of JM83/pGLP90C12S Anaerobically Lysed Cell Suspension at pH 7.0. The lysed cell suspension in 50 mM MOPS/5 mM EDTA, pH 7.0, was prepared and used for redox potentiometric analysis as described in Materials & Methods. Panel A: Spectra were recorded as previously described at 20 K. The poised potential that each sample was taken at is as shown for each spectrum, respectively. Spectra were normalized for tube calibration and the appropriate scaling factor is also highlighted [refer to Figuire 31]; Panel B: Estimation of Midpoint potential at - 385 mV with $n = 0.65$. The open squares represent the calculated values from the Nernst equation, while the shaded boxes are the data points.

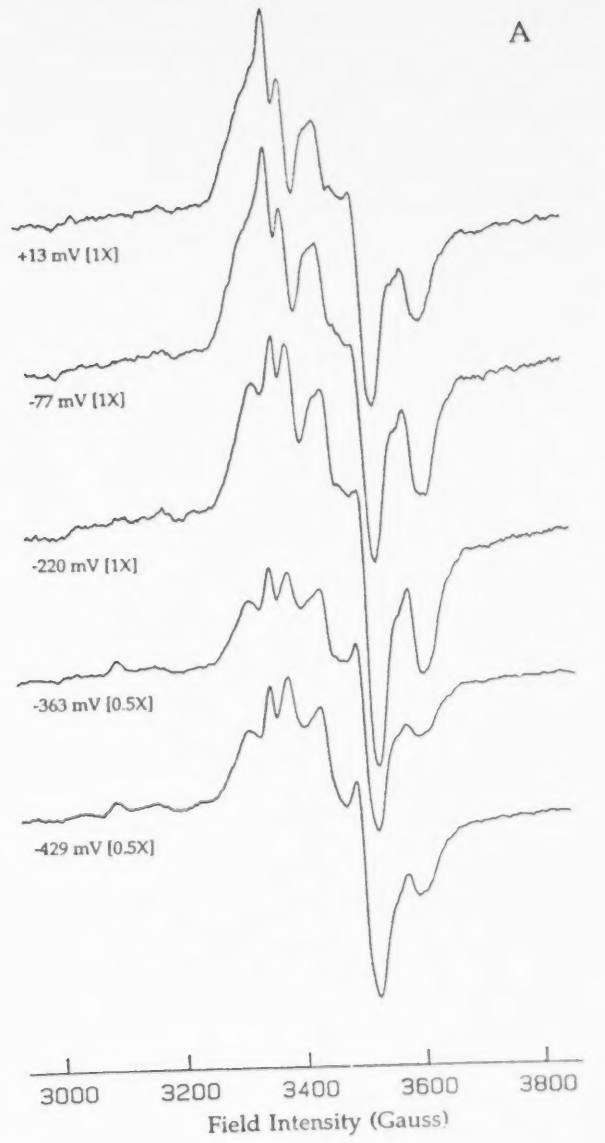
A
+13 mV [1X]
-77 mV [1X]
-220 mV [1X]
-363 mV [0.5X]
-429 mV [0.5X]
3000
3200
3400
3600
3800
Field Intensity (Gauss)

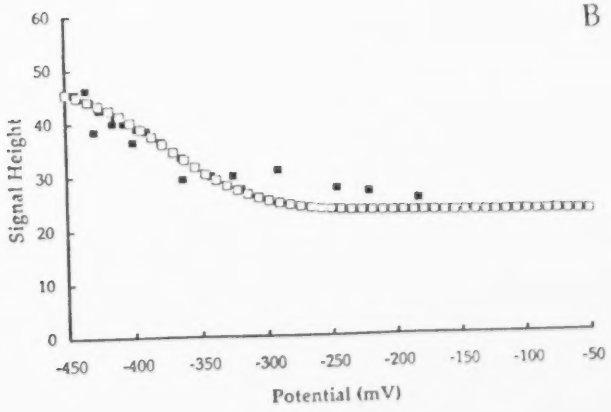
B
Signal Height
60
50
40
30
20
10
0
-450
-400
-350
-300
-250
-200
-150
-100
-50
Potential (mV)

VII. CONCLUDING REMARKS

The studies reported in this thesis were directed towards developing an understanding of the structural and functional role of GlpB as part of the anaerobic glycerol-3-phosphate dehydrogenase in *Escherichia coli*. The expression and the necessity of GlpB for growth were investigated and its interaction with the soluble catalytic dimer, GlpAC, as well as with the membrane, were examined. The remainder of the thesis was devoted to the characterization of the [Fe-S] redox center within GlpB. The general discussion which follows is designed to provide an overview connecting the experimental results.

A. Summary

The word 'operon' is invariably used to describe a single unit of transcription, containing one or more genes, under the control of a specific regulator protein acting in concert with its effector (Iuchi & Lin, 1993). Anaerobic glycerol-3-phosphate dehydrogenase is encoded by the *glpACB* operon. The existence of the third subunit was unknown until the cloning and sequencing of the operon (Cole *et al.*, 1988). Thus, a central issue was whether the *glpB* gene was expressed as part of the operon, and, if so, whether the gene product contributed to the enzyme in a structural and/or functional role. Based on the characteristics of other electron transfer enzymes, such as fumarate reductase and DMSO reductase, it was believed that GlpB was expressed and localized within the membrane. This localization of the polypeptide would allow for the transfer of reducing equivalents from the soluble catalytic dimer, GlpAC, via the membrane bound menaquinone pool, to the terminal electron acceptor fumarate or DMSO. Such transfer assumes a transient interaction of some sort between the soluble dimer and GlpB, occurring only in the presence of substrate and lasting only long enough for the reducing equivalents to be passed on. It was also possible that GlpB had a more structural role for the enzyme, acting as a membrane anchor for the dimer, with association disrupted on cell breakage. Growth on minimal medium supplemented with glycerol as the carbon source and fumarate as the hydrogen source would induce a simple respiratory chain, with GlpACB acting with fumarate reductase to form a functional complex, with the subsequent generation of ATP to allow the cell to grow.

The work presented in this thesis has confirmed some of the basic questions in relation to the hypothesis. I have demonstrated that GlpB was expressed and appeared to

be localized to the inner membrane. It evidently participated in the electron transfer role of the enzyme since the physiological substrate G3P was able to reduce the redox center within GlpB in the presence of the catalytic dimer, GlpAC. I have assigned the redox center in GlpB as a [2Fe-2S] center with an estimated midpoint potential of - 320 mV.

In my early studies [Chapter III], I confirmed the expression of *glpB* as part of the *glpACB* operon, and also showed that the third gene of the operon could be expressed on its own in the absence of the promoter proximal genes. GlpB appeared to be the 44 kDa polypeptide observed on SDS-polyacrylamide gels, but the level of expression from the bacteriophage T7 promoter was not sufficient enough for the purification of GlpB. The T7 expression studies also showed that GlpC is required for stabilization of GlpA as GlpA on its own formed aggregates, but when GlpC was co-expressed with GlpA, the 62 kDa polypeptide maintained its soluble nature. A functional enzyme was expressed with the inducible T7 promoter, with comparable activity to that observed during anaerobic induction of the endogenous *glp* promoter. This suggested that proper assembly of the polypeptides and cofactors occurred during aerobic growth.

GlpB was shown to be associated at least in part with the cytoplasmic membrane by expression studies and sucrose gradient sedimentation. GlpB though has proven intractable to detergent solubilization with anything less than denaturing detergents like sarkosyl and SDS, and to a lesser degree with cholic acid. In each case though, the identified redox center within GlpB, as analyzed by EPR, was significantly disrupted which hindered functional analysis of the polypeptide.

In Chapter IV, I examined the physiological role of GlpB. I first looked at the growth requirement of GlpB. To do so, I constructed a mutant strain which was defective in various *glp* genes [*glpK*, *glpACB* and *glpT*] and also glycerol dehydrogenase activity. Complementation studies demonstrated that all three subunits, GlpA, GlpC and GlpB were essential for growth. This provided evidence that *glpB* was functionally included in the *glpACB* operon. Intact cells overproducing GlpB exhibited a [Fe-S] signal in the reduced state as observed by EPR spectroscopy. The observed reduction was shown to be specific for the physiological substrate G3P, with oxidation occurring with the addition of fumarate. These experiments confirmed the essential role GlpB had in the transfer of electrons from the GlpAC dimer to the terminal electron acceptor.

The results presented in Chapter V concentrated on describing the overexpression, enrichment and characterization of GlpB as a fusion protein with glutathione S-transferase (GST). Partial enrichment of the GlpB was obtained [30 - 40

%] and the preparation did assemble the [Fe-S] centers within the fusion protein. I had difficulties with the solubility of the fusion protein and stability of the GlpB domain, but the EPR spectral analysis confirmed the presence of a [Fe-S] center. The signal in the reduced state was assigned as a rhombic signal with g values indicative of [Fe-S] centers. The signal exhibited an optimal temperature at lower values [< 20 K] which is indicative of a [4Fe-4S] center, but the power saturation behavior was atypical and showed extreme inhomogeneity of the molecules within the sample. The use of the GST fusion system, although producing usable quantities of GlpB, did not appear to produce a protein representative of the true physiological state of GlpB. These studies suggested that the [Fe-S] centers were formed prior to aggregation and the stability of the clusters was sensitive to the local environment as well as cluster damage due to over reduction with dithionite. Analysis of the amino terminal region of GlpB as a fusion with GST failed to provide conclusive evidence for this region acting as the source of cysteine ligands for the center. Due to the atypical EPR spectral behavior, the type of cluster within the GSTGlpB protein could not be assigned.

The remainder of the thesis concentrated on characterization of the redox center within cells overexpressing the *glpACB* operon. Intact cells overexpressing GlpB exhibited a rhombic EPR signal [$g_z = 2.00$, $g_y = 1.96$ and $g_x = 1.88$] in the reduced state which indicated the presence of [Fe-S] centers. As observed in other [Fe-S] systems, the lineshape of the signal showed slight variations among preparations, and this was believed to be due to slight differences in handling and distribution of the molecules containing the [Fe-S] centers within a particular sample. It was determined that the redox center was very susceptible to oxidative damage, and the characterization of the center was performed utilizing as anaerobic conditions as possible. The lineshape of the reduced signal closely resembled that observed for 2[4Fe-4S] ferredoxins with additional features at g = 2.04, 2.02 1.97, 1.94, 1.92 and 1.90 at very low temperatures [5 - 20 K]. The rhombic signal was most representative for the center however, especially when the contribution of the fumarate reductase FR1 center was taken into account.

Temperature dependence of the reduced signal indicated an optimum temperature of between 30 and 50 K which was more indicative of a [2Fe-2S] center than a [4Fe-4S] center. The signal saturated easily at low temperatures [< 20 K], which was also contrary to a fast relaxation behavior of a [4Fe-4S] center and was more representative of a [2Fe-2S] center. In all cases where either temperature or microwave power was varied, no evidence for the existence of a second cluster was found. This was confirmed during redox potentiometric analysis with intact and lysed cell suspensions, as only a

single midpoint potential of - 320 mV ± 30 mV at pH 7.0 was observed. The spectra at the various poised potentials all exhibited similar lineshapes which increased or decreased in intensity at the various potentials. No additional features were observed in the shoulders of the signal which would indicate the presence of a second cluster. Treatment of the GlpB polypeptide with 80 % DMSO also failed to yield evidence of a second cluster. The possibility of a second cluster should not be ruled out though as the second cluster may have a midpoint potential which was too low to allow it to be reduced with dithionite or alternatively, similar to Center 2 in fumarate reductase, had such broad features that it was originally not apparent [Cammack *et al.*, 1986]. The use of other spectroscopic techniques [nuclear magnetic resonance [NMR (Packer *et al.*, 1975)], advanced EPR techniques and at other frequencies [i.e S-band to detect weakly coupled nuclei], or magnetic circular dichroism (MCD) may help elucidate the presence of a second cluster.

The [2Fe-2S] cluster in GlpB showed a preference for alkaline conditions [pH 9.0], and exhibited a decrease in signal amplitude on the addition of the iron chelator o-phenanthroline. The cluster environment was also detrimentally affected by the presence of denaturants urea or guanidine hydrocloride and the resultant reduced spectra resembled reduced spectra of cells which do not overexpress GlpB. Site-directed mutagenesis, creating the GlpB mutant, C59S, suggested that this substitution disrupted the cluster as the spectra observed were similar to those seen with the denaturants or with oxidative damage. The mutation C12S did not appear to disrupt the cluster but did appear to alter the environment or stabilization of the cluster as the center became more susceptible to oxidative damage. The cysteine may have been replaced by another potential ligand, but one that was not as stable as in the wild type. The visible absorption spectra taken of wild type cells overexpressing GlpB confirmed the presence of the iron-sulfur center and also demonstrated a loss of the cluster with the C59S mutant. The mutagenesis of the cysteine residues at residue 12 and 59 suggested that the cysteine motifs in the amino terminal region of the protein did not coordinate the proposed 2[4Fe-4S] ferredoxin-like clusters. The results reported did suggest that cysteine$_{59}$ was involved in coordinating a [2Fe-2S] center.

B. Future Directions

A primary goal within the laboratory is the functional reconstitution of a respiratory chain complex within liposomes, comparable to that observed in the

physiological state of the cell. Although I met with little success in attaining this goal, I have contributed to the understanding of the mechanism of the anaerobic G3P dehydrogenase. Many questions remain unanswered.

1. Mode of Membrane Binding of GlpB

The soluble nature of the amino terminal GlpB GST fusion protein suggested that the carboxy terminal region was responsible for aggregation of the full length fusion protein. This aggregation was presumably due to inter-polypeptide interaction between the hydrophobic regions which normally interact with the hydrophobic membrane environment. I have shown that GlpB was probably associated with the cytoplasmic membrane but I was unable to determine how this was so. Conventional detergents which are normally used to solubilize inner membrane proteins failed to solubilize GlpB, suggesting a novel association. It is possible that GlpB interacts with the membrane via a lipid anchor and/or an amphipathic helix. Alternatively, similar to outer membrane porins (Nikaido, 1992) and with recently proposed glucose transporters (Fischbarg *et al.*, 1993), β-sheet structure may be involved. Conventional predictive algorithms in most part are not representative for β-sheet structure (Nikaido, 1992, Schiltz *et al.*, 1991) and hence the lack of predicted β structure in the primary GlpB sequence does not rule this possibility out.

As previously mentioned two sequence motifs in GlpB are potential membrane attachment sites, the two Cys-Cys-Gly motifs and the amphipathic helix. The Cys-Cys-Gly motif has been found to be the site of palmitylation in rhodopsin (Khorana, 1992), mammalian red cell membrane Rh polypeptide (Hartel-Schenk & Agre, 1988), as well as in various viral glycoproteins (Hobman *et al.*, 1992). This modification is involved in binding the protein to the membrane. While there is no evidence for a similar modification in prokaryotes, a fatty acid linkage of the protein to the membrane should be investigated as a possible mechanism for the association of GlpB with the cytoplasmic membrane. Preliminary solubilization attempts with hydroxylamine, which is known to cleave the thioester linkage (Hartel-Schenk & Agre, 1988), did not appear to alter the solubility of GlpB, but the optimum conditions for the system may not have been utilized. Site directed mutagenesis of the cysteine residues to serine has also been shown to alter the modification. Thus, one approach would be to construct the cysteine to serine substitutions for the two Cys-Cys-Gly motifs, to determine if these modifications will release GlpB from the membrane. The use of radiolabelled palmitate would make the

analysis more definitive as well. The results may not be entirely conclusive as GlpB association may also be due to the helix or β-sheet motifs.

To investigate the membrane association additional experiments can be conducted. Recently, photo-labelling has been a valuable tool in determination of regions of a polypeptide associating with the membrane (Brunner, 1993). 'Hydrophobic photolabelling of membranes' serves to identify integral proteins by selectively labelling the membrane-embedded polypeptide regions. This method can be particularly useful in cases, such as GlpB, where long, contiguous stretches of hydrophobic amino acid residues are absent. The method make use of photoreagents that can be immersed in the lipid bilayer, thus labelling only those polypeptide regions which make direct contact with the lipid bilayer. Individual amino acids can be identified by following a strategy involving isolation and chemical or enzymatic fragmentation of the labelled protein, followed by separation and Edman degradation of the labelled fragments (Brunner, 1993). Sun *et al.*, (1993) used [^{19}F] NMR in combination with site-directed mutagenesis at various positions to investigate the regions of D-Lactate dehydrogenase which may be involved in membrane association and were able to localize the association to a particular region of the protein. As GlpB also contains a number of tryptophan residues which could be labelled with [^{19}F], this technique may provide additional information as to the association of GlpB with the membrane. Alternatively, conventional series of truncated fusions of GST or β-lactamase which show no membrane interaction, may aid in determinating if the membrane binding site in GlpB is limited to a small linear region such as the amphipathic helix. Transmembranal topology analysis with GlpB - β-lactamase fusions relies on the observation that only periplasmically exposed β-lactamase gives rise to ampicillin resistance (Broome-Smith *et al.*, 1990, Weiner *et al.*, 1993). Ultimately, it would be ideal to be able to crystallize GlpB and determine its structure with high resolution X-ray crystallography, but very few investigators have met with success.

2. Interaction of GlpAC with GlpB

Although I have demonstrated that GlpB is in functional association with GlpAC, the evidence for the anchor function of GlpB is poor. Kuritzkes *et al.* (1984) have provided some evidence that when GlpB is absent, the activity in the cytoplasm increases from 85 - 95 % to 99 %, which they attributed to loss of the anchor subunit. In the course of my studies, the activity distribution usually did not vary from a 85 - 90 %

cytoplasmic/ 10 - 15 % membrane fraction ratio, which is in agreement with Cole *et al.* (1988) who showed that 90 % of the total enzyme activity was soluble. In many of these lysates and cellular fractions it was difficult to determine exactly how much of GlpB was in association with GlpAC. In an attempt to show that GlpAC and GlpB physically interact, it is suggested to carry out lysis and fractionation of cells in conditions where the interaction may be maintained i.e. anaerobically in the presence of excess substrate or reducing agents. From my anaerobic work done with EPR analysis, a large scale anaerobic chamber or room would be necessary to ensure all aspects of the experiment were kept anaerobic [i.e. cellular fractionation and gel electrophoresis] for the most conclusive results. A second approach would be the utilization of crosslinking reagents to see if GlpB physically interacts with GlpAC (Chelsky & Dahlquist, 1980; Robinson & Weiner, 1982). Although bifunctional arsenical reagents (Stevenson *et al.*, 1978) were utilized to attempt to show an association of GlpAC with GlpB, the Cys residues proposed to act as ligands for the arsenical reagent may have been inaccessible due to the mentioned palmitic acid attachment.

3. Electron Transfer Properties of GlpB

The absolute characterization of the redox center within GlpB has been hampered by contributions of other membrane bound enzymes such as fumarate reductase as well as GlpB's disrupted state outside of its membrane location. It would be interesting to be able to characterize the redox activity of GlpB in the absence of other bacterial proteins, but still within its membrane localization. Perhaps, expression in an alternative system such as *Xenopus laevis* oocytes may prove useful. Success has been achieved with various membrane proteins such as murine P-glycoprotein (Castillo *et al.*, 1990) and recently with the glycerol facilitator, GlpF in *Escherichia coli* (Maurel *et al.*, 1993; Maurel *et al.*, 1994) and a eukaryotic nucleoside transporter (Hogue, 1994). The high efficiency with which *Xenopus* oocytes translate injected mRNA and process the synthesized proteins have made this system a choice for characterization of membrane transport systems (Soreq & Seidman, 1992). The technology perhaps may be extended to the study of the GlpACB polypeptides.

a) [Fe-S] Cluster Coordination

Further to the characterization of the redox center in GlpB, it would be

informative to determine which ligands are responsible for coordinating the [2Fe-2S] center. This would involve furthering the site-directed mutagenesis experiments which I initiated, in the hopes of determining the four cysteine residues required for [2Fe -2S] cluster coordination. This analysis would rely on either destroying the individual cluster or altering the paramagnetic center as observed in DMSO reductase (Rothery & Weiner, 1991).

A means of determining the approximate location of an [Fe-S] cluster within a polypeptide is to use spin relaxation enhancement by an external probe such as holmium-EDTA (Meinhardt & Ohnishi, 1992) or dysprosium-EDTA (Rothery & Weiner, 1993) complexes. The relaxation properties of the redox species are altered and can be used to determine the distance of the species under investigation to the probe, by comparison to the effect the Dys^{3+}-EDTA complex has on a spin-labelled fatty acid. This allows for an estimate of the distance of the redox species from the probe. Such experiments may aid in determining the location of the GlpB [2Fe-2S] center, which I propose to be close to the surface of the protein as the EPR signal altered with changes to the bulk environment.

My initial mutagenic experiments and the study of the truncated GST fusion suggested that the native polypeptide conformation of GlpB was essential for proper coordination of the [2Fe-2S] cluster. It may be useful to conduct circular dichroism studies with the GlpB polypeptide to confirm the structural rearrangement of the polypeptide in its native state as well as with the various pH states and solvents [i.e. DMSO]. The mutant enzymes could also be compared to help distinguish between loss of cluster due to absence of a ligand residue or due to alteration in the folding pattern of the cluster.

b) Quinone Binding to GlpB

From its membrane location and its functional association with GlpAC, it is proposed that GlpB passes its reducing equivalents to the menaquinone pool. As such, it is proposed that GlpB is a quinone binding protein. Although the GlpB sequence exhibited no clear MK motif and an EPR visible quinone semi-radical species was not observed in my GlpB preparations, an approach to test the possibility is to isolate various herbicide resistant mutants in chromosomal GlpB. This technique utilizes a number of quinone analogs, which are commercially available [myxothiazol, HOQNO, antimycin, funicosilin tertbutryn, 5-Undecyl-6-hydroxy-4,7-dioxobenzothiazole (UHDBT), and stigmatellin] to find mutants in quinone function. In the case of the bacterial

photoreaction center of known three-dimensional structure (Deisenhofer *et al.*, 1985), it is known that atrazine and terbutryn resistant mutations directly affect the residues constituting the quinone binding pockets of this complex (Daldal *et al.*, 1989). The technique [myxothiazol, stigmatellin and mucidin] has also been successful with the identification of various mutants in *Rhodobacter capsulatus* cytochrome bc_1 complex (Daldal *et al.*, 1989), some of which are directly involved in the quinone pocket and others in regions linking various domains. The possibility of mutating the quinone binding pocket as well as surrounding residues suggests a mechanism by which the electron transfer pathway in GlpB could be studied.

c) Role of Histidine Residues

As previously described in the thesis, histidines are considered important residues in electron transfer as they have the potential to coordinate the binding of heme or other active redox metals. In *Rhodobacter sphaeroides*, the cytochrome *b* subunit of the bc_1 complex contains two heme components and is also the locus of both a quinol oxidizing site and a quinone reducing site (Hacker *et al.*, 1993). Analysis of the various histidines in GlpB with Degli Espositi's method of prediction for potential heme binding ligands (Degli Esposti, 1989), suggested that H_{167} and a few other histidines in the sequence may bind a heme. This could be tested with site directed mutagenesis to alter the residues and observe the effects on the function of GlpB.

d) Role of the Carboxy Terminal Cys Motif

Near the carboxy terminus of the GlpB sequence is the $CX_2CX_{11}CXH$ motif which resembles a zinc finger motif (Hase & Finkelstein, 1993) as well as being a potential site for coordinating of a [2Fe-2S] cluster (Cammack, 1991). An initial determination of the presence of zinc by plasma absorption mass spectroscopy would be informative, but conclusive results are more readily obtained with pure protein. Site-directed mutagenesis again would be useful in altering the appropriate cysteine residues and determining what changes occur.

In each of the cases where site-directed mutagenesis was suggested it would also be beneficial to characterize the designated mutation for growth characteristics. This would help determine if the residue is crucial for the electron-transfer pathway of the

enzyme. Prior to leaving the laboratory, with the aid of G. Shaw, I constructed a chromosomal knockout mutant of *glpACB*, which does not exhibit anaerobic growth on glycerol or G3P/fumarate media. Full characterization of the mutant is ongoing, but it should prove valuable in characterization of a number of the proposed mutants and the effects they cause.

4. Studies with GlpAC

Although the bulk of the work presented in this thesis has concentrated on the third subunit, questions still remain to be answered with the GlpAC subunits. Primarily, the site of the flavin cofactors has yet to be determined as well as the substrate binding site. Sequence analysis with GlpA and GlpD suggest an extended region of amino acids which may be the G3P binding site (Austin & Larson, 1991). Most of the glycolytic enzymes which have phosphorylated substrates or cofactors appear to contain active-site arginyl residues (Riordan *et al.*, 1977). GlpD (Austin & Larson, 1991) and GlpA (Cole *et al.*, 1988) both contain conserved arginyl residues which may aid in the binding of G3P. Sequence homology with other flavin enzymes have suggested two regions in the catalytic dimer for flavin binding, namely an FAD binding site in GlpA and an FMN binding site in GlpC (Cole *et al.*, 1988). The use of artificial flavins as active site probes (Ghisla & Massey, 1986) may aid in determining whether these conserved regions due indeed bind the flavin moieties. Some of these probes, such as 5-deazaflavin, lack the ability to stabilize radicals and to carry out 1 e^- transfers as in normal flavin. Deazaflavin is thus a good probe for the differentiation between 1 e^- and 2 e^- processes. Site directed mutagenesis can then be applied to determine the key residues essential for flavin binding, substrate binding and the overall catalytic mechanism. These experiments may also help elucidate those residues important in electron transfer to GlpB.

A main question regarding the dehydrogenase as a complex is the pathway of electron transfer. It is proposed that the catalytic site is within GlpA with the FAD participating in the catalytic mechanism, with the FMN site in GlpC enhancing activity by an allosteric mechanism (as suggested by Cole *et al.*, 1988). The two hydrogens are carried by the subunit to GlpB where the electrons reduce the [2Fe-2S] center in GlpB and the two protons are extruded to the other side of the membrane, via the reduction of the menaquinone to menaquinol. Various investigators (summarized in Cole *et al.*, 1985) also suggest the necessity of a *b*-type cytochrome following the dehydrogenase

but the role of this cytochrome is somewhat controversial. As presented in this thesis, features in the 555 and 558 nm region were observed in absortion spectra obtained with various whole cell preparations of JM83 and JM83 harboring the various *glp* plasmids [Chapter VI]. Such features have been previously assigned to two *b*-type cytochromes with reported midpoint potentials of + 140 mV and + 250 mV (Cole *et al.*, 1985). In view of the midpoint potentials of the various components in the G3PDH/MK/fumarate reductase complex, it is not clear how the cytochromes with such high midpoint potentials would be involved.

Another question which is essential to the understanding of electron transfer in GlpB is the detection of only one [Fe-S]. The transfer of two reducing equivalents must thus occur sequentially, unless other residues proposed in GlpB do bind other electron transfer species such as heme or another as yet undetected [Fe-S] center. The various mutagenesis experiments may help elucidate this question.

With the characterization of the third subunit in the *glpACB* operon as described in this thesis, our goal of understanding simple respiratory chains is now a step closer. The ultimate aim of reconstituting the G3PDH/fumarate reducatase or dimethyl sulfoxide reductase complex in liposomes may be attainable as the active research ongoing in the laboratory with DMSO reductase has also progressed to a stage where these reconstitution experiments may proceed. It will be interesting to determine how closely these systems will follow the physiological state of the cell.

BIBLIOGRAPHY

Abrahams, J. P., Lutter, R., Todd, R. J., van Raaij, M. J., Leslie, A. G. W., and J. E. Walker. 1993. Inherent asymmetry of the structure of F_1-ATPase from bovine heart mitochondria at 6.5 Å resolution. *EMBO J.* **12**:1775-1780.

Adman, E. T., Sieker, L. C., and L. H. Jensen. 1973. The structure of a bacterial ferredoxin. *J. Biol. Chem.* **248**:3987-3996.

Adman, E. T., Sieker, L. C., and L. H. Jensen. 1976. Structure of *Peptococcus aerogenes* ferredoxin: refinement at 2 Å reolution. *J. Biol. Chem.* **251**:3801-3806.

Allen, J. P., Feher, G., Yeates, T. O., Komiya, H., and D. C. Rees. 1987. Structure of the reaction center from *Rhodobacter sphaeroides* R-26: the cofactors. *Proc. Natl. Acad. Sci. USA.* **84**:5730-5734.

Allewell, N. M. 1993. Untangling the energetics of protein folding. *Trends Biochem. Sci.* **18**:1-2.

Ambudkar, S. V., Larson, T. J., and P. C. Maloney. 1986. Reconstitution of sugar phosphate transport systems of *Escherichia coli*. *J. Biol. Chem.* **261**:9083-9086.

Anraku, Y. and R. B. Gennis. 1987. The aerobic respiratory chain of *Escherichia coli*. *Trends Biochem. Sci.* **12**:262-266.

Argast, M. and W. Boos. 1980. Co-regulation in *Escherichia coli* of a novel transport system for *sn*-glycerol-3-phosphate and outer membrane protein Ic(c,E) with alkaline phosphatase and phosphate-binding protein. *J. Bacteriol.* **143**:142-150.

Aris, J. P., Klionsky, D. J., and R. D. Simoni. 1985. The F_0 subunits of the *Escherichia coli* F_1F_0-ATP synthase are sufficient to form a functional proton pore. *J. Biol. Chem.* **260**:11207-11215.

Asnis, R. E. and A. F. Brodie. 1953. A glycerol dehydrogenase from *Escherichia coli*. *J. Biol. Chem.* **203**:153-159.

Au, D. C.-T., Green, G. N., and R. B. Gennis. 1984. Role of quinones in the branch of the *Escherichia coli* respiratory chain that terminates in cytochrome *o*. *J. Bacteriol.* **157**:122-125.

Au, D. C.-T., Lorence, R. M., and R. B. Gennis. 1985. Isolation and characterization of an *E. coli* mutant lacking the cytochrome *o* terminal oxidase. *J. Bacteriol.* **161**:123-127.

Augier, V., Guigliarelli, B., Asso, M., Betrand, P., Frixon, C., Giordano, G., Chippaux, M., and F. Blasco. 1993. Site-Directed mutagenesis of conserved cysteine residues within the β-subunit of *Escherichia coli* Nitrate reductase. Physiological, biochemical and EPR characterization of the mutated enzymes. *Biochemistry* **32**:2013-2023.

Austin, D. and T. J. Larson. 1991. Nucleotide sequence of the *glpD* gene encoding aerobic sn-Glycerol 3-Phosphate dehydrogenase of *Escherichia coli* K-12. *J. Bacteriol.* **173**:101-107.

Balbas, P. and F. Bolivar. 1991. Design and construction of expression plasmid vectors in *Escherichia coli*. *Methods Enzymol.* **185**:14-37.

Baldwin, J. M., Henderson, R., Beckman, E., and F. Zemlin. 1988. Images of purple membrane at 2.8 Å resolution obtained by cryo-electron microscopy. *J. Mol. Biol.* **202**:585-591.

Ballesteros, J. A and H. Weinstein. 1992. Analysis and refinement of criteria for predicting the structure and relative orientation of transmembranal helical domains. *Biophys. J.* **62**:107-109.

Beinert, H. 1983. Semi-micro methods for analysis of labile sulfide and of labile sulfide plus sulfane sulfur in unusually stable iron-sulfur proteins. *Anal. Biochem.* **13**:373-378.

Beinert, H. and R. H. Sands. 1960. Studies on succinic and DPNH dehydrogenase preparations by paramagnetic resonance (EPR) spectroscopy. *Biochem. Biophys. Res. Commun.* **3**:41-46.

Beinert, H. 1990. Recent developments in the field of iron-sulfur proteins. *FASEB J.* **4**:2483-2491.

Bell, A. and S. Busby. 1994. Location and orientation of an activating region in the *Escherichia coli* transcription factor, FNR. *Mol. Microbiol.* **11**:383-390.

Bilous, P. T., Cole, S. T., Anderon, A. F., and J. H. Weiner. 1988. Nucleotide sequence of the *dmsABC* operon encoding the anaerobic dimethyl sulfoxide reductase of *Escherichia coli* HB101. *Mol. Microbiol.* **2**:785-795.

Bilous, P. T. and J. H. Weiner. 1985a. Dimethyl sulfoxide reductase activity by anaerobiocally grown *Escherichia coli* HB101. *J. Bacteriol.* **162**:1151-1155.

Bilous, P. T. and J. H. Weiner. 1985b. Proton translocation coupled to dimethyl sulfoxide reduction in anaerobically grown *Escherichia coli* HB101. *J. Bacteriol.* **163**:369-375.

Bilous, P. T. and J. H. Weiner. 1988. Molecular cloning and expression of the *Escherichia coli* dimethyl sulfoxide reductase operon. *J. Bacteriol.* **170**:1511-1518.

Birnboim, H., and J. Doly. 1979. A rapid extraction procedure for screening recombinant plasmid DNA. *Nucleic Acids Res.* **7**:1513-1525.

Blasco, F., Iobbi, C., Giordano, G., Chippaux, M., and V. Bonnefoy. 1989. Nitrate reductase of *Escherichia coli*. Completion of the nucleotide sequence of the *nar* operon and reassessment of the role of the α and β subunits in iron binding and electron transfer. *Mol. Gen. Genet.* **218**:249-256.

Blasco, F., Pommier, J., Augier, V., Chippaux, M., and G. Giordano. 1992. Involvement of the *narJ* or *narW* gene product in the formation of active nitrate reductase in *Escherichia coli*. *Mol. Microbiol.* **6**:221-230.

Blum, H., Cusanovich, M. A., Sweeney, W. V., and T. Ohnishi. 1981. Magnetic interactions between dysprosium complexes and two soluble iron-sulfur proteins. *J. Biol. Chem.* **264**:2199-2206.

Blum, H., Bowyer, J. R., Cusanovich, M. A., Waring, A. J., and T. Ohnishi. 1983. Spin-lattice relaxation rates of iron-sulphur proteins and heme proteins affected by dysprosium complexes and temperature. *Biochim. Biophys. Acta.* **748**:418-428.

Boekema, E. J., Berden, J. A., and M. G. van Heel. 1986. Structure of mitochondrial F_1-ATPase studied by electron microscopy and image processing. *Biochim. Biophys. Acta.* **851**:353-360.

Bowden, G. A., Paredes, A. M., and G. Georgiou. 1991. Structure and morphology of protein inclusion bodies in *Escherichia coli*. *Bio/Technology* **9**:725-730.

Boyer, P. D. 1972. Conformational coupling in oxidative phosphorylation and photophosphorylation. *Trends Biochem. Sci.* **2**:38-41.

Bragg, P. D. 1979. "Electron transport and energy-transducing systems in *Escherichia coli*" *In* Capaldi, R. A. (ed.) Membrane Proteins in Energy Transduction., Marcel Dekker Inc., New York, pp. 341-449.

Brice, J. M., Law, J. F., Meyer, D. J., and C. W. Jones. 1974. Energy conservation in *Escherichia coli* & *Klebsiella pneumoniae*. *Biochem. Soc. Trans.* **2**:523-526.

Broome-Smith, J. K., Tadayyon, M., and Y. Zhang. 1990. β-lactamase as a probe of membrane protein assembly and protein export. *Mol. Microbiol.* **4**:1637-1644.

Brown, E. D. and J. M. Wood. 1993. Conformational change and membrane association of the PutA protein are coincident with reduction of its FAD cofactor by proline. J. *Biol. Chem.* **268**:8972-8979.

Brumby, P. E. and V. Massey. 1967. Determination of nonheme iron, total iron, and copper. *Methods Enzymol.* **10**:463-474.

Brummer, J. 1993. New photolabeling and crosslinking methods. *Annu. Rev. Biochem.* **62**:483-514.

Bruschi, M. and F. Guerlesquin. 1988. Structure, function and evolution of bacterial ferredoxins. *FEMS Microbiol. Rev.* **54**:155-176.

Brusilow, W. S. A. 1993. Assembly of the *Escherichia coli* F_1F_0ATPase, a large multimeric membrane-bound enzyme. *Mol. Microbiol.* **9**:419-424.

Buchanan, B. B. and D. I. Arnon. 1970. Ferredoxins: chemistry and function in photosynthesis, nitrogen fixation, and fermentative metabolism. *Adv. Enzymol.* **33**:119-176.

Calhoun, M. W. and R. B. Gennis. 1993. Demonstration of separate genetic loci encoding distinct membrane-bound respiratory NADH dehydrogenases in *Escherichia coli*. *J. Bacteriol.* **175**:3013-3019.

Calhoun, M. W., Hill, J. J., Lemieux, L. J., Ingledew, W. J., Alben, J. O., and R. B. Gennis. 1993. Site-directed mutants of the cytochrome *bo* ubiquinol oxidase of *Escherichia coli*: amino acid substitutions for two histidines that are putative CuB ligands. *Biochemistry*. **32**:11524-11529.

Cammack, R. 1975. Effects of solvent on the properties of ferredoxins. *Biochem. Soc. Trans.* **3**, 482-488.

Cammack, R. 1986. "Iron-sulfur clusters in enzymes: pathways of electron transfer". *In* Iron-sulfur protein research. Matsubara, H. et al (eds.), Japan Sci. Soc. Press, Tokyp, Springer-Verlag, Berlin, pp. 40-55.

Cammack, R. 1991. Iron-sulphur clusters in enzymes - themes and variations. *Adv. Inorgan. Chem.* **38**:281-322.

Cammack, R., Patil, D. S., and V. M. Fernandez. 1985a. Electron-spin-resonance/electron-paramagnetic resonanance spectroscopy of iron-sulfur enzymes. *Biochem. Soc. Trans.* **13**:572-578.

Cammack, R., Patil, D. S., Condon, C., Owen, P., Cole, S. T. and J. H. Weiner. 1985b. "ESR spectroscopic studies of succinate dehydrogenase and fumarate reductase from *Escherichia coli*". *In* Bray, R. C., Engel, P. C., and S. G. Mayhew, eds. Flavins and Flavoproteins, Walter de Gruyter, Berlin, pp. 551-554.

Cammack, R., Patil, D. S., and J. H. Weiner. 1986. Evidence that center 2 in *Escherichia coli* fumarate reductase is a [4Fe-4S] cluster. *Biochim. Biophys. Acta.* **870**:545-551.

Cammack, R. and A. Watts. 1994. ESR: Instrumentation, General Theory and Operating Techniques [in preparation].

Cammack, R. and J. H. Weiner. 1990. Electron paramagnetic resonance spectroscopic characterization of dimethyl sulfoxide reductase of *Escherichia coli*. *Biochemistry* **29**:8410-8416.

Castillo, G., Vera, J. C., Yang, C-P. H., Horwitz, S. B. amd O. M. Rosen. 1990. Functional expression of murine mulitdrug resistance in *Xenopus laevis* oocytes. *Proc. Natl. Acd. Sci. USA.* **87**:4737-4741.

Castor, L. N. and B. Chance. 1959. Photochemical determination of the oxidases of bacteria. *J. Biol. Chem.* **234**:1587-1592.

Chalmers, J. L., Kim, E., Telfor, J. N., Wong, E. Y., Tacon, W. C., Shuler, M. L., and Wilson, D. B. 1990. Effects of temperature on *Escherichia coli* overproducing β-lactamase or human epidermal growth factor. *Appl. Environ. Microbiol.* 56:104-111.

Chelsky, D. and F. W. Dahlquist. 1980. Chemotaxis in *Escherichia coli*: Associations of protein components. *Biochemistry* **19**:4633-4639.

Chiang, R. C., Cavicchioli, R., and R. P. Gunsales. 1992. Identification and characterization of *narQ*, a second nitrate sensor-transmittor for nitrate-dependent gene regulation in *Escherichia coli*. *Mol. Microbiol.* **6**:1913-1923.

Chung, C. H. 1993. Proteases in *Escherichia coli*. *Science*. **262**:372-374.

Cole, S. T., Condon, C., Lemire, B., and J. H. Weiner. 1985. Molecular biology, biochemistry and bioenergetics of fumarate reductase, a complex membrane-bound iron-sulphur flavoenzyme of *Escherichia coli*. *Biochim. Biophys. Acta*. **811**:381-403.

Cole, S. T., Eiglmeier, K., Ahmed, S., Honore, N., Elmes, L., Anderson, W. F., and J. H. Weiner. 1988. Nucleotide sequence and gene-polypeptide relationships of the *glpABC* operon encoding the anaerobic sn-glycerol-3-phosphate dehydrogenase of *Escherichia coli* K-12. *J. Bacteriol.* **170**:2448-2456.

Compan, I. and D. Touati. 1994. Anaerobic activation of *arcA* transcription in *Escherichia coli*: roles of Fnr and ArcA. *Mol. Microbiol.* **11**:955-964.

Condon, C. and J. H. Weiner. 1988. Fumarate reductase of *Escherichia coli*: an investigation of function and assembly using *in vivo* complementation. *Mol. Microbiol.* **2**:43-52.

Conover, R. C., Kowal, A. T., Fu, W., Park, J-B, Aono, S., Adams, M. W. W., and M. K. Johnson. 1990. Spectroscopic characterization of the novel iron-sulfur cluster in *Pyrococcus furiosus* ferredoxin. *J. Biol. Chem.* **265**:8533-8541.

Cotter, D. P. and R. P. Gunsalus. 1989. Oxygen, nitrate and molybdenum regulation of *dmsABC* gene expression in *Escherichia coli*. *J. Bacteriol.* **171**:3817-3823.

Cotter, D. P. and R. P. Gunsalus. 1992. Contribution of the *fnr* and *arcA* gene products in coordinate regulation of the cytochrome o (*cyoABCDE*) and d (*cydAB*) oxidase genes in *Escherichia coli*. *FEMS Microbiol. Lett.* **91**:31-36.

Cramer, W. A. and D. B. Knaff. 1991. "Membrane structure and storage of free energy" *In* Cantor, C. R. (ed.) Energy Transduction in Biological Membranes., Springer-Verlag, New York, pp. 78-138.

Creighton, T. E. 1990. Protein folding. *Biochem J.* **270**:1-16.

Crimi, M. and M. Degli Esposti. 1991. Structural predictions for membrane proteins: the dilemma of hydrophobicity scales. *Trends Biochem. Sci* **16**:119.

Cronan Jr., J. E. and C. O. Rock. 1987. "Biosynthesis of Membrane Lipds". *In* Neidhardt, F. C. (ed.) *Escherichia coli* and *Salmonella typhimurium* Cellular and molecular biology, Vol 1. American Society for Microbiology, Washington, DC, pp. 474-497.

Crosa, J. H., Tolmasky, M. E., Actis, L. A., and S. Falkow. 1994. "Plasmids" *In* Gerhardt, P. (ed.) Methods for general and molecular bacteriology., American Society for Microbiology, Washington, D.C., pp. 365-386.

Dailey, H. A., Finnegan, M. G., and M. K. Johnson. 1994. Human ferrochelatase is an iron-sulfur protein. *Biochemistry* **33**:403-407.

Daldal, F., Tokito, M. K., Davidson, E., and M. Faham. 1989. Mutations conferring resistance to quinol (Q_z) inhibitors of the cyt bc_1 complex of *Rhodobacter capsulatus*. *EMBO J.* **8**:3951-3961.

Datta, D. B. 1987. *In* "A comprehensive introduction to membrane biochemistry" Floral Publishing, Madison, WI.

Davasse, V. and J-M. Moulis. 1992. Design and functional expression in *Escherichia coli* of a synthetic gene encoding *Clostridium pasteurianum* 2[4Fe-4S] ferredoxin. *Biochem. Biophys. Res. Comm.* **185**:341-349.

Degli Esposti, M. 1989. Prediction and comparison of the haem-binding sites in membrane haemoproteins. *Biochim. Biophys. Acta.* **977**:249-265.

Deisenhofer, J., Epp, O., Miki, L., Huber, R., and H. Michel. 1985. Structure of the protein subunits in the photosynthetic reaction centre of *Rhodopseudomonas viridis* at 3 Å resolution. *Nature* **318**:618-624.

deVetten, M. P. and P. Agre. 1988. The Rh polypeptide is a major fatty acid-acylated erthrocyte membrane protein. *J. Biol. Chem.* **263**:18193-18196.

DeWitt, J. G., Bentsen, J. G., Rosensweig, A. C., Hedman, B., Green, J., Pilkington, S., Papaefthiniou, G. G., Dalton, H., Hodgson, K. O., and S. J. Lippard. 1991. X-ray absorption, Mossbauer, and EPR studies of the dinuclear iron cneter in the hydroxylase component of methane monooxygenase. *J. Amer. Chem. Soc.* **113**:9219-9235.

Dickie, P. and J. H. Weiner. 1979. Purification and characterization of membrane-bound fumarate reductase from anaerobically grown *Escherichia coli*. *Can. J. Biochem.* **57**:813-821.

Downie, J. A., Gibson, F., and G. B. Cox. 1979. Membrane adenosine triphosphatases of prokaryotic cells. *Annu. Rev. Biochem.* **48**:103-131.

Dus, K., DeKlerk, H., Sletten, K., and R. G. Bartsch. 1967. Chemical characterization of high potential iron proteins from *Chromatium* and *Rhodopseudomonas gelatinosa*. *Biochim. Biophys. Acta.* **140**:291-311.

Dutton, P. L. 1978. Redox potentiometry: determination of midpoint potentials of oxidation-reduction components of biological electron-transfer systems. *Methods Enzymol.* **54**:411-434.

Ehrmann, M., Boos, W., Ormseth, E., Schweizer, H., and T. J. Larson. 1987. Divergent transcription of the sn-glycerol-3-phosphate active transport (*glpT*) and anaerobic sn-glycerol-3-phosphate dehydrogenase (*glpAglpCglpB*) genes of *Escherichia coli* K-12. *J. Bacteriol.* **169**:526-532.

Eiglmeier, K., Boos, W., and S. T. Cole. 1987. Nucleotide sequence and transcriptional startpoint of the *glpT* gene of *Escherichia coli*: extensive sequence homology of the glycerol-3-phosphate transport protein with components of the hexose-6-phosphate transport system. *Mol. Microbiol.* **1**:251-258.

Eiglmeier, K., Honore, N., Iuchi, S., Lin, E. C. C., and S. T. Cole. 1989. Molecular genetic analysis of FNR-dependent promoters. *Mol. Microbiol.* **3**:869-878.

Eisenberg, D. 1984. Three-dimensional structure of membrane and surface proteins. *Annu. Rev. Biochem.* **53**:595-623.

Elliott, J. I. and L. G. Ljungdahl. 1982. Isolation and characterization of an Fe_8-S_8 ferredoxin (Ferredoxin II) from *Clostridium thermoaceticum*. *J. Bacteriol.* **151**:328-333.

Englebrecht, S. and W. Junge. 1990. Subunit δ of H^+-ATPases: at the interface between proton flow and ATP. *Biochim. Biophys. Acta.* **1015**:379-390.

Fillingame, R. H., Mosher, M. E., Negrin, L. S., and R. K. Peters. 1983. H^+-ATPase of *Escherichia coli uncB402* mutation leads to a loss of χ subunits of F_0 sector. *J. Biol. Chem.* **258**:604-609.

Fillingame, R. H., Porter, B., Hermolin, J., and L. K. White. 1986. Synthesis of a functional F_0 sector of the *Escherichia coli* H^+-ATPase does not require synthesis of the alpha or beta subunits of F_1. *J. Bacteriol.* **165**:244-251.

Fischbarg, J., Cheung, M., Czegledy, F., Li, P., Iserovich, P., Kuang, K., Hubbard, J., Garner, M., Rosen, O. M., Golde, D. W., and J. C. Vera. 1993. Evidence that facilitative glucose transporters may fold as β-barrels. *Proc. Natl. Acad. Sci. USA.* **90**:11658-11662.

Flint, D. H., Emptage, M. K., and J. R. Guest. 1992. Fumarse A from *Escherichia coli*: purification and characterization as an iron-sulfur cluster containing enzyme. *Biochemistry* **31**:10331-10337.

Fox, B. G., Froland, W. A., Dege, J. E., and J. D. Lipscomb. 1989. Methane monooxygenase from *Methylosinus trichosorium* OB3b. *J. Biol. Chem.* **264**:10023-10033.

Freedberg, W. B. and E. C. C. Lin. 1973. Three kinds of controls affecting the expression of the *glp* regulon in *Escherichia coli*. *J. Bacteriol.* **115**:816-823.

Fu, R., Wall., J. D. and G. Voordouw. 1994. DcrA, a c-type heme-containing methyl-accepting protein from *Desulfovibrio vulgaris* Hildenborough, senses the oxygen concentration or redox potential of the environmnet. *J. Bacteriol.* **176**:344-350.

Fukuyama, K., Nagahara, Y., Tsukihara, T., Katsube, Y., Hase, T., and H. Matsubara. 1988. Tertiary structure of *Bacillus thermoproteolyticus* [4Fe-4S] ferredoxin, evolutionary implications for bacterial ferredoxins. *J. Mol. Biol.* **199**:183-193.

Fung, L. W-M., Pratt, E. A. and C. Ho. 1979. Biophysical and biochemical studies on the interaction of a membrnae-bound enzyme, D-lactate dehydrogenase of *Escherichia coli*, with phospholipids. *Biochemistry*. **18**:317-324.

Futai, M. 1973. Membrane D-lactate dehydrogenase from *Escherichia coli*: purification and properties. *Biochemsitry* **12**:2468-2474.

Futai, M. and H. Kanazawa. 1983. Structure and function of proton translocating adenosine triphosphatase (F_0F_1): biochemical and molecular biological approaches. *Microbiol. Rev.* **47**:285-312.

Futai, M. and Y. Tanaka. 1975. Localization of D-lactate dehydrogenase in membrane vesicles prepared by using a French press or ethylenediaminetetraacetate-lysozyme from *Escherichia coli*. *J. Bacteriol.* **124**:470-475.

Gaillard, J., Moulis, J-M, Auric, P., and J. Meyer. 1986. High multiplicity spin states of 2[4Fe-4Se]$^+$ Clostridial ferredoxins. *Biochemistry* **25**:464-468.

Gayda, J. P., Gibson, J. F., Cammack, R., Hall, D. O., and R. Mullinger. 1976. Spin lattice relaxation and exchange interaction in a 2-iron, 2-sulphur protein. *Biochim. Biophys. Acta.* **434**:154-163.

Gayda, J. P., Bertrand, P., Deville, A., Moer, C., Roger, G., Gibson, J. F., and R. Cammack. 1979. Temperature dependence of the electronic spin-lattice relaxation time in a 2-iron, 2-sulfur protein. *Biochim. Biophys. Acta.* **581**:15-26.

George, D. G., Hunt, L. T., Yeh, L-S. L., and W. C. Barker. 1985. New perspectives on bacterial ferredoxin evolution. *J. Mol. Evol.* **22**:20-31.

George, S. J., Armstrong, F. A., Hatchikian, E. C., and A. J. Thomson. 1989. Electrochemical and spectroscopic characterization of the conversion of the 7Fe into the 8Fe form of ferredoxin III from *Desulfovibrio africans*. *Biochem J.* **264**:275-284.

Georgiou, C. D., Dueweke, T. J., and R. B. Gennis. 1988. Regulation of expression of the cytochrome *d* terminal oxidase in *Escherichia coli* is transcriptional. *J. Bacteriol.* **170**:961-966.

Ghisla, S. and V. Massey. 1986. New flavins for old: artificial flavins as active site probes of flavoproteins. *Biochem J.* **239**:1-12.

Gott, P. and W. Boos. 1988. The transmembrane topology of the sn-glycerol-3-phosphate permease of *Escherichia coli* analysed by *phoA* and *lacZ* protein fusions. *Mol. Microbiol.* **2**:655-663.

Grabowski, R., Hofmeister, A. E. M., and W. Buckel. 1993. Bacterial L-serine dehydratases: a new family of enzymes containing iron-sulfur clusters. *Trends Biochem. Sci.* **18**:297-300.

Green, J., Trageser, M., Six, S., Unden, G., and J. R. Guest. 1991. Characterization of the FNR protein of *Escherichia coli*, an iron-binding trancriptional regulator. *Proc. R. Soc. Lond.* **244**:137-144.

Guigliarelli, B., Bertrand, P., More, C., Papavassiliou, P., Hatchikian, E. C., and J. P. Gayda. 1985. Interconversion between the 3Fe and 4Fe forms of the iron-sulfur clusters in the ferredoxin from *Thermodesulfobacterium commune*: EPR characterization and potentiometric titration. *Biochim. Biophys. Acta* **810**:319-324.

Gunsalus, R. P., Kalman, L. V., and R. R. Stewart. 1989. Nucleotide sequence of the *narL* gene that is involved in global regulation of nitrate controlled respiratory genes of *Escherichia coli*. *NucleicAcids Res.* **17**:1965-1975.

Gunsalus, R. P. 1992. Control of electron flow in *Escherichia coli*: coordinated transcription of respiratory pathway genes. *J. Bacteriol.* **174**:7069-7074.

Hacker, B., Barquera, B., Crofts., A. R. and R. B. Gennis. 1993. Characterization of mutations in the cytochrome *b* subunit of the bc_1 complex of *Rhodobacter sphaeroides* that affect the quinone reductase site (Q_c). *Biochemistry* **32**:4403-4410.

Haddock, B. A., Downie, J. A. and P. B. Garland. 1976. Kinetic characterization of the membrane-bound cytochromes of *Escherichia coli* grown under a variety of conditions by using a stopped-flow dual-wavelegth spectrophotometer. *Biochem. J.* **154**:285-294.

Hanahan, D., Jesse, J., and F. R. Bloom. 1991. Plasmid transformation of *Escherichia coli* and other bacteria. *Methods Enzymol.* **204**:63-113.

Hartel-Schenk, S. and P. Agre. 1988. Mammalian red cell membrane Rh polypeptides are selectively palmitoylated subunits of a macromolecular complex. *J. Biol. Chem.* **267**:5569-5574.

Hartman, J., Daram, P., Frizzell, R. A., Rado, T., Benos, D. J., and E. R. Sorscher. 1992. Affinity purification of insoluble recombinant fusion proteins containing glutathione-s-transferase. *Biotech. Bioengineer.* **39**:828-832.

Hase, C. C. and R. A. Finkelstein. 1993. Bacterial extracellular zinc-containing metalloproteases. *Microbiol. Rev.* **57**:823-837.

Hayashi, S. H. and E. C. C. Lin. 1967. Purification and properties of glycerol kinase from *Escherichia coli*. *J. Biol. Chem.* **242**:1030-1035.

Hayashi, S., Koch, J. P., and E. C. C. Lin. 1964. Active transport of L-α-glycerophosphate in *Escherichia coli*. *J. Biol. Chem.* **239**:3098-3105.

Hedderich, R., Albracht, S. P. J., Linder, D., Koch, J., R. K. Thauer. 1992. Isolation and characterization of polyferredoxin from *Methanobacterium thermoautotrophicum*. FEBS **298**:65-68.

Hederstedt, L. and T. Ohnishi. 1992. "Progress in succinate:quinone oxidoreductase research". *In* L Ernster (ed.) Molecular mechanisms in bioenergetics. Elsevier Science Publishers B. V., pp. 163-198.

Heller, K. B., Lin, E. C. C., and T. H. Wilson. 1980. Substrate specificity and transport properties of the glycerol facilitator of *Escherichia coli*. *J. Bacteriol.* **144**:274-278.

Henderson R. and P. N. T. Unwin. 1975. Three dimensional model of purple membrane obtained by electron microscopy. *Nature* **257**:28-33.

Hendrick, J. P. and F. U. Hartl. 1993. Molecular chaperone functions of heat-shock proteins. *Annu. Rev. Biochem.* **62**:349-384.

Hidalgo, E. and B. Demple. 1994. An iron-sulfur center essential for transcriptional activation by the redox-sensing SoxR protein. *EMBO J.* **13**:138-146.

Higgins, C. F. 1992. ABC Transporters: from microorganisms to man. *Ann. Rev. Cell. Biol.* **8**:67-113.

Hitchens, G. D. 1989. Electrode surface microstructures in studies of biological electron transfer. *Trends Biochem. Sci.* **14**:152-155.

Hobman, T. C, Woodward, L., and M. G. Farquhar. 1992. The rubella virus E1 glycoprotein is arrested in a novel post-ER, pre-Golgi compartment. *J. Cell. Biol.* **118**:795-811.

Hogue, D. 1994. Ph. D. Thesis. Functional and molecular studies on eucaryotic nucleoside transporters. University of Alberta, Edmonton, Canada.

Holden, H. M., Jacobson, B. L., Hurley, J. K., Tollin, G., Oh, B. H., Skjeldal, L., Chae, Y. K., Cheng, H., Xia, B., and J. L. Markley. 1994. Structure-function studies of [2Fe-2S] ferredoxins. *J. Bioenerg. Biomem.* **26**:67-88.

Hosler, J. P., Ferguson-Miller, S., Calhoun, M. W., Thomas, J. W., Hill, J., Lemieux, L., Ma, J., Georgiou, C., Fetter, J., Shapleigh, J., Tecklenburg, M. M. J., Babcock, G. T., and R. B. Gennis. 1993. Insight into the active-site structure and function of cytochrome oxidase by analysis of site-directed mutants of bacterial cytochrome aa_3 and cytochrome bo. *J. Bioenerg. Biomem.* **25**:121-136.

Hurley, J. H., Faber, H. R., Worthylake, D., Meadow, N. D., Roseman, S., Pettigrew, D. W., and Remington, S. J. 1993. Structure of the regulatory complex of *Escherichia coli* III^{Glc} with glycerol kinase. *Science.* **259**:673-677.

Ingledew, W. J. and R. K. Poole. 1984. The respiratory chain of *Escherichia coli*. *Microbiol. Rev.* **48**:222-271.

Ingledew, W. J. and M. Saraste. 1979. The reaction of cytochrome cd, with oxygen and peroxides. *Biochem. Soc. Trans.* **7**:167-168.

Innes, J. B. and G. W. Brudvig. 1989. Location and magnetic relaxation properties of the stable tyrosine radical in Photosystem II. *Biochemistry* **28**:1116-1125.

Iuchi, S. and E. C. C. Lin. 1988. *arcA* (*dye*), a global regulatory gene in *Escherichia coli* mediating repression of enzymes in the aerobic pathways. *Proc. Natl. Acad. Sci. USA.* **85**:1888-1892.

Iuchi, S., Cameron, D. C., and E. C. C. Lin. 1989. A second regulator gene (*arcB*) mediating repression of enzymes in aerobic pathways of *Escherichia coli*. *J. Bacteriol.* **171**:868-873.

Iuchi, S., Chepuri, V., Fu, H. A., Gennis, R. B., and E. C. C. Lin. 1990a. Requirement for terminal cytochromes in generation of the signal for the *arc* regulatory systems in *Escherichia coli*; study utilizing deletions and *lac* fusions of *cyo* and *cyd*. *J. Bacteriol.* **172**:6020-6025.

Iuchi, S., Matsuda, Z., Fujiwara, T., and E. C. C. Lin. 1990b. The *arcB* gene of *Escherichia coli* encodes a sensor-regulator protein for anaerobic repression of the *arc* modulon. *Mol. Microbiol.* **4**:715-727.

Iuchi, S., Cole, S. T., and E. C. C. Lin. 1990c. Multiple regulatory elements for the *glpA* operon encoding anaerobic glycerol-3-phosphate dehydrogenase and the *glpD* operon encoding aerobic glycerol-3-phosphate dehydrogenase in *Escherichia coli*: further characterization of respiratory control. *J. Bacteriol.* **172**:179-184.

Iuchi, S. and E. C. C. Lin. 1991. Adaptation of *Escherichia coli* to respiratory conditions: regulation of gene expression. *Cell* **66**:5-7.

Iuchi, S. and E. C. C. Lin. 1993. Adaptation of *Escherichia coli* to redox environments by gene expression. *Mol. Microbiol.* **9**:9-15.

Jennings, M. L. 1989. Topography of membrane proteins. *Annu. Rev. Biochem.* **58**:999-1027.

Johnson, M. K., Morningstar, J. E., Cecchini, G., and B. A. C. Ackrell. 1985. Detection of a tetranuclear iron-sulfur centre in fumarate reducatase from *Escherichia coli* by electron paramagnetic resonance spectroscopy. *Biochim. Biophys. Res. Commun.* **131**:756-762.

Johnson, M. K., Kowal, A. T., Morningstar, J. E., Oliver, M. E., Whittaker, K., Gunsales, R. P., Ackrell, B. A. C. and G. Cecchini. 1988. Subunit location of the iron-sulfur clusters in fumarate reductase from *Escherichia coli*. *J. Biol. Chem.* **263**:14732-14738.

Jollie, D. R. and J. D. Lipscomb. 1991. Formate dehydrogenase from *Methylosinus trichosporium* OB3b. *J. Biol. Chem.* **266**:21853-21863.

Jones, C. W. 1982. 'Bacterial respiration and photosynthesis'. *In* Coles, J. A., and C. J. Knowles (eds). Aspects of Microbiology 5. Nelson Canada Ltd., Don Mills., Ontario

Jones, H. M. and R. P. Gunsalus. 1987. Regulation of *Escherichia coli* fumarate reductase (*frdABCD*) operon expression by respiratory electron acceptor and the *fnr* gene product. *J. Bacteriol.* **169**:3340-3349.

Kaback, H. R. 1971. Bacterial membranes. *Methods Enzymol.* **22**:99-120.

Kassner, R. J. and W. Yang. 1977. A theoretical model for the effects of solvent and protein dielectric on the redox potentials of iron-sulfur clusters. *J. Amer. Chem. Soc.* **99**:4351-4355.

Kent, T. A., Emptage, M. H., Merkle, H., Kenendy, M. C., Beinert, H., and E. Munck. 1985. Mossbauer studies of aconitase. *J. Biol. Chem.* **260**:6871-6881.

Khorana, H. G. 1992. Rhodopsin, photoreceptor of the rod cell. *J. Biol. Chem.* **267**:1-4.

King, T. E. and R. O. Morris. 1967. Determination of acid-labile sulfide and sulfhydryl groups. *Methods Enzymol.* **10**:634-641.

Kistler, W. S., Hirsch, C. A., Cozzarelli, N. R., and E. C. C. Lin. 1969. Second pyridine nucleotide-independent L-α-Glycerophosphate dehydrogenase in *Escherichia coli* K-12. *J. Bacteriol.* **122**:1133-1135.

Kita, K., Konishi, K., and Y. Anraku. 1984a. Terminal oxidases of *Escherichia coli* aerobic respiratory chain. I. Purification and properties of cytochrome b_{556} - *o* complex from cells in the early exponential phase of aerobic growth. *J. Biol. Chem.* **259**:3368-3374.

Kita, K., Konishi, K., and Y. Anraku. 1984b. Terminal oxidases of *Escherichia coli* aerobic respiratory chain. I. Purification and properties of cytochrome b_{558} - *d* complex from cells grown with limited oxygen and evidence of branched electron-carrying systems. *J. Biol. Chem.* **259**:3375-3381.

Klausner, R. D., Rouault, T. A., and J. B. Harford. 1993. Regulating the fate of m-RNA: the control of cellular iron metabolism. *Cell* **72**:19-28.

Knoell, H. E., and J. Knappe. 1974. *Escherichia coli* ferredoxin, an iron-sulfur protein of the adrenodoxin type. *Eur. J. Biochem.* **50**:245-252.

Kohn, L. D., and H. R. Kaback. 1973. Mechanisms of active transport in isolated bacterial membrane vesicles. XV. Purification and properties of the membrane-bound D-lactate dehydrogenase from *Escherichia coli*. *J. Biol. Chem.* **248**:7012-1017.

Koval, A. T., Morningstar, J. E., Johnson, M. K., Ramsay, R. R., and T. P. Singer. 1986. Spectroscopic characterization of the number and type of iron-sulfur clusters in NADH:Ubiquinone Oxidoreductase. *J. Biol. Chem.* **261**:9239-9245.

Kovatchev, S., Vaz, W. L. C., and H. Eibl. 1981. Lipid dependence of the membrane-bound D-lactate dehydrogenase from *Escherichia coli*. *J. Biol. Chem.* **256**:10369-10374.

Kunkel, T. A. 1985. Rapid and efficient site-specific mutagenesis without phenotypic selection. *Proc. Natl. Acad. Sci. USA*. **82**:488-492.

Kuchta, R. D., Hanson, G. R., Holmquist, B., and R. H. Abeles. 1986. Fe-S Centers in lactyl-CoA dehydratase. *Biochemistry* **25**:7301-7307.

Kuhlbrandt, W., Wang, D. N., and Y. Fujiyoshi. 1994. Atomic model of plant light-harvesting complex by electron crystallography. *Nature* **367**:614-621.

Kuo, C-F., McRee, D. E., Fisher, C. L., O'Handley, S. F., Cunningham, R. P., and J. A. Tainer. 1992. Atomic structure of the DNA repair [4Fe-4S] enzyme endonuclease III. *Science* **258**:434-440.

Kuritzkes, D. R., Zhang, X-Y., and E. C. C. Lin. 1984. Use of ϕ(*glp-lac*) in studies of respiratory regulation of the *Escherichia coli* Anaerobic sn-Glycerol-3-phosphate dehydrogenase genes (*glpAB*). *J. Bacteriol.* **157**:591-598.

Laemmli, U. K. 1970. Cleavage of structural proteins during assembly of the head of bacteriophage T4. *Nature (London)* **227**:680-685.

Langen, R., Jensen, G. M., Jacob, U., Stephens, P. J., and A. Warshel. 1992. Protein control of iron-sulfur cluster redox potentials. *J. Biol. Chem.* **267**:25625-25627.

Larson, T. J., Schumacher, G., and W. Boos. 1982. Identification of the *glpT* encoded sn-glycerol-3-phosphate permease of *Escherichia coli*, an oligomeric integral membrane protein. *J. Bacteriol.* **152**:1008-1021.

Larson, T. J., Ye, S., Weissenborn, D. C., Hoffmann, H. J., and H. Schweizer. 1987. Purification and characterization of the repressor for the sn-glycerol-3-phosphate regulon of *Escherichia coli* K-12. *J. Biol. Chem.* **262**:15869-15874.

Larson, T. J., Cantwell, J. S., and A. T. van Loo-Bhattacharya. 1992. Interaction at a distance between mulitple operators controls the adjacent, divergently transcribed *glpTQ-glpACB* operons of *Escherichia coli* K-12. *J. Biol. Chem.* **267**:6114-6121.

Latour D. J. 1988. Ph. D. Thesis: The expression and assembly of *Escherichia coli* fumarate reductase. University of Alberta, Edmonton, Canada.

Latour, D. J. and J. H. Weiner. 1988. Regulation of *in vitro* expression of the *Escherichia coli frd* operon: alanine and Fnr represent positive and negative control elements. *Nucl. Acid. Res.* **16**:6330-6352.

Latour, D. J. and J. H. Weiner. 1989. Assembly of *Escherichia coli* fumarate reductase holoenzyme. *Biochem. Cell. Biol.* **67**:251-259.

Lawford, H. G. and B. A. Haddock. 1973. Respiration-driven proton translocation in *Escherichia coli*. *Biochem. J.* **136**:217-220.

Lazazzera, B. A., Bates, D. M., and P. J. Kiley. 1993. The activity of the *Escherichia coli* transcription factor FNR is regulated by a change in oligomeric state. *Genes & Development* **7**:1993-2005.

Lecker, S., Lill, R., Ziegelhoffer, T., Georgopoulos, C., Bassford Jr., P. J., Kumamoto, C. A., and W. Wickner. 1989. Three pure chaperone proteins of *Escherichia coli* - SecB, trigger factor and GroEL - form soluble complexes with precursor proteins *in vivo*. *EMBO J.* **8**:2703-2709.

Leong, L. M., Tan, B. H., and K. K. Ho. 1992. A specific stain for the detection of nonheme iron proteins in polyacrylamide gels. *Anal. Biochem.* **207**:317-320.

Lin, E. C. C. 1976. Glycerol dissimilation and it's regulation in bacteria. *Annu. Rev. Microbiol.* **30**:535-578.

Lin, E. C. C. 1987. 'Dissimilatory pathways for sugars, polyols, and carboxylates' *In* Neidhardt, F. C. (ed.) *Escherichia coli* and *Salmonella typhimurium* Cellular and molecular biology, Vol 1. American Society for Microbiology, Washington, DC, pp. 244-284.

Lin, E. C. C. and D. R. Kuritzkes. 1987. 'Pathways for anaaerobic electron transport' *In* Neidhardt, F. C. (ed.) *Escherichia coli* and *Salmonella thyphimurium* Cellular and Molecular Biology, Vol. 1. American Society for Microbiology, Washington DC., pp.201-221.

Liu, K. E. and S. J. Lippard. 1991. Redox properties of the hydroxylase component of methane monooxygenase from *Methylococcus capsulatus* (Bath). *J. Biol. Chem.* **266**:12836-12839.

Ludtke, D., Larson, T. J., Beck, C., and W. Boos. 1982. Only one gene is required for the *glpT*-dependent transport of sn-glycerol-3-phosphate in *Escherichia coli*. *Mol. Gen. Genet.* **186**:540-547.

Lutter, R., Saraste, M., van Walraven, H. S., Runswick, M. J., Finel, M., Deatherage, J. F., and J. E. Walker. 1993. F_1F_0-ATP synthase from bovine heart mitochondria: development of the purification of a monodisperse oligomycin-sensitive ATPase. *Biochem J.* **295**:799-806.

Magee, A. I., Koyama, A. H., Malfer, C., Wen., D., and M. J. Schlesinger. 1984. Release of fatty acids from virus glycoproteins by hydroxylamine. *Biochim. Biophys. Acta.* **798**:156-166.

Malkin, R. 1973. 'The chemical properties of ferredoxins' *In* Lovenberg, L. (ed.), Iron-sulfur proteins, Vol II., Academic Press, New York. pp.1-26.

Malkin, R. and A. J. Bearden. 1980. Bound iron-sulfur centers in photosynthetic membranes (higher plants and bacteria): physical detection and occurrence. *Methods Enzymol.* 69:238-249.

Mandel, M. and A. Higa. 1970. Calcium-dependent bacteriophage DNA infection. *J. Mol. Biol.* **53**:159-162.

Manoil, C., Mekalanos, J. J., and J. Beckwith. 1990. Alkaline phosphatase fusions: sensors of subcellular location. *J. Bacteriol.* **172**:515-518.

Manodori, A., Cecchini, G., Schroder, I., Gunsales, R. P., Werth, M. T. and M. K. Johnson. 1992. [3Fe-4S] to [4Fe-4S] cluster conversion in *Escherichia coli* fumarate reductase by site-directed mutagenesis. *Biochemistry* **31**:2703-2712.

Mason, J. R. and R. Cammack. 1992. The electron transport prroteins of hydroxylating bacterial dioxygenases. *Ann. Rev. Microbiol.* **46**:277-305.

Markwell, M. A., Haas, S. M., Bieber, L. L., and N. E. Tolbert. 1978. A modification of the Lowry procedure to simplify protein determination in membrnae and lipoprotein samples. *Anal. Biochem.* **87**:206-210.

Marston, F. A. O. 1986. The purification of eukaryotic polypeptides synthesized in *Escherichia coli. Biochem. J.* **240**:1-12.

Martin, A. E., Burgess, B. K., Stout, C. D., Cash., V. L., Dean, D. R., Jensen, G. M., and P. J. Stephens. 1990. Site-directed mutagenesis of *Azotobacter vinelandii* ferredoxin I: [Fe-S] cluster-driven proton rearrangement. *Proc. Natl. Acad. Sci. USA.* **87**:598-602.

Mathews, R., Charlton, S., Sands, R. H., and G. Palmer. 1974. On the nature of the spin coupling between the iron-sulfur clusters in the eight-iron ferredoxins. *J. Biol. Chem.* **249**:4326-4328.

Matsushita, K., Ohnishi, T., and H. R. Kaback. 1987. NADH-Ubiquinone oxidoreducatses of the *Escherichia coli* aerobic respiratory chain. *Biochemistry.* **26**:7732-7737.

Maurel, C., Reizer, J. M., Schroder, J. I., and M. J. Chrispeels. 1993. The vacuolar membrane protein γ-TIP creates water specific channels in *Xenopus* oocytes. *EMBO J.* 12:2241-2247.

Maurel, C., Reizer, J., Schroeder, J. I., Chrispeels, M. J., and M. H. Saier, Jr. 1994. Functional characterization of the *Escherichia coli* glycerol facilitator, GlpF, in *Xenopus* oocytes. *J. Biol. Chem.* (in press)

McCarthy, J. E. G. 1988. Expression of the *unc* genes in *Escherichia coli. J. Bioenerg. Biomem.* **20**:19-39.

Meinhardt, S. W. and T. Ohnishi. 1992. Determination of the position of the Q_i quinone binding site from the protein surface of the cytochrome bc_1 complex in *Rhodobacter capsulatus* chromatophores. *Biochim. Biophys. Acta.* 1100:67-74.

Mejean, V., Iobbi-Nivol, C., Lepelletier, M., Giorano, G., Chippaux, M., and M-C. Pascal. 1994. TMAO anaerobic respiration in *Escherichia coli*: involvement of the *tor* operon. *Mol. Microbiol.* **11**:1169-1179.

Meyer, J. and J. M. Moulis. 1981. Replacement of sulfide by selenide in the [4Fe-4S] clusters of the ferredoxin from *Clostridium pasteurianum. Biochiem. Biophys. Res. Commun.* **103**:667-673.

Miki, K. and E. C. C. Lin. 1973. Enzyme complex which couples glycerol-3-phosphate dehydrogenase to fumarate reduction in *Escherichia coli*. *J. Bacteriol.* **114**:767-771.

Miki, K. and E. C. C. Lin. 1975. Anaerobic energy-yielding reaction associated with transhydrogenation from glycerol-3-phosphate to fumarate by an *Escherichia coli* system. *J. Bacteriol.* **124**:1282-1287.

Miller, J. H. 1992. A short course in bacterial genetics: a laboratory manual and handbook for *Escherichia coli* and related bacteria. Cold Spring Harbor Laboratory Press., Cold Spring Harbor Laboratory, New York.

Miller, M. J. and R. B. Gennis. 1983. The purification and characterization of the cytochrome *d* terminal oxidase complex of the *Escherichia coli* aerobic respiratory chain. *J. Biol. Chem.* **258**:9159-9165.

Mitchell, P. 1961. Coupling of phosphorylation to electron and hydrogen transfer by a chemi-osmotic type of mechanism. *Nature (London).* **191**:144-148.

Monticello, R. A., and W. S. Brusilow. 1994. Role of the δ subunit in enhancing proton conduction through the F_0 of the *Escherichia coli* F_1F_0 ATPase. *J. Bacteriol.* **176**:1383-1389.

Morningstar, J. E., Johnson, M. K., Cecchini, G., Ackrell, B. A., and E. B. Kearney. 1985. The high potential iron-sulfur center in *Escherichia coli* fumarate reductase is a three-iron cluster. *J. Biol. Chem.* **260**:13631-13638.

Mortenson. L. E. 1964. Purification and analysis of ferredoxin from *Clostridium pasteurianum*. *Biochim. Biophys. Acta.* **81**:71-77.

Mortenson, L. E. and W. O. Gillum. 1980. Quantitative and qualitative characterization of the iron-sulfur centers of proteins. *Methods Enzymol.* **69**:779-792.

Moura, I., Tavares, P., Moura, J. J. G., Ravi, N., Huynh., B. H., Liu, M-Y., and J. LeGall. 1992. Direct spectroscopic evidence for the presence of a 6Fe cluster in an iron-sulfur protein isolated from *Desulfovibrio desulfuricans* (ATCC 27774). *J. Biol. Chem.* **267**:4489-4496.

Newton, N. A., Cox, G. B., and F. Gibson. 1971. The function of menaquinone (vitamin K_2) in *Escherichia coli* K-12. *Biochim. Biophys. Acta.* **244**:155-166.

Nikaido, H. and M. Vaara. 1987. 'Outer Membrane' *In* Neidhardt, F. C. (ed.) *Escherichia coli* and *Salmonella thyphimurium* Cellular and Molecular Biology, Vol. 1. American Society for Microbiology, Washington DC., pp.7-22.

Nikaido, H. 1992. Porins and specific channels of bacterial outer membranes. *Mol. Microbiol.* **6**:435-442.

Nikaido, H. and M. H. Saier, Jr. 1992. Transport proteins in bacteria: common themes and designs. *Science* **258**:936-942.

Nohno, T., Noji, S., Taniguchi, S., and T. Saito. 1989. The *narX* and *narL* genes encoding the nitrate-sensing regulators of *Escherichia coli* are homologous to a family of prokaryotic two component regulatory genes. *Nucl. Acids Res.* **17**:2947-2957.

Omer, C. A. and J. B. Gibbs. 1994. Protein prenylation in eukaryotic microorganisms: genetics, biology and biochemistry. *Mol. Microbiol.* **11**:219-225.

Orme-Johnson, W. H. 1973. Iron-sulfur proteins: structure and function. *Annu. Rev. Biochem.* **42**:159-204.

Orme-Johnson, W. H. and H. Beinert. 1969. Heterogeneity of paramagnetic species in two iron-sulfur proteins: *Clostridium pasteurianum* ferredoxin and milk xanthine oxidase. *Biochim. Biophys. Res. Commun.* **36**:337-342.

Orme-Johnson, W. H. and R. H. Sands. 1973. "Probing iron-sulfur proteins with EPR and ENDOR spectroscopy". *In* Lovenberg, W. (ed.) Iron-sulfur proteins. Academic Press, New York, pp. 195-238.

Packer, E. L., Sternlight, H., Lode, E. T. and J. C. Rabinowitz. 1975. The use of ^{13}C nuclear magnetic resonance of aromatic amino acid residues to determine the midpoint oxidation-reduction potential of each iron-sulfur cluster of *Clostridium acidi-urici* and *Clostridium pasteurianum* ferredoxins. *J. Biol. Chem.* **250**:2062-2072.

Palmer, G. and R. H. Sands. 1966. On the magnetic resonance of spinach ferredoxin. *J. Biol. Chem.* **241**:254.

Pao, G. M., Wu, L-F., Johnson, K. D., Hofte, H., Chrispeels, M. J., Sweet, G., Sandal, N. N., and M. H. Saier, Jr. 1991. Evolution of the MIP family of integral membrnae transport proteins. *Mol. Microbiol.* **5**:33-37.

Park, J-B., Fan, C., Hoffman, B. M, and M. W. W. Adams. 1991. Potentiometric and electron nuclear double resonance properties of the two spin forms of the $[4Fe\text{-}4S]^{+}$ cluster in the novel ferredoxin from the hyperthermophilic archaebacterium *Pyrocossus furiosus*. *J. Biol. Chem.* **266**:19351-19356.

Pascal, M. -C., Burini, J. F., and M. Chippaux. 1984. Regulation of trimethylamine N-oxide (TMAO) reductase of *Escherichia coli*: Analysis of *tor::Mud1* operon fusion. *Mol. Gen. Genet.* **195**:351-355.

Pascal, M. -C., Lepelletier, M., Giordano, G., and M. Chippaux. 1991. A regulatory mutant of trimethylamine N-oxide reductase of *Escherichia coli* K-12. *FEMS Microbiol. Lett.* **78**:297-300.

Paul, C. and J. P. Rosenbusch. 1985. Folding patterns of porin and bacteriorhodopsin. *EMBO J.* **4**:1593-1597.

Payne, M. J., Chapman, A., and R. Cammack. 1993. Evidence for an [Fe]-type hydrogenase in the parasitic protozoan *Trichomonas vaginalis*. *FEBS Lett.* **317**:101-104.

Peersen, O. B., Pratt, E. A., Truong, H-T., N., Ho, C., and G. S. Rule. 1990. Site-specific incorporation of 5-Fluorotryptophan as a probe of the structure and function of the membrane-bound D-Lactate dehydrogenase of *Escherichia coli*: a ^{19}F nuclear magnetic resonance study. *Biochemistry*. **29**:3256-3262.

Petrovich, R. M., Ruzicka, F. J., Reed, G. H., and P. A. Frey. 1992. Characterization of iron-sulfur clusters in lysine 2,3-aminomutase by electron paramagnetic resonance spectroscopy. *Biochemistry* **31**:10774-10781.

Pettigrew, D. W., Ma, D. P., Conrad, C. A., and J. R. Johnson. 1988. *Escherichia coli* glycerol kinase - cloning and sequencing of the *glpK* gene and the primary structure of the enzyme. *J. Biol. Chem.* 263:135-139.

Polglase, W. J., Pun, W. T., and J. Withaar. 1965. Lipoquinones of *Escherichia coli*. *Biochim. Biophys. Acta*. **118**:425-426.

Poole, R. K. and B. A. Haddock. 1975. Effects of sulphate-limited growth in continuous culture on the electron-transport chain and energy conservation in *Escherichia coli* K-12. *Biochem. J.* **152**:537-546.

Poole, R. K., Hatch, L., Cleeter, M. W. J., Gibson, F., Cox, G. B., and W. Guanghui. 1993. Cytochrome *bd* biosynthesis in *Escherichia coli*: the sequences of the *cydC* and *cydD* genes suggest that they encode the components of an ABC membrane transporter. *Mol. Microbiol.* **10**:421-430.

Poole, R. K. and W. J. Ingledew. 1987. "Pathways of electrons to oxygen" *In* Neidhardt, F. C. (ed.) *Escherichia coli* and *Salmonella typhimurium* Cellular and Molecular Biology, Vol. 1. American Society for Microbiology, Washington, DC., pp. 170-200.

Prince, R. C. and M. W. W. Adams. 1987. Oxidation-reduction properties of the two Fe_4S_4 clusters in *Clostridium pasteurianum* ferredoxin. *J. Biol. Chem.* **262**:5125-5128.

Puustinen, A., Finel, M., Haltia, T., Gennis, R. B., and M. Wilstrom. 1991. Properties of the two terminal oxidases of *Escherichia coli*. *Biochemistry*. **30**:3936-3942.

Rabin, R. S., Collins, L. A., and V. Stewart. 1992. *In vivo* requirement of integration host factor for *nar* (nitrate reductase) operon expression in *Escherichia coli* K-12. *Proc. Natl. Acad. Sci. USA*. **89**:8701-8705.

Rabin, R. S. and V. Stewart. 1993. Dual response regulators (NarL and NarP) interact with dual sensors (NarX and NarQ) to control nitrate- and nitrite-regulated gene expression in *Escherichia coli* K-12. *J. Bacteriol.* **175**:3259-3268.

Reeves, J. P., Hong, J-S., and H. R. Kaback. 1973. Reconstitution of D-lactate dependent transport in membrane vesicles from a D-lactate dehydrogenase mutant of *Escherichia coli*. *Proc. Natl. Acad. Sci. USA*. **70**:1971-1921.

Richards F. M. 1991. The protein folding problem. *Scientific American* **264**:54-63.

Robinson, J. J. 1982. Ph. D. Thesis: Studies on Glycerol-3-phosphate dehydrogenase and fumarate reductase of *Escherichia coli*. University of Alberta, Edmonton, Canada.

Robinson, J. J. and J. H. Weiner. 1982. Molecular properties of fumarate reductase isolated from the cytoplasmic membrane of *Escherichia coli*. *Can. J. Biochem.* **60**:811-816.

Rothery, R. A. and J. H. Weiner. 1991. Alteration of the iron-sulfur cluster composition of *Escherichia coli* dimethyl sulfoxide reductase by site-directed mutagenesis. *Biochemistry* **30**:8296-8305.

Rothery, R. A. and J. H. Weiner. 1993. Topological characterization of *Escherichia coli* DMSO reductase by electron paramagnetic resonancne spectroscopy of an engineered [3Fe-4S] cluster. *Biochemistry* **32**:5855-5861.

Rule, G. S., Pratt, E. A., Chin, C. C. Q., Wold, F., and C. Ho. 1985. Overproduction and nucleotide sequence of the respiratory D-Lactate dehydrogenase of *Escherichia coli*. *J. Bacteriol.* **161**:1059-1068.

Rupp, H., Rao, K. K., Hall, D. O. Cammack, R. 1978. Electron spin relaxation of iron-sulphur proteins studies by microwave power saturation. *Biochim. Biophys. Acta*. **537**:255-269.

Russel, M. and P. Model. 1984. Replacement of the fip gene of *Escherichia coli* by an inactive gene cloned on a plasmid. *J. Bacteriol.* **159**:1034-1039.

Saiki, R. K., Gelfand, D. H., Stoffel, S., Scharf, S. J., Higuchi, R., Horn, G. T., Mullis, K. B., and H. A. Erlich. 1988. Primer-directed enzymatic amplification of DNA with a thermostable DNA polymerase. *Science* **239**: 487-494.

Sambasivarao, D. and J. H. Weiner. 1991. Differentiation of the mulitple S- and N-oxide- reducing activities of *Escherichia coli*. *Curr. Microbiol.* **23**:105-110.

Sambrook, J., Fritsch, E. F., and T. Maniatis. 1989. Molecular cloning, a laboratory manual, second edition. Cold Spring Harbor Labaratory Press, Cold Spring Harbor, New York.

Sanger, F., Nicklen, S., and A. R. Coulson. 1977. DNA sequencing with chain-terminating inhibitors. *Proc. Natl. Acad. Sci. USA*. 74:5463-5467.

Savage, D. C. 1977. Microbial ecology of the gastrointestinal tract. *Annu. Rev. Microbiol.* **31**:107-133.

Schiltz, E., Kreusch, A., Nestel, U, and G. E. Scultz. 1991. Primary structure of porin from *Rhodobacter capsulatus*. *Eur. J. Biochem.* **199**:587-594.

Schroder, I., Darie, S., and R. P. Gunsalus. 1993. Activation of the *Escherichia coli* Nitrate reductase (*narGHJI*) operon by NarL and Fnr requires intergration host factor. *J. Biol. Chem.* **268**:771-774.

Schryvers, A. 1981. Ph. D. Thesis: The aerobic and anaerobic glycerol-3-phosphate dehydrogenases of *Escherichia coli*. University of Alberta, Edmonton, Canada.

Schryvers, A., Lohmeier, E., and J. H. Weiner. 1978. Chemical and functional properties of the native and reconstituted forms of the membrane-bound, aerobic glycerol-3-phosphate dehydrogenase of *Escherichia coli*. *J. Biol. Chem.* **253**:783-788.

Schryvers, A. and J. H. Weiner. 1981. The anaerobic sn-Glycerol-3-phosphate dehydrogenase of *Escherichia coli*. *J. Biol. Chem.* **256**:9959-9965.

Schryvers, A. and J. H. Weiner. 1982. The anaerobic sn-glycerol-3-phosphate dehydrogenase: cloning and expression of the *glpA* gene of *Escherichia coli* and identification of the *glpA* products. *Can. J. Biochem.* 60:224-231.

Schweizer, H., Sweet, G., and T. J. Larson. 1986. Physical and genetic structure of the *glpD-malT* interval of the Escherichia K-12 chromosome: identification of two new structural genes of the *glp* regulon. *Mol. Gen. Genet.* **202**:488-492.

Sefton, B. M. and J. E. Buss. 1987. The covalent modification of eukaryotic proteins with lipid. *J. Cell. Biol.* **104**:1449-1453.

Senior, A. E. 1992. Catalytic sites of *Escherichia coli* F_1-ATPase. *J. Bioenerg. Biomemb.* **24**:479-484.

Sharrocks, A. D., Green, J., and J. R. Guest. 1991. *In vivo* and *in vitro* mutants of FNR the anaerobic transcriptional regulator of *E. coli*. *Proc. R. Soc. Lond.* **245**:219-226.

Shaw, D. J., Rice, D. W., and J. R. Guest. 1983. Homology between CAP & Fnr, a regulator of anaerobic respiration in *Escherichia coli*. *J. Mol. Biol.* **166**:241-247.

Shethna, Y. I., Stombaugh, N. A., and R. H. Burris. 1971. Ferredoxin from *Bacillus polymyxa*. *Biochem. Biophys. Res. Commun.* **42**:1108-1116.

Silvestro, A., Pommier, J., and Giordano, G. 1988. The inducible trimethylamine N-oxide reductase of *Escherichia coli* K12: biochemical and immunological studies. *Biochim. Biophys. Acta.* **954**:1-13.

Silvestro, A., Pommier, J., Pascal, M. C., and G. Giordano. 1989. The inducible trimethylamine N-oxide reductase of *Escherichia coli* K-12: it's location and inducers. *Biochim. Biophys. Acta.* **999**:209-216.

Simons, P. C. and D. L. Vander Jagt. 1977. Purification of glutathione S-transferases from human liver by glutathione-affinity chromatography. *Anal. Biochem.* **82**:334-341.

Slater, E. C. 1953. Nature (London) Mechanism of phosphorylation in the respiratory chain. **172**:975-978.

Smith, D. B. and K. S. Johnson. 1988. Single-step purification of polypeptides expressed in *Escherichia coli* as fusions with glutathione S-transferase. *Gene* **67**:31-40.

Smith, M. W. and F. C. Neidhardt. 1983a. Proteins induced by anaerobiosis in *Escherichia coli*. *J. Bacteriol.* **154**:336-343.

Smith, M. W. and F. C. Neidhardt. 1983b. Proteins induced by aerobiosis in *Escherichia coli*. *J. Bacteriol.* **154**:344-350.

Soreq, H. and S. Seidman. 1992. *Xenopus* oocyte microinjection: from gene to protein. *Methods Enzymol.* **207**:225-265.

Spiro, S. and J. Guest. 1990. FNR and it's role in oxygen regulated gene expression in *Escherichia coli*. *FEMS Microbiol. Rev.* **75**:399-428.

Spiro, S., Roberts, R. E., and J. R. Guest. 1989. Fnr-dependent repression of the *ndh* gene of *Escherichia coli* and metal ion requirement for FNR-regulated gene expression. *Mol. Microbiol*, **3**:601-608.

Sprott, G. D., Koval, S. F., and C. A. Schnaitman. 1994. "Cell fractionation" *In* Gerhardt, P (ed.) Methods for general and molecular bacteriology., American Society for Microbiology, Washington, D.C., pp. 72-103.

Steenkamp, D. J., Singer, T. P., and H. Beinert. 1978. Participation of the iron-sulphur cluster and covalently bound coenzyme of trimethylamine dehydrogenase in catalysis. *Biochem J.* **169**:361-369.

Stewart, V., Parales, J., and S. M. Merkel. 1989. Structure of the genes *narL* and *narX* of the *nar* (nitrate reductase) locus in *Escherichia coli* K-12. *J. Bacteriol.* **171**:2229-2234.

Stewart, V. 1982. Requirement of Fnr & NarL functions for nitrate reductase expression in *Escherichia coli* K-12. *J. Bacteriol.* **151**:1320-1325.

Stewart, V. 1993. Nitrate regulation of anaerobic respiratory gene expression in *Escherichia coli*. *Mol. Microbiol.* **9**:425-434.

St. Martin, E. J., Freedburg, W. B., and E. C. C. Lin. 1977. Kinase replacement by a dehydrogenase for *Escherichia coli* glycerol utilization. *J. Bacteriol.* **131**:1026-1028.

Stock, J. B., Stock, A. M., and J. M. Mottonen. 1990. Signal transduction in bacteria. *Nature*. **344**:395-400.

Stombaugh, N. A., Burris, R. H., and W. Orme-Johnson. 1973. Ferredoxins from *Bacillus polymyxa*. *J. Biol. Chem.* **248**:7951-7956.

Stombaugh, N. A., Sundquist, J. E., Burris, R. H., and W. H. Orme-Johnson. 1976. Oxidation-reduction properties of several low potential iron-sulfur proteins and of methylviologen. *Biochemistry* **15**:2633-2641.

Studier, F. W., and B. A. Moffatt. 1986. Use of bacteriophage T7 RNA polymerase to direct selective high level expression of cloned genes. *J. Mol. Biol.* 189:113-130.

Studier, F. W., Rosenberg, A. H., Dunn, J. J., and J. W. Dubendorff. 1990. Use of T7 RNA polymerase to direct expression of cloned genes. *Methods Enzymol.* **185**:60-89.

Sun, Z-Y., Truong, H. T. N., Pratt, E. A., Sutherland, D. C., Kulig, C. E., Homer, R. J., Groetsch, S. M., Hsue, P. Y., and C. Ho. 1993. A ^{19}F-NMR study of the membrane-binding region of D-lactate dehydrogeanse of *Escherichia coli. Protein Science* **2**:1938-1947.

Sweeney, W. V. and B. A. McIntosh. 1978. Determination of cooperative interaction between clusters in *Clostridium pasteurianum* 2(4Fe-4S) ferredoxin. *J. Biol. Chem.* **254**:4499-4501.

Sweet, G., Gandor, C., Voegelle, R., Wittekindt, N., Beuerle, J., Truniger, V., Lin, E. C. C., and W. Boos. 1990. Glycerol facilitator of *Escherichia coli*: cloning of the *glpF* and identifiction of the *glpF* product. *J. Bacteriol.* **172**:424-430.

Ta, D. T. and L. E. Vickery. 1992. Cloning, sequencing, and overexpression of a [2Fe-2S] ferredoxin gene from *Escherichia coli. J. Biol. Chem.* **267**:11120-11125.

Tabor, S. and C. C. Richardson. 1985. A bacteriphage T7 RNA polymerase/promoter system for controlled exclusive expression of specific genes. *Proc. Natl. Acad. Sci. USA.* **82**:1074-1078.

Tabor, S. and C. C. Richardson. 1987. DNA sequence analysis with a modified bacteriophage T7 DNA polymerase. *Proc. Natl. Acad. Sci. USA.* **84**:4767-4771.

Tagaki, M., Tsuchiya, T., and M. Ishimoto. 1981. Proton translocation coupled to trimethylamine N-oxide reduction in anaerobically grown *Escherichia coli. J. Bacteriol.* **148**:762-768.

Tang, C. T., Ruch Jr., F. E., and E. C. C. Lin. 1979. Purification and properties of a nicotinamide adenine dinucleotide-linked dehydrogenase that serves an *Escherichia coli* mutant for glycerol metabolism. *J. Bacteriol.* **140**:182:187.

Tang, J. C. T., St. Martin, E. J., and E. C. C. Lin. 1982. Derepression of an NAD-linked dehydrogenase that serves an *Escherichia coli* mutant for growth on glycerol. *J. Bacteriol.* **152**:1001-1007.

Tang, C. and H. L. Henry. 1993. Overexpression in *Escherichia coli* and affinity purification of chick kidney ferredoxin. *J. Biol. Chem.* **268**:5069-5076.

Tartoff, K. D., and C. A. Hobbs. 1987. Improved media for growing plasmid and cosmid clones. *Bethesda Res. Lab. Focus* **9**:12.

Thomas, C. T. and M. G. McNamee. 1990. Purification of membrane proteins. *Methods Enzymol.* **182**:499-519.

Thomas, J. W., Lemieux, L. J., Alben, J. O., and R. B. Gennis. 1993. Site-directed mutagenesis of highly conserved residues in helix VIII of subunit I of the cytochrome *bo* ubiquinol oxidase from *Escherichia coli*: and amphipathic transmembrane helix that may be important in conveying protons to the binuclear center. *Biochemistry* **32**:11173-11180.

Thomson, A. J., Robinson, A. E., Johnson, M. K., Cammack, R., Rao., K. K., and D. O. Hall. 1981. Low-temperature magnetic circular dichroism evidence for the conversion of four-iron-sulphur cluster in a ferredoxin from *Clostridium pasteurianum* into three-iron-sulphur clusters. *Biochim. Biophys. Acta.* **637**:423-432.

Trageser, M., Spiro, S., Duchene, A., Kojro, E., Fahrenholz, F., Guest, J. R., and G. Unden. 1990. Isolation of intact FNR protein (M_r30000) of *Escherichia coli*. *Mol. Microbiol.* **4**:21-27.

Truniger, V., Boos, W., and G. Sweet. 1992. Molecular analysis of the *glpFKX* regions of *Escherichia coli* and *Shigella flexneri*. *J. Bacteriol.* **174**:6981-6991.

Truniger, V. and W. Boos. 1994. Mapping and Cloning of *gldA*, the structural gene of the *Escherichia coli* glycerol dehydrogenase. *J. Bacteriol.* **176**:1796-1800.

Vogelstein, B. and D. Gillespie. 1979. Preparative and analytical purification of DNA from agarose. *Proc. Natl. Acad. Sci. USA.* **76**:615-619.

Weiner, J. H. 1974. The localization of glycerol-3-phosphate dehydrogenase in *Escherichia coli*. *J. Membrane Biol.* **15**:1-14.

Weiner, J. H. and P. Dickie. 1979. Fumarate reductase of *Escherichia coli*; elucidation of the covalent-flavin component. *J. Biol. Chem.* **254**:8590-8593.

Weiner, J. H. and L. A. Heppel. 1972. Purification of the membrane-bound and pyridine nucleotide-independent L-glycerol-3-phosphate dehydrogenase from *Escherichia coli*. *Biochim. Biophys. Res. Commun.* **47**:1360-1365.

Weiner, J. H., Lemire, B. D., Elmes, L. M., Bradley, R. D., and D. G. Scraba. 1984. Overproduction of fumarate reductase in *Escherichia coli* induces a novel intracellular lipid-protein organelle. *J. Bacteriol.* **158**:590-596.

Weiner, J. H., Cammack, R., Cole, S. T., Condon, C., Honore, N., Lemire, B. D., and G. Shaw. 1986. A mutant of *Escherichia coli* fumarate reductase decoupled from electron transport. *Proc. Natl. Acad. Sci. USA.* **83**:2056-2060.

Weiner, J. H., MacIsaac, D. P., Bishop, R. E., and P. T. Bilous. 1988. Purification and properties of *Escherichia coli* dimethyl sulfoxide reductase, and iron-sulfur molbdoenzyme with broad substrate specificity. *J. Bacteriol.* **170**:1505-1510.

Weiner, J. H., Rothery, R. A., Sambasivarao, D. and C. A. Trieber. 1992. Molecular analysis of dimethyl sulfoxide reductase: a complex iron-sulfur molybdoenzyme of *Escherichia coli*. *Biochim. Biophys. Acta* **1102**:1-18.

Weiner, J. H., Shaw, G., Turner, R. J., and C. A. Trieber. 1993. The topology of the anchor subunit of dimethyl sulfoxide reductase of *Escherichia coli*. *J. Biol. Chem.* **268**:3238-3244.

Weissenborn, D. L., Wittekindt, N., and T. J. Larson. 1992. Structure and regulation of the *glpFK* operon encoding glycerol diffusion facilitator and glycerol kinase of *Escherichia coli* K-12. *J. Biol. Chem.* **267**:6122-6131.

Werth, M. T., Cecchini, G., Manodori, A., Ackrell, B. A. C., Schroder, I., Gunsales, R. P., and M. K. Johnson. 1990. Site-directed mutagenesis of conserved cysteine residues in *Escherichia coli* fumarate reductase: modification of the spectroscopic and electrochemical properties of the [2Fe-2S] cluster. *Proc. Natl. Acad. Sci. USA.* **87**:8965-8969.

Westenberg, D. J., Gunsales, R. P., Ackrell., B. A., Sices, H., and G. Cecchini. 1993. *Escherichia coli* fumarate reductase *frdC* and *frdD* mutants- identification of amino acid residues involved in catalytic activity with quinones. *J. Biol. Chem.* **268**:815-822.

Williams, D. C., VanFrank, R. M., Muth, W. T., Burnett, J. P. 1982. Cytoplasmic inclusion bodies in *Escherichia coli* producing biosynthetic human insulin proteins. *Science* **215**:687-689.

Williams, R. J. P. 1978. The multifarious couplings of energy transduction. *Biochim. Biophys. Acta.* 505:1-44.

Wilson, G. S. 1978 Determination of oxidation-reduction potentials. *Methods Enzymol.* **54**:396-410.

Wood, J. 1987. Membrane association of proline dehydrogenase in *Escherichia coli* is redox dependent. *Proc. Natl. Acad. Sci. USA.* **84**:373-377.

Woodland, M. P., Patil, D. S., Cammack, R., and H. Dalton. 1986. ESR studies of protein A of the soluble methane monooxygenase from *Methylococcus capsulatus* (Bath). *Biochim. Biophys. Acta.* **873**:237-242.

Yamamoto, I., Okubo, N., and Ishimoto, M. 1986. Further characterization of trimethylamine N-oxide reductase from *Escherichia coli*, a molydoprotein. *J. Biochem.* **99**:1773-1779.

Yamane, K., Akiyama, Y., Ito, K., and S. Mizushima. A positively charged region is a determinant of the orientation of cytoplasmic membrane proteins in *Escherichia coli*. *J. Biol. Chem.* **263**:21166-21171.

Yamato, I., Anraku, Y., and K. Hirosawa, K. 1975. Cytoplasmic membrane vesicles of *Escherichia coli*, a simple method for preparing the cytoplasmic and outer membranes. *J. Biochem.* **77**:705-718.

Ye, S. and T. J. Larson. 1988. Structures of the promoter and operator of the *glpD* gene encoding aerobic sn-glycerol-3-phosphate dehydrogenase of *Escherichia coli* K-12. *J. Bacteriol.* **170**:4209-4215.

Young, I. G., Rogers, B. L., Campbell, H. D., Jaworowski, A., and D. C. Shaw. 1981. Nucleotide sequence coding for the respiratory NADH dehydrogenase of *Escherichia coli*. *Eur. J. Biochem.* **116**:165-170.

Zambrano, M. M and R. Kolter. 1993. *Escherichia coli* mutants lacking NADH Dehydrogenase I have a competitive disadvantage in stationary phase. *J. Bacteriol.* **175**:5642-5647.

Zhao, N., Oh, W., Trybul, D., Thrasher, K. S., Kingsbury, T. J., and T. J. Larson. 1994. Characterization of the interaction of the *glp* repressor of *Escherichia coli* K-12 with single and tandem *glp* operator variants. *J. Bacteriol.* **176**:2393-2397.